Characterisation of a gene for photorepair in Escherichia coli K-12

Dorrell, Nicholas

Award date:
1993

Awarding institution:
University of Bath

CHARACTERISATION OF A GENE FOR PHOTOREPAIR IN *Escherichia coli* K12

Submitted by Nicholas Dorrell, B.Pharm.Hons., M.R.Pharm.S.

for the degree of

Doctor of Philosophy

of the University of Bath

1993

This research has been carried out in the School of Pharmacy and Pharmacology of the University of Bath under the supervision of S.H. Moss, M.Sc., Ph.D., M.R.Pharm.S.

COPYRIGHT

ProQuest LLC
789 East Eisenhower Parkway
P.O. Box 1346
Ann Arbor, MI 48106-1346

ABSTRACT

This study concentrates on the role of the putative *phr*A gene in the DNA repair process, photoreactivation, in *Escherichia coli* K-12. It was originally proposed that there were two genes, *phr*A and *phr*B, involved in the genetic control of photoreactivation. The *phr*B gene has been cloned, sequenced and extensively characterised, placing in doubt the relevance of the *phr*A gene. In our laboratory, previous workers have cloned a restriction fragment thought to contain the putative *phr*A gene, and shown an *in vivo* photoreactivable effect due to this restriction fragment. The work in this study is involved with the characterisation of the gene present on this restriction fragment.

The introduction includes a review of the literature regarding the controversy between *phr*A and *phr*B.

The experimental work is divided into three sections. The first section reports the sequencing of the restriction fragment, suggesting it does contain a gene which codes for a protein of approximately 38kDa.

The second section reports attempts to over-express the putative *phr*A gene product, including construction of two vectors designed to over-express the gene product.

In the third section, initial photoreactivation studies show the putative *phr*A gene does produce photorecovery above that observed in controls. Temperature and dose-rate studies suggest that part of the photorecovery observed in *phr*A$^+$ strains is produced by an unknown photoactive protein. A study of the near-UV sensitivity of *phr*A$^+$ *phr*B$^-$ and *phr*A$^-$ *phr*B$^-$ strains also suggests that the putative *phr*A gene increases resistance to near-UV killing.

These findings have been discussed with regard to the genetic control of photoreactivation in *Escherichia coli* K-12. The results of this study support the hypothesis that the putative

*phr*A gene is involved in photoenzymatic repair, and offers some explanations for the different findings reported in the literature regarding the activity of the putative *phr*A gene.

ACKNOWLEDGEMENTS

I would like to thank my supervisor Dr Steve Moss for his constant support, enthusiasm and encouragement over the last 3 years spent on this study. I would also like to thank Dr Abdul Ahmed and Dr Paul Towner for all their assistance and encouragement. Particular thanks are due to Dr Gail Adams, without whom this thesis would never have been written. I would like to thank SERC for financial support, Professor David Davies, Head of School, for providing facilities for the research, and all the technical staff in the School of Pharmacy and Pharmacology for all their efforts on my behalf.

ABBREVIATIONS

The following abbreviations have been used in this thesis :-

A	Adenine
amp	Ampicillin
ATP	Adenosine Triphosphate
bp / kbp	Base pairs / Kilo base pairs
BSA	Bovine Serum Albumin
C	Cytosine
C< >C	Cytosine - cytosine dimer
C< >T	Cytosine - thymine dimer
CPD	Cyclobutane pyrimidine dimer
Da	Daltons
DDDW	Deionised double-distilled water
DNA	Deoxy-ribonucleic acid
E.coli	*Escherichia coli*
EDTA	Ethylenediaminetetraacetic acid
EPR	Enzymatic photoreactivation
G	Guanine
IPTG	Isopropylthio-β-D-galactoside
PCS	Poly-cloning site
PR	Photoreactivation
PRE	Photoreactivating enzyme
Pyr < > Pyr	Pyrimidine dimer
RBS	Ribosome-binding site

RNA	Ribonucleic acid
SDS	Sodium dodecyl sulphate
str	Streptomycin
T	Thymine
T< >T	Thymine dimer
tet	Tetracycline
Tris	Tris(hydroxymethyl)aminomethane
UV	Ultraviolet
≅	Approximately

AMINO ACIDS

Amino acid	Three-letter code	One-letter code
Alanine	Ala	A
Arginine	Arg	R
Asparagine	Asn	N
Aspartic acid	Asp	D
Cysteine	Cys	C
Glutamine	Gln	Q
Glutamic acid	Glu	E
Glycine	Gly	G
Histidine	His	H
Isoleucine	Ile	I
Leucine	Leu	L
Lysine	Lys	K
Methionine	Met	M
Phenylalanine	Phe	F
Proline	Pro	P
Serine	Ser	S
Threonine	Thr	T
Tryptophan	Trp	W
Tyrosine	Tyr	Y
Valine	Val	V

NB: Not all these amino acids are referred to in this study. The full list is included for completion.

TABLE OF CONTENTS

CHAPTER ONE

INTRODUCTION

1.1 BACKGROUND

In this study, the genetic control of one of the DNA repair processes, photoreactivation, in *Escherichia coli* K-12 is examined, looking at UV-induced DNA damage and its repair.

The genetic material of a cell faces a continual challenge to its integrity from the environment. One of the principal functions of any cell is the prevention of an unacceptably high mutation rate. DNA damage can conveniently be grouped into two major 'classes', referred to as *Spontaneous* and *Environmental*, and collectively provides the substrate for many DNA repair processes and other cellular responses evolved to combat this threat. Ultra-violet light is an environmental cause of DNA damage.

Historically, the investigation of UV radiation damage to DNA marks the beginning of the study of the repair of DNA damage. It is relevant biologically as living organisms have had to contend with the genotoxic effects of solar UV radiation since the beginning of the evolution of life on this planet. The ultraviolet region of the electromagnetic spectrum can be divided into VACUUM- (< 190nm), FAR- (190nm-290nm), MID- (290nm-320nm) and NEAR- (320nm-400nm), and this terminology is used throughout this study. The terms UVC (far-UV), UVB (mid-UV) and UVA (near-UV) are also encountered in the literature, being particularly popular with reference to sunlight.

Photoreactivation is one of the three main types of DNA repair mechanisms. It is characterised by the requirement of light to initiate the repair of DNA damage. The most important type of repair in this group is termed *Enzymatic Photoreactivation.*

Enzymatic photoreactivation is defined as a DNA repair process that requires the presence of a photoreactivating enzyme, DNA photolyase. DNA photolyase binds specifically to ultraviolet radiation-induced cyclobutane pyrimidine dimers in DNA, and upon exposure of the photolyase-dimer complex to wavelengths in the range of 300nm-500nm, results in the splitting of the dimerised pyrimidines back to their monomeric form.

In *Escherichia coli*, it was once proposed that their were two photolyase molecules produced from two separate genes, termed *phr*A and *phr*B (Sutherland and Hausrath, 1979). Since then, however, the role of the *phr*A gene has been questioned by the work of A. Sancar and co-workers in particular, and finally dismissed as a photolyase (Husain and Sancar, 1987a). However, work in our laboratory has shown a role for the *phr*A gene in photorepair in *Escherichia coli*. The aim of this study was to try and confirm this role of the *phr*A gene in light-repair in *Escherichia coli* K-12, and try and provide an explanation for the conflicting reports that exist in the literature.

1.2 UV DAMAGE TO CELLS

The work in this study is concerned with UV-induced DNA damage, however it is important to remember that DNA is not the only target for UV-induced damage. It was previously proposed that the cytotoxic effects of UV radiation increased with decreasing wavelength. However, Gates (1930) recognised that bacteria exhibited a maximum UV absorption at approximately 260nm which was associated with a concomitant increase in cell lethality. Thus interaction with a specific target molecule, later shown to be DNA, was suggested. Many of the biological effects of UV radiation have now been attributed to the formation of specific photoproducts in DNA.

Cyclobutane pyrimidine dimers and pyrimidine (6-4) pyrimidone photoproducts are the two main classes of cytotoxic, mutagenic and carcinogenic DNA photoproducts produced by ultraviolet light irradiation of cells (Friedberg, 1985; Brash, 1988; Mitchell and Nairn, 1989). These are reviewed in detail here, as well as, briefly, other DNA photoproducts and non-DNA damage produced by UV irradiation.

1.2.1 CYCLOBUTANE PYRIMIDINE DIMERS

When DNA is exposed to radiation at wavelengths approaching its absorption maximum (about 260nm), adjacent pyrimidines become covalently linked by formation of a four-membered ring structure resulting from the saturation of their respective 5,6 double bonds (Beukers and Berends, 1960). Theoretically, these dimers can exist in twelve isomeric forms; however, only four of them (*cis-syn, cis-anti, trans-syn and trans-anti*) are formed in significant amounts (Khattak and Wang, 1972) - see Figure 1.1.

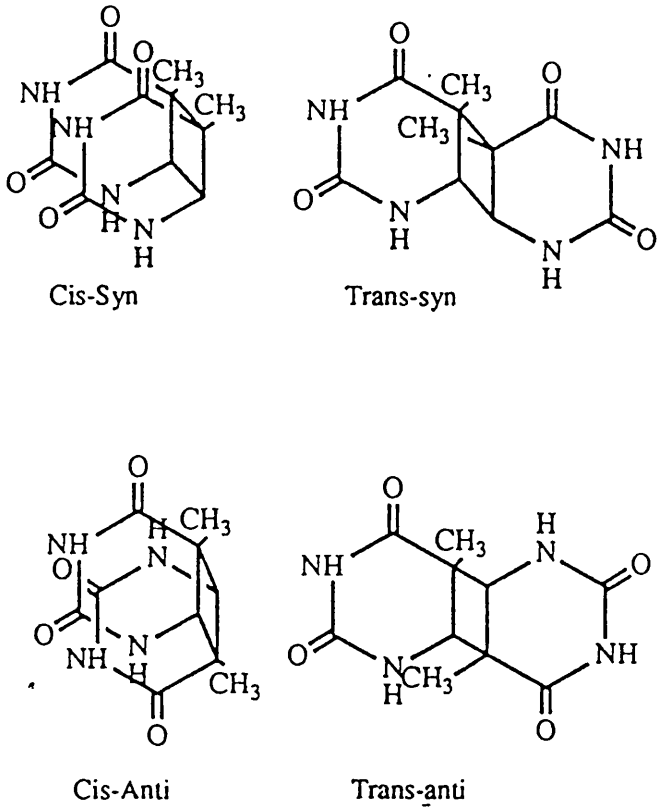

Figure 1.1. The four biological forms of thymine dimers formed in DNA.

In double-stranded DNA, the *cis-syn* isomer is the only dimer formed - see Figure 1.2. This preponderance of the *cis-syn* isomer is a consequence of steric factors, as the strain involved in the formation of this isomer within DNA is relatively small, in contrast to the other three forms (Heelis *et al.*, 1993). Nonetheless, some distortion of the double helix is inevitable. A recent NMR study (Taylor *et al.*, 1990) showed that the *cis-syn* T< >T dimer causes a minor perturbation in the helical axis of DNA, and weakens, but does not break, the hydrogen bonds between the dimerised thymines and opposite bases.

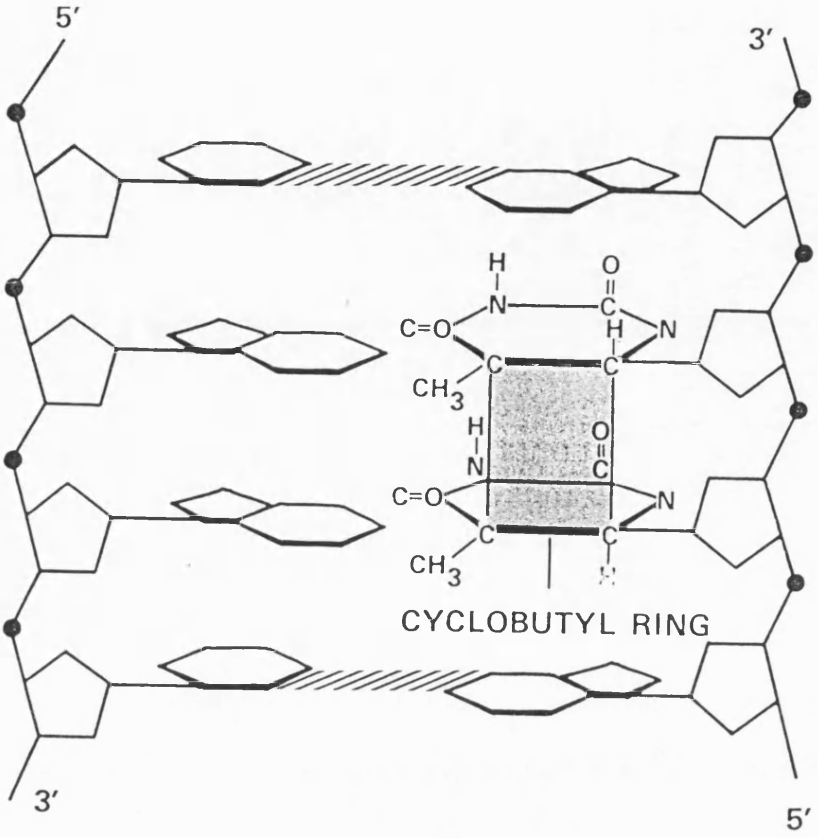

Figure 1.2. A *cis-syn* cyclobutane pyrimidine dimer.

Dimers can form between any combination of thymine (or uracil) and cytosine. Setlow and Carrier (1966) found that in 265nm irradiated *E. coli*, which has an approximately equal G-C and A-T content, the percentage ratio of cytosine-cytosine (C< >C), cytosine-thymine (C< >T) and thymine-thymine (T< >T) dimers was 7, 34 and 59 respectively.

The formation of pyrimidine dimers during irradiation of DNA is a reversible process that can be represented as :-

$$Py + Py \underset{}{\overset{UV}{\rightleftharpoons}} Py <> Py$$

Since under normal conditions the equilibrium is shifted far to the right, dimer formation is favoured over dimer reversal (Setlow, 1968). However, if *E. coli* DNA radio-labelled in thymine is continuously irradiated with 254nm UV-light, the thymine-containing pyrimidine dimer content (thymine-thymine, plus thymine-cytosine dimers) of the DNA does not increase beyond 7% of the total thymine content (Radany *et al.*, 1981). This steady state reflects a dynamic equilibrium in which the rates of dimer formation (which is pseudo zero order, to a good approximation) and reversal (which is first order in dimer content) are equal (Radany *et al.*, 1981).

This observation was supported by Gordon and Haseltine (1982) who showed not only that at high doses of UV light, dimer formation reached a maximum which was unaffected by further irradiation; but also that the dose at which the maximum level of dimers was reached varied for different types of dimers. The steady-state level for C< >C dimers is reached at a 254nm fluence of $\cong$ 500 Jm^{-2}, while for T< >T dimers, fluences in excess of 2000 Jm^{-2} are required. In addition, it was shown that the absolute level of dimerisation varied at individual dimer sites. The level varied from less than 1% at sites of potential C< >C dimers to as high as 10% for some T< >T sites. Flanking nucleotides in double-stranded DNA also influence the steady-state level of dimer formation. In general, the equilibrium level of dimers is greater for TT sites flanked on both sides by A, than for TT sites flanked on the 5' side by an A and on the 3' side by G. However, this immediate nucleotide flanking effect was not sufficient to account for all the variations observed.

Thus the formation of cyclobutane pyrimidine dimers in DNA is not a random phenomenon as was first believed. Also, pyrimidine dimer contents in a particular sequence of UV-irradiated DNA cannot necessarily be extrapolated to other sequences of DNA or other irradiation conditions. Despite this, the cyclobutane pyrimidine dimer has served well as the classic 'test lesion' for analysis of DNA repair.

1.2.2 PYRIMIDINE - PYRIMIDONE (6-4) PHOTOPRODUCTS

The pyrimidine - pyrimidone (6-4) photoproduct (referred to throughout this study as the (6-4) photoproduct), which is observed in UV-irradiated DNA at TC, CC and TT sequences, is formed when the 5-6 bond of the 5' base initially forms bonds across the exocyclic group at the 4 position of the 3' base. The bond holding the exocyclic group to the 4 carbon then spontaneously breaks, transferring this group to the 5' base and leaving a 6-4 bond (Wang, 1976) - see Figure 1.3.

Lippke *et al.* (1981) found that the TC (6-4) photoproduct was formed preferentially, followed by formation at the CC and occasionally the TT sites. In double-stranded DNA, (6-4) photoproduct formation was not evident at CT sequences (Franklin *et al.*, 1982). Although the cyclobutane pyrimidine dimer is formed in approximately 10-fold greater abundance than the (6-4) photoproduct upon exposure of DNA to low fluences of 254nm radiation (Lippke *et al.*, 1981), the frequency distribution of dimers did not correlate with the frequency of mutations observed in *E. coli* by Brash and Haseltine (1982). At certain sequences, the rate of formation of the (6-4) photoproduct exceeded that of cyclobutane pyrimidine dimers, even at very low fluences in the range 10 - 50 Jm^{-2}.

Chan *et al.* (1986) measured the action spectrum for the formation of (6-4) photoproducts and found it to be indistinguishable from the pyrimidine dimer-formation action spectrum. Below 300nm, both action spectra closely paralleled the DNA absorption spectrum. More cyclobutane pyrimidine dimers were formed by far-UV than (6-4) photoproducts, but the ratio varied according to site. Yamada and Hieda (1992) showed a similarity in wavelength dependence of the formation of the cyclobutane pyrimidine dimers and the (6-4) photoproducts of thymine over the region 150nm to 290nm, with a maximum at 270nm.

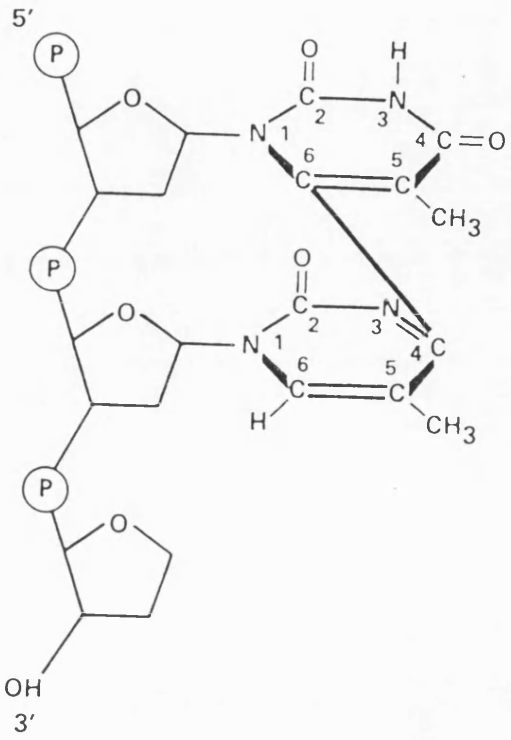

Figure 1.3. A thymine-cytosine (6-4) photoproduct.

It has been proposed (Brash, 1988) that the (6-4) photoproduct is the major UV-mutagenic photoproduct in *E. coli*. The cytotoxic, mutagenic and carcinogenic properties of cyclobutane pyrimidine dimers and (6-4) photoproducts have been extensively reviewed elsewhere (Brash, 1988; Mitchell and Nairn, 1989).

Johns *et al.* (1964) reported that the (6-4) photoproduct, known to them only as TpT4, could be converted quantitatively at 313nm to a new photoproduct, TpT3, and back again at 240nm. Such photochemical behaviour is quite similar to that observed for simpler pyrimidinones which have been shown to be photoisomerised to their Dewar isomers at wavelengths greater than 300nm.

Taylor and Cohrs (1987) showed that the (6-4) photoproduct is photoisomerised to its Dewar isomer with irradiation at $\lambda > 300$nm and discovered the structure of TpT3, the Dewar isomer of the (6-4) photoproduct - see Figure 1.4. They showed that the Dewar isomer was produced by direct photolysis with biologically relevant wavelengths of light ($\lambda > 280$nm), suggesting that (6-4) photoproducts produced during exposure of DNA to sunlight might be converted primarily to their Dewar isomers.

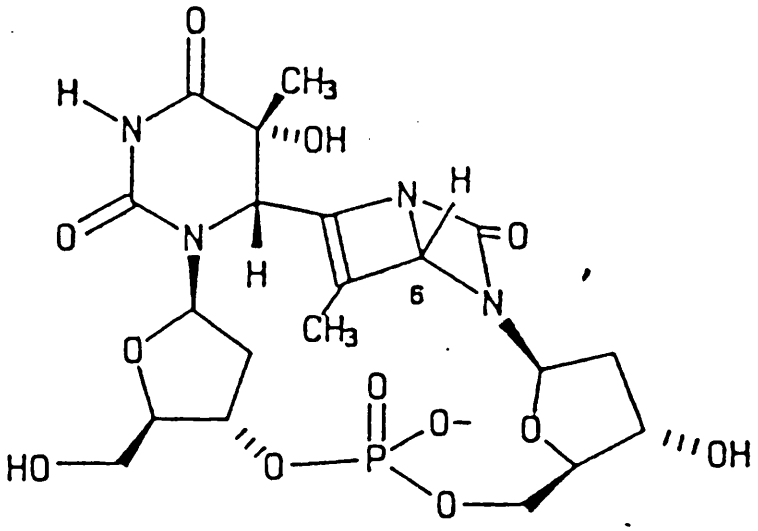

Figure 1.4. Structure of the Dewar isomer of the (6-4) photoproduct.

1.2.3 OTHER UV-INDUCED DNA PHOTOPRODUCTS

A variety of other DNA photoproducts are formed by irradiation with ultraviolet light. These include noncyclobutane-type pyrimidine adducts, thymine glycols, pyrimidine hydrates, DNA-protein cross links (all reviewed in Friedberg, 1985), 8,8-adenine dehydrodimers (Gasparro and Fresco, 1986), a purine photoproduct produced at 265nm (Gallagher and Duker, 1986), and a photoproduct at TA sequences (Bose and Davies, 1984). All the above mentioned UV radiation-induced damage results principally from the direct absorption of photons by bases in DNA. Sensitised photoreactions of DNA also occur (Friedberg, 1985).

1.2.4 UV-INDUCED NON-DNA DAMAGE

Whilst the action spectra for lethality in many species has been shown to closely follow the absorbance of DNA up to 313nm, beyond this point many of the lethal responses are probably due to photon absorption by other chromophores causing either DNA molecular alterations or other effects lethal to the cell. The targets for near-UV killing have been reviewed by Jagger (1985) and include DNA itself, DNA repair systems and membranes.

Tyrrell *et al.* (1973) have demonstrated destruction of the *E. coli* photoreactivating enzyme by 365nm radiation. The observation that near-UV radiation survival curves exhibit large shoulders before dropping off steeply at higher fluences, suggests that damage to DNA repair systems may be an important factor in determining ultraviolet radiation lethality.

Kelland *et al.* (1983) have shown that at wavelengths above 310nm, cell membrane damage was induced in *Escherichia coli* K-12, reaching a peak at 334nm, then gradually decreasing. Thus, cell membrane damage may be a significant contributor to near-UV radiation-induced cell lethality.

This is supported by work by Keyse *et al.* (1983), who showed a marked decrease in the sensitivity of an excision repair deficient xeroderma pigmentosum strain compared to a normal human skin fibroblast strain at wavelengths longer than 313nm. This suggested that the importance of pyrimidine dimers as the lethal lesion decreases with increasing wavelength, showing that different mechanisms of inactivation operate at wavelengths longer than 313nm, other than damage to DNA itself.

1.3 PHOTOREACTIVATION

In this section the basic mechanisms of photoreactivation are discussed. A more specific review of enzymatic photoreactivation in *E. coli* with relation to this study is included in Section 1.5. Enzymatic photoreactivation is not the only type of photorecovery reported in the literature.

1.3.1 ENZYMATIC PHOTOREACTIVATION

Enzymatic photoreactivation is a light-dependent process involving the enzyme catalysed monomerisation of *cis-syn* cyclobutane pyrimidine dimers - see Figure 1.5.

The enzyme, DNA photolyase, binds to the pyrimidine dimers in DNA in a light-independent step, forming a stable enzyme-substrate complex, which absorbs a photon, leading to the splitting of the cyclobutane ring and hence formation of the original monomers - see Figure 1.6.

The action of DNA photolyase is well described by the classic Michaelis-Menten scheme for enzyme catalysis with the important exception that catalysis is light-initiated.

$$\text{PRE} + \text{Pyr}<>\text{Pyr} \leftrightarrow \text{PRE} - \text{Pyr}<>\text{Pyr} \xrightarrow{h_\nu} \text{PRE} + 2\text{Pyr}$$

This light dependence of the catalysis step has made it possible to study the two steps of DNA repair processes, *Binding* and *Catalysis*, individually both *in vivo* and *in vitro*. However, early studies on mechanistic aspects of DNA repair by photolyase were hindered for the lack of sufficient quantities of pure enzymes because the enzyme is present in low concentrations in all organisms possessing it.

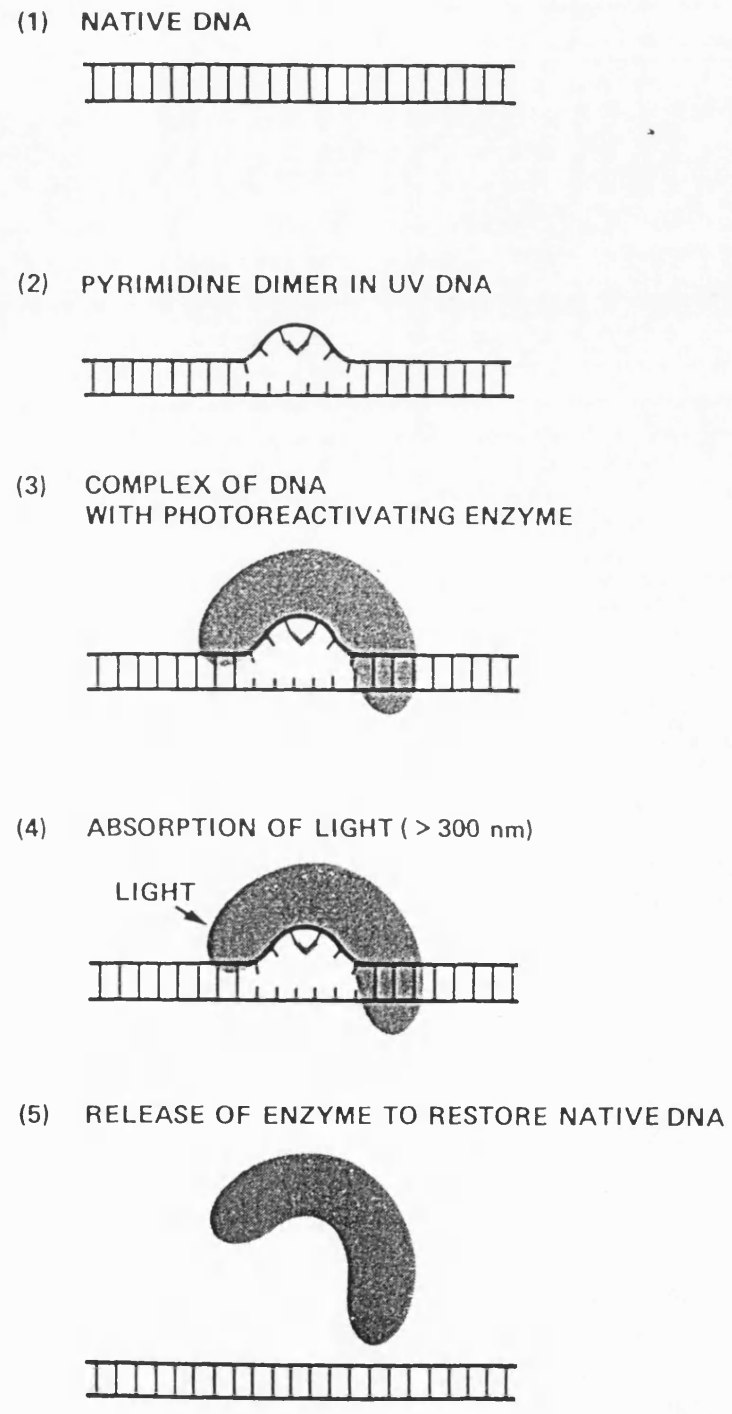

Figure 1.5. Schematic illustration of the photoreactivation of ultraviolet-induced cyclobutane pyrimidine dimers in DNA.

In the last decade, the gene encoding photolyase has been cloned from several organisms and sequenced, and the enzyme overproduced permitting purification of several hundred milligrams of pure photolyase. This was followed by the structural identification of co-factors involved in photoreactivation. Furthermore, recent studies using a combination of site-specific mutagenesis, flash photolysis, and other spectroscopic methods have significantly improved the understanding of the mechanism of DNA repair by photolyases.

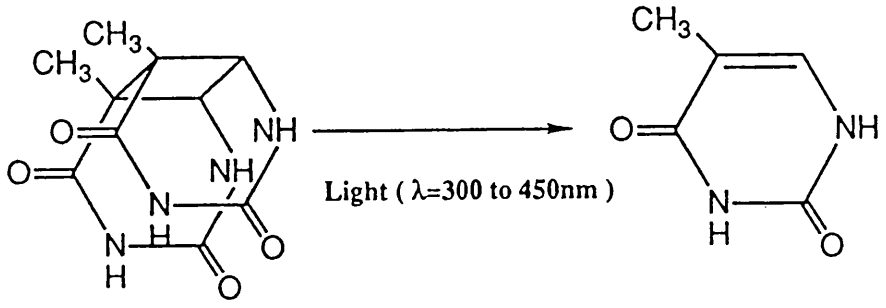

Figure 1.6. Splitting of a *cis-syn* thymine dimer by DNA photolyase.

So far, only a few photolyases have been characterised (Sancar, 1990). All contain two chromophore/co-factors. One is always flavin adenine dinucleotide (FAD) or its radical (FADH•) (Sancar and Sancar, 1984), the other, commonly known as the 'second chromophore', can be either 5,10-methenyltetrahydrofolate (MTHF) (Johnson *et al.*, 1988) or 7,8-didemethyl-8-hydroxy-5-deazariboflavin (8-HDF) (Eker *et al.*, 1990) - see Figure 1.7.

The shape and maximum wavelength of absorption or action spectrum of photolyases in the wavelength region 300nm - 500nm are dominated by the second chromophore (Kim and Sancar, 1993). Accordingly, the enzymes have been classified into two groups : the folate class, which has its action spectrum maximum at 360nm to 390nm, in which the photolyase from *E. coli* falls; and the deazaflavin class, which has its action spectrum maximum at 430nm to 460nm.

Comparison of the amino acid sequences (Sancar, 1990) reveals 30-40% homology in the photolyases of widely divergent species. In particular, the carboxy-terminal 140 amino acids are 50-60% identical among all photolyases, suggesting that this region might be involved in DNA and/or FAD binding, because enzymes from all species contain FAD and appear to bind DNA by the same mechanism (Kim and Sancar, 1993). In contrast, the amino-terminal halves of the enzymes display a much lower level of homology and appear to be conserved within each class of photolyases, suggesting that the amino-terminal halves are more likely to be the second chromophore binding-sites.

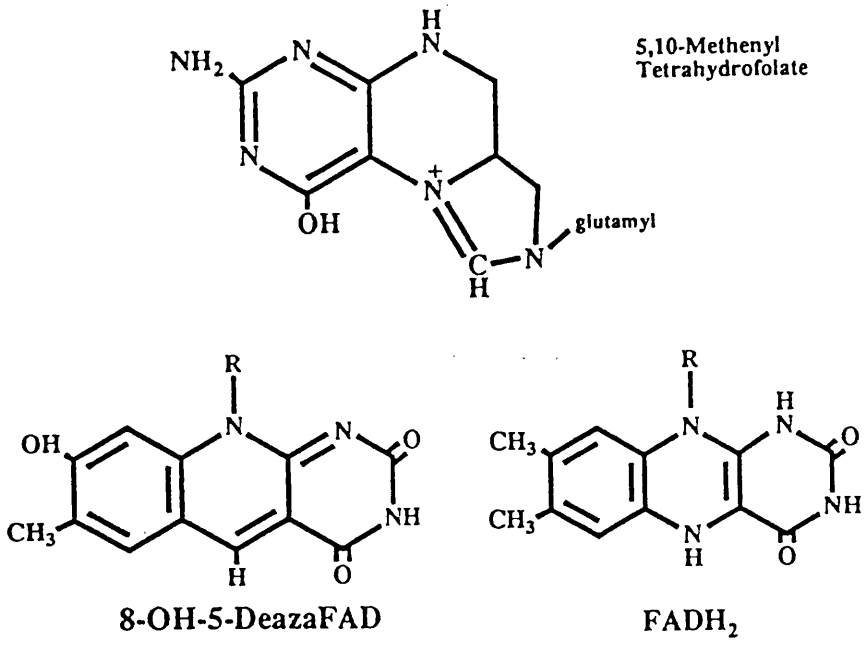

Figure 1.7. The chromophores of DNA photolyases.

In *E. coli*, the flavin chromophore/co-factor was identified by Jorns *et al.* (1984) and the folate chromophore/co-factor by Johnson *et al.* (1988). The mechanism for the splitting of the cyclobutane ring *in vitro* proceeds via the photoreduction of the flavin radical ($FADH^{\bullet}$) to give the fully reduced form ($FADH^{-}$), followed by dimer repair by the photoexcited reduced form (Payne *et al.*, 1987). The folate acts in a secondary capacity as an antenna molecule, absorbing a photon of light and transferring energy to the $FADH^{\bullet}$ at the catalytic centre. $FADH^{-}$ in turn transfers an electron to the pyrimidine dimer to generate a radical ion pair, resulting in dimer splitting. The enzyme-bound folate in *E. coli* photolyase does not decompose or dissociate during multiple turnovers of the reaction, and thus the catalytic folate in photolyase provides the only known example of a catalytic folate among the many known enzymatic reactions that use folate co-factors (Hamm-Alvarez *et al.*, 1990). The roles of the co-factors in photolyases are extensively reviewed by Kim and Sancar (1993).

Photolyases are extremely efficient in recognising pyrimidine dimers over nondimerised pyrimidines (Husain and Sancar, 1987b). In *E. coli*, this high level of discrimination could be very important because of the low number of photolyases per cell, and these should be able to selectively bind to a single pyrimidine dimer in 10^7 nucleotides and repair it immediately, as one dimer left unrepaired could be lethal to the cell. Photolyases are thought to achieve this high level of discrimination by recognising the pyrimidine dimer itself through random diffusion rather than through facilitated binding via unidimensional diffusion along the phosphodiester backbone, originally proposed as a sequential repair model by Davies *et al.* (1970).

The mode of interaction of photolyases with pyrimidine dimers is relatively well defined by chemical and enzymatic footprint experiments using enzymes from *Escherichia coli* (EUBACTERIA), *Methanbacterium thermoautotrophicum* (ARCHAEBACTERIA), and *Saccharomyces cerevisiae* (EUKARYOTA), and a unique 43bp double-stranded substrate containing a single pyrimidine dimer at the centre (Husain *et al.*, 1987; Kiener *et al.*, 1989;

Baer and Sancar, 1989). These studies revealed that photolyases from the three different kingdoms make essentially the same contacts immediately around the pyrimidine dimer, and that the most important contacts on DNA were the phosphodiester bond immediately 5' and the three phosphodiester bonds immediately 3' to the dimer on the damaged strand, and to a lesser extent, the phosphate opposite the dimer on the complementary strand. This suggested that a substrate of the structure pT< >TpNpNp would be required and sufficient for high affinity binding by photolyase. Of the four phosphates that appeared to be contacted by the chemical footprinting, only one or two are thought to be bound through salt bridges, consistent with the findings that the enzyme-DNA complex formation is relatively insensitive to the ionic strength of the reaction (Sancar *et al.*, 1987). The other phosphates are presumed to make hydrogen bonds. As mentioned in Section 1.2.1, pyrimidine dimers are known to induce a kink or bending in DNA and local disruption of hydrogen bonds in the vicinity of the dimer. The fact that this localised region in DNA corresponds to the common contacts, pT< >TpNpNp, made by photolyases from three different kingdoms, suggests that the configuration of the phosphodiester backbone, as well as the cyclobutane ring of the dimer, are the important structural features in damaged DNA for rapid recognition and tight binding by photolyase. A study investigating the effect of sequence on the binding and repair of pyrimidine dimers by photolyase has shown that changes in the sequence surrounding a pyrimidine dimer has very little effect on binding by *E. coli* DNA photolyase (Svoboda *et al.*, 1993).

The thermodynamic and kinetic properties of photolyase-DNA interactions are well understood. Similarly, the structures of the chromophores, their roles in photoreactivation, and the photochemical and the photophysical processes involving, and electron transfer to effect, photosplitting of the cyclobutane ring of pyrimidine dimers, have been elucidated. The remaining significant task, until recently, was the elucidation of the three-dimensional structure of the enzyme and enzyme-substrate complex. Park *et al.* (1993) have recently

reported the crystallisation and the preliminary crystallographic analysis of *Escherichia coli* DNA photolyase. Rapid developments in this area are now to be expected.

(6-4) photoproducts are not restored to normal by the *E. coli* photoreactivating enzyme *in vivo* and *in vitro* (Brash *et al.*, 1985; Brash and Haseltine, 1985). Thus cyclobutane pyrimidine dimers and (6-4) photoproducts can be distinguished biologically, which is a useful experimental technique.

1.3.2 INDIRECT PHOTOREACTIVATION

This phenomenon became apparent when photoreactivation using near-UV light was observed with 254nm UV-irradiated *E. coli* B *phr*, a strain lacking photoreactivating enzyme. The effect did not occur with 405nm photoreactivating light and was not due to the splitting of the thymine dimers (Jagger *et al.*, 1969). In contrast to enzymatic photoreactivation, these workers suggested that this 'indirect' photoreactivation resulted from enhancement of dark repair processes. This was subsequently proved by Ramabhadran and Jagger (1976) who demonstrated that near-UV irradiation induced a growth delay which facilitated the excision repair process. The mechanism of near-UV radiation-induced growth delay has been reviewed by Jagger (1985). Briefly, near-UV radiation induces a photoadduct between 4-thiouridine in the 8-position and a cytidine in the 13-position of certain rare forms of tRNA. This lowers the rate at which the tRNA accepts amino acids, which in turn decreases the rate of protein synthesis. This presence of uncharged tRNAs in the cell leads to an increase in the levels of guanosine tetraphosphate and guanosine pentaphosphate and a decrease in the rate of stable RNA accumulation with consequent growth delay.

This phenomenon also occurs if the cells are exposed to the near-UV photoreactivating light before far-UV irradiation, and in this case is termed *Photoprotection.*

1.3.3 SENSITISED PHOTOREVERSAL

Sensitised photoreversal is a non-enzyme-dependent reaction that splits pyrimidine dimers in DNA. This process has been observed with tryptophan and tryptophan-containing oligopeptides, such as lys-trp-lys, as well as with a protein coded by gene 32 of phage T4, which is particularly rich in tryptophan (Hélène and Charlier, 1977).

The mechanism is thought to involve an electron transfer from the excited indole ring of tryptophan to the dimer, possibly mediated by base-stacking interactions of the tryptophanyl residue with the pyrimidine dimer in DNA. This type of photoreactivation is not observed with wavelengths of photoreactivating light greater than 300nm (Sutherland and Griffin, 1980).

Tryptophan also plays a role in the photoreduction of $FADH^{\bullet}$ at the active site of *E. coli* DNA photolyase (Li *et al.*, 1991). All 15 tryptophan residues in *E. coli* DNA photolyase were replaced with phenylalanine, individually, by site-directed mutagenesis. It was found that the W306F mutation abolished photoreduction of $FADH^{\bullet}$ without affecting the substrate binding of the enzyme. Unpublished work referred to by Kim and Sancar (1993) claims unambiguous evidence that W306 is indeed involved in the reduction of the flavin radical.

It has been shown that the wavelengths effective in photoreactivation extend into the far-UV range where, in addition to the two co-factors, the aromatic residues of the enzyme absorb significantly (Payne and Sancar, 1990; Kim *et al.*, 1992). Photolyase is active only when the flavin is in the fully reduced form (Enz - $FADH^{-}$). Using the W306F mutant enzyme to evaluate the catalytic role of tryptophan(s) in *E. coli* DNA photolyase, Kim *et al.* (1992) showed that photolysis of T< >T with the mutant enzyme occurred at 280nm, but not at 366nm. It was shown that the repair was caused by a single tryptophan residue, identified as W277 in *E. coli* DNA photolyase.

As well as direct repair of pyrimidine dimers, W277 in *E. coli* DNA photolyase is also involved in specific binding to the dimers (Li and Sancar, 1990), suggesting that W277 is in the DNA binding site of the photolyase.

1.3.4 DIRECT PHOTOREVERSAL

As has been discussed already in Section 1.2.1, irradiation of DNA containing pyrimidine dimers at wavelengths between 200nm and 300nm results in the direct reversal of some fraction of the dimers until a new equilibrium between monomerisation and dimerisation is attained (Setlow, 1968). This phenomenon is referred to as *Direct Photoreversal*, but is not believed to be a biologically important process.

1.3.5 TYPE III PHOTOREACTIVATION

Jagger *et al.* (1970) defined three distinct molecular phenomena that result in photoreactivation. One is enzymatic photoreactivation, which was termed *Type I Photoreactivation.* The second phenomenon is indirect photoreactivation, termed *Type II Photoreactivation*, while the third phenomenon, termed *Type III Photoreactivation*, was first described in *Streptomyces griseus* and is characterised by a λ_{max} of 313nm with a narrow wavelength range (300nm to 360nm) and the absence of dose-rate and temperature effects. This suggested a direct photochemical reaction without the mediation of an enzyme. It has since been shown that 313nm light photoreverses (not to the original bases) mostly (6-4) photoproducts and, to a much lesser extent, pyrimidine dimers (Ikenaga *et al.*, 1971). Taylor and Cohrs (1987) demonstrated that the (6-4) photoproduct is photoisomerised to its Dewar isomer with irradiation at $\lambda > 300$nm.

The terminology of Type I, Type II and Type III Photoreactivation is used widely in the literature.

The statement that Type III Photoreactivation is characterised by an absence of dose-rate and temperature effects is quoted regularly in the literature (*e.g.* Husain *et al.*, 1988). Reference to the original work by Jagger *et al.* (1970) shows that they found the dose-rate dependence of photoreactivation in *Streptomyces griseus* was strong at 436nm, moderate at 366nm and only slight at 313nm over a range of fluence-rates of 10-1000 erg $mm^{-2}sec^{-1}$ (1-100 Wm^{-2}); and that temperature dependence was considerable at 436nm and only slight at 313nm over a range of temperatures between 2°C and 37°C. Therefore, the statement that Type III Photoreactivation is characterised by an absence of dose-rate and temperature effects is not literally true, but a good approximation.

1.4 OTHER DNA REPAIR PROCESSES

The cellular responses to DNA damage can be divided into three categories :-

1) Reversal of the damage.
2) Excision of the damage.
3) Tolerance of the damage.

The first two responses involve recognition and repair of the damage prior to replication, while the third response facilitates tolerance of persisting damage during and after replication.

The nature of this study concentrates solely on the reversal of UV-induced damage by photoreactivation repair processes. A summary of the other two responses is included for completeness, as it is important to remember that in wild-type strains, these responses work side-by-side.

1.4.1 EXCISION REPAIR

The forms of DNA damage that can be repaired by direct reversal are apparently limited in number. An important DNA repair mechanism observed in nature is one in which damaged or inappropriate bases are excised from the genome and replaced by the normal nucleotide sequence and chemistry. This cellular response to DNA damage is appropriately referred to as *Excision Repair*. For a comprehensive review on excision repair in general, see Friedberg (1985).

One of these repair processes is the nucleotide excision repair pathway. This system deals with a strikingly diverse array of structurally unrelated lesions, including various UV-induced photoproducts, such as cyclobutane pyrimidine dimers and (6-4) photoproducts.

The nucleotide excision repair pathway consists of five steps : damage recognition, incision of the damaged strand on both sides of the lesion and at some distance from it, excision of the lesion-containing oligonucleotide, synthesis of new DNA using the undamaged strand as a template, and ligation. The reaction is, in principle, error-free.

The key proteins involved in the nucleotide excision repair pathway are Uvr A-D (for a review, see Hoeijmakers, 1993; Sancar and Tang, 1993). The nucleotide excision repair process is thought to start when two molecules of Uvr A dimerise in the presence of ATP and complex with one molecule of Uvr B (Lin and Sancar, 1992). The heterotrimer binds to DNA; its weak 5'-3' DNA helicase activity may then allow it to translocate along one of the strands of the helix, scanning it for distorting lesions (Grossman and Yeung, 1990). If such a lesion is encountered, translocation stops and Uvr B is hooked onto the DNA, inducing a specific DNA conformation that includes a kink and a locally denatured region. The Uvr A molecules dissociate, allowing Uvr C to bind (Lin and Sancar, 1992). The Uvr BC complex then makes two incisions in the damaged strand. One, located eight phosphodiester bonds 5' of the lesion, is probably catalysed by Uvr C. The other incision, five or four bonds 3' of the lesion, is presumably made by Uvr B (Sancar and Rupp, 1983). The concerted action of Uvr D (which is also a helicase) and DNA polymerase I accomplishes the release of the 12-13-mer containing the damaged site, turnover of the bound Uvr B and Uvr C, and synthesis of an undamaged copy of the sequence that has been removed (Lin and Sancar, 1992). Finally, DNA ligase seals the nicks in the repaired strand. See Figure 1.8 for a diagrammatic representation of this repair process.

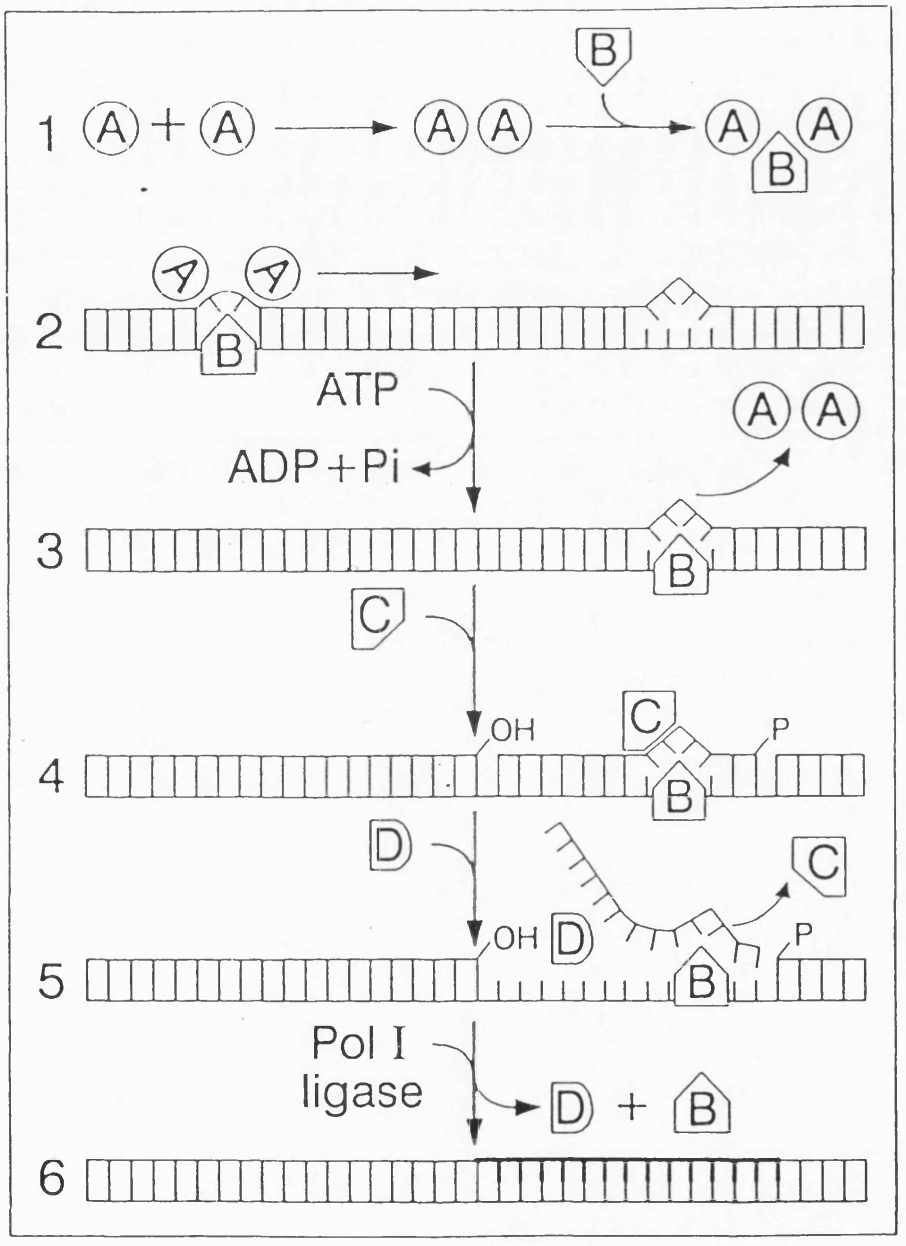

Figure 1.8. Diagrammatic representation of the nucleotide excision repair pathway in *Escherichia coli*.

A, B, C, and D, molecules of Uvr A, B, C, and D respectively.

Pol I, DNA polymerase I; ligase, DNA ligase;

This system can not only detect an impressive spectrum of damaged structures, ranging from thymine glycols to bulky chemical adducts and inter- and intra-strand crosslinks; it can also differentiate between two strands of a gene and assign a higher priority to eliminating DNA damage in the transcribed strand than in the non-transcribed (coding) strand. In *E. coli* it has been shown that the *mfd* (mutation frequency decline) gene is necessary for strand-specific repair (Selby *et al.*, 1991). The Mfd protein appears to target the transcribed strand for repair by recognising a stalled RNA polymerase molecule, blocked by a lesion in the transcribed strand, and actively recruiting the repair enzyme to the transcription blocking lesion as it dissociates the stalled RNA polymerase (Selby and Sancar, 1993). The Mfd protein has previously been termed a transcription-repair coupling factor (TRCF).

The *E. coli* photoreactivating enzyme also interacts with the nucleotide excision repair pathway. As well as monomerising cyclobutane pyrimidine dimers in its own right, during light-repair; in addition it facilitates the repair of these lesions by the nucleotide excision repair pathway during dark-repair (Yamamoto *et al.*, 1983a; Yamamoto *et al.*, 1983b; Hays *et al.*, 1985; Sancar and Smith, 1989). Therefore, DNA photolyase is not only a DNA repair enzyme in its own right but also an auxiliary protein in the nucleotide excision repair pathway.

Another excision repair enzyme of interest regarding this study, is the T4 endonuclease V, which is involved in the direct excision repair of cyclobutane pyrimidine dimers. In *E. coli* cells infected with bacteriophage T4, T4 endonuclease V, encoded by the *denV* gene of the bacteriophage, is responsible for the first step in the excision repair pathway of UV-damaged DNA. The T4 endonuclease V catalyses two distinct reaction steps (Macmillan *et al.*, 1981; Dodson and Lloyd, 1989); the incision of the N-glycosyl bond at the 5'-side of the pyrimidine dimer and the cleavage of the apyrimidinic phosphodiester bond. It has been suggested that T4 endonuclease V can bind non-specifically to DNA via electrostatic

interactions and can thus scan along the DNA duplex before binding to a pyrimidine dimer.

Interestingly, this enzymatic activity had never been found in any other organisms, either prokaryotes or eukaryotes, with the exception of *Micrococcus luteus* (Friedberg, 1985; Sancar and Sancar, 1988). However, Hamiliton *et al.* (1992) have reported that an enzyme functionally similar to the above activity exists in *Saccharomyces cerevisiae.* Whether there is T4 endonuclease V-like activity in *E. coli* has yet to be shown.

Both cyclobutane pyrimidine dimers and (6-4) photoproducts are excised from UV-induced damaged DNA by the *E. coli uvr*ABC repair system (Franklin and Haseltine, 1984).

1.4.2 DNA DAMAGE TOLERANCE AND POST-REPLICATION REPAIR

The cellular responses involved in DNA damage tolerance have important biological consequences. With respect to individual dividing cells, these responses provide potential mechanisms for survival in the face of replicative arrest, possibly allowing for DNA repair to occur once template DNA containing base damage has been replicated. Also some damage tolerance mechanisms are associated with a significant increase in mutation frequency, thus providing the potential for genetic diversification within a population. For a comprehensive review on DNA damage tolerance in general, see Friedberg (1985).

There are at least two mechanisms whereby cells can resume DNA synthesis on templates containing replicative blocks and in so doing, enhance their potential for survival. One is by reinitiating DNA synthesis some distance downstream from the blocks (essentially circumnavigating them), thereby creating gaps of discontinuities in the daughter DNA strands, which subsequently become filled in by some mechanism. The second is by

continuing DNA synthesis past the template lesion in a continuous mode after an initial arrest.

One of the best understood processes is termed *Post-Replication Repair*. Post-replication repair is best explained with the aid of a diagram - see Figure 1.9. Briefly, post-replication repair deals with, for example, a pyrimidine dimer that interferes with replication, during which the parental DNA strands unwind at the replication fork and two daughter strands are synthesised (1). The pyrimidine dimer prevents base pairing along a stretch of one parental strand, producing a post-replication gap opposite a stretch of single-strand DNA (2). RecA protein, the product of the *rec*A gene, binds to the single-strand region (3) and aligns it with a homologous region of the sister duplex. The interaction of RecA with single-stranded DNA is stabilised by the *ssb* gene product, DNA single-stranded binding protein. When homologous pairing is achieved, an enzyme nicks the duplex (4). RecA switches the free-end of the duplexes parental strand into the gap, producing a crossed-strand exchange (5). The upper heteroduplex can now be repaired by DNA polymerase. With the correct sequence in place opposite the pyrimidine dimer, RecA is released (6). Finally, two cuts are made by an enzyme at the site of the crossed-strand exchange (7). The pyrimidine dimer is still present in one of the daughter strands (8). For a review, see Howard-Flanders (1981).

Based on cell survival studies, two independent pathways for post-replication repair in *E. coli* have been proposed. One is dependent on the *rec*F gene (Rothman *et al.*, 1975) and the other is dependent on the *rec*B, *uvr*D and *lex*A genes (Wang and Smith, 1981). The *rec*F-dependent pathway promotes the repair of daughter-strand gaps, whereas the *rec*B-dependent pathway repairs DNA double-strand breaks arising from unrepaired daughter-strand gaps (Wang and Smith, 1983; Wang and Smith, 1986).

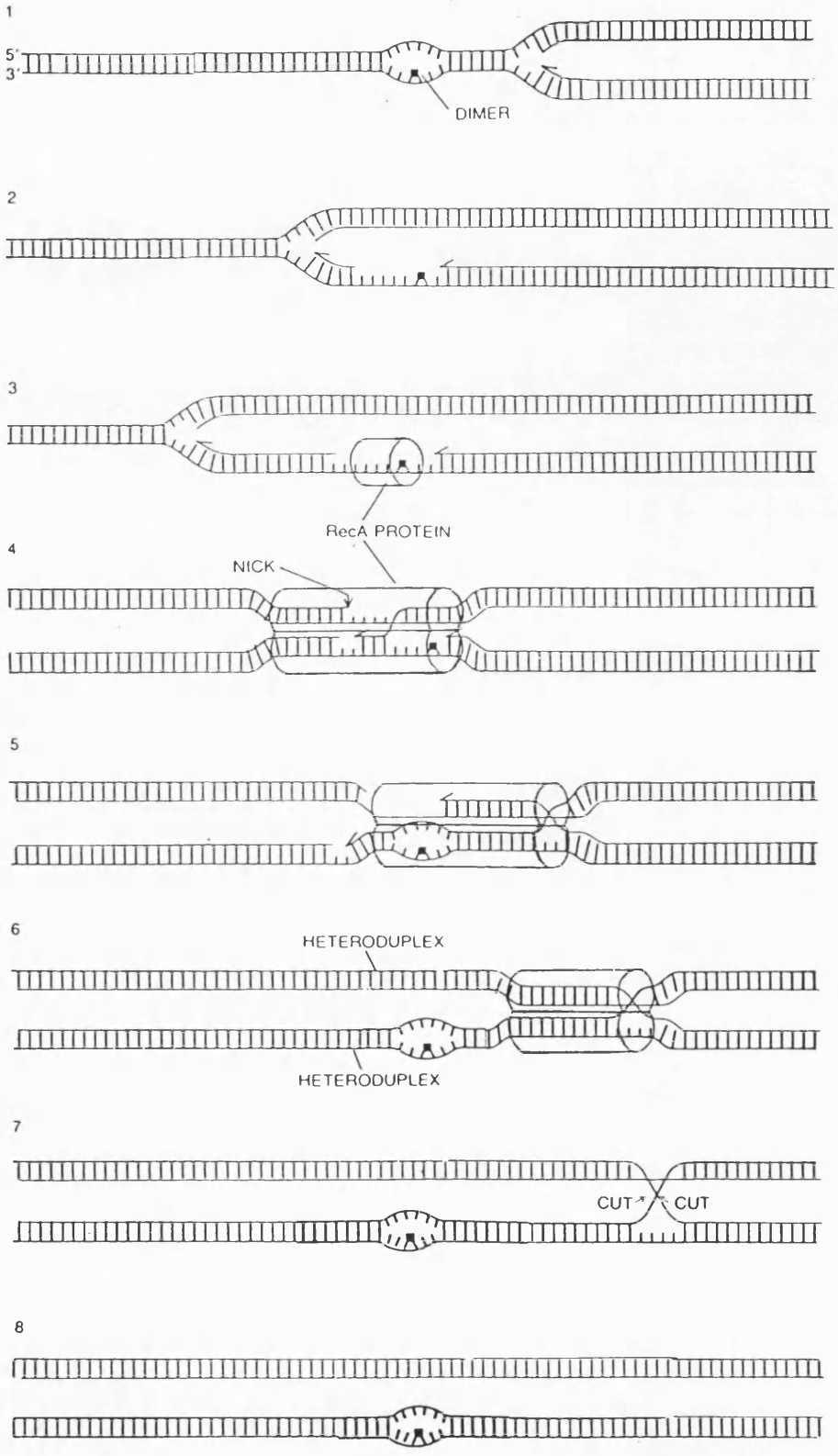

Figure 1.9. Diagrammatic representation of the post-replication repair pathway in *Escherichia coli*.

1.4.3 THE SOS REGULATORY SYSTEM OF *Escherichia coli.*

E. coli exhibits a complex and diverse response to many conditions which damage DNA or inhibit DNA replication. The SOS regulatory network of *E. coli* is triggered by treatments that damage DNA or block the normal replication of the chromosome. The origin of the term 'SOS' to describe this phenomenon was a conference on mutagenesis held in Rochester, New York, in 1973. Miroslav Radman coined the phrase SOS primarily to emphasise the dramatic nature of this cellular response to a distress signal, i.e., DNA damage (Friedberg, 1985). It is often misinterpreted to imply a last-ditch attempt by the cell to survive the lethal effects of DNA damage after other cellular responses have failed. Biochemical and genetic data have demonstrated that the SOS response is under the control of the *rec*A and *lex*A genes (Little and Mount, 1982; Walker, 1984). The RecA protein is required for the induction of the SOS genes, and also for the process of homologus recombination (Witkin, 1976). The LexA protein is the common repressor of at least 18 genes, including *rec*A and *lex*A. The RecA protein is reversibly converted to a protease by an inducing signal after DNA damage. It is thought that at least part of this activating signal *in vivo* is the single-stranded DNA that is generated after inhibition of DNA replication (Walker, 1984), although the exact nature of the signal is not yet known. Once activated, the RecA protease can cleave or promote the self-cleavage of the LexA repressor, resulting in the expression of the SOS genes (Little *et al.*, 1980; Little, 1984). Under these conditions, several cellular activities such as enhanced DNA repair ability, enhanced mutagenesis, and inhibition of cell division (filamentation) among others are displayed. SOS induction also leads to increases in both RecA and LexA protein synthesis. When DNA lesions are repaired, the inducing signal is no longer produced, and RecA protein becomes inactive. Thus, balance between LexA and the activated form of RecA protein is destroyed, LexA repressor accumulates, and the SOS genes are newly

repressed. In cells containing temperate phages such as λ and ϕ80, activated RecA protein also promotes the cleavage of the phage repressors leading to prophage induction.

Fernandez de Henestra *et al.* (1991) introduced a broad host range plasmid containing an operon fusion between the *rec*A and *lac*Z genes of *E. coli* into various aerobic and facultative gram-negative bacteria to study the expression of the *rec*A gene after DNA damage. All the bacteria tested, except *Xanthomonas campestris* and those of the genus *Rhodobacter*, were able to repress and induce the *rec*A gene of *E. coli* in the absence and in the presence of DNA damage respectively. This indicates that the SOS system is present in bacterial species of several families and that the LexA-binding site must be highly conserved in them. This supported work by Sedgwick and Goodwin (1985) who introduced a plasmid carrying the *E. coli lex*A gene into six *Enterobacteria* species. The results suggested that the SOS regulatory mechanism is widespread in *Enterobacteria* and functionally conserved.

There is evidence to suggest that the *cis-syn* cyclobutane pyrimidine dimer is the significant SOS-inducing lesion in UV-induced DNA damage in *E. coli*. Removal of the pyrimidine dimers by photoreactivation blocks induction of the SOS response (Brash and Haseltine, 1985).

1.5 OCCURRENCE OF PHOTOREACTIVATION ACTIVITY IN *Escherichia coli*

The subject of this study centres on the genetic control of photoreactivation in *Escherichia coli*. Therefore this section concentrates on the occurrence of photoreactivation and the photoreactivating enzymes in *Escherichia coli*.

1.5.1 HISTORICAL BACKGROUND

Although Albert Kelner is generally credited with the discovery of photoreactivation in 1949, a photoreactivation type of process was reported in 1933 by Hausser and von Oehmcke (see Jagger, 1960). These workers observed that UV radiation-induced darkening of banana skin could be prevented by post-UV irradiation exposure to near UV light (366nm) and visible light.

The systematic study of enzymatic photoreactivation did not begin until the late 1940's with the nearly simultaneous publications by Kelner and Renato Dulbecco. Whilst investigating the effect of post-irradiation temperature on the UV-survival of certain strains of *Streptomyces griseus*, Kelner (1949) reported that exposure of UV-irradiated suspensions to visible light resulted in an increase in survival rate of 100,000 to 400,000-fold, whereas controls kept in the dark did not. Dulbecco (1949) reported a similar observation with T-bacteriophages in *E. coli* and coined the term *Photoreactivation.*

It was not until the late 1950's, however, that studies with extracts of *E. coli* and baker's yeast demonstrated that photoreactivation is an enzyme-mediated phenomenon. Rupert *et al.* (1958) used crude cell extracts and the *Haemophilus influenzae* transformation assay to measure photoreactivating enzyme activity *in vitro*. This suggested that the photorepairable lesion was situated in the DNA and that the agent was enzymatic in nature.

At this point, the nature of the substrate was not known. Beukers and Berends (1960) and Wang (1960) found that UV-irradiation of a frozen thymine solution yielded a dimeric thymine photoproduct which was identical to the main photoproduct in UV-irradiated DNA. Subsequent irradiation of the thawed solution led to the reappearance of the characteristic thymine absorption spectrum. Beukers and Berends (1960) suggested that this reversible alteration of DNA by UV-irradiation might be related to biological photoreactivation. However, Wang (1960) showed that irradiation of thymine dimers in solution with 370nm photoreactivating light did not lead to the reappearance of thymine monomers. Wulff and Rupert (1962) were able to show loss of thymine dimers from ^{3}H-thymine labelled DNA by the combined action of the cell-free extract of baker's yeast and photoreactivating light. This suggested that enzymatic photoreactivation involved the splitting of pyrimidine dimers into their constituent monomers, and was proven by the work of Setlow and Setlow (1962).

Photoreactivating enzyme, or DNA photolyase, has been detected in many organisms. Considering the role of UV irradiation as a source of genetic damage in biological evolution, it is not surprising that organisms have developed specific methods for the repair of pyrimidine dimers. Studies on the enzymes found in different organisms have revealed a remarkable functional and structural conservation (reviewed by Sancar, 1990).

1.5.2 THE CONTROVERSY BETWEEN *phr*A AND *phr*B

Although *E. coli* was the first organism in which DNA photolyase activity was demonstrated *in vitro* (Rupert *et al.*, 1958), the combination of high cellular nuclease activities and the low copy number of the enzyme per cell made purification of the enzyme difficult. Thus much of the early characterisation was of the *in vivo* process using the flash photolysis method (reviewed by Harm *et al.*, 1971).

Sutherland *et al.* (1972) studied photoenzymatic repair in mutants with deletions extending from *chl*A to either *att*λ or through to *gal*, and concluded that the *phr* locus was between *gal* and *att*λ - see Figure 1.10. An *E. coli* strain lysogenic for a λ specialised transducing phage carrying the *gal-att*λ region was constructed, and a 2000-fold increase in photoreactivating enzyme activity was obtained upon induction. An enzyme with apparent photoreactivating enzyme activity was isolated and characterised (Sutherland *et al.*, 1973).

However, Youngs and Smith (1978) and Sancar and Rupert (1978) presented data which conclusively placed the *phr* gene counter-clockwise of *gal* between *kdp* and *glt*A, contradicting the findings of Sutherland *et al.* (1972).

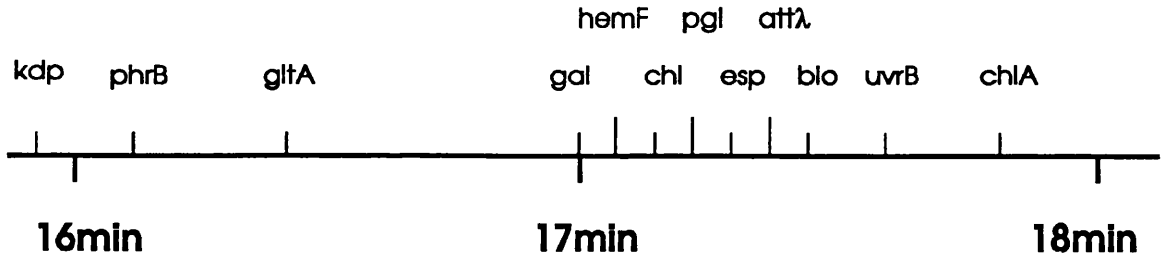

Figure 1.10. The genetic map of the *E. coli* chromosome between 16 and 18 mins, showing the genes relevant to this section.

Sutherland and Hausrath (1979) investigated photoreactivation in deletion mutants lacking the *gal-attλ* region and found them to be photoreactivable, although at a reduced rate, in contrast to the findings of Sutherland *et al.* (1972). They proposed that the gene in the *gal-attλ* region at 17min should be termed *phr*A, and the gene mapped by Youngs and Smith (1978) and Sancar and Rupert (1978) at 15.9min should be termed *phr*B. The recalibrated *E. coli* linkage map (Bachmann, 1983) placed *phr*A at 17.3min and *phr*B at 16.2min.

Sancar *et al.* (1983) have cloned and amplified the *phr*B gene product, and have isolated, purified and sequenced the photolyase gene and protein (Sancar *et al.*, 1984a; Sancar *et al.*, 1984b). Husain and Sancar (1987a) investigated the genetics of photoreactivation in *E. coli* in detail. They found that deletion of the *gal-attλ* region increased the sensitivity of *E. coli* to near-UV radiation, but had no effect on the rate or extent of photoreactivation. However, point mutations in, or deletion of, the *phr*B gene drastically reduced both the rate and extent of photoreactivation but did not totally eliminate it. They concluded that extensive illumination of cells deleted in the *phr*B gene results in an increase in cell survival, suggesting that another mechanism exists in *E. coli* to photoreverse (inefficiently) the effect of far-UV irradiation by subsequent exposure to near-UV or visible light. Further studies (Husain *et al.*, 1988) showed that the residual photoreactivation in *phr*B mutants is not associated with reversal of pyrimidine dimers. It was suggested the residual photoreactivation was attributable to the direct photoconversion of the (6-4) photoproducts to their Dewar isomers by Type III photoreactivation.

Thus Husain and Sancar (1987a) proposed that the gene in the *gal-attλ* region termed *phr*A should not be described as such, since their findings showed deletion of this gene had no effect on the rate or the extent of photoreactivation; and that the gene product should not be called a photolyase because the protein did not play any physiologically significant role in photoreactivation *in vivo*, according to their results. With this, *phr*A was effectively dismissed from the literature.

1.5.3 THE EVIDENCE FOR phrA

Sutherland *et al.* (1973) purified a DNA photoreactivating enzyme from induced cells of an *E. coli* strain having a lysogenic λ-bacteriophage carrying the *gal-att*λ chromosomal region (Sutherland *et al.*, 1972). The purified enzyme tended to form aggregates, but Snapka and Sutherland (1980) developed a purification procedure to minimise aggregation. The purified enzyme had a molecular weight of approximately 40kDa and was associated with RNA (10 - 15 nucleotides per enzyme molecule).

Sutherland *et al.* (1986) characterised the substrate range of the 40kDa PRE isolated by Snapka and Sutherland (1980). The enzyme was at least as active on *cis-syn* cyclobutane pyrimidine dimers in supercoiled DNA as in linear DNA, but inactive on dimers in RNA. Both the phosphodiester bond internal to the deoxyriboses of the pyrimidines of the dimer and the N-glycosyl bond joining the pyrimidine to deoxyribose must be intact for enzyme action. The enzyme was shown to have no activity towards (6-4) photoproducts in DNA. Sutherland *et al.* (1986) also studied extracts from wild-type *E. coli* and found they contained PRE activity corresponding to a 40kDa species and a 50kDa species, which they suggested were the gene products of *phr*A and *phr*B.

Sutherland and Hausrath (1979) investigated the photoreactivation kinetics of wild-type and Δ(*gal-att*λ) strains and reported that whereas the Δ(*gal-att*λ) strains could indeed be photoreactivated, the rate of photoreactivation was much slower in strains with this deletion. Husain and Sancar (1987a) attempted to reproduce these results, but were unable to do so. They found, however, that deletions of the *gal-att*λ region increased the sensitivity of the strains to near-UV light killing. They suggested that this may be due to the accumulation of coproporphyrin in the cell, due to deletion of the *hem*F gene which is located in the *gal-att*λ interval (Bachmann, 1983), which in turn photosensitises to near-UV killing.

Hejmadi and Verma (1987) were also able to isolate a 40kDa PRE using the method developed by Snapka and Sutherland (1980), and showed that in the absence of the RNA cofactor, the 40kDa PRE binds with DNA regardless of the presence of pyrimidine dimers. This suggested that the RNA cofactor is somehow involved in the site-selection for the 40kDa PRE on DNA containing pyrimidine dimers. Verma *et al.* (1990) showed that binding of the 40kDa PRE with UV-irradiated DNA protects the RNA cofactor against subsequent digestion with RNase, and suggested a qualitative model for the structure of the photolyase:UV-irradiated DNA complex, based on the stacking interactions between a base of the RNA cofactor and the destacked purines on the complementary strand opposite to the pyrimidine dimer.

Smith *et al.* (1987) studied photoreactivation after 254nm UV irradiation in a dark-repair-deficient *phr*B mutant (DY326) and in a strain deleted at the proposed *phr*A locus (AS44). They showed apparent enzymatic repair in the *phr*B mutant, which was abolished when the mutation was transduced into the *phr*A mutant. They also showed an apparent decrease in the production of active PRE molecules in the *phr*A mutant compared to a non-isogenic *phr* $^+$ strain (AB2480), and that photoreactivation proceeds at a rate 30% of that of the *phr* $^+$ strain. They concluded that the *phr*B gene is the major structural gene for PRE molecules, but that a gene in the region of the putative *phr*A locus also had an effect on photoenzymatic repair in *E. coli*, and indeed could code for a second photolyase molecule.

Smith and Moss (1987) studied the efficiency of photoreactivation with respect to the wavelength of photoreactivating light in the same dark-repair-deficient *phr* $^+$, *phr*A and *phr*B mutants, and showed a structureless peak over the range 360nm to 400nm for all three strains. This data suggested that the light dependent repair observed in the *phr*B mutant was similar to enzymatic photoreactivation and may be mediated by an unknown photoactive protein.

Smith and Moss (1988) cloned a SphI restriction fragment from λ*gal* transducing 'phage DNA specifically carrying the gal-attλ region and demonstrated the appearance of a photoreactivable response in a photoreactivation-deficient *phr*A *phr*B mutant (AS46), and an increase in the rate of photoreactivation when the plasmid carrying the restriction fragment (pAS01) was transformed into the *phr*A mutant (AS44). When the plasmid pAS01 was transformed into the *phr*B mutant (DY326) no increase in the rate or extent of photoreactivation was observed. They concluded that although a gene present on the plasmid fulfilled the role of the *phr*A gene, and confirmed the hypothesis that a gene in the *gal-attλ* region does affect the rate of photoenzymatic repair in *E. coli*; the evidence to date did not permit the conclusion that this gene codes for a protein having photolyase-like activity. A similar conclusion was drawn by Smith (1987).

Thus, the evidence for *phr*A is rather confusing. Some of the more speculative claims made by Sutherland and Hausrath (1979) were that *phr*A$^-$ *phr*B$^+$ mutants photoreactivate ultraviolet-induced killing at a rate 20% of normal and they contained approximately 20% of the normal photoreactivating enzyme level. Statements such as these have gone a long way to discredit *phr*A research. It would be easy to dismiss the work of B.M. Sutherland and co-workers as A. Sancar and co-workers have done in both *E. coli* (Husain and Sancar, 1987a) and human cells (Li *et al.*, 1993). However, as far as *E. coli* is concerned, the work by Hejmadi and Verma (1987) and Verma *et al.* (1990) using the same photoreactivating enzyme as purified by Snapka and Sutherland (1980) must not be overlooked.

It is hoped that the work performed during this study will help to clarify the role of *phr*A in photoreactivation in *Escherichia coli.*

1.5.4 THE PROSPECTIVE ROLE OF THE *phr*A GENE

Following the reports by Husain and Sancar (1987a) and Husain *et al.* (1988), which effectively dismissed *phr*A from a role in photorepair in *E. coli*, the role of *phr*A with respect to the results obtained in our laboratory needs to be reviewed.

The reports by the above authors could be correct as stated, and the *phr*A gene does not play any significant role in photoreactivation *in vivo*. However, the report by Husain *et al.* (1988) used a strain deleted in both *phr*B and *phr*A as the *phr*$^-$ mutant. Therefore, even if the *phr*A gene product is not involved in the repair of pyrimidine dimers, that statement can not be concluded from this work. Interestingly, it is not mentioned whether the *phr*A$^+$ *phr*B$^-$ mutant used by Husain and Sancar (1987a) was assayed for removal of pyrimidine dimers. It would seem logical to have assayed this strain to finally confirm that *phr*A is not involved with the repair of pyrimidine dimers.

Another explanation could be that the photoreactivation conditions used by Husain and Sancar (1987a) were not conducive to activate the *phr*A gene product. The fluence-rate used by Sutherland and Hausrath (1979) was quoted as 192.5 Wm^{-2}, however Husain and Sancar (1987a) found this fluence-rate to be quite lethal over a 20 minute period of photoreactivation, and used a fluence-rate of 5 Wm^{-2}. It should be noted that fluence-rates of polychromatic light are inherently unreliable, and in particular may be distorted by the presence of infra-red radiation. Smith *et al.* (1987) found that saturating irradiance conditions were reached at approximately 7-8 Wm^{-2}. Was the fluence-rate of the photoreactivating light used by Husain and Sancar (1987a) too low for the activity of *phr*A to be seen?

It has been reported that a new photoreactivating enzyme has been discovered in *Drosphilia melanogaster* which specifically repairs (6-4) photoproducts (Todo *et al.*, 1993). Studies by these workers showed that *E. coli* possesses a protein that specifically binds (6-4) photoproducts, but an initial assay for its photoreactivation-mediating activity

was negative. The biological function of this (6-4) photoproduct-binding factor remains to be determined. The *phr*A gene product could be this (6-4) photoproduct-binding factor, and is possibly a photoreactivating enzyme specific for (6-4) photoproducts. The level of repair seen in the *phr*A$^+$ *phr*B$^-$ strain studied in our laboratory is consistent with the amount of (6-4) photoproducts likely to be induced by the UV-irradiation conditions. As stated in Section 1.2, cyclobutane pyrimidine dimers and (6-4) photoproducts are the most abundant of the total UV-induced photoproducts, constituting 70-80% and 20-30% of the total photoproducts respectively (Svoboda *et al.*, 1993).

Therefore, three major possibilities exist for the role of *phr*A in *Escherichia coli* :-

i) No significant role in photoreactivation.

ii) Photoreactivation by repair of pyrimidine dimers at higher fluence-rates of photoreactivating light.

iii) Photoreactivation by repair of (6-4) photoproducts.

The aim of this study was to characterise the probable gene on the insert in pAS01 (Smith and Moss, 1988), with the intention of trying to confirm one of the above explanations.

CHAPTER TWO

MATERIALS AND METHODS

2.1 GENERAL METHODOLOGY

2.1.1 WATER

All water used for preparative work throughout this study was freshly double glass distilled by a bi-distillation Fistreem still (FISONS LTD) fitted with a Fistreem pre-deioniser (FISONS LTD). It is referred to throughout this study as deionised double-distilled water (DDDW).

2.1.2 GLASSWARE

Glassware was decontaminated where necessary by autoclaving at 121°C for 30 minutes (DRAYTON CASTLE LABORATORY STERILISER). All glassware was washed in DDDW and then rinsed three times before drying overnight in a drying oven (GALLENKAMP). Glassware was then sealed with aluminium foil and sterilised by dry heat at 160°C for 4 hours (GALLENKAMP STERILISING OVEN).

2.1.3 GROWTH OF ORGANISMS

The organisms used in this study were all *Escherichia coli* K-12 strains. A list describing the genotypes and sources of all the organisms used is included in APPENDIX A. A

similar list detailing the plasmids used in this study is also included in APPENDIX A. The organisms used were routinely grown up from stock LB agar plates - see Section 2.1.4.

MEDIA USED FOR THE GROWTH

LB broth was routinely used as the growth medium for all experiments, except for the studies on UV-survival and photoreactivation experiments where Oxoid CM1 nutrient broth was used. A full list of media used in this study is included in APPENDIX B2.

The media was made up in DDDW and allowed to stand for 15 minutes. 100ml volumes were dispensed into 150ml medical screw-cap flat bottles (BEATSON-CLARKE) and sterilised by autoclaving at 121°C for 15 minutes. These were stored in the dark at room temperature prior to use.

INCUBATION

Cultures were incubated in either an Immersion Water Bath (GALLENKAMP BKS350) or a Hot Air Incubator (GALLENKAMP ILLUMINATED COOLED ORBITAL INCUBATOR). Unless otherwise stated, the temperature was set at 37°C ± 0.5°C and shaking at 100 cycles per minute, with the safety "cut off" set at 45°C. Both the temperature and the number of cycles per minute were monitored routinely.

AERATION APPARATUS

A forced aeration system used to standardise the amount of air to each culture vessel was used for all UV-survival and photoreactivation studies. Compressed air was passed through a course cotton wool pre-filter connected to a Rotameter flow meter (ROTAMER, CROYDON) which regulated the flow-rate to 10ml per minute to each culture vessel. The air was sterilised by passage through a 25mm diameter, 0.45μm pore-size Sartorius membrane filter (SARTORIUS GMBH, GERMANY) positioned immediately before the entrance port to the culture vessel. This apparatus has been described previously (Hodges, 1979).

METHODOLOGY

A loopful of surface-grown culture was inoculated into an appropriate vessel containing an appropriate amount of pre-warmed growth medium. For small culture volumes, a 30ml sterile Universal Container (STERILIN, FELTHAM) containing 10ml of pre-warmed growth medium was used. For larger culture volumes, a 250ml pyrex, screw-cap, conical flask containing 40ml - 100ml of pre-warmed growth medium was used. For strains carrying antibiotic resistance plasmids, the appropriate antibiotic was added to the growth medium. The vessel was incubated in either a shaking water bath or in the hot air shaking incubator for a length of time appropriate to the experiment. For the UV-irradiation and photoreactivation studies, the flask was connected to the aeration apparatus and incubated in a shaking water bath for 24 hours. A secondary liquid culture was prepared by inoculating 99ml of pre-warmed growth medium with 1ml of primary culture, and incubated as described above for 24 hours. These culture conditions were adhered to strictly to minimise the variation in photoreactivability measured by Tyrrell *et al.* (1972).

2.1.4 STORAGE OF ORGANISMS.

Stock cultures of all strains were sealed in sterile plastic tubes, packed in plastic vials and stored in the vapour phase of a liquid nitrogen refrigerator (UNION CARBIDE LTD) at a temperature of approximately −161°C.

Stocks for routine use were also prepared, by adding 0.15ml sterile glycerol to 0.85ml of bacterial culture, vortexing the culture to ensure the glycerol was evenly dispersed, then transferring the culture to a sterile, labelled, storage tube, equipped with a screw-cap and an air-tight gasket (INTER-MED, DENMARK). The culture was stored at −161°C, as described above. The sterile glycerol was prepared by dispensing 20ml aliquots into 30ml straight-sided glass containers, sealed and sterilised at 121°C for 15 minutes.

For routine use, a sterile inoculating needle was used to scrape the surface of the above frozen culture and immediately streaked onto a LB agar plate containing the appropriate antibiotic(s). The agar for these plates was prepared as described in APPENDIX B2 and 20ml volumes of molten agar were poured into 9cm sterile petri dishes (STERILIN LTD, FELTHAM). After inoculation, the plates were incubated at 37°C for 48 hours in a LEEC PCF2 incubator (LEEC, NOTTINGHAM). The plates were sealed with parafilm (NESCOFILM) and stored in an inverted position at 4°C. These plates were discarded after two weeks. The phenotype of each strain was routinely verified by assessing growth on the appropriate defined media plates.

2.1.5 MATERIALS

PIPETTES

Four Gilson pipettes (GILSON MEDICAL ELECTRONICS, FRANCE) with volume ranges 1.0ml - 5.0ml (MODEL P5000), 0.1ml - 1.0ml (MODEL P1000), 10µl - 2000µl (MODEL P200) and 0.5µl - 20µl (MODEL P20) were used, in conjunction with the appropriate plastic tips. After use the tips were washed and boiled in glass distilled water, dried and packed into BS6257 specification autoclave bags (DRG HOSPITAL SUPPLIES) or plastic tip boxes (GILSON MEDICAL ELECTRONICS, FRANCE) before sterilisation by autoclaving at 121°C for 15 minutes.

ANTIBIOTIC SOLUTIONS

Stock solutions of all the antibiotics used in this study were prepared to a concentration as described in Table 2.1. Solutions made up in DDDW were sterilised through a 25mm diameter 0.22µm pore-size Sartorius membrane filter, while solutions made up in ethanol required no sterilisation (Sambrook *et al.*, 1989). Solutions were stored in light resistant, sterile containers in the dark at -20°C.

ANTIBIOTIC	STOCK SOLUTIONS		WORKING CONCENTRATIONS
	CONCENTRATION	STORAGE TEMPERATURE	
AMPICILLIN	50mg/ml in H_2O	-20°C	50 - 100µg/ml
STREPTOMYCIN	10mg/ml in H_2O	-20°C	50µg/ml
TETRACYCLINE	5mg/ml in ethanol	-20°C	15µg/ml

Table 2.1. Summary of antibiotics used with working and stock concentrations.

DILUTION TUBES

All serial dilution's were performed in 15cm x 1.9cm rimless, thick-walled, pyrex glass tubes, fitted with Oxoid aluminium caps. The tubes were prepared as described under "Glassware", dried and sterilised by dry heat at 160°C for 4 hours.

SPREADERS

These were prepared from glass quill, sealed at each end and having a 60° bend approximately two-thirds along its length. They were prepared as described under "Glassware", dried, packed into autoclave bags and sterilised by autoclaving at 121°C for 15 minutes.

DILUTION MEDIUM

M9 salts solution (Anderson, 1946) was used as the dilution fluid. M9 salts solution was prepared from two stock concentrates, M9A and M9B (see APPENDIX B1). M9 salts solution ('M9') was prepared by aseptically mixing 100ml of M9A concentrate and 400ml of M9B concentrate and making up to 5 litres with DDDW. Approximately 100ml

volumes of this solution were transferred to 150ml medical, screw-cap, flat bottles and sterilised by autoclaving at 121°C for 15 minutes. The pH of this solution was 6.9 at 20°C.

SOLUTIONS AND OTHER REAGENTS

All other solutions and other reagents used in this study are described in APPENDIX B.

PLATING MEDIA

LB agar was used as plating media throughout this study, unless otherwise stated. Oxoid CM3 nutrient agar was used for the UV-irradiation and photoreactivation studies. The formulae are given in APPENDIX B2 and the method of preparation is described in Section 2.1.4.

All plates were stored at 4°C in the dark for up to 4 days. Immediately before use they were 'overdried' by placing in an inverted position at 37°C for 60 minutes under ventilated conditions.

MANIPULATIONS

All manipulations requiring aseptic technique were performed in a horizontal laminar flow cabinet (MICROFLOW, INTER-MED). Experimental protocols not requiring sterile conditions were performed at the bench.

2.2 MOLECULAR CLONING TECHNIQUES

The majority of the molecular cloning techniques used in this study are from, or have been adapted from Sambrook *et al.* (1989).

2.2.1 SOLUTIONS, RESTRICTION AND MODIFYING ENZYMES, AND OTHER REAGENTS

SOLUTIONS

Details of all the solutions used for molecular cloning are included in APPENDIX B1.

RESTRICTION ENZYMES

Unless otherwise stated, restriction enzymes were purchased from PHARMACIA, stored at -20°C in 10µl aliquots, and used in accordance with the manufacturers instructions.

MODIFYING ENZYMES

All modifying enzymes were purchased from PHARMACIA, stored at -20°C in 10µl aliquots, and used in accordance with the manufacturers instructions.

REACTION BUFFER

Unless otherwise stated, the reaction buffer used was ONE-PHOR-ALL PLUS (PHARMACIA), supplied as a 10x concentrate.

OTHER REAGENTS

Details of all the other reagents used in this study are included in APPENDIX B.

2.2.2 ISOLATION AND PURIFICATION OF PLASMID DNA

For the requirements of this study, the quantity and quality of plasmid DNA obtained by the alkaline lysis 'mini-prep' method described below was sufficient.

1.3ml of an overnight culture of the bacterial strain containing the plasmid was transferred to a 1.5ml microcentrifuge tube (ELKAY PRODUCTS INC) and centrifuged at full speed for 1 minute in a microcentrifuge (MSE MICROCENTUAR) to pellet the cells. The media was removed using a sterile glass pipette. 100µl of ice-cold SOLUTION I was added to the cells, and the pellet resuspended by vigorous vortexing, then incubated on ice for 5 minutes. 200µl of SOLUTION II was added, and the microcentrifuge inverted five times to gently mix the contents, then incubated on ice for 5 minutes. 150µl of SOLUTION III was added, and the contents vortexed for 10 seconds to disperse SOLUTION III through the viscous bacterial lysate, then incubated on ice for 5 minutes, then centrifuged at full speed for 5 minutes. The supernatant was transferred to a new microcentrifuge tube and 450µl of phenol:chloroform:iso-amyl alcohol (25:24:1) added. The contents were vortexed for 20 seconds and then centrifuged at full speed for 2 minutes. The upper aqueous layer was carefully transferred to a new microcentrifuge tube and 1ml of 96% ethanol (-20°C) added to precipitate the plasmid DNA. The contents were vortexed for 20 seconds and incubated at -20°C for 60 minutes. The DNA was pelleted by centrifugation at full speed for 5 minutes, then the supernatant carefully discarded. The pellet was carefully rinsed with 70% ethanol (room temperature), briefly spun on the centrifuge for 1 minute and the supernatant carefully removed. The DNA pellet was dried by placing in a vacuum desiccator for 2 minutes and air drying at room temperature for 5 minutes. The DNA was redissolved in 50µl of TE (pH 8.0 containing DNA-ase free RNA-ase 20µg/ml), unless otherwise stated elsewhere. The contents were briefly vortexed, spun down and stored at -20°C.

2.2.3 CALCULATION OF THE CONCENTRATION OF DNA IN SOLUTION

This was calculated by the spectrophotometric measurement of the amount of ultra-violet irradiation absorbed by the bases in solution. 10µl of DNA solution was diluted to 1.0ml with TE (pH 8.0) and using TE (pH 8.0) as a blank, readings for the OD_{260} and OD_{280} were made using a spectrophotometer (MILTON ROY SPECTRONIC 601). The reading at 260nm allows calculation of the concentration of nucleic acid in the sample. An OD_{260} of 1.0 corresponds to approximately 50µg/ml for double-stranded DNA. The ratio OD_{260} / OD_{280} provides an estimate of the purity of the nucleic acid. Pure preparations of DNA have an OD_{260} / OD_{280} of 1.8. If there is contamination with protein or phenol, the OD_{260} / OD_{280} will be significantly less (Sambrook *et al.*, 1989).

2.2.4 RESTRICTION ENZYME DIGESTION OF PLASMID DNA

Plasmid DNA can be analysed by cleavage with restriction enzymes. Restriction enzyme digestion reactions were set up as follows :-

DNA SOLUTION	≅ 10µg
RESTRICTION ENZYME	≅ 10 units
RESTRICTION BUFFER (10X CONCENTRATE)	2µl
STERILE DDDW	to 20µl

The reaction mixture was briefly vortexed, spun down and incubated at 37°C for 1 hour in a water bath. 1 unit of restriction enzyme will digest 1µg of λDNA in 50µl Assay Buffer in 1 hour at 37°C, according to the manufacturers data sheet. After incubation, 3µl of gel-

loading buffer was added, briefly vortexed, spun down and stored at -20°C until ready to load onto an agarose gel.

2.2.5 ANALYSIS OF RESTRICTION FRAGMENTS BY AGAROSE GEL ELECTROPHORESIS

Electrophoresis through agarose or polyacrylamide gels is the standard method used to separate, identify and purify DNA fragments. Routinely, a 0.8% agarose gel was used, which separates linear DNA molecules in the range 0.6 - 9 kbp (Sambrook *et al*, 1989).

PREPARATION OF A GEL

240mg of electrophoresis grade agarose (BDH, POOLE) was added to 30ml TAE buffer and dissolved by heating in a boiling water bath for 5 minutes with constant swirling, until all the agarose 'lenses' had dissolved. The solution was cooled to about 60°C, then ethidium bromide solution was added to a final concentration of 0.5μg/ml. The ends of a clean, dry, plastic electrophoresis tray (BIO-RAD) were sealed with autoclave tape and either an 8- or 15-tong plastic comb positioned 1.0mm above the plate surface at one end of the tray. The molten gel was poured carefully into the tray and allowed to cool and set for 30 - 45 minutes at room temperature.

LOADING AND RUNNING A GEL

The comb and sealing tape were carefully removed, and the gel mounted in an electrophoresis tank (BIO-RAD MINI-SUB DNA CELL) with a nominal capacity of 250ml. The gel was covered with TAE buffer to a depth of just over 1mm, making sure that all the 'wells' were filled. 12μl (8 wells) or 7μl (15 wells) of sample was loaded into each well as required, using 3μl of λDNA/HindIII as a marker in one of the outside lanes. When all the wells were loaded, the lid of the tank was closed and a voltage of 60V applied using a

250/2.5 Power Supply (BIO-RAD). The gels were run for between 60 - 120 minutes. The TAE buffer was recirculated around the tank by a flow-inducer (WATSON-MARLOW, FALMOUTH), so it flowed from the cathode to the anode.

VISUALISATION AND PHOTOGRAPHY OF A GEL

The fluorescent dye, ethidium bromide (Sharp *et al*, 1973), which is present in the agarose gel contains a planar group that intercalates between the stacked bases of DNA. Ultraviolet radiation at 254nm is absorbed by the DNA and transmitted to the dye, the energy re-emitted at 590nm in the red-orange region of the visible spectrum. The fixed position of this planar group and its close proximity to the bases causes ethidium bromide bound to DNA to display an increased fluorescent yield compared to free dye. Thus small amounts of DNA can be detected in the presence of free ethidium bromide in the gel.
At anytime during electrophoresis, the gel tray could be removed from the tank, and the DNA fragments viewed on a UV Products Transilluminator. When the DNA fragments had migrated as far as was required, the gel was photographed with a CU-5 Fotodyne camera and Type 55 Polaroid Film.

2.2.6 ISOLATION AND PURIFICATION OF DNA FROM AGAROSE GELS

The isolation and purification of DNA, usually a restriction fragment from a restriction enzyme digest of plasmid DNA, was performed using the Sephaglas Band Prep Kit (PHARMACIA). This kit provides a simple and rapid method for extracting individual DNA bands from agarose gels following electrophoresis. The method utilises a novel matrix, Sephaglas BP. Sephaglas BP is well suited to DNA purification for two reasons; a) DNA can be bound to it selectively, then eluted into a buffer of low ionic strength for direct use in a variety of common laboratory procedures; and b) the chaotropic salt required for

binding (sodium iodide), denatures proteins and dissolves agarose. The kit is able to isolate from an agarose gel plug DNA of sufficient purity for subsequent ligation, according to the manufacturers data sheet.

The DNA was loaded onto an agarose gel and run for 60 - 120 minutes until the fragment required had separated from the other bands. The gel was viewed using 366nm UV light (DESAGA UVIS 254nm / 366nm LIGHT SOURCE) to minimise damage to the DNA. A piece of the gel containing the required fragment was cut out of the gel with a scalpel, chopped into small pieces and transferred to a pre-weighed clean 1.5ml microcentrifuge tube, then weighed to calculate the weight of the agarose slice. 250µl of Gel Solubiliser (250µl minimum, or 1µl for each mg of agarose) was added, vortexed vigorously, and incubated at 60°C for 10 minutes until the agarose slice had dissolved. 5µl of Sephaglas BP (5µl for each estimated µg of DNA) was added to the dissolved agarose slice, vortexed gently, then incubated at room temperature for 5 minutes, vortexing gently every minute to resuspend the Sephaglas. The contents were centrifuged at full speed in a microcentrifuge for 1 minute, and the supernatant carefully discarded. 40µl of Wash Buffer (or 8x the volume of Sephaglas added previously) was added to the Sephaglas pellet, vortexed gently to resuspend the pellet, then centrifuged for 1 minute. The supernatant was carefully removed. This wash-step was repeated twice. The tube was inverted, and the pellet allowed to air-dry for 10 minutes. 10µl of Elution Buffer (10µl minimum, or 0.5x the volume of Sephaglas added previously), vortexed gently to resuspend the Sephaglas pellet, incubated for 5 minutes at room temperature, with periodic agitation, then centrifuged for 1 minute. The supernatant was carefully transferred to a clean microcentrifuge tube, taking care not to disturb the Sephaglas pellet. This elution step was repeated to obtain a better yield of DNA. The concentration of the DNA was calculated using the spectrophotmetric assay described in Section 2.2.3. The DNA was now pure enough to proceed directly to the next stage, without further purification.

2.2.7 ALKALINE PHOSPHATASE TREATMENT OF RESTRICTED PLASMID DNA

Treatment of linear DNA molecules produced by restriction enzyme cleavage with calf-intestinal alkaline phosphatase (PHARMACIA) results in the removal of the 5'-terminal phosphate residues and prevents self-ligation. This is a useful technique when cloning restriction fragments into vectors.

Restricted DNA (1-20μg) in a reaction volume of 50μl is dephosphorylated by the addition of ≅ 0.1 units of alkaline phosphatase and incubation at 37°C for 30 minutes. Afterwards, the alkaline phosphatase can be inactivated by incubating at 85°C for 15 minutes, then allowing the reaction mixture to cool at room temperature for 30 minutes. Using this protocol, less than 1% of the input DNA should retain its terminal phosphate groups, according to the manufacturers data sheet.

2.2.8 LIGATION OF LINEAR DNA MOLECULES

Ligation of a segment of foreign DNA to a linearised plasmid vector involves the formation of new bonds between phosphate residues located at the 5'-termini of double-stranded DNA and adjacent 3'-hydroxyl moieties. Four new phosphodiester bonds are formed if all of the four 'ends' carry 5'-phosphate residues, however if the plasmid DNA has been dephosphorylated, only two new phosphodiester bonds can be formed. The resulting hybrid molecules carry two single-stranded nicks that are repaired after the hybrids have been introduced into competent bacteria.

For all cloning purposes in this study, bacteriophage T_4 DNA ligase (PHARMACIA) was used to catalyse *in vitro* the formation of phosphodiester bonds between adjacent 5'-phosphate and 3'-hydroxyl residues in the presence of ATP. The advantage of bacteriophage T_4 DNA ligase was that it will join blunt-ended termini efficiently under

normal reaction conditions as well as cohesive termini. The constituents of the ligation mixtures used are given in the relevant RESULTS section.

2.2.9 PREPARATION OF COMPETENT CELLS

5ml of LB broth was inoculated with a single colony of the chosen bacteria from a LB agar plate. This was incubated at 37°C overnight. 40ml of pre-warmed LB broth was inoculated with 0.4ml of overnight culture and incubated at 37°C until the $OD_{550} \equiv 0.5$ (mid-log phase), usually 3 - 4 hours. The cells were transferred in 20ml aliquots to ice-cold sterile Universal Containers, and the cultures cooled on ice for 10 minutes. The cultures were then centrifuged at 4000rpm at 4°C for 10 minutes in a centrifuge (MSE CHILSPIN, FISONS). The media was removed with a sterile glass pipette, and the containers inverted to drain off the last traces of media. The cells were resuspended in 5ml ice-cold sterile 0.1M $CaCl_2$ and incubated on ice for 30 minutes, then centrifuged at 4000rpm at 4°C for 10 minutes. The supernatant was removed with a sterile glass pipette, and the containers inverted to drain off the last traces of supernatant. The cells were resuspended in 1ml of ice-cold sterile 0.1M $CaCl_2$ and stored at 4°C for 16 hours, then used for transformation. The above procedures were carried out under aseptic conditions. Dagert and Ehrlich (1979) have shown that competent cells may be stored at 4°C for 24 - 48 hours in $CaCl_2$ solution. The efficiency of transformation increases four- to six-fold during the first 12 - 24 hours of storage, then decreases to the original level.

2.2.10 TRANSFORMATION OF PLASMID DNA INTO COMPETENT CELLS

It has been shown that bacteria treated with ice-cold $CaCl_2$ and then briefly heated can be transfected with bacteriophage λ DNA, plasmid DNA and *E.coli* chromosomal DNA.

Apparently, the treatment induces a transient state of "competence" in the recipient bacteria, during which they are able to take up DNAs derived from a variety of sources. Many methods have been devised with the aim of increasing the transformation efficiency. The method used in this study has been derived from Sambrook *et al.* (1989).

A sterile thin-walled glass tube (HOSLAB, ILFORD, ESSEX) was chilled on ice for 5 minutes, then 300µl of competent cells and 5µl of plasmid DNA (either purified plasmid DNA or a ligation mixture - ≅ 0.05µg DNA) were added and mixed by gentle swirling, then incubated on ice for 30 minutes. The cells were heat-shocked by placing the tube in a water bath at 50°C for 45 seconds, then incubated on ice for 1 - 2 minutes. 1ml of pre-warmed LB broth was added to the tube, mixed gently, then the contents transferred to a sterile Universal Container and incubated at 37°C for 1 hour with shaking. 8.7ml of pre-warmed LB broth was added along with the appropriate antibiotic depending on the resistance conferred by the plasmid. The contents were mixed by gentle swirling and then incubated at 37°C for 12 hours with shaking. The resulting culture was streaked out onto LB agar plates supplemented with the appropriate antibiotic and incubated at 37°C for 48 hours. The resulting individual colonies were then screened by isolating the plasmid DNA and restriction enzyme analysis as described previously.

2.2.11 CONTROLS FOR LIGATION AND TRANSFORMATION EXPERIMENTS

Various controls were performed alongside the ligation and transformation experiments to verify the validity of the final result. These are described in the appropriate RESULTS section later on.

2.2.12 PRODUCTION OF SYNTHETIC OLIGONUCLEOTIDES

Synthetic oligonucleotides were required for a variety of purposes in this study, from primers for DNA sequencing to synthetic linkers for sub-cloning.

The synthetic oligonucleotides were prepared using a DNA Synthesiser Model 381A (APPLIED BIOSYSTEMS) in pre-packed disposable Synthesis Columns (SEVERN BIOTECH LTD) by Dr Paul Towner in the Department of Biochemistry, University of Bath. The synthetic oligonucleotide was bound to a resin in the column. The synthetic oligonucleotide was extracted and isolated as follows :-

A 1ml syringe was filled with 1ml of concentrated ammonia solution and fixed to one end of the column. A 5ml syringe was fixed to the other end of the column, and used to draw 0.3ml of concentrated ammonia solution into the column. This was left for 60 minutes at room temperature, then a further 0.2ml of concentrated ammonia solution was drawn into the column. This was repeated until all of the concentrated ammonia solution had passed through the column. The concentrated ammonia solution containing the oligonucleotide was transferred to a 1.5ml screw-capped microcentrifuge tube, which was placed into a 7.5ml Universal Container (STERILIN, FELTHAM) containing 0.5ml of concentrated ammonia solution. This was placed into a water bath at 55°C overnight (a minimum of 6 hours), to remove the amino-protecting groups. The solution was transferred to an ice-cold 30ml Universal Container and 5ml of 96% ethanol (-20°C) added, followed by 3ml of glacial acetic acid, added slowly down the side of the tube. The contents were mixed and incubated at -20°C for 60 minutes. The oligonucleotide was collected by centrifugation at 2000rpm for 10 minutes in a MSE Chilspin. The supernatant was carefully removed, and the oligonucleotide rinsed carefully with 5ml of 70% ethanol at room temperature. This was carefully removed, and the oligonucleotide pellet dried under vacuum for 3 minutes, then air-dried at room temperature for 10 minutes. The oligonucleotide was redissolved in 200µl of sterile DDDW. The concentration of the oligonucleotide was calculated as

described in Section 2.2.3, however an OD_{260} of 1.0 corresponds to ≅ 37μg/ml of oligonucleotide DNA rather than 50μg/ml for double-stranded DNA (Sambrook *et al.*, 1989).

2.3 SEQUENCING TECHNIQUES

Details of the preparation of DNA for sequencing are included in Section 3.3.3.

2.3.1 EQUIPMENT

A Sequi - Gen Nucleic Acid Sequencing Cell (BIO-RAD) was used for the sequencing experiments. This was a modular, high resolution, vertical slab gel electrophoresis instrument designed for DNA / RNA sequencing. The dimensions of the cell plate were 21cm (width) by 50cm (height). The actual gel area was 17cm by 50cm.

The Sequi - Gen Cell used a new type of upper buffer chamber called an Integral Plate / Chamber (IPC). The IPC was the inner glass plate and buffer chamber bonded together with a permanent adhesive at the sides and bottom edges of the plate. This formed a thin, 0.5cm buffer chamber that extended over the entire area of the gel plate. A platinum electrode wire, strung across the bottom of the IPC, functioned as the cathode.

The IPC assembly consisted of the IPC, an outer glass plate and a pair of clamps. A gel mould was formed when 0.4mm plastic spacers were clamped between the glass plates of the IPC assembly. After a gel had been cast, the IPC assembly was placed in an upright position in the lower buffer chamber (Universal Base), and locked into place with a stabiliser bar. Buffer was poured into the upper buffer chamber (minimum volume 575ml) and lower buffer chamber (minimum volume 350ml) until it contacted the top and bottom of the gel. Two safety covers were used to cover the upper and lower buffer chambers. The upper safety cover was attached to the 'plugs' at the top of each clamp, and the lower safety cover was attached to the 'plugs' on the lower buffer chamber. The anode was a platinum electrode wire strung across the bottom of the lower buffer chamber, between the two 'plug attachments'. The upper buffer carried the current from the cathode up to the

top of the plates where the gel was exposed. The lower buffer contacted the gel at the bottom edge of the plates.

2.3.2 PREPARATION BEFORE ASSEMBLY OF THE GEL

The glass plates were thoroughly cleaned with detergent and rinsed with warm tap water. The plates were dried with paper towels, making sure that all traces of detergent were removed from the edges of the plates. Both plates were rinsed with DDDW and then 95% ethanol just prior to assembly, wiping off any dust with a lint-free paper tissue moistened with 95% ethanol at the point of assembly.

The IPC glass plate was siliconised before use, and this was repeated after five gels had been run. This allowed easy removal of the IPC plate from the outer plate, as the gel would stick preferentially to the unsiliconised outer plate. The plate was cleaned and rinsed as described above, placed horizontally glass face up in a fume cupboard, and a solution of Sigamacote® (SIGMA) rubbed onto the glass plate using lint-free paper tissue, ensuring that the whole of the glass surface was treated. The plate was then cleaned and rinsed again before assembly.

All plastic parts (buffer chambers, stabiliser bar, combs, spacers and casting tray) were rinsed with detergent in lukewarm tap water, rinsed well with warm tap water, rinsed with DDDW, and allowed to drip dry on clean paper towels. The spacers were wiped with lint-free paper tissue moistened with 95% ethanol prior to assembly.

Clean plates and spacers were the key to pouring gels without bubbles or leaks.

2.3.3 ASSEMBLING THE GLASS PLATES

The IPC was placed on the bench, horizontally glass face up. The spacers were placed on the long edges of the IPC plate, and the outer glass plate was placed on top of the spacers,

with the cleaned side face down. The outer plate and spacers were aligned with the bottom edge of the inner glass plate, so that the two glass plates were flush at the bottom. The clamps were slid over the gel plate assembly, one clamp at a time. Each clamp was attached at one end first, then slid onto the gel plate assembly until it snapped into place along the entire length. The spacers and outer glass plate were checked to be flush at the bottom with the inner glass plate.

2.3.4 PREPARATION OF POLYACRYLAMIDE SOLUTIONS

All polyacrylamide solutions used in this work were prepared from purchased Stock Solutions (SEQUAGEL). A gel concentration of 6% v/v was used and prepared as follows :-

SEQUAGEL CONC	14ml
SEQUAGEL DIL	40ml
SEQUAGEL BUFFER	6ml

For Sealing Gels, the following solution was prepared :-

6% GEL SOLUTION	10ml
SEQUAGEL CONC	1ml
TEMED	50µl
AMMONIUM PERSULPHATE (25% w/v)	70µl

This was mixed by swirling and used immediately as described later.

For sequencing gels, the following solution was prepared :-

6% GEL SOLUTION	50ml
TEMED	50µl
AMMONIUM PERSULPHATE (25% w/v)	67µl

This was mixed by swirling and used as described later.

2.3.5 CASTING THE GEL

The bottom edge of the gel was sealed as follows. A foam cushion and filter paper sealing strip were placed into the clean, dry casting tray with the paper on top. The sealing gel was prepared, mixed immediately and poured over the entire length of the paper sealing strip, so it became completely saturated. The IPC assembly was placed on top of the sealing strip (bottom of the glass plates in contact with the strip), and the screws on the casting tray tightened to bind the casting tray tightly to the clamps of the IPC assembly. The movement of the sealing gel into the space between the gel plates by capillary action was checked along the full width of the gel. The sealing strip was allowed to set for 60 minutes

Once the sealing gel had polymerised, the IPC assembly was laid on the bench at an angle of approximately 15°, and the casting gel prepared. The gel solution was drawn into a 50ml plastic syringe, and the IPC assembly tilted so that the gel solution entered the glass plates near one spacer. This reduced the formation of bubbles during filling, any bubbles that formed were removed by gently tapping the glass plate.

After pouring, the IPC assembly was laid nearly flat at an angle of approximately 5°. The flat end of a 'sharkstooth' comb (BETHESDA RESEARCH LABORATORIES) was inserted between

the gel plates before the gel had polymerised. This was clamped at both sides to ensure that the plates held firmly against the comb, using two 'bulldog' clips.
Once the gel had polymerised, a paper towel was laid across the top of the gel and saturated with DDDW. The gel was left overnight to 'age'.

2.3.6 SETTING UP FOR OPERATION

The casting tray was detached and the sealing strip pulled away from the bottom of the gel. The 'sharkstooth' comb was removed, and the well formed immediately rinsed with DDDW to remove any unpolymerised acrylamide.
The IPC assembly was placed into the lower buffer chamber and the stabiliser bar inserted. The upper buffer chamber was filled with 0.5x TBE buffer to about 1cm from the top of the chamber. The lower buffer chamber was filled with 350ml - 500ml of the same buffer.
A Gel Temperature Indicator (BIO-RAD) was attached to the outer glass plate near the centre of the gel to monitor the temperature during electrophoresis. The 'sharkstooth' comb was replaced into the well at the top of the gel, 'teeth' down to form the loading wells. The 'teeth' penetrated the gel by about 1mm. The safety covers were attached and the gel pre-run for 45 minutes at 1800V using a Model 3000xi Computer Controlled Electrophoresis power supply (BIO-RAD). This was to warm the gel up to operating temperature ($\cong$ 50°C). The level of the buffer in the upper buffer chamber was monitored regularly, and topped up when required so that it always covered the top of the gel.

2.3.7 LOADING AND RUNNING THE GEL

The power supply was turned off, the upper safety cover removed, and the samples loaded onto the gel, via the 'sharkstooth' wells, as described in Section 3.3.3. Prior to loading, the wells were rinsed with buffer using a pasteur pipette to remove any dissolved urea. The

samples were always loaded onto a 'hot' (45° - 50°C) gel using a P20 Gilson pipette. Once the samples were loaded, the upper safety cover was replaced.

The gel was run at a constant power of 45W. It was found that this power produced a constant gel temperature of ≅ 50°C. Running at constant power also resulted in more reproducible runs.

2.3.8 DISASSEMBLY OF THE GEL

The power supply was switched off and both safety covers removed. The stabiliser bar was detached and the IPC assembly removed. The buffer was poured out of the IPC assembly, and the inside and outside rinsed. The clamps were removed from the IPC, and the inner glass plate carefully removed by prying gently at the top of the gel.

2.3.9 FIXING AND DRYING THE GEL

The gel on the outer glass plate was fixed in 2 litres of Fixing Solution (Acetic Acid : Methanol : DDDW / 1 : 1 : 8) solution for 15 minutes. This process removed hygroscopic urea, which would inhibit drying. The gel was then transferred to a fresh sheet of Whatman 3mm filter paper. This was achieved by laying the filter paper on top of the gel, gently rubbing it flat with a test tube, and then peeling back the filter paper from one end. The gel was covered with Saran Wrap ™, and the edges trimmed to fit the slab gel dryer (BIO-RAD MODEL 583 GEL DRYER). The gel was dried at 80°C under vacuum for 90 minutes. The Saran Wrap ™ was removed and the gel trimmed again to fit the film exposure cassette (SIGMA, 14in x 17in).

2.3.10 AUTORADIOGRAPHY

The gel was placed in the film exposure cassette, gel face up and secured using masking tape, and the edges of the gel marked with a black marker pen. One piece of High Performance Autoradiography Film (HYPERFILM ™ - β MAX - AMERSHAM) was removed from its box under red light conditions and placed over the gel surface, shiny side up, using the edge markers as a guide. The cassette was closed and clamped shut, and the film left for 48 hours exposure. After this time, the film was removed under red light and placed in a Developing solution (KODAK LX-24 X-RAY DEVELOPER) until the sequence bands appeared. The film was then transferred to a Rinsing solution (1% v/v acetic acid in water) and then transferred to a Fixing solution (KODAK FX-40 X-RAY LIQUID FIXER) until the hazy appearance of the film had disappeared. The film was rinsed again and then hung up to dry.

2.3.11 PRODUCTION OF SYNTHETIC PRIMERS

The start point for sequencing the forward section of the insert was the M13 Universal Primer, and for the reverse section the M13 Reverse Primer. These were purchased from USB, OHIO, USA. Approximately 300bps from the primer could be read accurately on the autoradiographs. A clear section was taken of between 17 and 20 base pairs and a new synthetic primer produced as described in Section 2.2.12. The primers were diluted with sterile DDDW to a final concentration of 0.5pmol/μl.

2.4 EXPRESSION TECHNIQUES

Intact native proteins can be produced in *E.coli* by providing a strong, regulated promoter and an efficient ribosome-binding site - see Section 4.3. Levels of expression may vary from less than 1% to more than 30% of the total cell proteins.

2.4.1 GROWTH OF INDUCED CULTURES

An overnight culture of the plasmid of interest, present in a suitable host, was prepared in LB broth supplemented with the appropriate antibiotic(s). The induction culture was prepared by inoculating 50ml of pre-warmed LB broth supplemented with the appropriate antibiotic(s) with 0.5ml of overnight culture. This culture was incubated at 37°C for 2 hours with shaking until the culture had reached approximately mid-log phase - for the two host strains used (JM83 and JM105) this was equivalent to an OD_{550} of about 0.5. IPTG was aseptically added to the culture to a final concentration of 1.0 mM. A 1ml sample was aseptically removed and transferred to a 1.5ml microcentrifuge tube. The culture was returned to the incubator, taking this point as T = 0. The culture was incubated for to 24 hours, with 1ml samples taken at T = 2, 4, 6, 12, and 24.

2.4.2 PREPARATION OF SAMPLES

The bacteria were recovered from the 1ml of culture by centrifugation at full speed for 1 minute. The medium was carefully removed using a sterile glass pipette, leaving the bacterial pellet as dry as possible.

The pellet was resuspended by vortexing in 50µl of sterile H_20, then 50µl of 2 x SDS gel-loading buffer was added, and the contents vortexed for 20 seconds. The sample was placed in a boiling water bath for 5 minutes. The sample was centrifuged for 10 minutes,

then 50µl of the supernatant transferred to a fresh microcentrifuge tube. The samples were stored at -20°C until ready to load onto a SDS-polyacrylamide gel for analysis.

2.4.3 SDS-POLYACRYLAMIDE GELS

Almost all analytical electrophoresis of proteins is carried out in polyacrylamide gels under conditions that ensure dissociation of the proteins into their individual polypeptide subunits and that minimise aggregation. Most commonly, the strongly anionic detergent SDS is used in combination with a reducing agent and heat to dissociate the proteins before they are loaded onto the gel - see Section 2.4.2. Because the amount of SDS is almost always proportional to the molecular weight of the polypeptide and is independent of the sequence, SDS-polypeptide complexes migrate through polyacrylamide gels in accordance with the size of the polypeptide. By using markers of a known molecular weight, it is therefore possible to estimate the molecular weight of the polypeptide chain(s), and to see if over-expression of a certain protein is occurring over a set of samples taken at different time intervals from the same culture.

EQUIPMENT

A Mini-PROTEAN II (BIORAD) dual slab cell was used to prepare and run the SDS-polyacrylamide gels in conjunction with a Model 200/2.0 Power Supply (BIORAD). The glass plates and the plastic components were cleaned and prepared in a similar fashion to that described in Sections 2.3.2 and 2.3.3. The kit was assembled and used in accordance with the manufacturers instructions.

2.4.4 PREPARATION OF POLYACRYLAMIDE SOLUTIONS

All polyacrylamide solutions used in this work were prepared from purchased Stock Solutions (PROTOGEL). Gel concentrations of 12% for the stacking gels and 4% for the resolving gels were used.

For resolving gels, the following solution was prepared :-

STERILE DDDW	3.35ml
PROTOGEL	4.0ml
1.5M TRIS (pH 8.8)	2.5ml
SDS (20% w/v)	50µl
AMMONIUM PERSULPHATE (25% w/v)	100µl
TEMED	5µl

This was mixed by swirling and used as described later.

For stacking gels, the following solution was prepared :-

STERILE DDDW	6.1ml
PROTOGEL	1.3ml
0.5M TRIS (pH 6.8)	2.5ml
SDS (20% w/v)	50µl
AMMONIUM PERSULPHATE (25% w/v)	100µl
TEMED	10µl

This was mixed by swirling and used as described later.

2.4.5 CASTING THE GEL

A comb was placed completely into the assembled glass plate sandwich, and a mark made 1cm below the teeth of the comb with a marker pen. A freshly prepared resolving gel solution was added slowly down the gap present at the top of the glass plates, up to the level of mark. This was covered with a layer of 50% v/v methanol and left to polymerise for 60 minutes. The methanol was removed by shaking, the top of the gel rinsed with DDDW, then covered with a layer of 0.375M Tris (pH8.8), wrapped tightly in Saran Wrap ™ and left overnight at room temperature to 'age'.

The top of the gel was rinsed with DDDW and shaken dry. A freshly prepared stacking gel solution was then added on top of the resolving gel until it had filled the rest of the space between the two glass plates. A comb was inserted into the stacking gel, making sure that no air bubbles formed, then left to polymerise for 45 minutes.

2.4.6 SETTING UP FOR OPERATION

The comb was carefully removed from the stacking gel, the 'wells' rinsed with DDDW and shaken dry. The gel apparatus was assembled according to the manufactures instructions, and placed into the lower buffer chamber. The buffer used was Tris-glycine-SDS electrophoresis buffer. A 10x stock solution (BIORAD) was purchased and diluted to a working concentration as required. 300ml of buffer was prepared, and added to the upper buffer chamber until the buffer covered the smaller, but not the larger, glass plate. The remaining buffer was poured into the lower buffer chamber.

2.4.7 LOADING AND RUNNING THE GEL

The samples were loaded onto the gel in 5µl volumes. A molecular weight marker was loaded into the first lane. The marker used was SDS-PAGE Molecular Weight Standard - Low Range (BIORAD), which contains six molecular weight markers ranging between 14,400 Da and 97,400 Da. The full list of the molecular weights of the markers is given in Section 4.3.1. The marker was prepared for use by diluting 1µl in 19µl of SDS-gel loading buffer, placed in a boiling water bath for 5 minutes, and centrifuged for 10 minutes at full speed. The supernatant transferred to a fresh microcentrifuge tube. The marker was stored at -20°C until ready to load onto a SDS-polyacrylamide gel. The lid of the lower buffer chamber was connected and attached to the power supply. The gel was run at a constant voltage of 180V for about 45 minutes, until the blue marker present in the SDS-gel loading buffer had reached the bottom of the gel.

2.4.8 DISASSEMBLY OF THE GEL

The power supply was switched off, the lid removed, and the gel plates snapped out of the holding apparatus. The top plate was carefully removed, then the stacking gel and the spacers removed also. The resolving gel was carefully lifted of the bottom plate using one of the spacers.

2.4.9 STAINING AND DESTAINING THE GEL

The gel was stained in Coomassie Brilliant Blue Stain (see APPENDIX B1) on a gently rocking platform for 60 minutes. The gel was then destained by immersion in a Destaining / Fixing Solution (Methanol : Acetic Acid : DDDW / 4 : 1 : 5) on a gently rocking

platform. The destaining / fixing solution was changed four to five times over a 2 to 3 hour period.

2.4.10 MOUNTING AND DRYING THE GEL

The gel was mounted onto a clean piece of Whatman 3mm filter paper and dried in a similar fashion to that described in Section 2.3.9 for 30 minutes.

2.5 UV IRRADIATION AND PHOTOREACTIVATION TECHNIQUES

2.5.1 GENERAL METHODOLOGY

WASHING / DILUTION FLUID

M9 salts solution was used to wash and resuspend cells, and also as the dilution fluid. Its preparation has been described in Section 2.1.5.

HARVESTING CELLS

A 24 hour liquid secondary culture was prepared as described in Section 2.1.4. 1ml was pipetted into a sterile 1.5ml microcentrifuge tube, and centrifuged at full speed in a microcentrifuge for 1 minute, to pellet the cells. The media was removed using a sterile glass pipette, and the cells resuspended in 0.5ml of ice-cold sterile M9. The cells were pelleted by centrifuging at full speed for 1 minute. This step was repeated twice, to rinse the cells three times. The cells were resuspended in 1.0ml of ice-cold sterile M9 and transferred to a sterile dilution tube containing 9.0ml of ice-cold sterile M9.

After harvesting, an estimate of the viability of the cell suspension was provided by measurement of the absorbance of the suspension at 470nm, and referring to a previously determined calibration curve for the particular organism - see APPENDIX E for an example. The OD_{470} of 1ml of cell suspension was measured against a blank of 1ml of M9 in plastic cuvettes (ELKAY PRODUCTS INC). The Beer-Lambert relationship does not apply to optical densities greater than 0.35, so cell suspensions exceeding this value were diluted accordingly. The cell suspension was diluted with ice-cold sterile M9 to a final volume of 15.0ml in a sterile 15cm x 2.5cm rimless, pyrex glass boiling tube to give an approximate cell count of 1×10^7 colony forming units per ml.

METHOD OF ASSESSMENT OF VIABILITY

The viable count of the bacterial cell suspension was determined by an initial 20-fold dilution, produced by transferring 0.2ml of the test suspension into 3.8ml of M9 in a dilution tube. When survival was low after UV-irradiation, a 2-fold dilution was prepared by adding 0.4ml of the test suspension to 0.4ml of M9. A subsequent series of 10-fold dilution's were performed as necessary by transferring 0.5ml of the diluted test suspension to 4.5ml of M9. Each dilution was thoroughly mixed using a Whirlimix (FISONS LTD). A 0.2ml aliquot of the required dilution was pipetted onto the surface of each of three nutrient agar plates, and spread uniformly with a sterile glass spreader. A range of dilution's were plated to yield colony counts in the 20 -200 range. The plates were allowed to stand for 30 minutes, then incubated in an inverted position in the dark at 37°C for 48 hours. The number of visible colonies (without magnification) on each plate were counted. The mean value of the three plates, together with the dilution factor, was used to determine the number of viable bacteria in the test suspension.

INVESTIGATION OF THE ERRORS INVOLVED IN VIABLE COUNT ASSESSMENT BY THIS TECHNIQUE

The two principle sources of error which may be introduced arise from a) the pipettes may not deliver accurate or precise volumes, and b) the mixing of the bacterial test suspension after each dilution stage may be insufficient for the count to truly reflect the viability of the test suspension.

The error arising from the pipettes was assessed every 3 months by weighing out six individual volumes of DDDW delivered under experimental conditions - see Table 2.2. The conditions used simulated 'in-use' conditions, the pipettes were reset on each occasion and a fresh tip fitted. The DDDW was equilibrated to room temperature for 15 minutes before testing. The results are very similar to the errors calculated by Smith (1987).

The efficiency of the mixing of the bacterial test suspension was assessed by performing six individual serial dilution's of the same test suspension and determining the viability by plating 0.2ml aliquots onto the surface of four nutrient agar plates per dilution series. The experimental results are given in Table 2.3. Again, the results are very similar to the errors calculated by Smith (1987).

VOLUME (ML)	PIPETTE	MEAN (g)
0.2	P1000	0.1961 ± 0.0012
0.5	P1000	0.4932 ± 0.0031
3.8	P5000	3.7819 ± 0.0016
4.5	P5000	4.4903 ± 0.0021

Table 2.2. Investigation of the errors introduced in viable count assessment by the use of Gilson pipettes.

SAMPLE	PLATE COUNTS	DILUTION FACTOR	VIABLE COUNT
1	50, 58, 61, 55	10^5	$5.58 \pm 0.43 \times 10^6$
2	52, 63, 49, 58	10^5	$5.55 \pm 0.62 \times 10^6$
3	44, 48, 60, 54,	10^5	$5.15 \pm 0.70 \times 10^6$
4	55, 54, 59, 56	10^5	$5.60 \pm 0.22 \times 10^6$
5	47, 56, 51, 63	10^5	$5.43 \pm 0.69 \times 10^6$
6	49, 61, 54, 62	10^5	$5.65 \pm 0.61 \times 10^6$

Table 2.3. Investigation of the errors introduced during serial dilution and plating of the bacterial suspension.

Therefore, the calculated errors introduced by the experimental protocol were in the same order as previously calculated by Smith (1987) for the same protocol.

2.5.2 IRRADIATION PROCEDURES

All ultra-violet light experiments were carried out in a 'dark-room' under illumination from red fluorescent tubes (ATLAS LTD, 80W) which do not emit at wavelengths below 540nm. This did not cause concurrent photoreactivation of damage to DNA and was further confirmed by action spectra studies for photoreactivation (Smith, 1987)

FAR UV-RADIATION (254nm)

The source used was a 5cm Penray lamp (ULTRAVIOLET PRODUCTS INC, SAN GABRIEL, C.A. JnC SC-1) fitted with a G-275 filter, which results in 95% of the emission at 254nm. Mains electricity to the lamp was supplied through a voltage stabiliser (ADVANCED ELECTRONICS, CV 100A). The lamp was used in a horizontal position in the apparatus shown in Figure 2.1. The irradiation vessel was positioned 20cm directly beneath the UV source, with a shutter regulating exposure, positioned between. This was an iris camera shutter (G.B. KERSHAW 630) with a 2cm aperture and fitted with a cable release. The shutter was electronically tripped using a relay switch and the exact exposure time recorded on a millisecond timer (MARCONI INSTRUMENTS LTD). The irradiation vessel was a jacketed, straight-sided glass bowl, with an internal diameter of 5.2cm. Adequate stirring was ensured by passing a stream of filtered, humidified air onto the surface of the test suspension through a side jet. 9ml of bacterial test suspension was irradiated. The fractional increase in the distance between the source and the surface of the suspension after removal of each 0.2ml aliquot was considered to be insignificant. A flow of compressed air was directed over the source filter to prevent any build up of ozone. The bacterial suspension was equilibrated at 25°C prior to irradiation, which was subsequently carried out at room temperature.

This apparatus has been described previously (Smith, 1987).

METHODOLOGY

After the appropriate growth period, the bacterial cells were harvested and resuspended in ice-cold sterile M9 to give a final viable count of approximately 1 x 10^7 colony forming units per ml. The period of time between harvesting and irradiation of the bacterial suspension was standardised at 20 minutes. The Penray lamp was switched on at least 20 minutes before use. The bacterial suspension was equilibrated to 25°C in a water bath for the last 5 minutes of the 20 minute period. 9ml of the bacterial cell suspension was transferred to the irradiation vessel which had been sterilised by 254nm UV radiation from the Penray light source for 20 minutes. A 0.2ml aliquot was removed for an initial viable count assessment and after each subsequent fluence to determine the surviving fraction.

2.5.3 DETERMINATION OF THE FLUENCE RATE OF ULTRAVIOLET RADIATION

254nm SOURCE

The fluence rate was determined by routine chemical actinometry (Hatchard and Parker, 1956). The method uses potassium ferroxalate as the actinometer and relies on the light-catalysed production of Fe^{2+} ions in a solution of $K_3Fe(C_2O_4)_3$. The solution absorbs light completely in the UV region, the yield is independent of the fluence rate and the quantum yield of the reaction is constant.

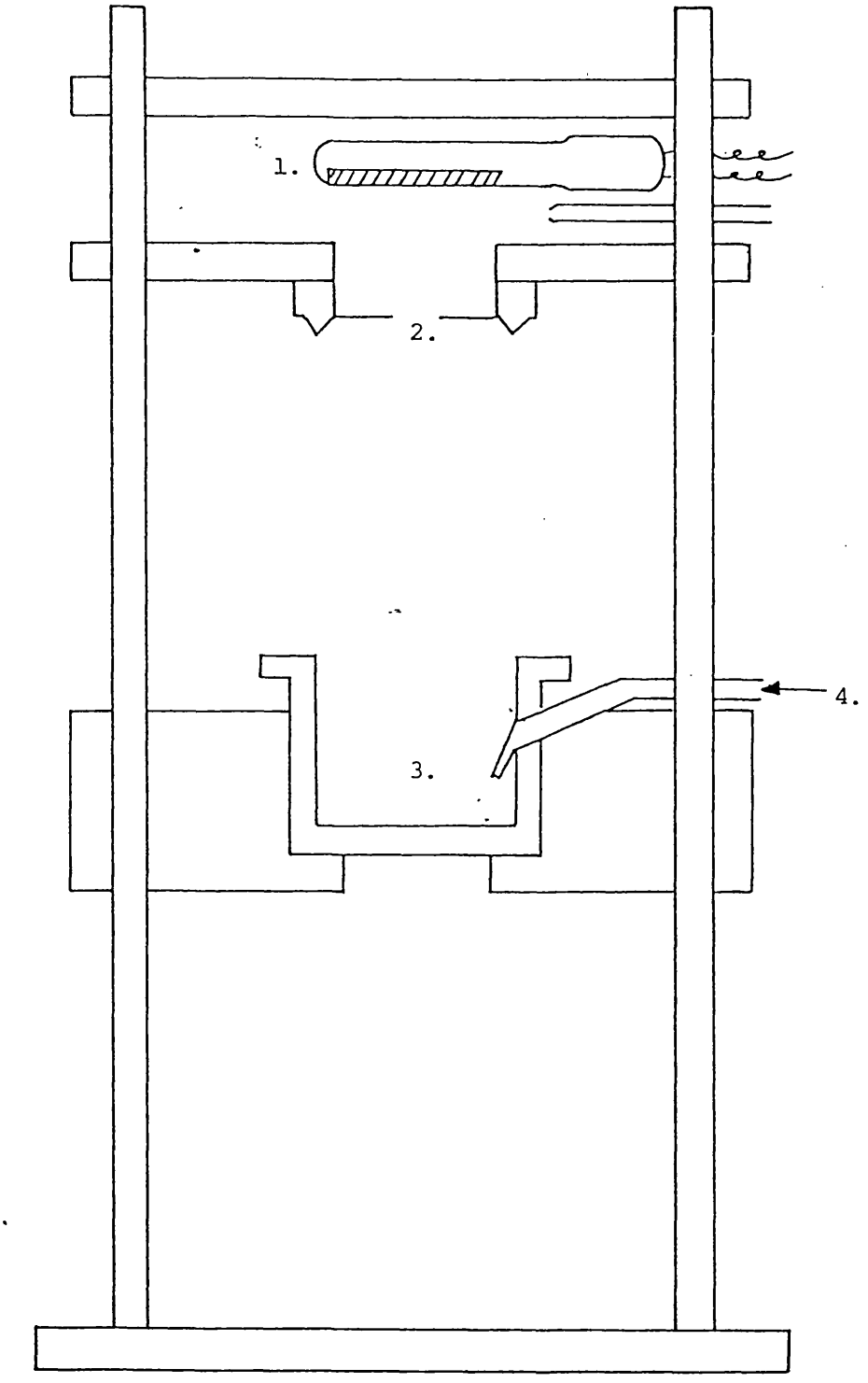

Figure 2.1. Diagram of the apparatus for 254nm UV-irradiation.

UV Source	(1)	Irradiation Vessel	(3)
Shutter	(2)	Air Inlet	(4)

Actinometry was performed under red light according to the method of Jagger (1967), by irradiation of 8.8ml of actinometer solution in the irradiation vessel. It was intended that this method would take into account any internal reflection arising from the use of the glass irradiation vessel. A calibration curve of optical density at 510nm against amount of ferrous ions (shown in APPENDIX E) was constructed and used to determine the amount of ferrous ions formed by the radiation. The fluence rate was calculated from this, using the constant pertaining to 254nm as described by Jagger (1967).

CALIBRATION OF A THERMOPILE

Conversion of incident energy from microvolts to fluence rate was made by reference to the calibration for a thermopile determined by potassium ferroxalate actinometry. A number of fluence rates obtained at different distances from the UV source were determined by chemical actinometry and plotted against the thermopile reading for a Oriel 7101 detector. This graph is shown in Figure 2.2. From the slope of this graph a conversion factor for millivolts to Wm^{-2} of 0.03597 was calculated.

2.5.4 PHOTOREACTIVATION PROCEDURES

APPARATUS

The apparatus is shown diagrammatically in Figure 2.3. All fittings were mounted on an optical bench. This apparatus has been described previously (Smith, 1987).

LIGHT SOURCE

Continuous broad-band light was produced by a Tutor 2 Projector (RANK ALDIS, POWER 300W - MAX LAMP 24V 250W).

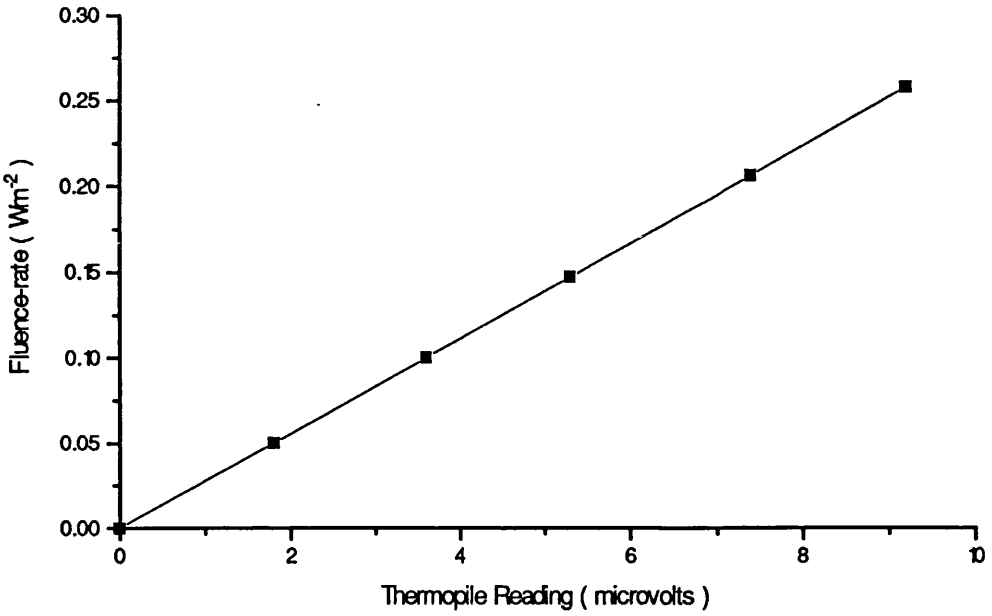

Figure 2.2. Calibration curve for the Oriel 7101 thermopile, plotting fluence rate determined by actinometry against the thermopile reading in microvolts.

FILTERS

The continuous broad-band light was filtered through a 2cm pathlength solution containing 1.2% copper sulphate and 1.4% cobaltous sulphate and a purple glass filter (EALING 26-3384). The resulting transmission spectrum is shown in Figure 2.4. The transmitted light was a continuous band of wavelengths between 350nm and 420nm, which is the biologically effective region for photoreactivation (Smith, 1987; Jagger *et al.*, 1969). No measurable transmission was recorded in the infra-red range.

ILLUMINATION VESSEL

The bacterial suspension for photoreactivation was placed in a 1cm pathlength glass cuvette (UNICAM) fitted with a plastic lid. These were stored in 70% ethanol, dried by a stream of compressed air and sterilised by 254nm radiation from a Penray lamp for 15 minutes.

TEMPERATURE CONTROL UNIT

This consisted of a rectangular glass vessel 10cm x 10cm x 2.5cm with two optically flat surfaces (EALING LTD) and an aluminium lid assembly, incorporating an insert to hold the illumination vessel in the light path. A continuous flow of water was supplied to the vessel through one tube from a water bath (GRANT SE MODEL) at 25°C by means of a flow-inducer (WATSON-MARLOW, FALMOUTH), and removed by a constant level syphon tube. The rate of flow was set so that the flow of water into the illumination vessel was approximately the same as the flow out via the syphon tube. Temperature equilibration was achieved in approximately 4 minutes and maintained throughout within ± 0.1°C.

For experiments requiring the temperature to be above 25°C, water was supplied from a different water bath (GRANT JB MODEL) set at the required temperature to give the necessary temperature in the temperature control unit.

For experiments requiring the temperature to be below 25°C, water was supplied from a different water bath (GRANT JB MODEL) cooled using a Bath Cooler (U-COOL, NESLAB) set at the required temperature to give the necessary temperature in the temperature control unit.

Routine temperature measurements were made throughout each experiment using a Comark probe thermometer.

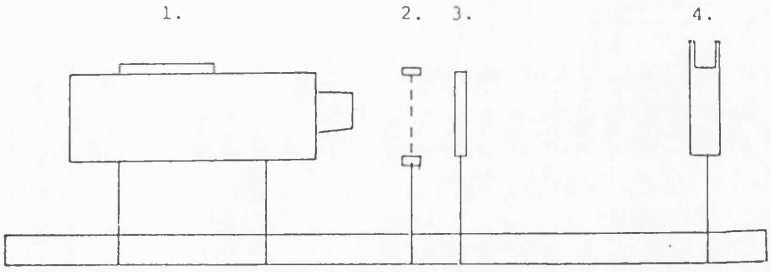

Figure 2.3. Diagram of the apparatus used for photoreactivation.

Projector	(1)	Temperature Control Unit and	
Shutter	(2)	Illumination Vessel	(4)
Filter Holders	(3)		

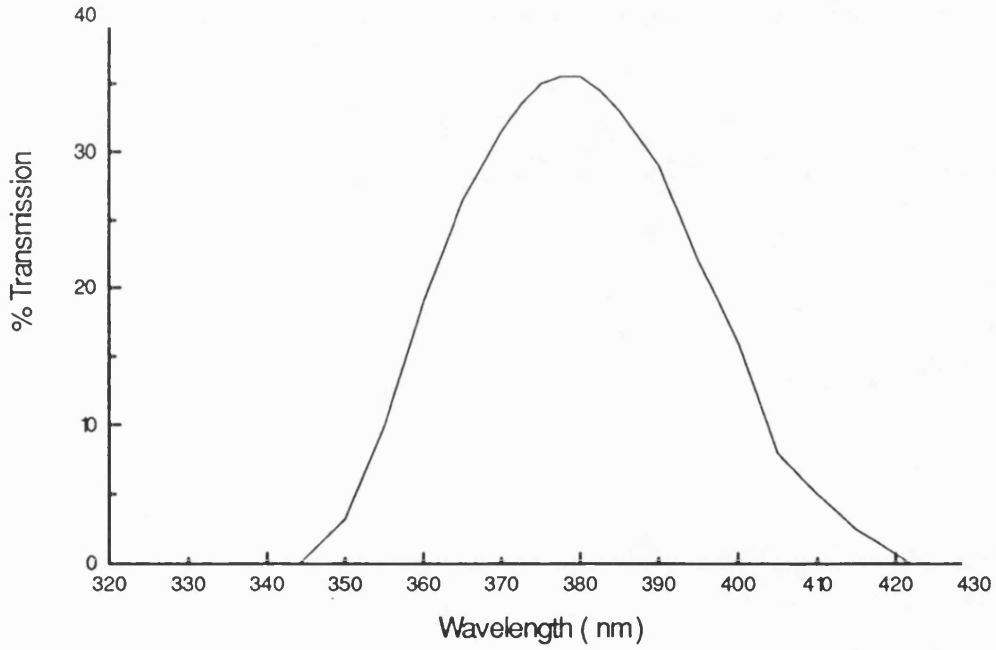

Figure 2.4. Transmission properties of the filters used in the photoreactivating experiments.

METHODOLOGY

After UV-irradiation, the bacterial suspension to be photoreactivated was held in a 25°C water bath for 20 minutes to allow formation of any photoreactivating enzyme - substrate complexes. 3.0ml of the bacterial suspension was transferred to an illumination vessel. 3.0ml of unirradiated bacterial suspension was also transferred to an illumination vessel, to act as a control. The cuvettes were then placed in the temperature control unit. A piece of opaque material (the 'Shutter') was placed between the projector assembly and the irradiation vessel, after which the lamp was switched on. This screen was removed at the same instant that the stop watch was started to time the photoreactivation period.

Separate UV-irradiated samples were used for each photoreactivating exposure, since it has been shown that fractionated doses have an increased effect (Tyrrell, 1971).

A comparative estimate of the fluence rate was made using another calibrated thermopile, an Oriel 7102 detector, which was positioned such that its window corresponded to the front face of the glass cuvette. A conversion factor of 0.025 was calculated as described in Section 2.5.3 and used to convert millivolts to Wm^{-2}.

CHAPTER THREE

CLONING AND SEQUENCING OF THE *phr*A GENE

3.1 INTRODUCTION

The first objective of this study was to sequence the insert from pAS01, which is thought to contain the *phr*A gene (Smith and Moss, 1988). In order to achieve this aim, the insert was subcloned into plasmid pUC19. The reasoning for this was pUC19 has the M13 Universal Primer and M13 Reverse Primer sites (Messing *et al.* 1981) either side of the polycloning site, into which the SphI-SphI restriction fragment in pAS01 could be cloned and then easily sequenced. The sequencing was performed using the chain termination method of Sanger *et al.* (1977). The resulting sequence was analysed using the Staden and GCG programmes on the SERC Daresbury Seqnet computer system.

3.2 METHODS

The majority of the cloning and sequencing techniques have already been described in Chapter 2.

The preparation of plasmid DNA prior to sequencing and other relevant methods are described in detail in the following section.

3.3 RESULTS

3.3.1 SUB-CLONING OF THE INSERT IN pAS01 INTO pUC19

PREPARATION OF THE SphI-SphI RESTRICTION FRAGMENT FROM pAS01

Plasmid pAS01 was isolated and purified as described in Section 2.2.2. The concentration of the purified plasmid DNA was calculated as described in Section 2.2.3. 20μg of pAS01 plasmid DNA was digested with an excess of restriction enzyme SphI for 2 hours at 37°C to ensure complete digestion. The resulting SphI-SphI restriction fragment was isolated and purified as described in Section 2.2.6. The concentration of the purified fragment DNA was calculated as described in Section 2.2.3.

PREPARATION OF VECTOR DNA

Plasmid pUC19 (see Figure 3.1) was isolated and purified as described in Section 2.2.2. The concentration of the purified plasmid DNA was calculated as described in Section 2.2.3. The plasmid DNA was digested with an excess of restriction enzyme SphI for 2 hours at 37°C to ensure complete digestion. A small sample was run on an agarose gel to confirm that digestion had taken place. The restriction enzyme was inactivated by incubating at 85°C for 30 minutes, then allowing the reaction mixture to cool at room temperature for 30 minutes.

The pUC19 / SphI restricted DNA was treated with Alkaline Phosphatase to dephosphorylate the sticky ends of the linear DNA, to prevent self-ligation, as described in Section 2.2.7. The Alkaline Phosphatase was inactivated by incubating at 85°C for 15 minutes, then allowing the reaction mixture to cool at room temperature for 30 minutes.

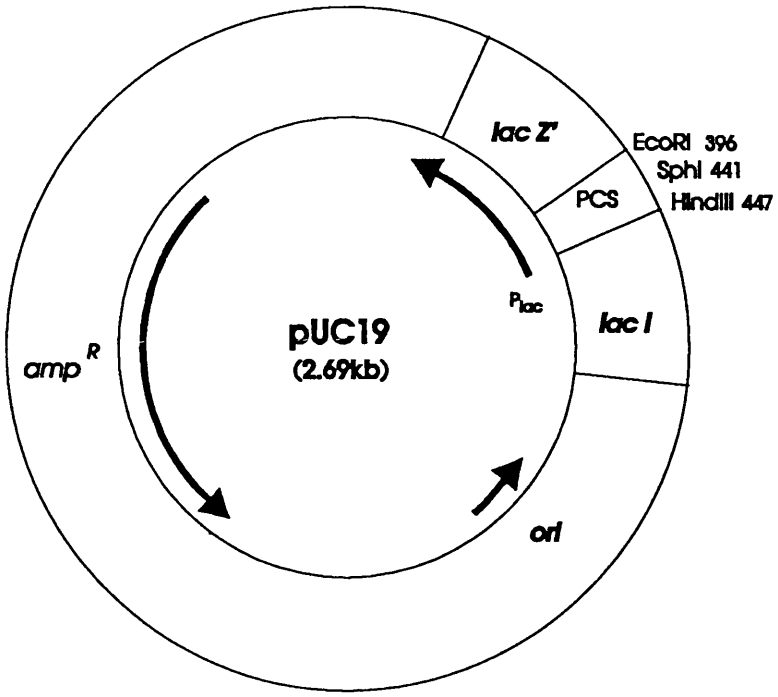

Figure 3.1. Diagram of pUC19, showing the important features.

LIGATION OF INSERT AND VECTOR DNA

The insert DNA was ligated to the vector DNA in the following ligation mixture :-

pUC19 / SphI	≅ 0.1μg
SphI - SphI RESTRICTION FRAGMENT	≅ 0.15μg
STERILE DDDW	to 7μl

This reaction mixture was incubated at 45°C for 5 minutes to melt any cohesive bonds that had formed, then cooled on ice for 5 minutes. Then the following were added :-

BUFFER (10X CONCENTRATE)	1µl
ATP (10mM)	1µl
T_4 DNA LIGASE (1 unit/µl)	1µl

This was mixed by vortexing, spun down and incubated at 15°C for 10 hours.

Two separate ligation mixtures were set up, termed LIGATION A and LIGATION B.

PRODUCTION OF COMPETENT JM83 CELLS

Fresh competent cells of JM83 were prepared as described in Section 2.2.9. These were stored at 4°C for 16 hours and then used for transformation.

TRANSFORMATION OF LIGATION MIXTURE INTO JM83

Transformation of the competent JM83 cells with the ligation mixtures were performed as described in Section 2.2.10. The 12 hour liquid cultures were streaked out onto LB / amp plates and incubated at 37°C for 48 hours. Growth was seen on plates from both LIGATION A and LIGATION B.

CONTROLS

The following controls were performed alongside the ligation mixture described above :-

a) LIGATION MIX - NO ENZYME

The T_4 DNA ligase was omitted from the ligation mixture. No growth was seen after incubation in the LB / amp broth after 12 hours at 37°C or after streaking onto LB / amp plates after incubation for 48 hours at 37°C.

b) LIGATION MIX - NO INSERT DNA

The insert DNA was omitted from the ligation mixture. Growth was seen after incubation in the LB / amp broth after 12 hours at 37°C and after streaking onto LB / amp plates after incubation for 48 hours at 37°C. Restriction analysis showed the plasmid present to be indistinguishable from pUC19.

c) TRANSFORMATION MIX - NO LIGATION MIX

No ligation mixture was added to the competent cells of JM83, which then underwent the transformation procedure. No growth was seen after incubation in the LB / amp broth after 12 hours at 37°C or after streaking onto LB / amp plates after incubation for 48 hours at 37°C.

d) COMPETENT CELLS - VIABILITY TEST

The competent cells of JM83 were streaked out on LB, LB / amp and LB / str plates and incubated at 37°C for 48 hours. No growth was seen on LB / amp plates, while growth occurred on the LB and LB / str plates.

3.3.2 ANALYSIS OF THE NEW PLASMIDS

Plasmid DNA was isolated from individual colonies in batches of twelve as described in Section 2.2.2. The plasmids were restricted with restriction enzyme EcoRI and then loaded onto an agarose gel and run for 90 minutes, using pUC19 / EcoRI as a control. Plasmids which showed up on the gel to be heavier than pUC19 were then restricted with restriction enzyme SphI to see if the insert DNA could be cut out of the plasmids. This proved to be the case for all plasmids tested. These plasmids were then restricted with restriction enzymes HindIII and EcoRV (a restriction enzyme known to have one site

within the SphI - SphI restriction fragment from pAS01). The results showed two different plasmids had been produced, depending on the orientation of the SphI - SphI restriction fragment in pUC19 - see Agarose Gel 3.1. These were termed pND01 and pND02 - see Figures 3.2 and 3.3.

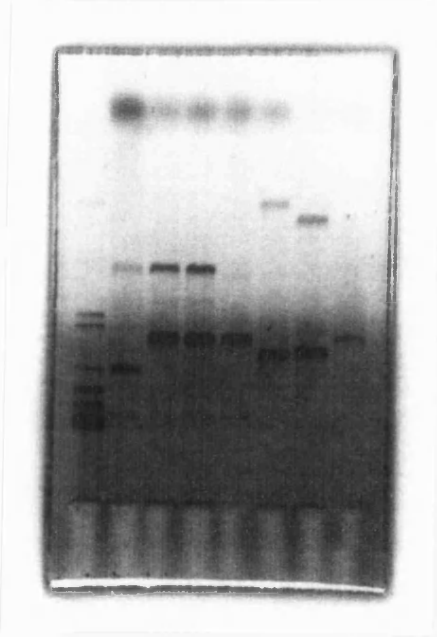

Agarose Gel 3.1. Restriction digests of plasmids pAS01, pND01, pND02 and pUC19.
Lane 1, λDNA / HindIII; Lane 2, pAS01 / SphI; Lane 3, pND01 / SphI;
Lane 4; pND02 / SphI; Lane 5, pUC19 / SphI; Lane 6, pND02 / HindIII + EcoRV;
Lane 7, pND01 / HindIII + EcoRV; Lane 8, pUC19 / HindIII + EcoRV.

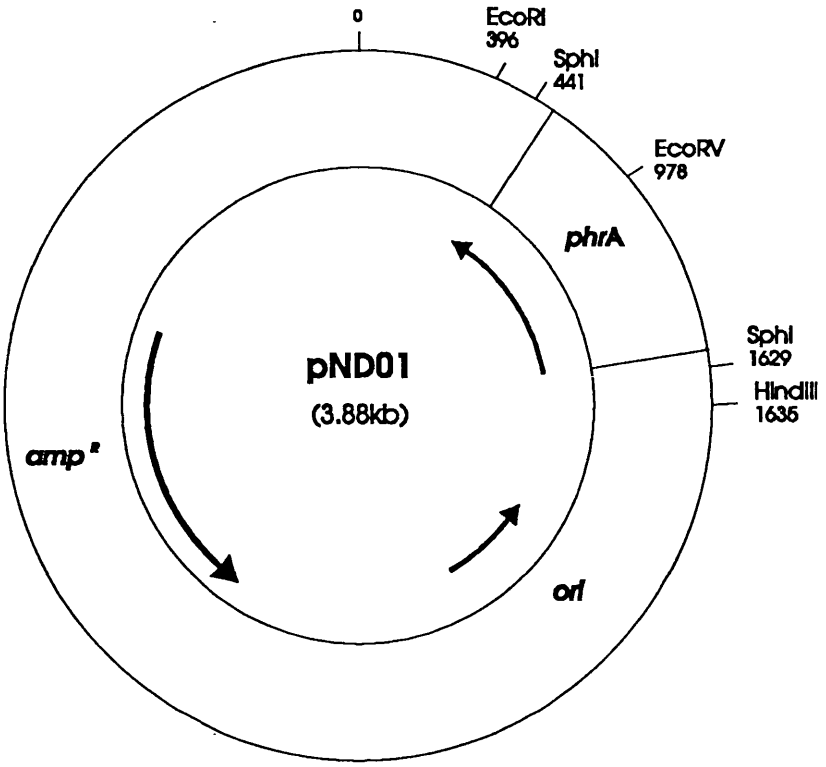

Figure 3.2. Diagram of pND01, showing the important features.

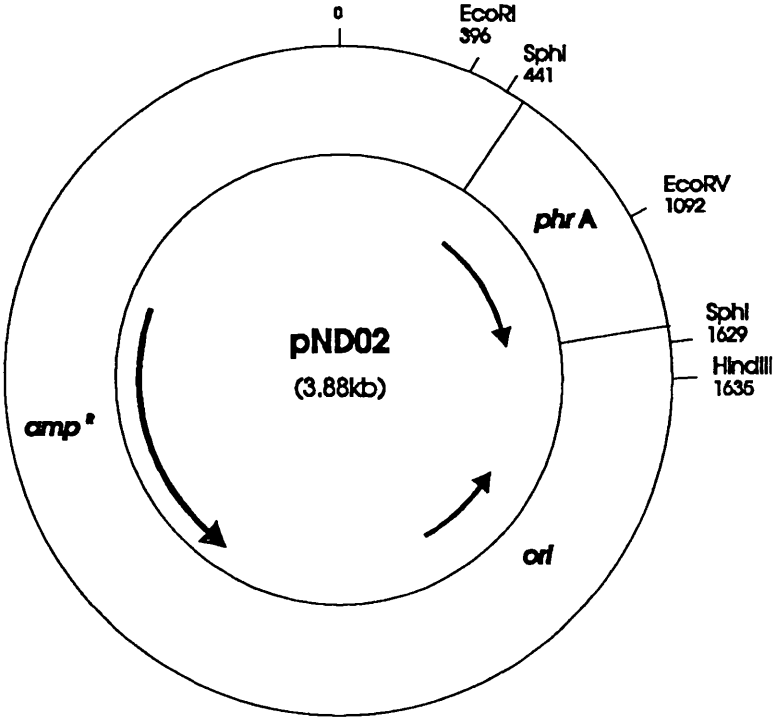

Figure 3.3. Diagram of pND02, showing the important features.

3.3.3 SEQUENCING OF THE INSERT IN pND01

The SphI - SphI restriction fragment inserted into pUC19 to form pND01 was sequenced using the chain termination method of Sanger *et al* (1977). Sequencing was performed using the Sequenase® Version 2.0 kit (USB, OHIO, USA). The preparation of polyacrylamide gels for sequencing, materials used and the treatment of the gel after electrophoresis have been described previously in Section 2.3.

DENATURING PLASMID DNA

Plasmid pND01 was isolated and purified as described in Section 2.2.2, and resuspended in TE (pH 7.5). The concentration of the plasmid DNA was calculated as described in Section 2.2.3, and diluted to ≅ 0.5μg/μl with TE (pH 7.5). The plasmid DNA was prepared for sequencing by denaturing with NaOH and then removing the NaOH and other impurities by spun-column chromatography. The following reaction mixture was set up :-

pND01 PLASMID DNA	20μl	(≅ 10μg)
DENATURING SOLUTION (1M NaOH, 1mM EDTA)	5μl	

This was vortexed briefly, spun down and incubated at room temperature for 30 minutes. A Sephacryl S-400 column (PHARMACIA) was prepared in accordance with the manufacturers instructions. The denaturing reaction mixture was slowly pipetted onto the flat upper surface of the compacted bed of Sephacryl S-400, and the column centrifuged for 2 minutes at 1500 rpm. The eluted solution contained purified denatured plasmid DNA in approximately 25μl of TE (pH 7.5).

ANNEALING

The following annealing reaction mixture was set up :-

PURIFIED DENATURED PLASMID DNA	7µl
PRIMER (0.5pmol/µl)	1µl
REACTION BUFFER (5X CONCENTRATE)	2µl

This was mixed by vortexing briefly, spun down and incubated at 65°C for 2 minutes, then allowed to cool slowly from 65°C to room temperature over 30 minutes. The annealed mixture was stored on ice until ready for labelling (no longer than 4 hours).

LABELLING

The following labelling reaction mixture was set up :-

ANNEALED MIXTURE (TEMPLATE / PRIMER)	10µl
DTT (0.1M)	1µl
[α - ^{35}S] dATP	1µl
LABELLING MIX	2µl
SEQUENASE ® VERSION 2.0 (1.5units/µl)	2µl

This was mixed by vortexing briefly, spun down and incubated at room temperature for 5 minutes.

TERMINATION

Prior to the labelling reaction, 2.5µl of ddGTP / ddATP / ddTTP / ddCTP were placed in four separate microcentrifuge tubes. The tubes were pre-warmed at 37°C for at least 1 minute. 3.5µl of labelling mix was added to each tube, vortexed briefly, spun down, and

incubated at 37°C for 5 minutes. 4µl of 'STOP' solution was added to each tube, vortexed briefly, spun down, and stored on ice until ready to load onto a polyacrylamide sequencing gel, prepared as described previously in Section 2.3.

LOADING

A sample of each tube G - A - T- C (approximately 2.5 - 3.0µl) was incubated at 75-80°C for 2 minutes, then chilled briefly on ice. This was to prevent most nucleic acid secondary structures from re-annealing. The samples were then immediately loaded onto a polyacrylamide sequencing gel in the order G - A - T- C. This order was strictly adhered to - see Section 2.3.7.

RUNNING A GEL

Samples were loaded onto a polyacrylamide sequencing gel at different time intervals to run between 9 hours and 1 hour, depending on the part of the sequence to be read. The gels were run, disassembled, soaked in methanol:acetic acid:water, dried and exposed to autoradiography film, as described in Section 2.3.

READING THE SEQUENCE

The film was developed and dried as described in Section 2.3.10. As soon as it was dry, the left and right sides of the gel were identified, and the film labelled with the date, primer details and the times run.

The sequence was read over a light box (COPILITE, HALCO SUNBURY CO LTD) and was recorded twice by myself and Dr A.H. Ahmed. The autoradiographs are shown in Appendix C.

SEQUENCING CLOSE TO THE PRIMER

It has been shown (Tabor and Richardson, 1989) that di-deoxy-nucleotide triphosphates are incorporated by Sequenase ® Version 2.0 more efficiently relative to deoxy-nucleotide triphosphates in the presence of Mn^{2+}. Thus the addition of Mn^{2+} to normal sequencing reactions (with fixed di-deoxy to deoxy ratios) reduces the average length of DNA synthesised, intensifying bands corresponding to sequences close to the primer.

Using the reaction conditions described previously, it was possible to read about 100 bases away from the primer. By reducing the amount of template DNA in the 'ANNEALING' reaction to about 1μg, adding 1μl of Mn^{2+} buffer to the 'LABELLING' reaction, and reducing the 'LABELLING' and 'TERMINATION' reaction times to 2 minutes, it was possible to read up to 20 bases away from the primer.

BUILDING UP THE SEQUENCE

The entire length of the SphI - SphI restriction fragment was sequenced for both strands using the M13 Universal and M13 Reverse Primers as starting points. Thus points of compression within the sequence on one strand could be "ironed out" by sequencing the complementary strand. This method also reduced the possibility of errors when reading the sequence, as any discrepancy was highlighted immediately.

PRIMERS

Using the above sequencing method, it was possible to read accurately up to about 300bps from the primer. The forward and reverse strands of the insert DNA were sequenced using the primers indicated in Table 3.1. Problems were initially encountered using the M13 Reverse Primer. This was due to the strain of pUC19 used been one of a series of rogue strains of pUC19, which have a 'C' base missing at position 33, between the 'T' and 'A' - see Figure 3.5. This disrupts the annealing of the M13 Reverse Primer (Dr P. Towner,

Personal Communication). This was overcome by synthesising a new 1st Reverse Primer as indicated in Table 3.1.

FORWARD PRIMERS		REVERSE PRIMERS	
NAME	SEQUENCE	NAME	SEQUENCE
M13 UNIVERSAL PRIMER	5'-GTAAAACGACGGCCAGT-3'	1ST REVERSE PRIMER	5'-ACGCCAAGCTTGCATGC-3'
2ND FORWARD PRIMER	5'-CCTGTAGTGGTTCATCG-3'	2ND REVERSE PRIMER	5'-AGTTTGTCCAGTTTGCT-3'
3RD FORWARD PRIMER	5'-CCTGTAACCTTGCGGAT-3'	3RD REVERSE PRIMER	5'-CATCCGCAAGGTTACAG-3'
4TH FORWARD PRIMER	5'-AGCAAACTGGACAAACT-3'	4TH REVERSE PRIMER	5'-CGATGAACCACTACAGG-3'

Table 3.1. Primers used in the sequencing of the insert.

3.3.4 THE SEQUENCE OF THE INSERT IN pND01

NUCLEOTIDE SEQUENCE

The resulting sequence was 1188bp in length, flanked by SphI restriction sites at both ends, as expected, and with the sequences expected for plasmid pUC19 either side of the SphI site within the polycloning site on that plasmid - see Figure 3.5. The sequence was analysed using the Staden and GCG programmes on the Daresbury Seqnet computer system.

No significant open reading frame was found on the forward strand of the sequence, using the GCG program 'FRAMES'. Upon reversing and complementing the sequence, an open reading frame starting from an ATG start codon was discovered which covered 1020 bases - see Figure 3.4.

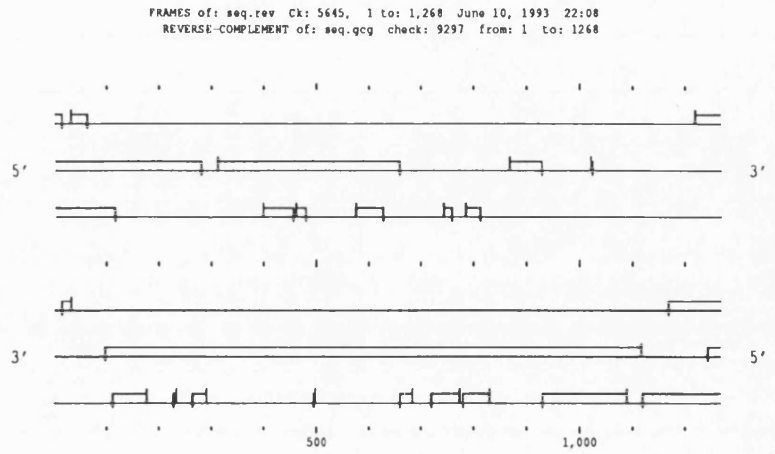

Figure 3.4. Open Reading Frames on the Forward and Reverse Strand of the Insert.

Preceding the ATG start codon, areas were identified which bore similarity to the consensus sequences for *E.coli* transcriptional and translational signals. These are discussed in more detail in Section 3.4.

pUC19 →

1 AACAATTTCA CACAGGAAAC AGCTATGACC ATATTACGCC AAGCTTGCAT

|→ SphI - SphI Restriction Fragment

51 GCAACTGGCG CAGCAGTTCG GTATTACCGG CCCTCCTGGA CCGACGCTTT

|→ RBS

101 AAATACCTTT CCACTGGCGA GACGCGAAAA ACCCTGCTGT GTC*AGG*CGCT

----- ⇒ Gene

151 G*ATG*TCGGAG CCTGACTTGT TGATTCTTGA TGAGCCGTTC GATGGCCTGG

201 ATGTTGCCTC ACGTCAGCAG CTGGCTGAGC GACTCGCCTC GTTACATCAG

251 TCCGGTATTA CTCTGGTACT GGTGCTCAAT CGCTTCGATG AGATCCCGGA

301 GTTTGTCCAG TTTGCTGGCG TGCTGGCGGA TTGCACGTTA GCGGAAACTG

351 GCGCTAAAGA GGAACTGCTC CAACAAGCAC TCGTCGCGCA ACTGGCGCAT

401 AGTGAACAGC TTGAAGGTGT GCAACTGCCG GAGCCGGATG AACCTTCAGC

451 ACGTCACGCC TTACCCGCCA ACGAACCGCG CATTGTGCTG AACAATGGCG

501 TGGTTTCTTA TAACGATCGC CCCATTCTTA ATAACCTTAG CTGGCAGGTG

551 AATCCAGGCG AACACTGGCA AATTGTCGGG CCAAATGGTG CAGGAAAATC

601 GACGTTATTA AGCCTGGTTA CTGGCGATCA TCCGCAAGGT TACAGCAACG

651 ATTTGACGGC TTTTCGACGA CGTGCCGGCA GCGGCGAAAC CATCTGGGAT

701 ATCAAAAAGC ATATCGGTTA CGTCAGCAGT AGTTTGCATC TGGATTACCG

751 GGTCAGCACT ACCGTGCGTA ATGTGATTCT TTCTGGCTAT TTTGATTCGA

801 TTGGCATTTA TCAGGCCGTT TCGGATCGCC AGCAAAAACT GGTGCAGCAG

851 TGGCTGGATA TTCTCGGCAT TGATAAACGC ACGGCTGACG CTCCGTTCCA

901 TAGTCTTTCC TGGGGACAGC AGCGTCTGGC GCTGATTGTC CGCGCACTGG

951 TGAAACATCC GACGTTGCTT ATTCTCGATG AACCACTACA GGGGCTTGAT

1001 CCGCTGAATC GCCAGCTTAT CCGCCGTTTT GTTGATGTGC TGATTAGCGA

1051 AGGTGAAACG CAATTGTTGT TTGTTTCGCA CCACGCTGAA GATGCGCCTG

1101 CCTGTATTAC CCATCGTCTT GAGTTCGTGC CGGACGGTGG ACTCTATCGC

.....-----.....Termination Sequence.....

1151 TATGTGCTGA CAAAAATATA T*TGA*GTCGGT AGTGCTGACC TTCGCGGAGG

..... |→ pUC19

1201 CGGCCTTAGC ACCCTCTCCG GCCAACGGTT **CGACGCATGC** CTGCAGGTCG

|→

1251 ACTCTAGAGG ATCCCCGG

Figure 3.5. The sequence of the insert from pND01.

AMINO ACID SEQUENCE

The coding region of the open reading frame codes for a protein of 340 amino acids, with a calculated molecular weight of 37,894 Da. This is a very similar size to the protein isolated by Snapka and Sutherland (1980), however the amino acid composition is very different to the one presented by these workers. This is discussed in Section 3.4. The amino acid sequence is presented in Figure 3.6.

116	GGC	GAG	ACG	CGA	AAA	ACC	CTG	CTG	TGT	CAG	GCG	CTG
	Met	Ser	Glu	Pro	Asp	Leu	Leu	Ile	Leu	Asp	Glu	Pro
152	ATG	TCG	GAG	CCT	GAC	TTG	TTG	ATT	CTT	GAT	GAG	CCG
	Phe	Asp	Gly	Leu	Asp	Val	Ala	Ser	Arg	Gln	Gln	Leu
188	TTC	GAT	GGC	CTG	GAT	GTT	GCC	TCA	CGT	CAG	CAG	CTG
	Ala	Glu	Arg	Leu	Ala	Ser	Leu	His	Gln	Ser	Gly	Ile
224	GCT	GAG	CGA	CTC	GCC	TCG	TTA	CAT	CAG	TCC	GGT	ATT
	Thr	Leu	Val	Leu	Val	Leu	Asn	Arg	Phe	Asp	Glu	Ile
260	ACT	CTG	GTA	CTG	GTG	CTC	AAT	CGC	TTC	GAT	GAG	ATC
	Pro	Glu	Phe	Val	Gln	Phe	Ala	Gly	Val	Leu	Ala	Asp
296	CCG	GAG	TTT	GTC	CAG	TTT	GCT	GGC	GTG	CTG	GCG	GAT
	Cys	Thr	Leu	Ala	Glu	Thr	Gly	Ala	Lys	Glu	Glu	Leu
332	TGC	ACG	TTA	GCG	GAA	ACT	GGC	GCT	AAA	GAG	GAA	CTG
	Leu	Gln	Gln	Ala	Leu	Val	Ala	Gln	Leu	Ala	His	Ser
368	CTC	CAA	CAA	GCA	CTC	GTC	GCG	CAA	CTG	GCG	CAT	AGT
	Glu	Gln	Leu	Glu	Gly	Val	Gln	Leu	Pro	Glu	Pro	Asp
404	GAA	CAG	CTT	GAA	GGT	GTG	CAA	CTG	CCG	GAG	CCG	GAT
	Glu	Pro	Ser	Ala	Arg	His	Ala	Leu	Pro	Ala	Asn	Glu
440	GAA	CCT	TCA	GCA	CGT	CAC	GCC	TTA	CCC	GCC	AAC	GAA
	Pro	Arg	Ile	Val	Leu	Asn	Asn	Gly	Val	Val	Ser	Tyr
476	CCG	CGC	ATT	GTG	CTG	AAC	AAT	GGC	GTG	GTT	TCT	TAT
	Asn	Asp	Arg	Pro	Ile	Leu	Asn	Asn	Leu	Ser	Trp	Gln
512	AAC	GAT	CGC	CCC	ATT	CTT	AAT	AAC	CTT	AGC	TGG	CAG
	Val	Asn	Pro	Gly	Glu	His	Trp	Gln	Ile	Val	Gly	Pro
548	GTG	AAT	CCA	GGC	GAA	CAC	TGG	CAA	ATT	GTC	GGG	CCA
	Asn	Gly	Ala	Gly	Lys	Ser	Thr	Leu	Leu	Ser	Leu	Val
584	AAT	GGT	GCA	GGA	AAA	TCG	ACG	TTA	TTA	AGC	CTG	GTT
	Thr	Gly	Asp	His	Pro	Gln	Gly	Tyr	Ser	Asn	Asp	Leu
620	ACT	GGC	GAT	CAT	CCG	CAA	GGT	TAC	AGC	AAC	GAT	TTG
	Thr	Ala	Phe	Arg	Arg	Arg	Ala	Gly	Ser	Gly	Glu	Thr
656	ACG	GCT	TTT	CGA	CGA	CGT	GCC	GGC	AGC	GGC	GAA	ACC
	Ile	Trp	Asp	Ile	Lys	Lys	His	Ile	Gly	Tyr	Val	Ser
692	ATC	TGG	GAT	ATC	AAA	AAG	CAT	ATC	GGT	TAC	GTC	AGC
	Ser	Ser	Leu	His	Leu	Asp	Tyr	Arg	Val	Ser	Thr	Thr
728	AGT	AGT	TTG	CAT	CTG	GAT	TAC	CGG	GTC	AGC	ACT	ACC
	Val	Arg	Asn	Val	Ile	Leu	Ser	Gly	Tyr	Phe	Asp	Ser
764	GTG	CGT	AAT	GTG	ATT	CTT	TCT	GGC	TAT	TTT	GAT	TCG
	Ile	Gly	Ile	Tyr	Gln	Ala	Val	Ser	Asp	Arg	Gln	Gln
800	ATT	GGC	ATT	TAT	CAG	GCC	GTT	TCG	GAT	CGC	CAG	CAA

	Lys	Leu	Val	Gln	Gln	Trp	Leu	Asp	Ile	Leu	Gly	Ile
836	AAA	CTG	GTG	CAG	CAG	TGG	CTG	GAT	ATT	CTC	GGC	ATT
	Asp	Lys	Arg	Thr	Ala	Asp	Ala	Pro	Phe	His	Ser	Leu
872	GAT	AAA	CGC	ACG	GCT	GAC	GCT	CCG	TTC	CAT	AGT	CTT
	Ser	Trp	Gly	Glu	Glu	Arg	Leu	Ala	Leu	Ile	Val	Arg
908	TCC	TGG	GGA	CAG	CAG	CGT	CTG	GCG	CTG	ATT	GTC	CGC
	Ala	Leu	Val	Lys	His	Pro	Thr	Leu	Leu	Ile	Leu	Asp
944	GCA	CTG	GTG	AAA	CAT	CCG	ACG	TTG	CTT	ATT	CTC	GAT
	Glu	Pro	Leu	Gln	Gly	Leu	Asp	Pro	Leu	Asn	Arg	Gln
980	GAA	CCA	CTA	CAG	GGG	CTT	GAT	CCG	CTG	AAT	CGC	CAG
	Leu	Ile	Arg	Arg	Phe	Val	Asp	Val	Leu	Ile	Ser	Glu
1016	CTT	ATC	CGC	CGT	TTT	GTT	GAT	GTG	CTG	ATT	AGC	GAA
	Gly	Glu	Thr	Gln	Leu	Leu	Phe	Val	Ser	His	His	Ala
1052	GGT	GAA	ACG	CAA	TTG	TTG	TTT	GTT	TCG	CAC	CAC	GCT
	Glu	Asp	Ala	Pro	Ala	Cys	Ile	Thr	His	Arg	Leu	Glu
1088	GAA	GAT	GCG	CCT	GCC	TGT	ATT	ACC	CAT	CGT	CTT	GAG
	Phe	Val	Pro	Asp	Gly	Gly	Leu	Tyr	Arg	Tyr	Val	Leu
1124	TTC	GTG	CCG	GAC	GGT	GGA	CTC	TAT	CGC	TAT	GTG	CTG
	Thr	Lys	Ile	Tyr	Stop	.	.	.	.	.	.	.
1160	ACA	AAA	ATA	TAT	TGA	GTC	GGT	AGT	GCT	GAC	CTT	CGC

1 MSEPDLLILDEPFDGLDVASRQQLAERLASLHQSGITLVLVLNRFDEIPEFV

53 QFAGVLADCTLAETGAKEELLQQALVAQLAHSEQLEGVQLPEPDEPSARH

103 ALPANEPRIVLNNGVVSYNDRPILNNLSWQVNPGEHWQIVGPNGAGKSTL

153 LSLVTGDHPQGYSNDLTAFRRRAGSGETIWDIKKHIGYVSSSLHLDYRVST

204 TVRNVILSGYFDSIGIYQAVSDRQQKLVQQWLDILGIDKRTADAPFHSLSW

255 GQQRLALIVRALVKHPTLLILDEPLQGLDPLNRQLIRRFVDVLISEGETQLL

307 FVSHHAEDAPACITHRLEFVPDGGLYRYVLTKIY

Figure 3.6. The amino acid sequence of the major open reading frame on the insert sequenced from pND01, showing the three letter codes for the amino acids against the nucleotide sequence (above) and the numbered single letter codes for the amino acids (below).

REGISTRATION OF THE SEQUENCE

Upon searching on the EMBL and GenBank databases for similar nucleotide and protein sequences using the GCG programs 'FASTA' and 'TFASTA', no significant matches were found. The open reading frame was thus termed the putative *phr*A gene.

A search was also performed on a DAP parallel computer for the amino acid sequence against the Owl Database Release 19.0 (February 1993) by Dr S.M. Keyse. In general, these searches are faster and more sensitive than equivalent searches performed on a conventional computer. No significant matches were found, however, a lot of matches were made to transport / membrane pump-type proteins. The significance of this is not yet known.

The sequence was registered with the European Molecular Biology Laboratory in Hiedleberg, Germany, in April 1993. The Accession Number is X69182. The gene was registered as the putative *phr*A gene, coding for a photolyase enzyme.

3.3.5 ANALYSIS OF THE SEQUENCE

With the variety of different computer programs available for analysing sequences, it would have been very easy to over analyse the sequence. The computer analysis of the putative *phr*A gene was initially kept to a minimum, concentrating rather on experimental work.

CODON PREFERENCE ANALYSIS

One of the most useful pieces of sequence data is codon preference analysis. The program used was the GCG program 'CODON PREFERENCE'. This program is a frame-specific gene finder that tries to recognise protein coding sequences by virtue of the similarity of their codon usage to a codon frequency table, or by the bias of their composition (usually GC) in the third position of each codon.

The three reading frames of the sequence were analysed. The average codon preference for the frame with the open reading frame was 0.7327 (Frame 2), compared with 0.5470 (Frame 1) and 0.5698 (Frame 3) for the other two frames - see Figure 3.7. This is comparable with the codon preference analysis of *phr*B, for example, where the average codon preference for the frame encoding the gene is 0.6124, compared to 0.5345 and 0.5555 for the other two frames.

PROTEIN ANALYSIS

Using the GCG program 'MOTIFS', the peptide sequence for the putative *phr*A gene was analysed for sequence motifs. The program works by searching through protein sequences for the patterns defined in the *PROSITE Dictionary of Protein Sites and Patterns.*

The one match found was for an ATP / GTP-binding site motif A (P-loop). It has been shown (Saraste *et al.*, 1990) that an appreciable proportion of proteins that bind ATP or GTP share a number of more or less conserved sequence motifs. The best conserved of

these motifs is a glycine-rich region, which probably forms a flexible loop between a beta-strand and an alpha-helix. This loop interacts with one of the phosphate groups of the nucleotide. This sequence motif is generally referred to as the 'A' consensus sequence or the 'P-loop'. The consensus pattern and the matching area on the putative *phr*A gene product are shown in Figure 3.8.

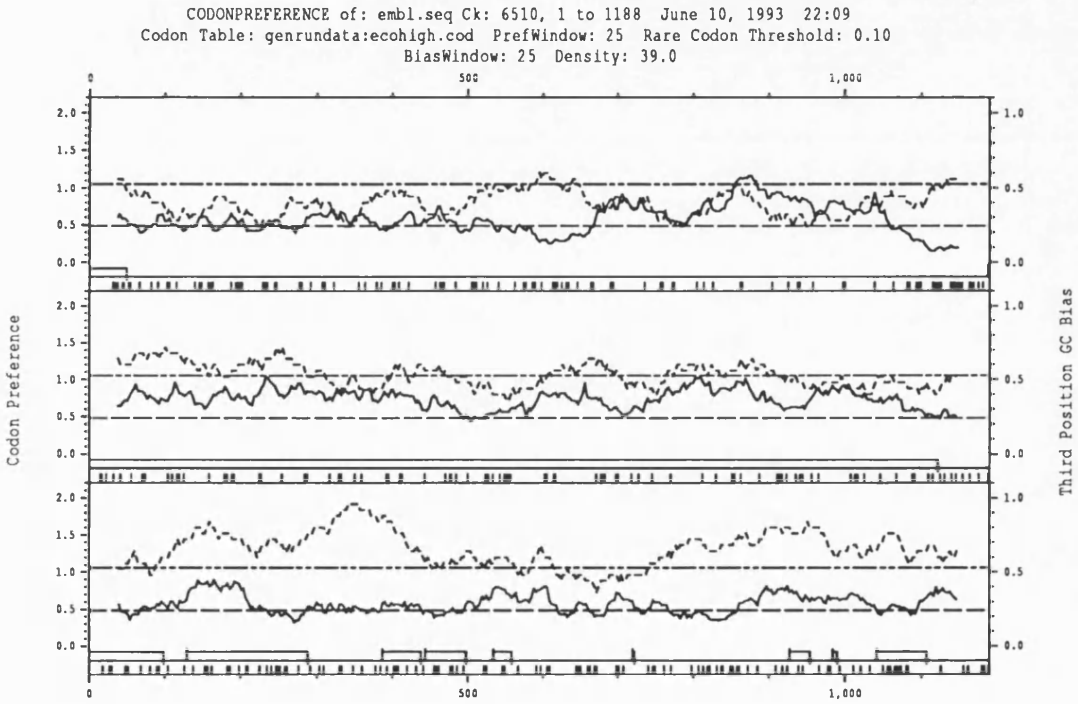

Figure 3.7. Codon preference analysis of the three reading frames.

The matching area on the protein sequence is found between positions 542 to 564 - see Figure 3.6. The significance of this ATP / GTP binding site is as yet unknown. It is hoped that maybe either the expression studies on the putative *phr*A gene product (Chapter 4) or the *in vivo* photoreactivation studies (Chapter 5) could cast further light on this matter.
No match was found to the DNA Photolyase motif, which was found when the peptide sequence from *phr*B was analysed using the 'MOTIFS' program.

[AG] - x (4) - G - K - [ST]

142 G - P - N - G - A - G - K - S 149

Figure 3.8. The consensus sequence of the P-loop (above) and the match with the putative *phr*A gene product (below).

RESTRICTION ENZYME ANALYSIS

Using the Staden program 'NIP', the theoretical restriction enzyme sites for the sequenced insert and plasmid vector pUC19 were obtained - see Figures 3.9 and 3.10. The term 'Cut Position' is used to indicate the number of the base immediately 5' to the cut produced by digestion with the relevant restriction enzyme. This confirmed previous work which had showed that there was an EcoRV site within the insert from pAS01. Restriction digests of plasmids pAS01, pND01, pND02 and pUC19 were performed to confirm this theoretical data in practice.

NAME	SEQUENCE	CUT POSITION	FRAGMENT LENGTHS
HindIII	A'AGCTT	42	41
SphI	GCATG'C	52	10
DraI	TTT'AAA	101	49
PvuII	CAG'CTG	221	120
EcoRV	GAT'ATC	701	480
SphI	GCATG'C	1240	539
PstI	CTGCA'G	1246	6
BamHI	G'GATCC	1260	14
			9

Figure 3.9. Important restriction enzyme sites in the 1268bp sequence obtained from the reverse-strand sequencing of pND01.

NB: The insert from pAS01 is between the two SphI sites at 48 and 1236.

NAME	SEQUENCE	CUT POSITION	FRAGMENT LENGTHS
PvuII	CAG'CTG	309	718
EcoRI	G'AATTC	397	88
BamHI	G'GATCC	418	21
PstI	CTGCA'G	440	22
SphI	GCATG'C	446	6
HindIII	A'AGCTT	448	2
PvuII	CAG'CTG	631	183
DraI	TTT'AAA	1566	935
DraI	TTT'AAA	1585	19
DraI	TTT'AAA	2277	692

Figure 3.10. Important restriction enzyme sites in the 2698bp plasmid vector pUC19. Plasmid pUC19 is numbered by the standard numbering system for the pUC plasmids (Sambrook *et al.*, 1989).

3.4 DISCUSSION

Sequencing of the insert from pAS01 showed that there was an open reading frame present which could code for a protein of 37, 894Da. This is similar in size to the *phr*A gene product studied by Snapka and Sutherland (1986). Having found an open reading frame beginning with an ATG start codon, other features associated with *E.coli* genes were investigated. Areas were identified which bore similarity to the consensus sequences for *E.coli* transcriptional and translational signals.

TRANSCRIPTION SIGNALS

Transcriptional promoters in *E.coli* generally exhibit common features (Rosenburg and Court, 1979, Siebenlist *et al*, 1980, Aoyama *et al*, 1983): a) centred approximately 10 base pairs 5' to the mRNA start, site a heptameric sequence TATAATG, called a Pribnow box, is found; b) centred about 35 base pairs upstream from the mRNA start site, the sequence TTGACA occurs; c) the distance between the Pribnow box and the -35 sequence is 17±2 base pairs.

Within the region 5' to the translational start site of the gene, two areas exhibit varying degrees of homology to the consensus promoter - see Figure 3.11. Of these two, the one with the Pribnow box at position 110-116 and a -35 sequence at 87-92 has the best match to a consensus promoter, however the one with the Pribnow box at position 135-141 and a -35 sequence at either 109-114 or 114-119 is much closer to the mRNA start site - see Figure 3.5.

Certain common features have also been noted near or at sites of transcription termination in *E.coli* (Rosenberg and Court, 1979): a) preceding the termination site is a region of hyphenated dyad symmetry; b) termination occurs at a site 20 ± 4 nucleotides from the centre of symmetry and usually within a region containing several consecutive

T residues; and c) a G / C - rich sequence variable in length (3 - 11 contiguous G / C base pairs) are found preceding the stop-site.

Using the GCG program 'TERMINATOR', an area 3' to the translational termination point of the gene (between 1168 and 1218 - see Figure 3.5) was identified as a possible termination sequence for the gene. This contains a G / C - region of dyad symmetry, and the presence of a T rich region 22 base pairs 3' to the centre of dyad symmetry suggests that this region constitutes the transcriptional termination site of the gene - see Figure 3.12.

		-35 SEQUENCE		PRIBNOW BOX	
CONSENSUS SEQUENCE:		TTGACA		TATAATG	
OPTION 1	:	87	TGGACC	110	TCCACTG
OPTION 2	:	109	TTCCAC	135	TGCTGTG
OPTION 3	:	114	CTGGCG	135	TGCTGTG

Figure 3.11. Transcriptional promoters of the putative *phr*A gene.

```
          Stop                          --------  -->
1168  A TAT TGA GTC        1193  CGC GGA GGC GGC CT•T AGC ACC CTC TCC
      T ATA ACT CAG              GCG CCT CCG CCG GA•A TCG TGG GAG AGG
                                                  <--  ---------

          ----
1223  CGG TTC GA
      GCC AAG CT
```

Figure 3.12. Termination Sequence for the putative *phr*A gene.

TRANSLATIONAL SIGNALS

Translational signals also have consensus sequences, originally proposed by Shine and Dalgarno (1974) for the ribosome-binding site. This consists of a consensus sequence 3-9bp in length and 3-11bp 5' from the mRNA start site (Sambrook *et al*, 1989). At position 144-146, the sequence AGG is found. This is the same ribosome-binding site as found in the *trp*A gene (Platt and Yanotsky, 1975). This ribosome-binding site is found 5 nucleotides prior to the initiator methionine of the gene. Translation of the gene terminates at a UGA corresponding to the TGA at nucleotides 1172-1174 in the DNA sequence - see Figure 3.5.

CODON USAGE

Use of synonymous codons in structural genes is non-random. In *E.coli* the frequency of use of different synonymous codons is directly related to the abundance of cognate tRNAs (Ikemura, 1981). The significance of this observation is not known; however it has been noted that rarely used codons appear less frequently in highly expressed genes than in genes which are expressed at a low level (Ikemura, 1981, Konigsberg and Godson, 1983). It has been proposed that codon usage affects the efficiency of translation and therefore the level of gene expression. Using the same analysis technique used by Sancar *et al* (1984b) comparing the codon usage in *phr*B to that in 25 non-regulatory proteins from *E.coli* (Konigsberg and Godson, 1983), it can be seen that there is a definite bias in favour of the use of rare and infrequent codons in the putative *phr*A gene. The frequency of synonym usage is actually reversed (*i.e.* an infrequently used synonym in *E.coli* non-regulatory proteins becomes the most frequently used) for Phe, Gly, His, Ile, Asn, Arg, Ser, Thr, Val, and Tyr. Also the usage of the rare codons AUA (Ile), UCG (Ser), CCU and CCC (Pro), ACG (Thr), CAA (Gln), AAU (Asn), and AGG (Arg) is increased, to a level of 9.7% of the total codon usage, in comparison to that in phrB of 7.8% and 4% in the 25 non-regulatory proteins. See Table 3.2.

		*phr*A		*E.coli*			*phr*A		*E.coli*
AMINO ACID	CODON	TOTAL CODONS	SYNONYM USE %	SYNONYM USE %	AMINO ACID	CODON	TOTAL CODONS	SYNONYM USE %	SYNONYM USE %
ALA (A)	GCU	7	29	28	ASN (N)	AAU^{R}	7	58	24
	GCC	7	29	19		AAC	5	42	76
	GCA	4	17	23	PRO (P)	CCU^{R}	3	17	9
	GCG	6	25	30		CCC^{R}	2	10	6
CYS (C)	UGU	1	50	42		CCA	3	17	20
	UGC	1	50	58		CCG	10	56	65
ASP (D)	GAU	19	86	51	GLN(Q)	CAA^{R}	8	36	27
	GAC	3	14	49		CAG	14	64	73
GLU (E)	GAA	12	60	73	ARG (R)	CGU	7	35	58
	GAG	8	40	27		CG C	9	45	35
PHE (F)	UUU	6	60	44		CGA	3	15	2
	UUC	4	40	56		CGG	1	5	3
GLY (G)	GGU	7	30	47.5		AGA	0	0	1
	GGC	11	48	40.5		AGG^{R}	0	0	0.25
	GGA	3	13	5	SER (S)	UCU	2	9	27
	GGG	2	9	7		UCC	2	9	26
HIS (H)	CAU	8	67	39		UCA	2	9	8
	CAC	4	33	61		UCG^{R}	6	26	11
ILE (I)	AUU	14	70	37		AGU	4	17	6
	AUC	5	25	62		AGC	7	30	22
	AUA^{R}	1	5	1	THR (T)	ACU	4	29	24
LYS (K)	AAA	7	88	77		ACC	3	21	51
	AAG	1	12	23		ACA	1	7	6
LEU (L)	UUA	5	10	6.1		ACG^{R}	6	43	20
	UUG	7	14	8	VAL (V)	GUU	6	23	38
	CUU	10	20	9		GUC	6	23	13
	CUC	7	14	7		GUA	1	4	23
	CUA	1	2	2		GUG	13	50	27
	CUG	19	40	69	TRP (W)	UGG	5	100	100
MET (M)	AUG	1	100	100	TYR (Y)	UAU	6	67	41
						UAC	3	33	59

Table 3.2. Codon usage in the putative *phr*A gene compared with that in 25 *Escherichia coli* non-regulatory genes.

^{R} indicates rare codons in *Escherichia coli.*

It has been shown (Sancar *et al.*, 1984b) that under inducing conditions, this bias in favour of infrequently used or rare codons results in reduced amounts of protein being produced, in comparison with a gene that utilises more commonly used codons. It is

therefore predicted that the level of the putative *phr*A gene product in *E.coli* in its natural state is very low. The occurrence of the *phr*B gene product in the natural state is only about 10 molecules of photolyase per cell (Harm *et al.*, 1968). If this is regulated by the degree of rare codon usage, predicted as 7.8%, then the occurrence of the putative *phr*A gene product, with a predicted rare codon usage of 9.7%, is likely to be in the order of one to two molecules per cell. This could help to explain the relatively small effect that the putative *phr*A gene contributes to the rate and extent of photoreactivation.

It is also predicted that engineering the over-expression of the putative *phr*A gene product is likely to be difficult. If the rate of production of the protein is limited in the natural state by the intracellular levels of the tRNAs corresponding to the rare or infrequently used codons, then even by cloning the gene into an efficient expression vector with a strong promoter and ribosome-binding site, the level of protein may still be small. This was the next step in the study, and is discussed in Chapter 4.

COMPARISON WITH SUTHERLANDS *phr*A ENZYME

Snapka and Sutherland (1980) reported the purification and properties of a PRE from *E.coli* with a molecular weight of 36,800Da, later revised to slightly less than 40kDa (Sutherland *et al.*, 1986). This was claimed to be the *phr*A gene product. The reported amino acid composition of this enzyme is very different from the theoretical amino acid composition of our putative *phr*A gene product, predicted from the sequence obtained in this study.

The photoreactivating enzyme isolated by Snapka and Sutherland (1980) consists of 298 amino acids, with the absence of any tryptophan residues. The protein predicted from the putative *phr*A gene would consist of 340 amino acids, with 5 tryptophan residues. The molecular weights of the two proteins are very similar, though this is unlikely to be of any significance.

This would suggest that the enzyme studied by Sutherland and co-workers, and later by Hejmadi and Verma (1987) and Verma *et al.* (1990), is a different enzyme from that responsible for the activity studied in our laboratory at Bath.

There is a possibility that if the putative *phr*A gene product does bind to pyrimidine dimers *in vivo* then repair could proceed via a tryptophan-mediated photolysis of the dimers - see Section 1.3.3. However, this is an unlikely explanation for the photorecovery seen with AS46 / pAS01 (Smith and Moss, 1988) as this type of photoreactivation is not observed with wavelengths of photoreactivating light greater than 300nm (Sutherland and Griffin, 1980). The photoreactivating light used in our laboratory has no significant transmission properties below 340nm - see Figure 2.4.

It was hoped that the work on both the expression of the gene product of the putative *phr*A gene (Chapter 4) and the *in vivo* photoreactivation experiments would shed more light on the above points.

In conclusion, sequencing the insert from pAS01 shows there is an open reading frame present which codes for a protein of approximately 40kDa. These were termed the putative *phr*A gene and the putative *phr*A gene product respectively. This work would suggest that the photorecovery seen when pAS01 is transformed into the repair-deficient strain AS46 (Smith and Moss, 1988), is due to the protein produced from the gene present on the insert present on that plasmid.

CHAPTER FOUR

EXPRESSION OF THE GENE PRODUCT

4.1 INTRODUCTION

Having sequenced the insert from pAS01, and identified a potential open reading frame coding for a protein of approximately 40kDa, the next step was to try and over-express this protein. Work in our laboratory with the maleate dehydrogenase gene (*mdh*) cloned into plasmid vector pUC19, termed plasmid pAH13, had showed over-production of the enzyme when cultures of JM83 / pAH13 had been induced with 1mM IPTG (A.H. Ahmed - unpublished results). Thus the starting point for this part of the work was attempting to try and induce over-production of the gene product from plasmid pND01 to a level that could be detected using SDS - PAGE techniques.

4.2 METHODS

The induction and expression techniques and the use of SDS - PAGE to analyse the results have already been described in Chapter 2.
Other relevant methods are described in detail in the following section.

4.3 RESULTS

In all of the induction / expression experiments, cultures of JM83 / pAH13 induced with 1mM IPTG were used as a positive control - see Section 4.3.8. This was to show that the experimental conditions were conducive to induction of a gene product using IPTG, as it was predicted that it would be difficult to express the putative *phr*A gene product - see Section 3.4.

4.3.1 INDUCTION OF pND01 AND pND02

Overnight cultures of JM83 / pND01 and JM83 / pND02, with JM83 / pUC19 and JM83 used as controls, were grown up in LB broth supplemented with 100µg/ml ampicillin and 50µg/ml streptomycin. Induction cultures were prepared as described in Section 2.4.1. The cultures were grown over a 24 hour period and sampled at different time intervals as described in Section 2.4.1. The samples were treated as described in Section 2.4.2. A SDS polyacrylamide gel was prepared as described in Section 2.4.3 and 5µl of marker loaded onto the first lane of each gel. 5µl of each sample was then loaded onto the remaining lanes of the gels, and the gel run for approximately 60 minutes, until the blue marker in the loading buffer had reached the bottom of the gel. The gel assembly was disassembled, the gel stained and destained as described in Section 2.4.4. The results are shown in SDS-PA Gels 4.1 to 4.4. The sizes of the molecular weight markers are, in decreasing size, 97,400 Da, 66,200 Da, 45,000 Da, 31,000 Da, 21,500 Da and 14,400 Da.

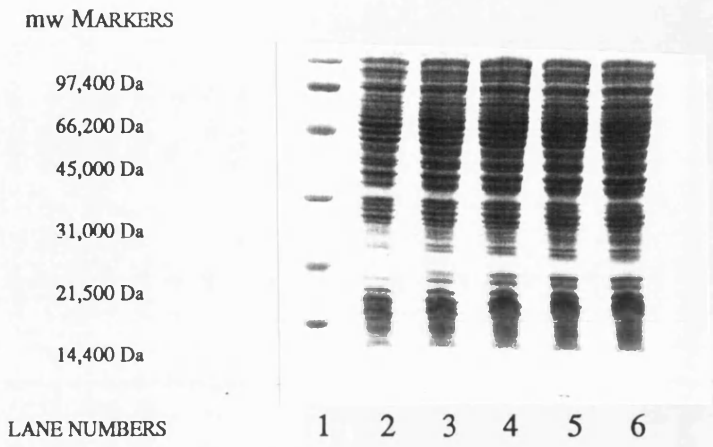

SDS-PA Gel 4.1. JM83 / pND01 induced with 1mM IPTG over 24hrs.
Lane 1, Markers; Lane 2, 2hrs; Lane 3, 4hrs; Lane 4, 6hrs; Lane 5, 12hrs; Lane 6, 24hrs

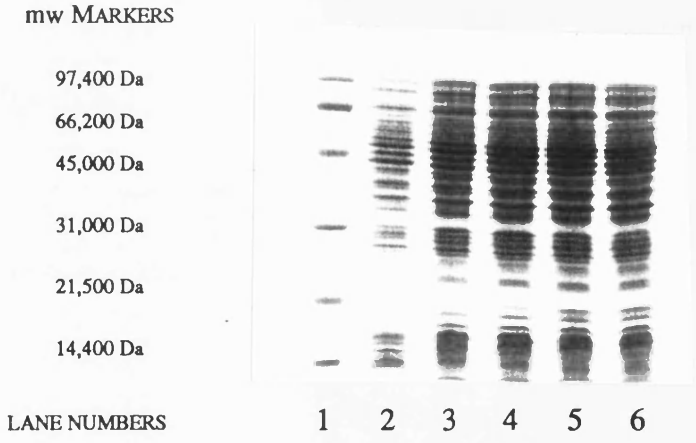

SDS-PA Gel 4.2. JM83 / pND02 induced with 1mM IPTG over 24hrs.
Lane 1, Markers; Lane 2, 2hrs; Lane 3, 4hrs; Lane 4, 6hrs; Lane 5, 12hrs; Lane 6, 24hrs

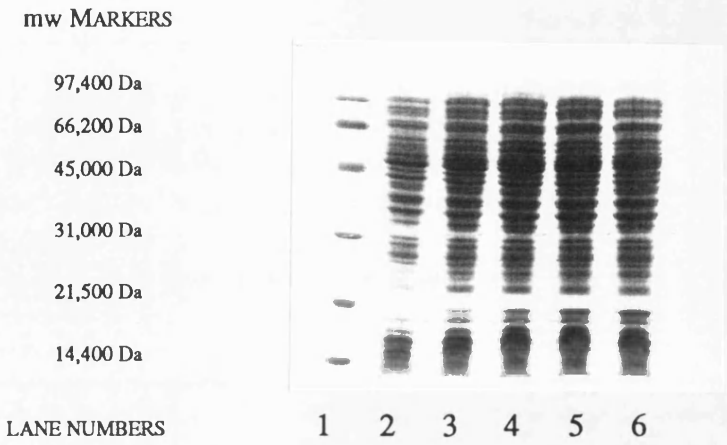

SDS-PA Gel 4.3. JM83 / pUC19 induced with 1mM IPTG over 24hrs.
Lane 1, Markers; Lane 2, 2hrs; Lane 3, 4hrs; Lane 4, 6hrs; Lane 5, 12hrs; Lane 6, 24hrs

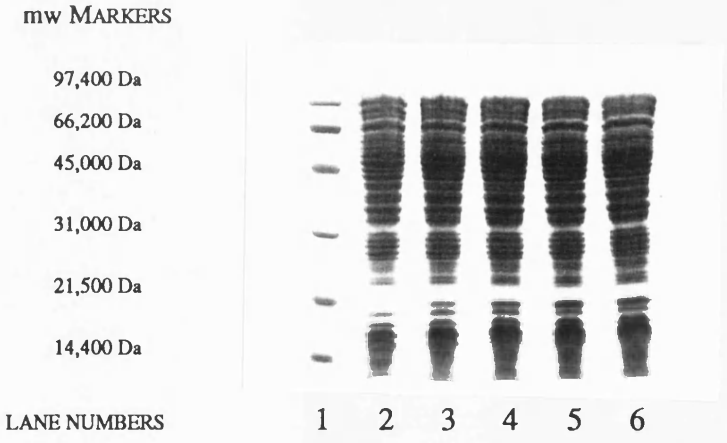

SDS-PA Gel 4.4. JM83 induced with 1mM IPTG over 24hrs.
Lane 1, Markers; Lane 2, 2hrs; Lane 3, 4hrs; Lane 4, 6hrs; Lane 5, 12hrs; Lane 6, 24hrs

4.3.2 SUB-CLONING OF THE PUTATIVE GENE INTO AN EXPRESSION VECTOR - PART I

Due to the failure to show any expression of the gene product from pND01, the next step was to sub-clone the insert containing the putative *phr*A gene into a specialist expression vector. The chosen expression vector was pKK223-3 (Brosius and Holy, 1984) which was purchased from PHARMACIA - see Figure 4.1. pKK223-3 contains the strong *tac* promoter which, in an appropriate host such as JM105 (Yanisch-Perron *et al*, 1985), is regulated by the *lac* repressor and induced by the addition of IPTG to the medium. Immediately downstream of the *tac* promoter is the pUC8 multiple cloning site and the strong *rrn*B ribosomal terminator, which stabilises this vector-host system by inhibiting read-through transcription initiated from the *tac* promoter in the parent plasmid. Genes containing a ribosome-binding site and an ATG start codon may be expressed by insertion into the PstI or HindIII sites. The ribosome-binding site on the plasmid can be utilised to express inserts cloned into the EcoRI site if the start codon is within 10 -15 base pairs from the ribosome-binding site. Plasmid pKK223-3 was transformed into competent cells of JM105 as described in Section 2.2.10.

The initial approach was to utilise the *tac* promoter on the expression vector and the ribosome-binding site located in front of the putative gene. This approach was chosen because :- a) it was a much simpler and quicker cloning procedure than trying to insert the ORF of the putative gene in position to utilise the ribosome-binding site on the expression vector, and b) it would test the 'efficiency' of the proposed ribosome-binding site 'AGG'.

By taking a PstI - HindIII restriction fragment from pND02 and inserting it into the expression vector pKK223-3 digested with PstI and HindIII, the putative gene would be inserted in the correct orientation with the *tac* promoter.

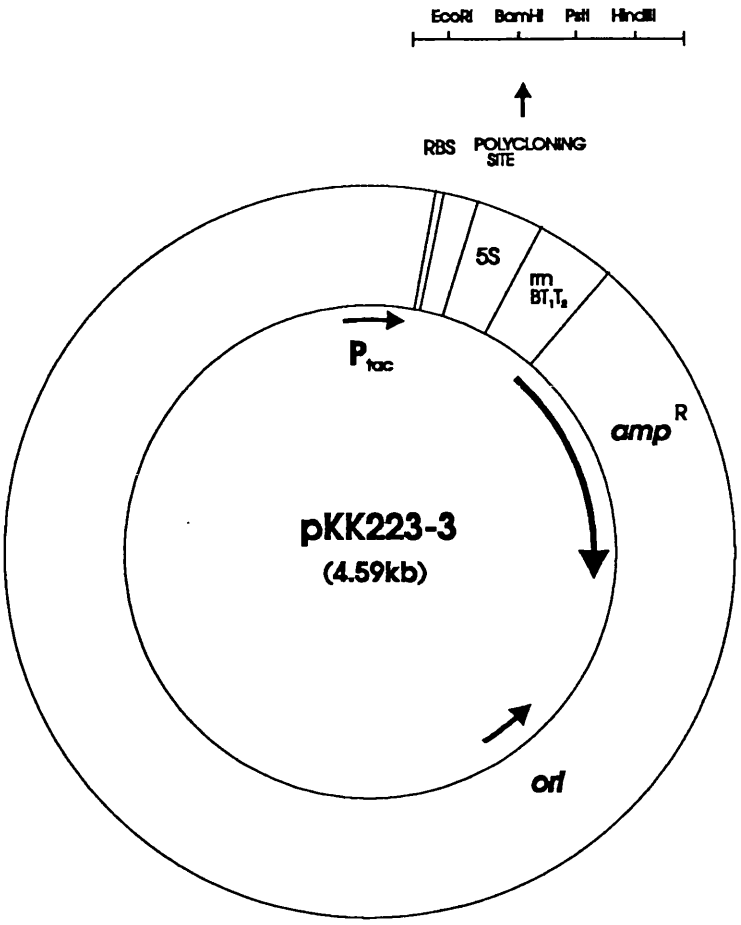

Figure 4.1 Plasmid expression vector pKK223-3, showing the important features.

PREPARATION OF THE PstI-HindIII RESTRICTION FRAGMENT FROM pND02

Plasmid pND02 was isolated and purified as described in Section 2.2.2. 20μg of pND02 plasmid DNA was digested with an excess of restriction enzymes PstI and HindIII for 2 hours at 37°C to ensure complete digestion. The resulting PstI-HindIII restriction fragment was isolated and purified as described in Section 2.2.6. The concentration of the purified fragment DNA was calculated as described in Section 2.2.3.

PREPARATION OF VECTOR DNA

Plasmid pKK223-3 was isolated and purified as described in Section 2.2.2. The concentration of the purified plasmid DNA was calculated as described in Section 2.2.3. 10μg of pKK223-3 plasmid DNA was digested with an excess of restriction enzymes PstI and HindIII for 2 hours at 37°C to ensure complete digestion. Half the sample was run on an agarose gel to confirm that digestion had taken place. The restriction enzymes were inactivated by incubating at 85°C for 30 minutes, then allowing the reaction mixture to cool at room temperature for 30 minutes.

The pKK223-3 / PstI / HindIII restricted DNA was treated with Alkaline Phosphatase to dephosphorylate the sticky ends of the linear DNA, to prevent self-ligation, as described in Section 2.2.7. The Alkaline Phosphatase was inactivated by incubating at 85°C for 15 minutes, then allowing the reaction mixture to cool at room temperature for 30 minutes.

LIGATION OF INSERT AND VECTOR DNA

The insert DNA was ligated to the vector DNA in the following ligation mixture :-

pKK223-3 / PstI / HindIII	≅ 0.1μg
PstI - HindIII RESTRICTION FRAGMENT	≅ 0.15μg
STERILE DDDW	to 7μl

This reaction mixture was incubated at 45°C for 5 minutes to melt any cohesive bonds that had formed, then cooled on ice for 5 minutes. Then the following were added :-

BUFFER (10x CONCENTRATE)	1μl
ATP (10mM)	1μl
T_4 DNA LIGASE (1 unit/μl)	1μl

This was mixed by vortexing, spun down and incubated at 15°C overnight (a minimum of 6 hours).

Two separate ligation mixtures were set up, termed LIGATION A and LIGATION B.

PRODUCTION OF COMPETENT JM105 CELLS

Fresh competent cells of JM105 were prepared as described in Section 2.2.9. These were stored at 4°C for 16 hours and then used for transformation.

TRANSFORMATION OF LIGATION MIXTURE INTO JM105

Transformation of the competent JM105 cells with the ligation mixture was performed as described in Section 2.2.10. The 12 hour liquid culture was streaked out onto LB / amp plates and incubated at 37°C for 48 hours. Growth was seen on plates from LIGATION A and LIGATION B.

CONTROLS

The following controls were performed alongside the proper ligation mixture :-

a) LIGATION MIX - NO ENZYME

The T_4 DNA ligase was omitted from the ligation mixture. No growth was seen after incubation in the LB / amp broth after 12 hours at 37°C or after streaking onto LB / amp plates after incubation for 48 hours at 37°C.

b) LIGATION MIX - NO INSERT DNA

The PstI-HindIII restriction fragment was omitted from the ligation mixture. Growth was seen after incubation in the LB / amp broth after 12 hours at 37°C and after streaking onto LB / amp plates after incubation for 48 hours at 37°C. Restriction analysis showed the plasmid present to be indistinguishable from pKK223-3.

c) TRANSFORMATION MIX - NO LIGATION MIX

No ligation mixture was added to the competent cells of JM105, which then underwent the transformation procedure. No growth was seen after incubation in the LB / amp broth after 12 hours at 37°C or after streaking onto LB / amp plates after incubation for 48 hours at 37°C.

d) COMPETENT CELLS - VIABILITY TEST

The competent cells of JM105 were streaked out on LB, LB / amp and LB / str plates and incubated at 37°C for 48 hours. No growth was seen on LB / amp plates, while growth occurred on the LB and LB / str plates.

4.3.3 ANALYSIS OF THE NEW PLASMIDS

Plasmid DNA was isolated from individual colonies in batches of twelve as described in Section 2.2.2. The plasmids were restricted with restriction enzyme EcoRI and then loaded onto an agarose gel and run for 90 minutes, using pKK223-3 / EcoRI as a control. Plasmids which showed up on the gel to be heavier than pKK223-3 were then restricted with restriction enzymes PstI and HindIII to see if the insert DNA could be cut out of the plasmids. This proved to be the case for all plasmids tested. These plasmids were then restricted with restriction enzymes SphI and HindIII + EcoRV to test for the same insert as in pAS01. This test was positive for all plasmids tested - see Agarose Gel 4.1. This new plasmid was termed pND03 - see Figure 4.2.

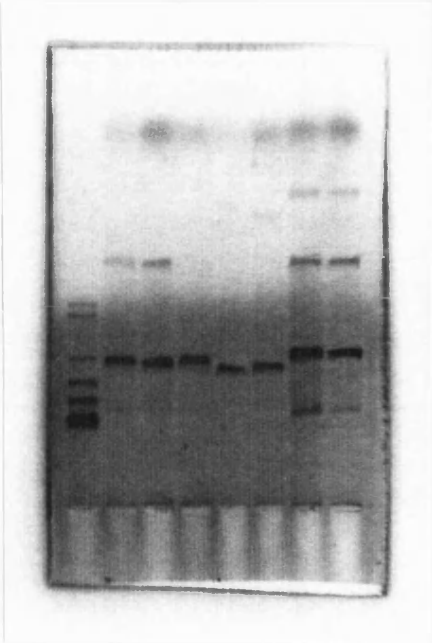

Agarose Gel 4.1. Restriction digests of plasmids pND03, pND04 and pKK223-3.
Lane 1, λDNA / HindIII; Lane 2, pND03 / PstI + HindIII;
Lane 3, pND04 / PstI + HindIII; Lane 4; pKK223-3 / PstI + HindIII;
Lane 5, pND03 / HindIII + EcoRV; Lane 6, pND04 / HindIII + EcoRV;
Lane 7, pND03 / SphI; Lane 8, pND04 / SphI.

The above protocol was also used to produce the control plasmid with the insert containing the gene in the reverse orientation. The only difference was that the PstI - HindIII restriction fragment used was isolated from pND01 instead of pND02. The restriction analysis used on the resulting transformant plasmids was the same as above, but different sized fragments were produced upon restriction analysis with restriction enzymes HindIII and EcoRV - see Agarose Gel 4.1. This new plasmid was termed pND04 - see Figure 4.3. The purpose of the control plasmid pND04 was to check that no protein was expressed from the reversed and complemented strand of the insert DNA from pAS01.

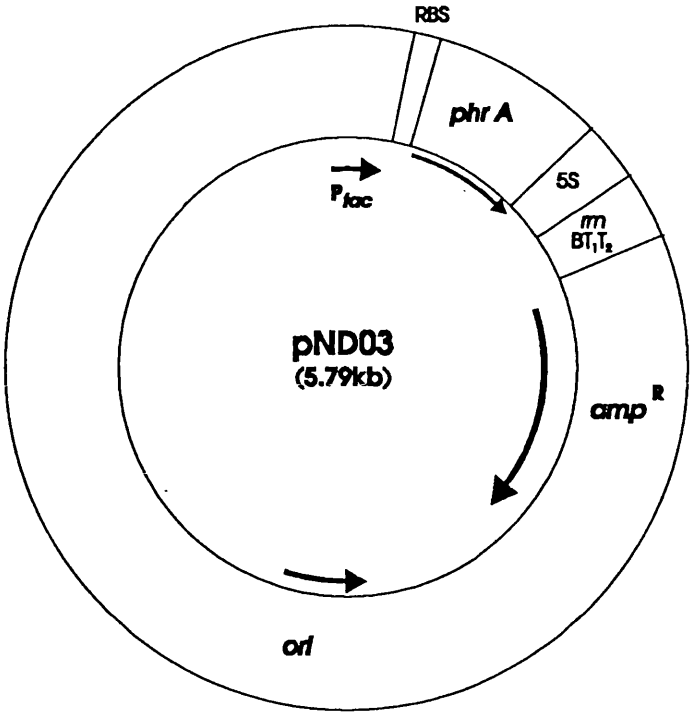

Figure 4.2. Plasmid pND03, showing the important features.

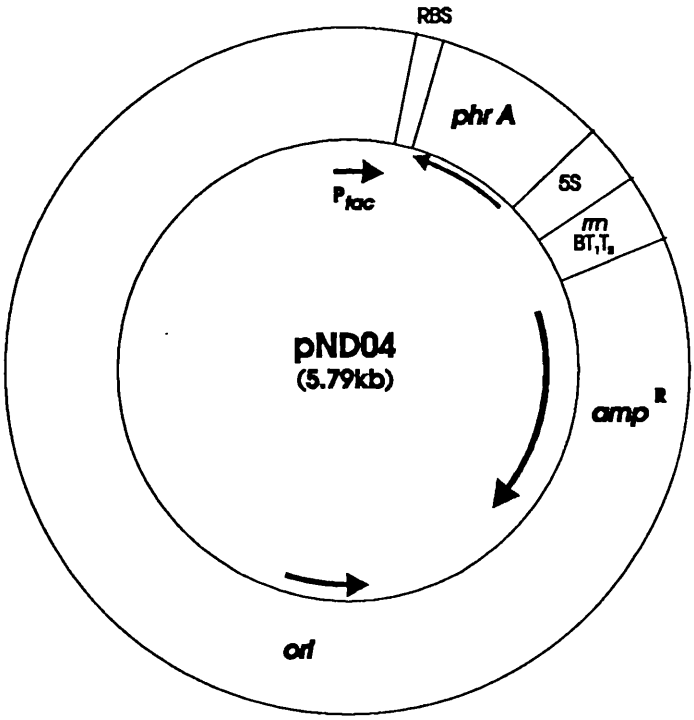

Figure 4.3. Plasmid pND04, showing the important features.

4.3.4 INDUCTION OF pND03 AND pND04

Overnight cultures of JM105 / pND03 and JM105 / pND04, with JM105 / pKK223-3 and JM105 used as controls, were grown up in LB broth supplemented with 100µg/ml ampicillin and 50µg/ml streptomycin. Induction cultures were prepared as described in Section 2.4.1. The cultures were grown over a 24 hour period and sampled at different time intervals as described in Section 2.4.1. The samples were treated as described in Section 2.4.2. A SDS polyacrylamide gel was prepared as described in Section 2.4.3 and 5 µl of marker loaded onto the first lane of each gel. 5µl of each sample was then loaded onto the remaining lanes of the gels, and the gel run for approximately 60 minutes, until the blue marker in the loading buffer had reached the bottom of the gel. The gel assembly was disassembled, the gel stained and destained as described in Section 2.4.4. The results are shown in SDS-PA Gels 4.5 to 4.8.

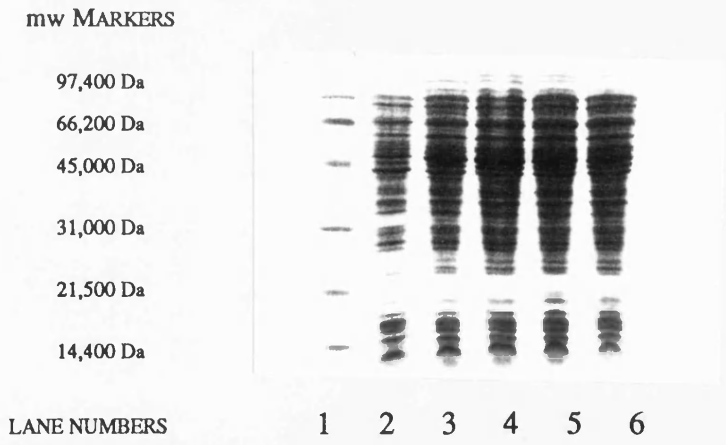

SDS-PA Gel 4.5. JM105 / pND03 induced with 1mM IPTG over 24hrs.
Lane 1, Markers; Lane 2, 2hrs; Lane 3, 4hrs; Lane 4, 6hrs; Lane 5, 12hrs; Lane 6, 24hrs

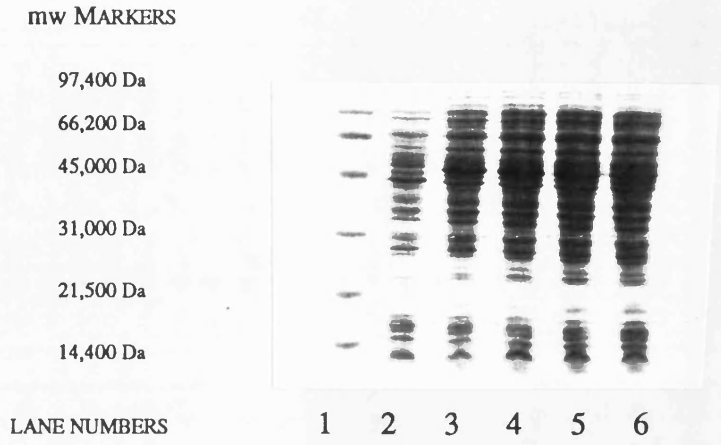

SDS-PA Gel 4.6. JM105 / pND04 induced with 1mM IPTG over 24hrs.
Lane 1, Markers; Lane 2, 2hrs; Lane 3, 4hrs; Lane 4, 6hrs; Lane 5, 12hrs; Lane 6, 24hrs

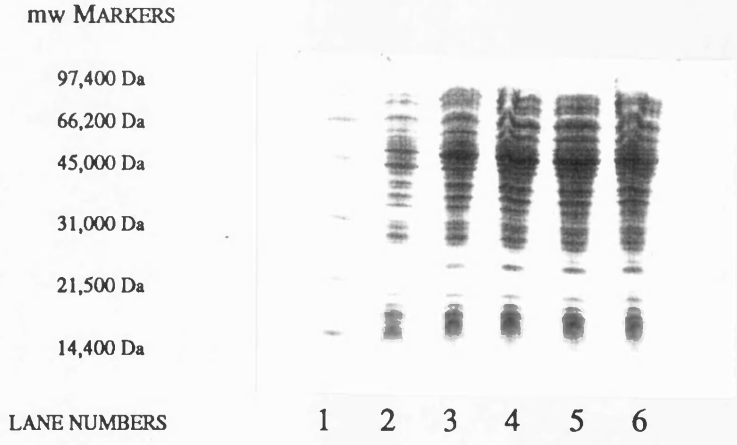

SDS-PA Gel 4.7. JM105 / pKK223-3 induced with 1mM IPTG over 24hrs.
Lane 1, Markers; Lane 2, 2hrs; Lane 3, 4hrs; Lane 4, 6hrs; Lane 5, 12hrs; Lane 6, 24hrs

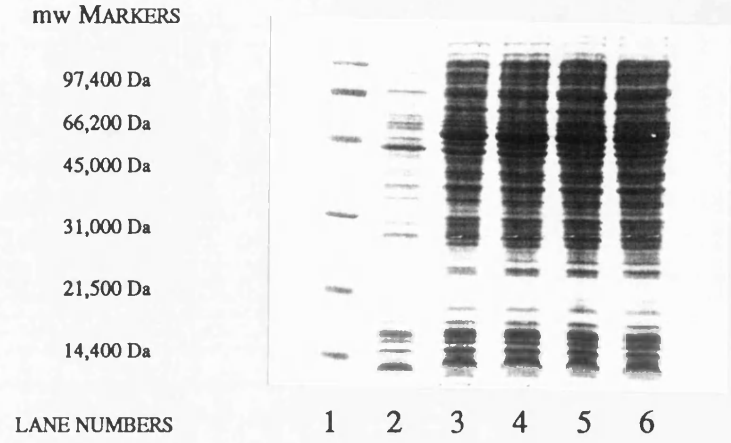

SDS-PA Gel 4.8. JM105 induced with 1mM IPTG over 24hrs.
Lane 1, Markers; Lane 2, 2hrs; Lane 3, 4hrs; Lane 4, 6hrs; Lane 5, 12hrs; Lane 6, 24hrs

4.3.5 SUB-CLONING OF THE PUTATIVE GENE INTO AN EXPRESSION VECTOR - PART II

Due to the failure to show any major expression of the gene product from pND03, the next step was to place the open reading frame of the putative *phr*A gene in frame with the promoter and the ribosome-binding site of the expression vector, pKK223-3. This involved inserting the gene in the EcoRI site on pKK223-3 so that the initiation codon ATG was between 10 to 15 base pairs downstream (3') to the ribosome-binding site on pKK223-3 - see Figure 4.4.

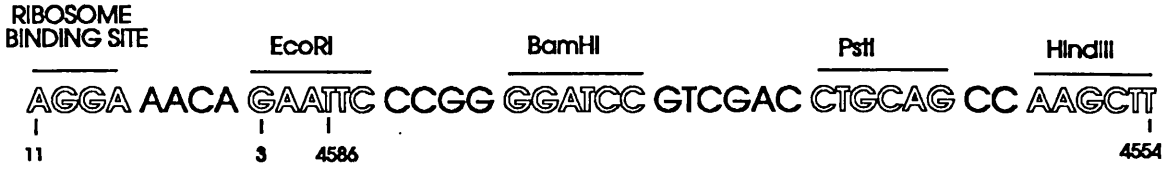

Figure 4.4. The ribosome-binding site and polycloning site of pKK223-3.

There is no EcoRI site in the insert DNA from pAS01, and no obvious restriction site to achieve easy cloning. The plan decided upon involved producing a large quantity of the insert DNA from plasmid pND02, plus parts of the polycloning site from pUC19 at either end, by the Polymerase Chain Reaction (PCR) method so a partial digest of this fragment DNA with NlaIV (which cuts the insert twice, once just downstream of the ATG start codon and once in the middle of the putative *phr*A gene) could be achieved, then isolating the fragment with the cut just downstream of the ATG start codon. This fragment DNA was ligated to a synthetic oligonucleotide specially prepared to match the portion of the gene, including the ATG start codon, which had been removed by the restriction enzyme, NlaIV, and also including an engineered EcoRI site at the 5' end. This fragment was then reduced by restriction cleavage with restriction enzymes EcoRI and HindIII and inserted into the expression vector, pKK223-3, previously restricted with the same two restriction enzymes - see Figure 4.5.

PCR PRODUCTION OF A DNA FRAGMENT CORRESPONDING TO THE INSERT FROM PLASMID pND02

Two synthetic primers from both ends of the insert from plasmid pND02, one forward (5' end) and one reversed and complemented (3' end), were prepared and purified as described in Section 2.2.12.

Forward primer	20-mer	TCT AGA GTC GAC CTG CAG GC
Reverse primer	20-mer	ACG CCA AGC TTG CAT GCG TC

The concentration of the purified primers were calculated as described in Section 2.2.3, and diluted to approximately 0.1µg/µl with sterile DDDW. Plasmid pND02 was isolated and purified as described in Section 2.2.2, the concentration of the purified plasmid DNA calculated as described in Section 2.2.3, and diluted to approximately 1.0ng/µl with sterile TE (pH8.0). The following reaction mixture was then set up :-

PLASMID pND02 DNA (1ng/µl)	10µl
FORWARD PRIMER (0.1µg/µl)	10µl
REVERSE PRIMER (0.1µg/µl)	10µl
dNTPs (5mM)	5µl
BUFFER (10X CONCENTRATE)	10µl
STERILE DDDW	55µl

A couple of drops of PCR oil (SIGMA) were added on top of the reaction mixture to reduce evaporation, then 0.5µl Taq DNA Polymerase was added, mixed by vortexing briefly, and spun down. The tube containing the reaction mixture was placed in the heating block of a DNA Thermal Cycler (PERKIN ELMER CETUS). The PCR reaction was initiated using the following heat and time settings pre-programmed in the memory of the DNA Thermal Cycler :-

DENATURING STEP	94°C for 60 seconds, then,
ANNEALING STEP	50°C for 90 seconds, then,
POLYMERISATION STEP	72°C for 120 seconds, then repeat.

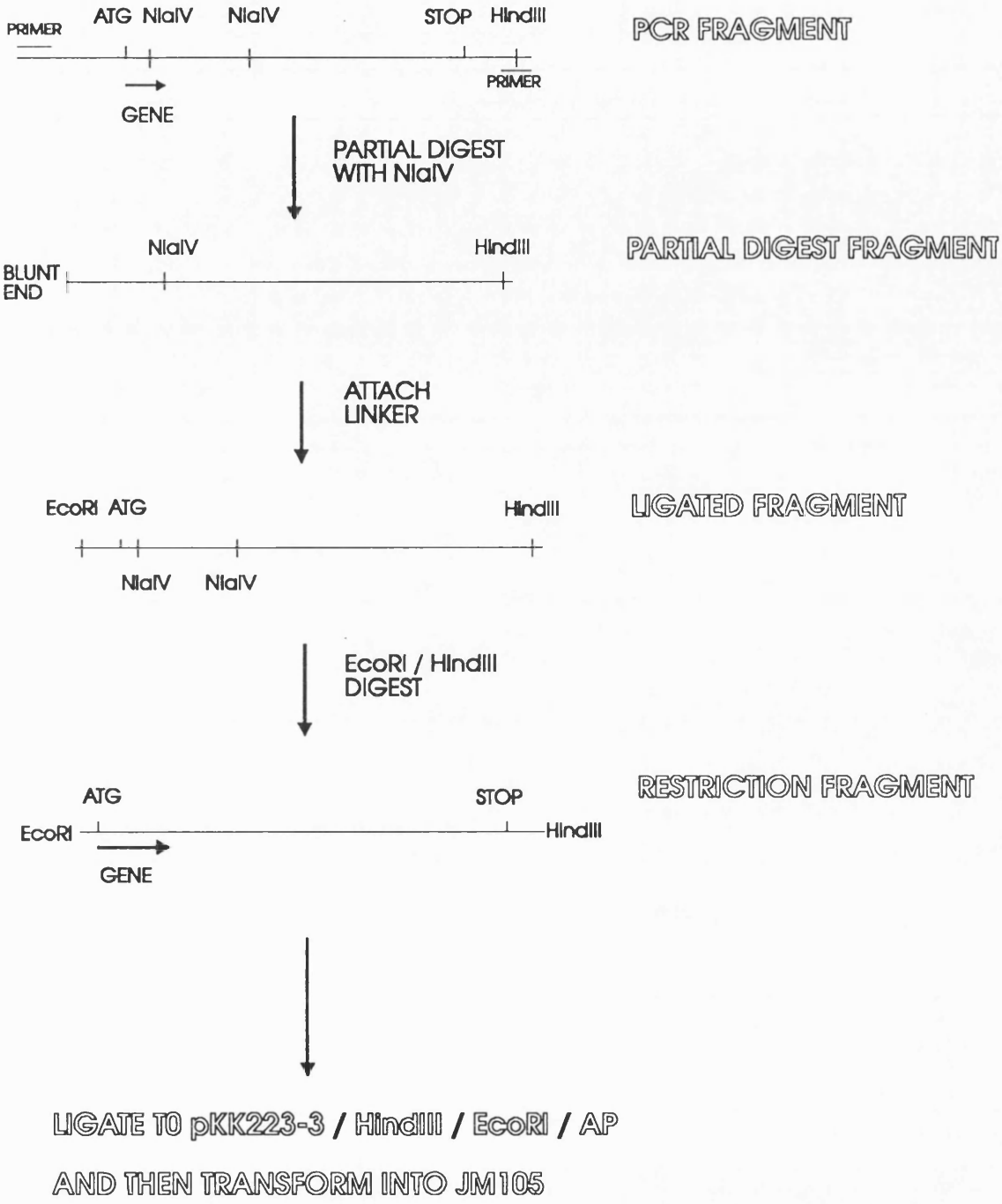

Figure 4.5. Diagram showing the steps involved in the production of pND05.

The PCR reaction was programmed for 30 cycles, then the DNA Thermal Cycler cooled the reaction mixture to 4°C. The reaction mixture was extracted with an equal volume of chloroform : iso-amyl alcohol (24:1) to remove the PCR oil. The upper aqueous layer was carefully transferred to a new microcentrifuge tube and 1ml of 96% ethanol (-20°C) added to precipitate the DNA. The contents were vortexed for 20 seconds, then incubated for 60 minutes at -20°C. The DNA was pelleted by centrifugation at full speed for 5 minutes, then the supernatant carefully discarded. The pellet was carefully rinsed with 70% ethanol (room temperature), briefly spun on the centrifuge for 1 minute and the supernatant carefully removed. The DNA pellet was dried by placing in a vacuum desiccator for 2 minutes and air drying at room temperature for 5 minutes. The DNA was redissolved in 30 µl of TE (pH 8.0 containing DN-ase free RN-ase 20µg/ml). The contents were briefly vortexed, spun down and stored at -20°C. The concentration of the PCR fragments was calculated as described in Section 2.2.3. The size of the PCR fragments was identified by running a sample on a 0.8% agarose gel, which confirmed the major fragment to be approximately 1200bps. The nature of this major fragment was checked by restriction analysis with restriction enzyme EcoRV.

PARTIAL DIGESTION OF THE PCR FRAGMENT WITH NlaIV

The theoretical nature of the 1223bp major PCR fragment is shown in Figure 4.6.

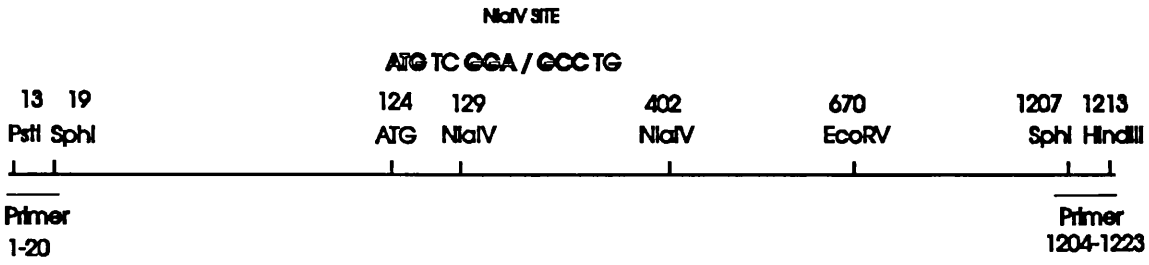

Figure 4.6. Diagram of the major PCR fragment, showing the important features.

The next step was to perform a partial digest of the 1223bp DNA fragment with restriction enzyme NlaIV at position 129, but not at position 402. NlaIV cuts DNA leaving blunt-ended fragments. Restriction enzyme NlaIV, BSA (100x concentrate) and N4 Buffer (10x concentrate) were purchased from NEW ENGLAND BIOLABS.

The following reaction mixture was set up :-

PCR FRAGMENT (1.5μg/μl)	10μl
BUFFER (10X CONCENTRATE)	2μl
BSA (100X CONCENTRATE)	0.2μl
NlaIV (1unit/μl)	1μl
STERILE DDDW	6.8μl

This was incubated on ice for 10 minutes, then 3μl of Gel-Loading Buffer added and mixed. A sample was run on a 1.5% agarose gel - see Agarose Gel 4.2, which showed three major fragments :- one ≅ 1200bp, one ≅ 1100bp, and one ≅ 800bp; which corresponded to undigested DNA, digested DNA at site 129, and digested DNA at site 402 respectively - see Figure 4.6. The fragment of ≅ 1100bp was the desired piece of DNA.

This fragment was isolated and purified as described in Section 2.2.6. The concentration of the purified DNA was calculated as described in Section 2.2.3.

PREPARATION OF THE SYNTHETIC OLIGONUCLEOTIDE LINKER

The linker was designed to be a mirror-image from the middle of the EcoRI site, so that whichever end ligated to the blunt-end of the partial NlaIV-digested PCR fragment, it would leave the ATG start codon 3' of the EcoRI site - see Figure 4.7.

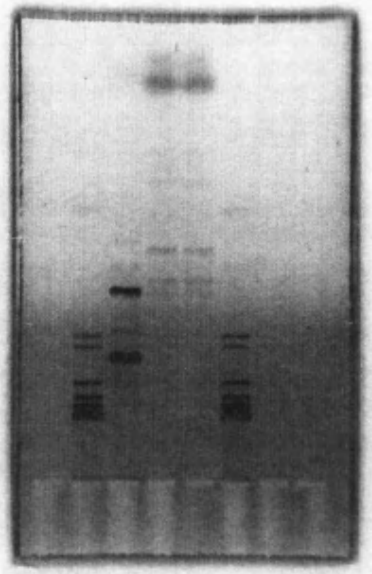

Agarose Gel 4.2. Restriction digests of plasmid pND02 and the PCR fragment.
Lane 2, λDNA / HindIII; Lane 3, pND02 / BamHI + HindIII;
Lane 4; PCR fragment / NlaIV; Lane 5, PCR fragment / NlaIV;
Lane 6, λDNA / HindIII.

Two synthetic oligonucleotides (20-mers) were prepared and purified as described in Section 2.2.12. The concentration of the purified oligonucleotides were calculated as described in Section 2.2.3, and diluted with sterile DDDW to approximately 2μg/μl. 50μl of each oligonucleotide were combined in a fresh microcentrifuge tube, so that the oligonucleotides would hybridise to form a double-stranded piece of DNA. The concentration of the linker was calculated as described in Section 2.2.3.

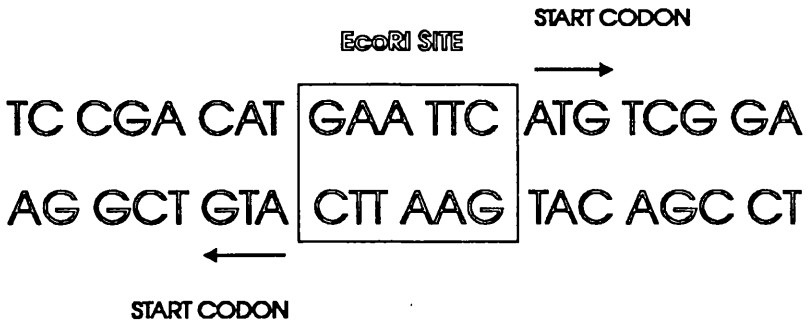

Figure 4.7. Diagram of the synthetic oligonucleotides, showing the important features.

ENZYMATIC PHOSPHORYLATION OF THE NON-PHOSPHORYLATED LINKER

Only phosphorylated molecules are substrates for bacteriophage T_4 DNA ligase, so the non-phosphorylated linker required treatment with bacteriophage T_4 polynucleotide kinase and ATP, before it could be joined to DNA. The following reaction mixture was set up :-

LINKER DNA (2.9μg/μl)	2μl
BUFFER (10X CONCENTRATE)	2μl
ATP (10mM)	2μl
BACTERIOPHAGE T_4 POLYNUCLEOTIDE KINASE (10U/μl)	1μl
STERILE DDDW	3μl

The reaction mixture was incubated at 37°C for 90 minutes. The bacteriophage T_4 polynucleotide kinase was inactivated by incubating the reaction mixture at 65°C for 10 minutes, then allowing the reaction mixture to cool at room temperature for 15 minutes (S. Pearson, Pharmacia - Personal Communication). The phosphorylated linker was now ready for attachment to the partial NlaIV digested PCR fragment.

LIGATION OF THE PHOSPHORYLATED LINKER TO THE BLUNT-ENDED FRAGMENT FROM THE PARTIAL NlaIV DIGEST

The following ligation mixture was set up :-

BLUNT-ENDED DNA (0.15μg/μl)	2μl
PHOSPHORYLATED LINKER (0.2μg/μl)	5.5μl
ATP (10mM)	1μl
BUFFER (10X CONCENTRATE)	2μl

These were all mixed at 0°C, then the following added at room temperature :-

PEG 8000 (40%w/v)	7.5μl
T_4 DNA LIGASE (8U/μl)	2μl

The ligation mixture was incubated at 20°C for 8 hours. The ligase enzyme was then inactivated by incubating the reaction mixture at 65°C for 20 minutes, then allowing the reaction mixture to cool at room temperature for 30 minutes.

RESTRICTION ENZYME DIGESTION OF THE NEW DNA FRAGMENT

The following reaction mixture was set up :-

LIGATION MIXTURE	20μl
BUFFER (10X CONCENTRATE)	20μl
STERILE DDDW	53μl
EcoRI (25U/μl)	4μl
HindIII (15U/μl)	3μl

This was incubated at 37°C for 4 hours, then an extra 2µl of EcoRI and 1µl of HindIII were added, and the reaction mixture incubated at 37°C for a further 60 minutes. After incubation, 2µl of 0.5M EDTA (pH 8.0) was added to the reaction mixture, mixed by vortexing, and spun down. 200µl of phenol : chloroform : isoamyl alcohol (25 : 24 : 1) was added to the reaction mixture, mixed by vortexing, and centrifuged at full speed for 3 minutes. The upper aqueous layer was carefully transferred to a fresh microcentrifuge tube. The restriction fragment was purified by spun-column chromatography, to remove smaller fragments of DNA which would interfere with the subsequent ligation reaction. A Sephacryl S-400 column (PHARMACIA) was prepared in accordance with the manufacturers instructions. 50µl of the reaction mixture was slowly pipetted onto the flat upper surface of the compacted bed of the column, and the column centrifuged for 2 minutes at 1500 rpm. The eluted solution contained the purified DNA restriction fragment in approximately 50µl of TE (pH 8.0) buffer. The DNA was precipitated by addition of 10µl of 3M sodium acetate solution and 220µl of 96% ethanol (-20°C), then incubated at -20°C for 2 hours. The DNA was collected by centrifugation at full speed for 10 minutes. The supernatant was carefully removed, and the DNA rinsed with 200µl of 70% ethanol (room temperature), which was then carefully removed. The DNA was air-dried for 10 minutes, then redissolved in 8µl of TE (pH 8.0). The DNA restriction fragment was now ready for ligation with pKK223-3.

PREPARATION OF VECTOR DNA

Plasmid pKK223-3 was isolated and purified as described in Section 2.2.2. The concentration of the purified plasmid DNA was calculated as described in Section 2.2.3. 10µg of pKK223-3 plasmid DNA was digested with an excess of restriction enzymes EcoRI and HindIII for 2 hours at 37°C to ensure complete digestion. Half the sample was run on an agarose gel to confirm that digestion had taken place. The restriction enzymes

were inactivated by incubating at 85°C for 30 minutes, then allowing the reaction mixture to cool at room temperature for 30 minutes.

The pKK223-3 / EcoRI / HindIII restricted DNA was treated with Alkaline Phosphatase to dephosphorylate the sticky ends of the linear DNA, to prevent self-ligation, as described in Section 2.2.7. The Alkaline Phosphatase was inactivated by incubating at 85°C for 15 minutes, then allowing the reaction mixture to cool at room temperature for 30 minutes.

LIGATION OF THE DNA FRAGMENT AND VECTOR DNA

The DNA fragment containing the *phr*A gene was ligated to the vector DNA in the following ligation mixture :-

pKK223-3 / EcoRI / HindIII (≅ 0.1μg/μl)	1μl
FRAGMENT DNA / EcoRI / HindIII (≅ 0.04μg/μl)	6μl

This reaction mixture was incubated at 45°C for 5 minutes to melt any cohesive bonds that had formed, then cooled on ice for 5 minutes. Then the following were added :-

BUFFER (10X CONCENTRATE)	1μl
ATP (10mM)	1μl
T_4 DNA LIGASE (1 unit/μl)	1μl

This was mixed by vortexing, spun down and incubated at 16°C overnight (a minimum of 6 hours).

Two separate ligation mixtures were set up, termed LIGATION A and LIGATION B.

PRODUCTION OF COMPETENT JM105 CELLS

Fresh competent cells of JM105 were prepared as described in Section 2.2.9. These were stored at 4°C for 16 hours and then used for transformation.

TRANSFORMATION OF LIGATION MIXTURE INTO JM105

Transformation of the competent JM105 cells with the ligation mixture was performed as described in Section 2.2.10. The 12 hour liquid culture was streaked out onto LB / amp plates and incubated at 37°C for 48 hours. Growth was seen on plates from LIGATION A and LIGATION B.

CONTROLS

The following controls were performed alongside the proper ligation mixture :-

a) LIGATION MIX - NO ENZYME

The T_4 DNA ligase was omitted from the ligation mixture. No growth was seen after incubation in the LB / amp broth after 12 hours at 37°C or after streaking onto LB / amp plates after incubation for 48 hours at 37°C.

b) LIGATION MIX - NO INSERT DNA

The EcoRI / HindIII digested DNA fragment was omitted from the ligation mixture. Growth was seen after incubation in the LB / amp broth after 12 hours at 37°C and after streaking onto LB / amp plates after incubation for 48 hours at 37°C. Restriction analysis showed the plasmid present to be the same as pKK223-3.

c) TRANSFORMATION MIX - NO LIGATION MIX

No ligation mixture was added to the competent cells of JM105, which then underwent the transformation procedure. No growth was seen after incubation in the LB / amp broth

after 12 hours at 37°C or after streaking onto LB / amp plates after incubation for 48 hours at 37°C.

d) COMPETENT CELLS - VIABILITY TEST

The competent cells of JM105 were streaked out on LB, LB / amp and LB / str plates and incubated at 37°C for 48 hours. No growth was seen on LB / amp plates, while growth occurred on the LB and LB / str plates.

4.3.6 ANALYSIS OF THE NEW PLASMID

Plasmid DNA was isolated from individual colonies in batches of twelve as described in Section 2.2.2. The plasmids were restricted with restriction enzyme EcoRI and then loaded onto an agarose gel and run for 90 minutes, using pKK223-3 / EcoRI as a control. Plasmids which showed up on the gel to be heavier than pKK223-3 were then restricted with restriction enzymes EcoRI and HindIII to see if the insert DNA could be cut out of the plasmids. This proved to be the case for all plasmids tested. These plasmids were then restricted with restriction enzymes SphI and HindIII + EcoRV to test for the same insert as in pAS01 - see Agarose Gel 4.3. This test was positive for all plasmids tested. This new plasmid was termed pND05 - see Figure 4.8.

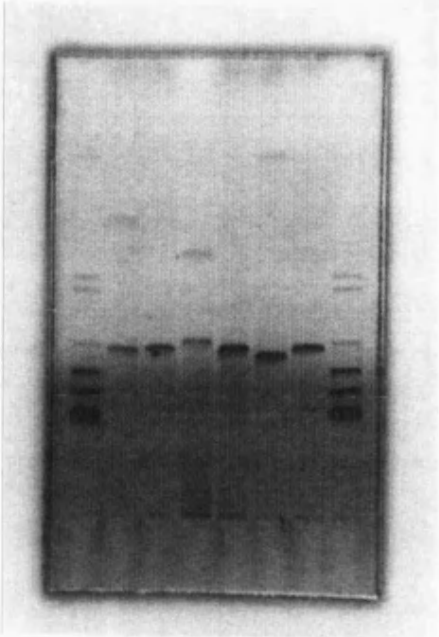

Agarose Gel 4.3. Restriction digests of plasmids pND05 and pKK223-3.

Lane 1, λDNA / HindIII; Lane 2, pND05 / EcoRI + HindIII;

Lane 3, pKK223-3 / EcoRI + HindIII; Lane 4; pND05 / SphI; Lane 5, pKK223-3 / SphI;

Lane 6, pND05 / HindIII + EcoRV; Lane 7, pKK223-3 / HindIII + EcoRV.

4.3.7 INDUCTION OF pND05

An overnight culture of JM105 / pND05 was grown up in LB broth supplemented with 100μg/ml ampicillin and 50μg/ml streptomycin. Induction cultures were prepared as described in Section 2.4.1. The cultures were grown over a 24 hour period and sampled at different time intervals as described in Section 2.4.1. The samples were treated as described in Section 2.4.2. A SDS polyacrylamide gel was prepared as described in Section 2.4.3 and 5μl of marker loaded onto the first lane of each gel. 5μl of each sample was then loaded onto the remaining lanes of the gels, and the gel run for approximately 60 minutes, until the blue marker in the loading buffer had reached the bottom of the gel. The

gel assembly was disassembled, the gel stained and destained as described in Section 2.4.4. The results are shown in SDS-PA Gel 4.9. Refer to SDS-PA Gels 4.7 and 4.8 for controls (JM105 / pKK223-3 and JM105)

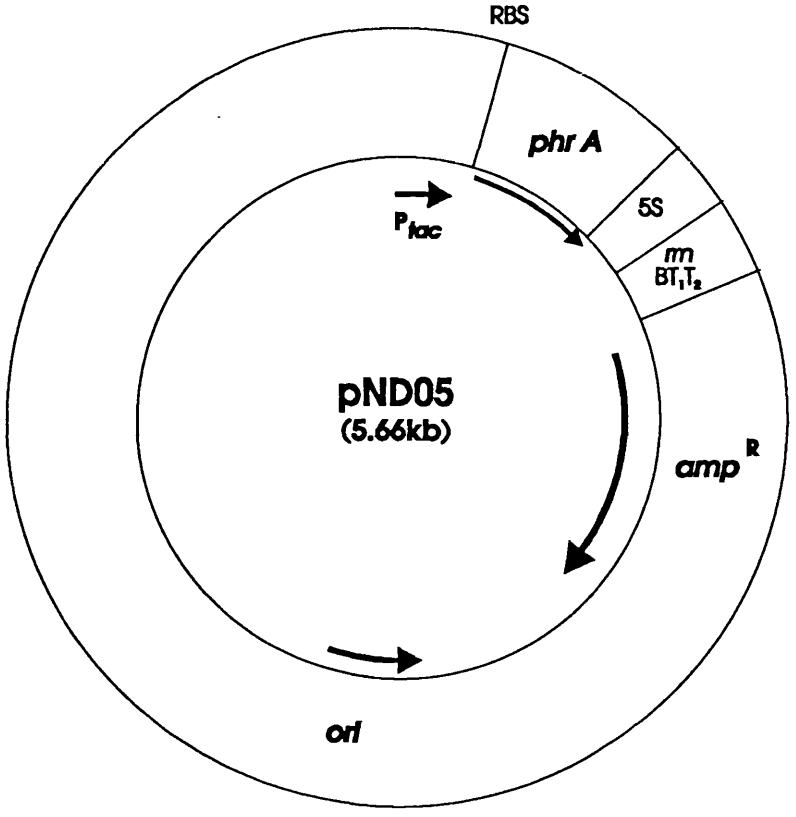

Figure 4.8. Diagram of pND05, showing the important features.

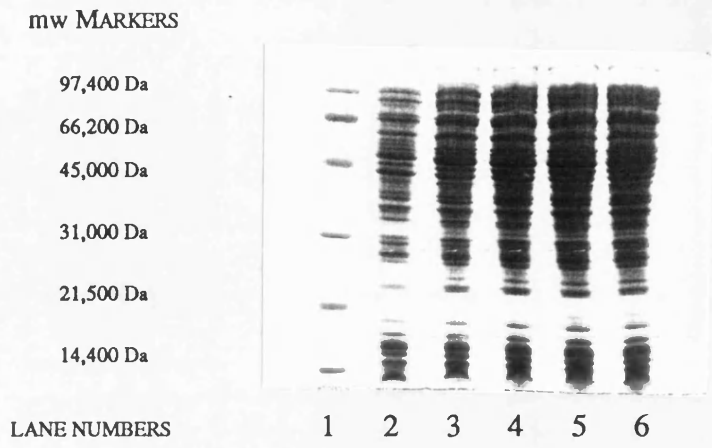

SDS-PA Gel 4.9. JM105 / pND05 induced with 1mM IPTG over 24hrs.
Lane 1, Markers; Lane 2, 2hrs; Lane 3, 4hrs; Lane 4, 6hrs; Lane 5, 12hrs; Lane 6, 24hrs

As can be seen from comparing SDS-PA Gels 4.5 and 4.9, there seems to be no discernible difference between JM105 / pND03 and JM105 / pND05 under the experimental expression conditions used.

4.3.8 INDUCTION OF pAH13

As stated at the beginning of Section 4.3, a positive control (JM83 / pAH13, which contains the *mdh* gene inserted in the polycloning site of pUC19) was run alongside the test induction cultures, to show that the experimental expression conditions were conducive to over-producing a protein from a plasmid.

An overnight culture of JM83 / pAH13 was grown up in LB broth supplemented with 100 µg/ml ampicillin and 50µg/ml streptomycin. An induction culture was prepared as described in Section 2.4.1. The culture was grown over a 24 hour period and sampled at

different time intervals as described in Section 2.4.1. The sample was treated as described in Section 2.4.2. A SDS polyacrylamide gel was prepared as described in Section 2.4.3 and 5µl of marker loaded onto the first lane of each gel. 5µl of each sample was then loaded onto the remaining lanes of the gels, and the gel run for approximately 60 minutes, until the blue marker in the loading buffer had reached the bottom of the gel. The gel assembly was disassembled, the gel stained and destained as described in Section 2.4.4. The results are shown in SDS-PA Gel 4.10. Refer to SDS-PA Gels 4.3 and 4.4 for controls (JM83 / pUC19 and JM83)

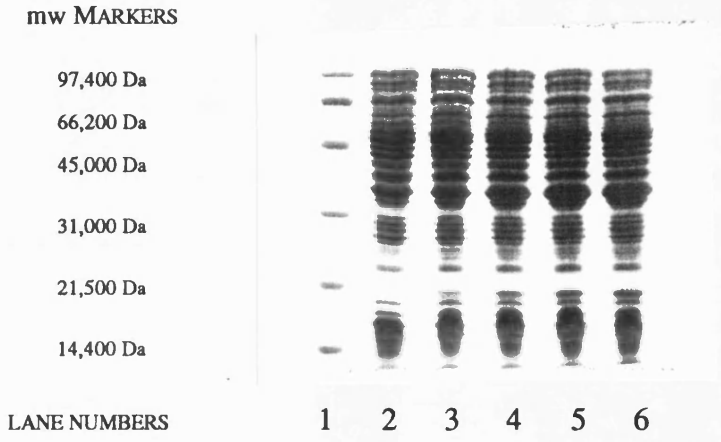

SDS-PA Gel 4.10. JM83 / pAH13 induced with 1mM IPTG over 24hrs.
Lane 1, Markers; Lane 2, 2hrs; Lane 3, 4hrs; Lane 4, 6hrs; Lane 5, 12hrs; Lane 6, 24hrs

4.4 DISCUSSION

The attempt to over-express the putative *phr*A gene product from pND01 involved the use of the promoter sequences and the ribosome-binding site identified 5' to the ATG start codon in Section 3.4. No protein band was identified in the region of the expected size of the putative *phr*A gene product, or in any other region, above the background protein bands of the two controls - see SDS-PA Gels 4.1, 4.3 and 4.4. No protein band of any size was identified from the induction of pND02, above the background protein bands of the two controls - see SDS-PA Gels 4.2, 4.3 and 4.4.

The attempt to over-express the putative *phr*A gene product from pND03 involved the use of the strong *tac* promoter on the pKK223-3 expression vector (Brosius and Holy, 1984) and the ribosome-binding site identified 5' to the ATG start codon in Section 3.4. Again, no protein band was identified above the background protein bands of the two controls - see SDS-PA Gels 4.5, 4.7 and 4.8. No protein band of any size was identified from the induction of pND04, above the background protein bands of the two controls - see SDS-PA Gels 4.6, 4.7 and 4.8.

The attempt to over-express the putative *phr*A gene product from pND05 involved the use of the strong *tac* promoter and the ribosome-binding site on the pKK223-3 expression vector (Brosius and Holy, 1984). Again, no protein band was identified above the background protein bands of the two controls - see SDS-PA Gels 4.9, 4.7 and 4.8.

The predicted difficulties in over-expressing the putative *phr*A gene product (see Section 3.4) were thus encountered during this section of the study. In the three vector systems utilised to carry the putative *phr*A gene (pND01, pND03 and pND05) there was no discernible expression of the putative *phr*A gene product.

One possible explanation for this could be that the staining system used (Coomassie Brilliant Blue Stain) was not sensitive enough to pick up the low levels of the putative *phr*A gene product produced by the induction process. The smallest amount of protein

that can be usually detected by staining with Coomassie Brilliant Blue is around 0.1μg (Sambrook *et al.*, 1989). Staining with silver salts is approximately 100-1000 fold more sensitive than staining with Coomassie Brilliant Blue stain (Sambrook *et al.*, 1989), and is capable of detecting as little as 0.1-1.0ng of protein in a single band. This would have been the next step in the expression studies had time allowed. Also, running the samples on a larger gel using a larger gel apparatus, such as a PROTEAN II xi (BIO-RAD) dual slab cell for example, could show up lower levels of protein due to better separation of the gel bands.

Another explanation could be that the inducing chemical (IPTG) was not functioning in the correct manner. The positive control experiments show that the IPTG used was functioning as an inducer under the experimental expression conditions used. IPTG, as well as having an inducing effect, can, at certain concentrations, act as an inhibitor of gene expression (S. Pearson, Pharmacia - Personal Communication). However, different concentrations of IPTG were tried for pND03 and pND05, between 0.1 - 5.0 mM IPTG in the final culture (results not shown). This produced no difference from the expression seen in SDS-PA Gels 4.5 and 4.9 at any of the concentrations tried. Therefore, this was unlikely to be the cause of the lack of expression of the putative *phr*A gene product.

The results from the *in vivo* studies of pND01, pND03 and pND05 reported in Chapter 5 cast an interesting light over the expression of the putative *phr*A gene product from these three vectors, suggesting that some increase in gene expression is taking place in these vectors. Therefore, the problems encountered in this section of the study, the likely causes and the possible remedies, will be discussed in more detail in Chapter 6, during the final discussion of the work in this study.

CHAPTER FIVE

UV-IRRADIATION AND PHOTOREACTIVATION STUDIES

5.1 INTRODUCTION

The initial aim of this part of the study was to try and reproduce the work of Smith (1987) (which showed photoreactivation of about 1 log cycle after UV-irradiation reduction of 4 log cycles of strain AS46 / pAS01) with the plasmids produced in this study carrying the putative *phr*A gene transformed into AS46, which is a *phr*A *phr*B mutant - see APPENDIX A. It has been proposed (Husain and Sancar, 1987a; Husain *et al.*, 1988) that the photoreactivation seen in *phr*B mutants is due to Type III photoreactivation. This type of photoreactivation is characterised by a λ_{max} of 313nm with a narrow wavelength range (300nm to 360nm), and the absence of dose-rate and temperature effects - see Section 1.3.5. Reference to Figure 2.4 shows the photoreactivating light used in this study would allow some Type III photoreactivation to occur. Experiments to study the effects of changes in the temperature at which exposure to the photoreactivating light takes place, and changes in the fluence rate of the photoreactivating light, were carried out.

5.2 METHODS

The UV-irradiation, photoreactivation techniques and experimental conditions have already been described in Chapter 2.

Other relevant methods are described in detail in the following section.

5.3 RESULTS

The first stage in this part of the study was to transform the plasmids produced in Chapter 3 (pND01) and Chapter 4 (pND03) into the *phr*A *phr*B mutant, AS46. Plasmid pND05 (Chapter 4) was not produced until much later on.

5.3.1 TRANSFORMATION OF AS46 WITH THE PLASMIDS PRODUCED IN THIS STUDY

For a valid comparison with the first results obtained for photoreactivation with the cloned putative *phr*A gene (Smith, 1987; Smith and Moss, 1988), the *phr*A *phr*B mutant, AS46, was used as the host strain.

PREPARATION OF PLASMID DNA

Each plasmid was isolated and purified as described in Section 2.2.2. The concentration of the DNA was calculated as described in Section 2.2.3, and diluted with TE (pH 8.0) to give a final concentration of 0.01μg/μl.

PRODUCTION OF COMPETENT AS46 CELLS

Fresh competent cells of AS46 were prepared as described in Section 2.2.9. These were stored at 4°C for 16 hours and then used for transformation.

TRANSFORMATION OF PLASMIDS INTO AS46

Transformation of the competent AS46 cells with the plasmid DNA was performed as described in Section 2.2.10. The 12 hour liquid cultures were streaked out onto LB / amp plates in duplicate, and incubated at 37°C for 48 hours. Growth was seen on all plates.

ANALYSIS OF THE PLASMIDS

Plasmid DNA was isolated from individual colonies in batches of four as described in Section 2.2.2. The plasmids were restricted with restriction enzyme EcoRI and then loaded onto an agarose gel and run for 90 minutes, using the relevant stock plasmid, restricted with EcoRI, as a control. Plasmids which matched the size of the control plasmid were further analysed with relevant restriction enzymes to further confirm the validity of the plasmid in question.

5.3.2 INITIAL PHOTOREACTIVATION STUDIES

The initial photoreactivation studies were carried out at 25°C. Strains AS46 / pND01 and AS46 / pND03 were studied using strains AS46 / pUC19 and AS46 / pKK223-3 as controls, respectively. It was hoped that AS46 / pND03 would show a greater rate of photoreactivation than AS46 / pND01, and maybe even a greater extent of recovery, due to better expression of the putative *phr*A gene product in AS46 / pND03. Although no discernible difference in the expression of the putative *phr*A gene product was detected during the expression studies (see Section 4.3), if the putative *phr*A gene product was produced in only slightly higher amounts in pND03 to pND01 (even just two molecules per cell rather than one), a greater effect would be expected if the putative *phr*A gene product is indeed photoactive.

SURVIVAL CURVES

Initial 254nm UV survival curves were produced for all organisms. 24 hour secondary cultures of each organism were grown up as described in Section 2.1.4, the cells harvested as described in Section 2.5.1, and irradiated to reduce the surviving fraction by approximately 4 log cycles in four doses as described in Section 2.5.2. The results are shown in Figures 5.1, 5.2, 5.3 and 5.4.

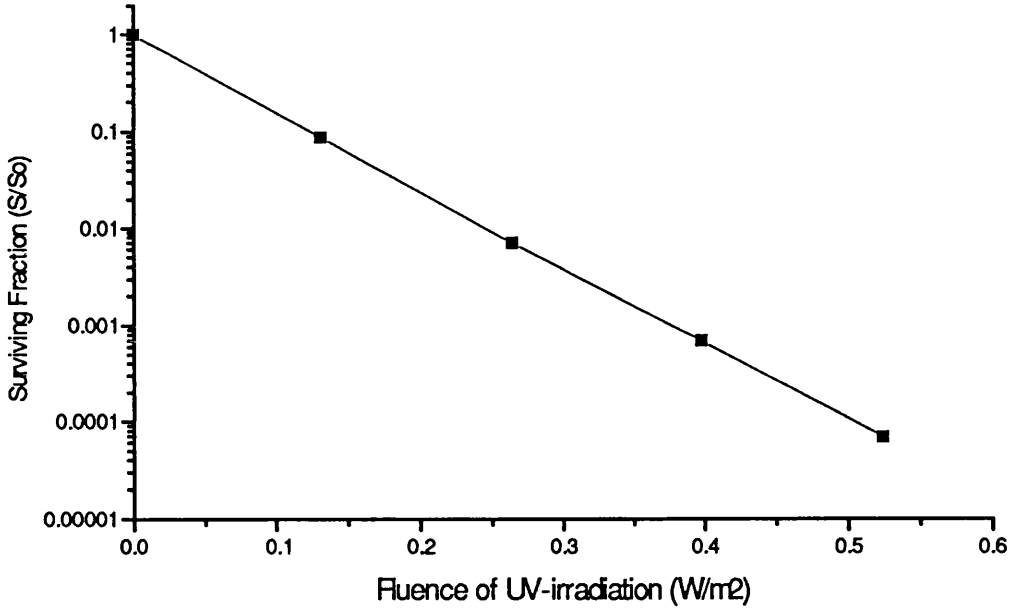

Figure 5.1. Survival Curve for UV-irradiated AS46/pND01 (■).

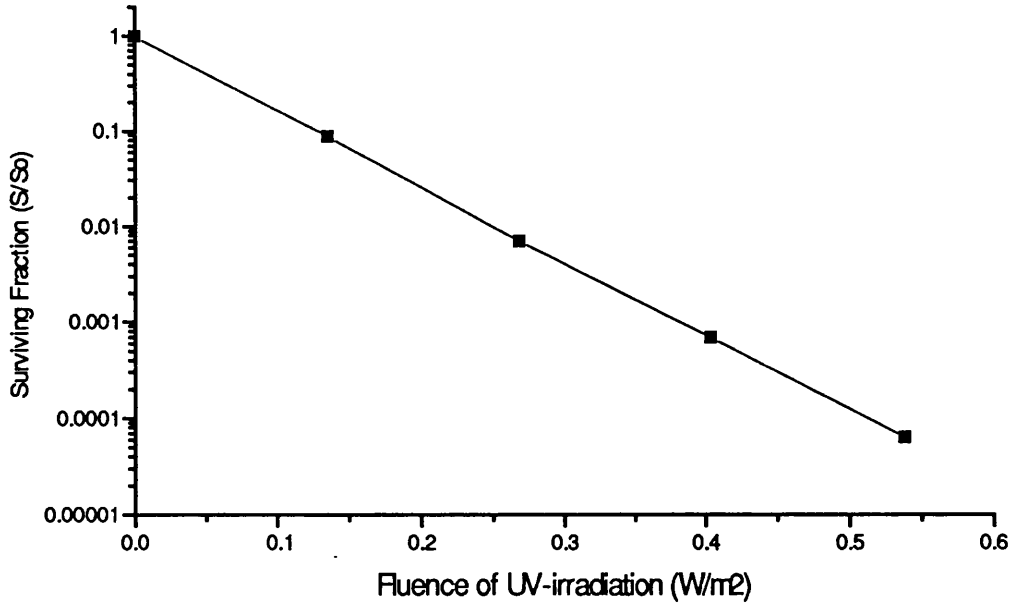

Figure 5.2. Survival Curve for UV-irradiated AS46/pUC19 (■).

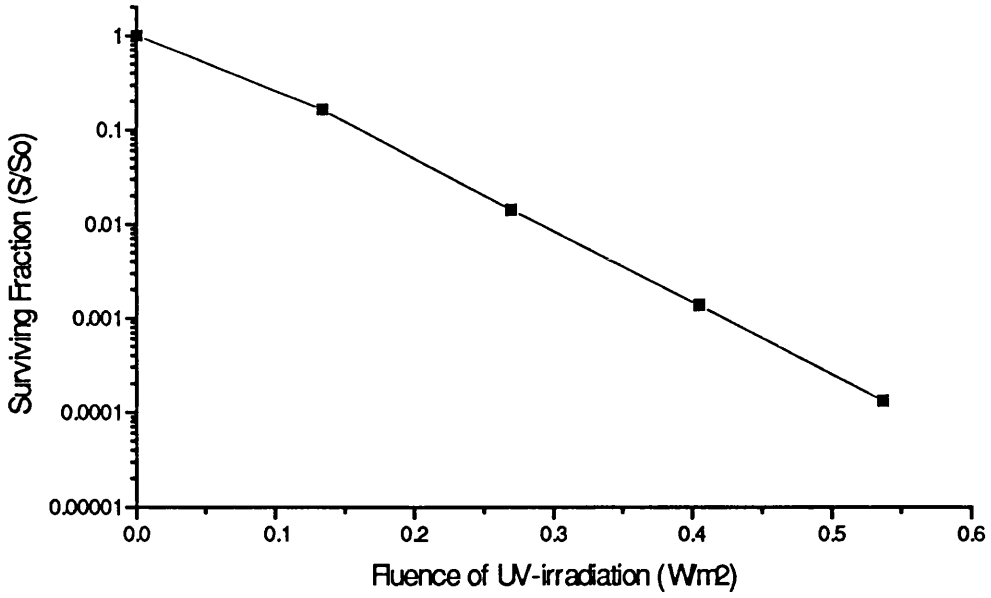

Figure 5.3. Survival Curve for UV-irradiated AS46/pND03 (■).

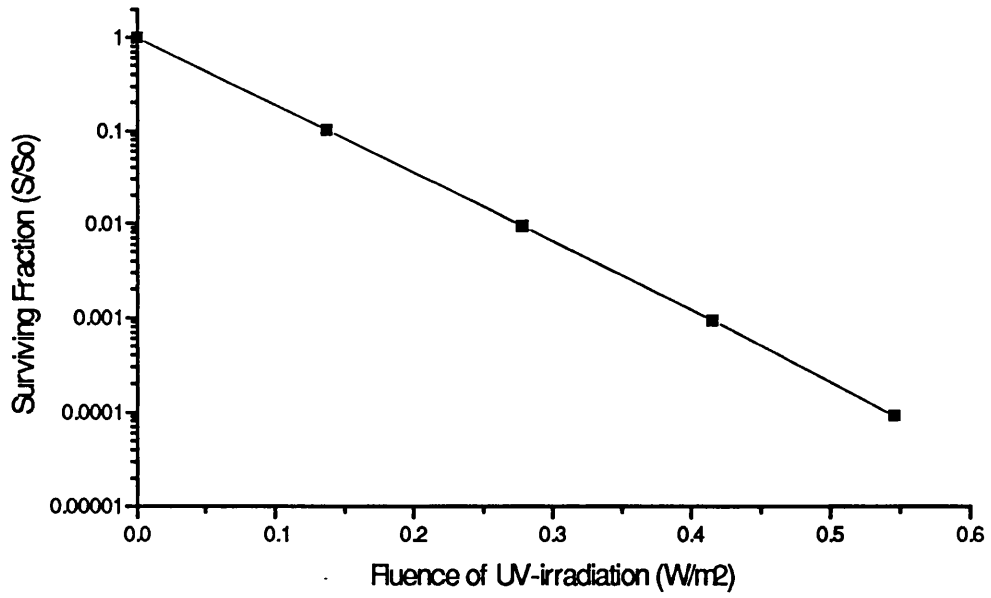

Figure 5.4. Survival Curve for UV-irradiated AS46/pKK223-3 (■).

PHOTOREACTIVATION

24 hour secondary cultures of both organisms were produced, harvested and irradiated as described above to reduce the surviving fraction to approximately 1 x 10^3 colony forming units per ml. The irradiated cells were incubated at 25°C for 20 minutes to allow any enzyme-substrate complexation to occur, then the cells were transferred to an illumination vessel which was placed in the temperature control unit. The irradiated cells were then exposed to photoreactivating light as described in Section 2.5.4 for a period of 120 minutes at a constant temperature of 25°C, sampling at 30 minutes intervals. Unirradiated cells were also exposed to the photoreactivating light at the same time and samples taken at 30 minute intervals as well. A sample of irradiated cells were held in the dark at 25°C and samples taken at 30 minute intervals as well. The results are shown in Figures 5.5, 5.6, 5.7 and 5.8. Throughout this work, all experiments were performed in triplicate, and one experiment presented in graphical form as a representative example.

The results show that all the strains studied showed a degree of recovery upon exposure to the photoreactivating light following UV irradiation, compared to the same UV-irradiated cells held in the dark. However, the strains carrying the *phr*A gene (AS46 / pND01 and AS46 / pND03) showed a degree of recovery greater than that seen in the strains carrying the plasmid vector alone (AS46 / pUC19 and AS46 / pKK223-3). The data was analysed quantitatively by examining the mean increase in survival from the three sets of results for each experiment for each strain studied. This was calculated from the surviving fractions at T = 0 and T = 120, by measuring the logarithmic increase in S/So at T = 120 from T = 0 - see Table 5.1.

STRAIN AND PHENOTYPE	INCREASE IN SURVIVAL
AS46 / pND01 ($phrA^+$)	0.62 0.02
AS46 / pUC19 ($phrA^-$)	0.40 0.11
AS46 / pND03 ($phrA^+$)	0.84 0.07
AS46 / pKK223-3 ($phrA^-$)	0.50 0.04
AS46 ($phrA^-$)	0.33 0.14

Table 5.1. Increase in mean survival after 120 minutes of photoreactivation at 25°C.

These results suggested two important points :-

a) Strain AS46 is not totally photoreactivation-repair deficient as reported by Smith (1987), which is in keeping with the results published by Husain and Sancar (1987a), who suggested that no known *E. coli* strain was totally deficient in photoreactivation.

b) The *phr*A gene product does affect the rate and maybe the extent of photoreactivation in *E. coli.*

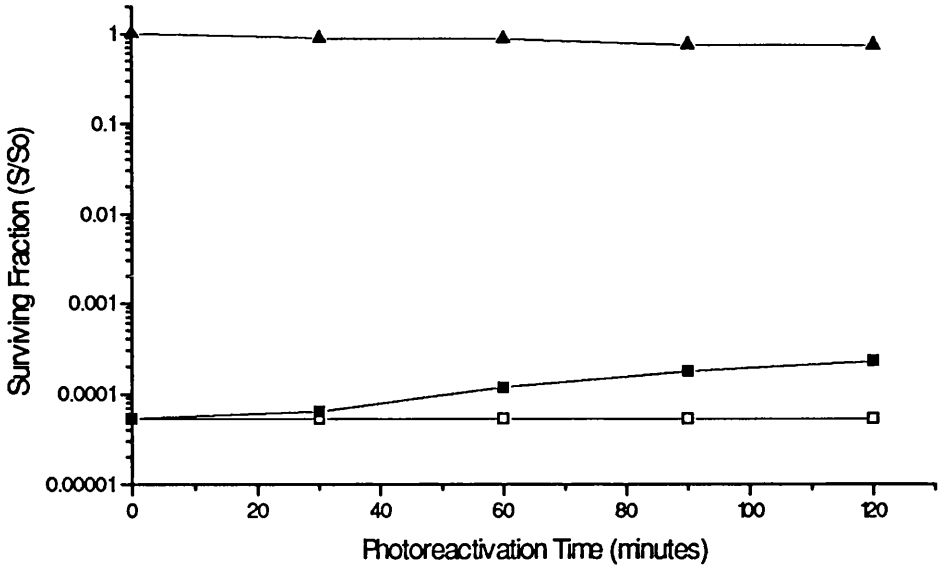

Figure 5.5. Photoreactivation of UV-irradiated AS46/pND01 (■) at 25°C. The controls are UV-irradiated AS46/pND01 (□) in the dark and unirradiated AS46/pND01 (▲) in the photoreactivating light.

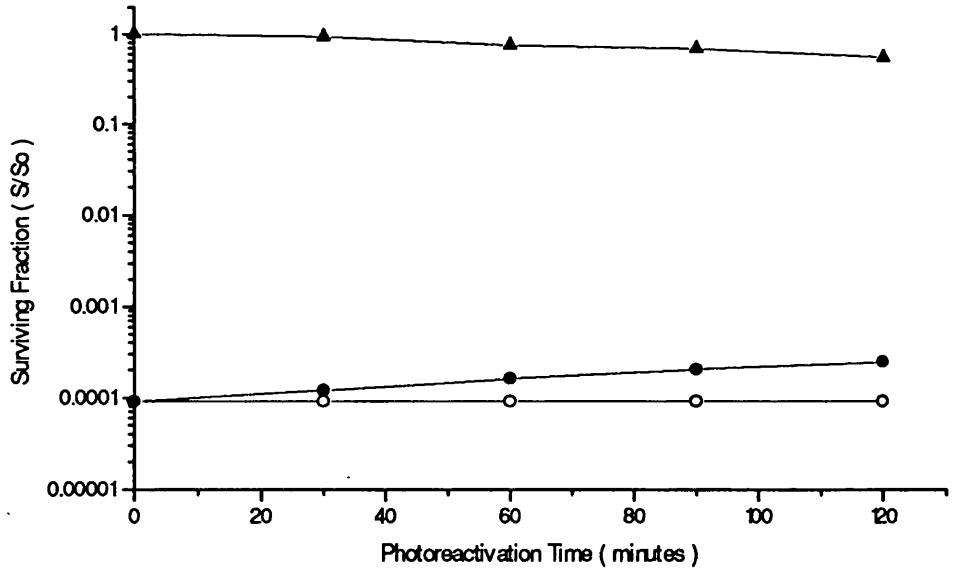

Figure 5.6. Photoreactivation of UV-irradiated AS46/pUC19 (●) at 25°C. The controls are UV-irradiated AS46/pUC19 (○) in the dark and unirradiated AS46/pUC19 (▲) in the photoreactivating light.

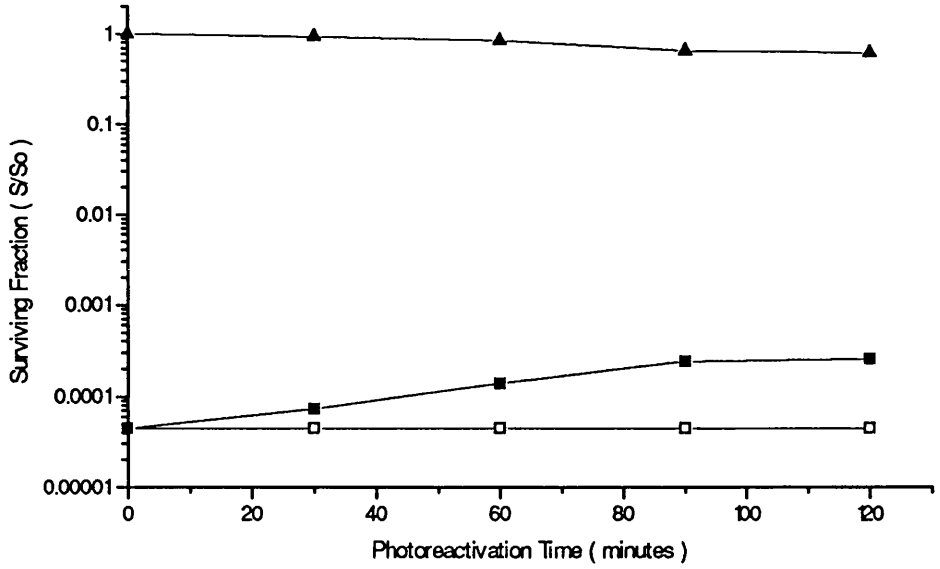

Figure 5.7. Photoreactivation of UV-irradiated AS46/pND03 (■) at 25°C. The controls are UV-irradiated AS46/pND03 (❑) in the dark and unirradiated AS46/pND03 (▲) in the photoreactivating light.

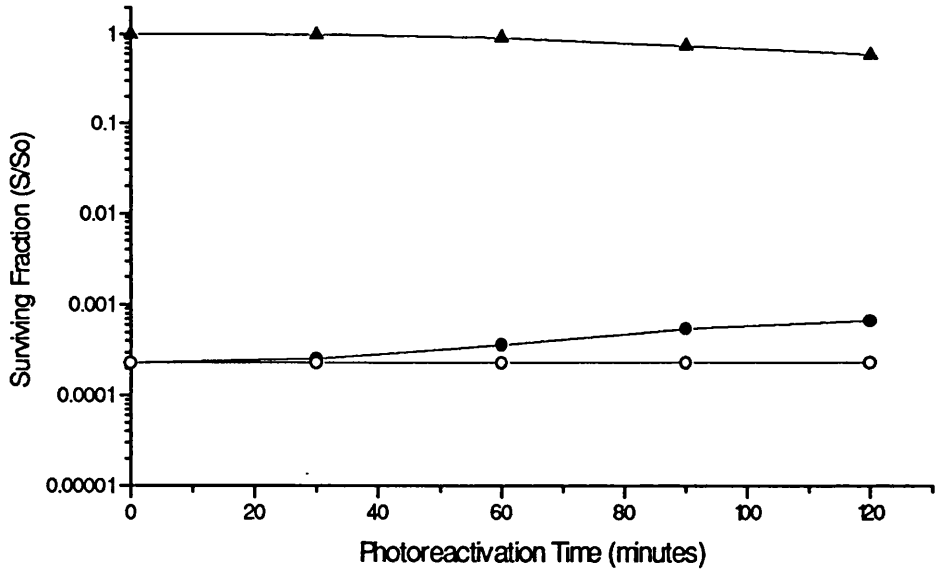

Figure 5.8. Photoreactivation of UV-irradiated AS46/pKK223-3 (●) at 25°C. The controls are UV-irradiated AS46/pKK223-3 (○) in the dark and unirradiated AS46/pKK223-3 (▲) in the photoreactivating light.

The same photoreactivation experiment as described above was performed with AS46, which also showed a degree of light-repair compared to dark-repair over a 120 minute period of exposure to photoreactivating light - see Figure 5.9 and Table 5.1. However, the degree of repair was no way near the level of 30% of the lethal damage reported by Husain and Sancar (1987a) in *phr*B and *phr*A *phr*B mutants exposed to 5 hours of photoreactivating light.

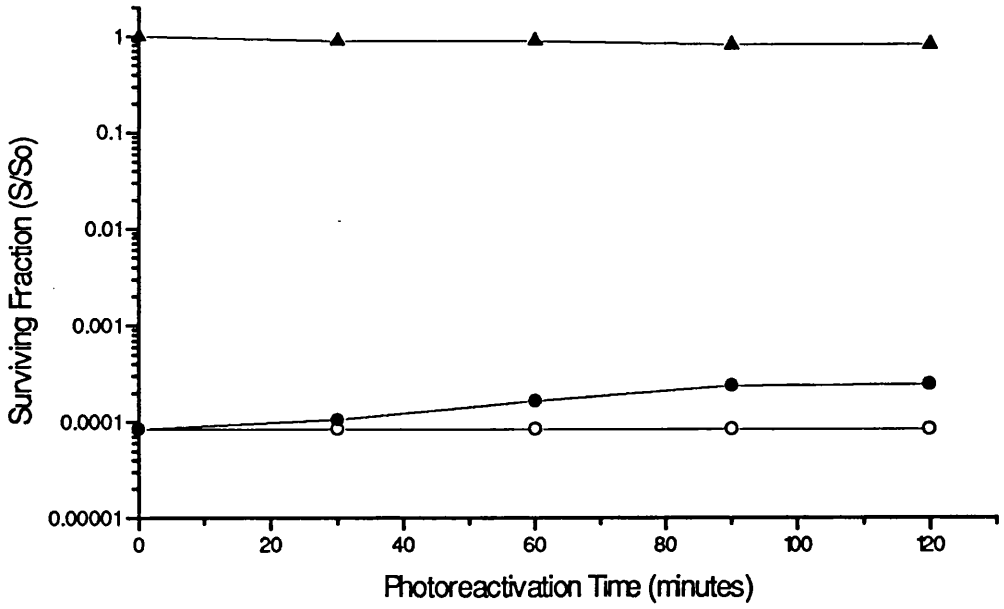

Figure 5.9. Photoreactivation of UV-irradiated AS46 (●) at 25°C. The controls are UV-irradiated AS46 (○) in the dark and unirradiated AS46 (▲) in the photoreactivating light.

The rate and extent of repair in strain AS46 / pND03 was higher over a 120 minute period of exposure to photoreactivating light than that seen in strain AS46 / pND01 - see Table 5.1. Therefore in the following temperature and dose-rate studies, AS46 / pND03 was used as the test strain and AS46 / pKK223-3 used as the control strain.

5.3.3 TEMPERATURE DEPENDENCE STUDIES

It has been claimed that the photoreactivation seen in *phr*B mutants is due to Type III photoreactivation (Husain and Sancar, 1987a). One of the features of Type III photoreactivation is the absence of the effect of temperature changes on the rate of recovery. Thus the photoreactivation experiments were performed at 37°C, 25°C and at 10°C to see if temperature was a factor in the repair seen in strains AS46 / pND03 and AS46 / pKK223-3.

PHOTOREACTIVATION AT DIFFERENT TEMPERATURES

24 hour secondary cultures of both organisms were produced, harvested and irradiated as described above to reduce the surviving fraction to approximately 1 x 10^3 colony forming units per ml. The irradiated cells were incubated at 25°C for 20 minutes to allow any enzyme-substrate complexation to occur, then the cells were transferred to an illumination vessel which was placed in the temperature control unit and allowed to equilibrate to the experimental temperature for a further 5 minutes. The irradiated cells were then exposed to photoreactivating light as described in Section 2.5.4 for a period of 120 minutes, sampling at 30 minutes intervals. Unirradiated cells were also exposed to the photoreactivating light at the same time and samples taken at 30 minute intervals as well. A sample of irradiated cells were held in the dark at the experimental temperature and samples taken at 30 minute intervals as well. The results are shown in Figures 5.10, 5.7, 5.11, 5.12, 5.8 and 5.13.

The results showed that the temperature at which photoreactivation takes place had a dramatic effect on the rate and extent of repair of strain AS46 / pND03 and very little effect on the rate and extent of repair of strain AS46 /pKK223-3 - see Table 5.2. This is discussed in Section 2.4.

STRAIN AND PHENOTYPE	INCREASE IN SURVIVAL
AS46 / pND03 ($phrA^+$) at 37°C	1.01 0.01
AS46 / pND03 ($phrA^+$) at 25°C	0.84 0.07
AS46 / pND03 ($phrA^+$) at 10°C	0.27 0.12
AS46 / pKK223-3 ($phrA^-$) at 37°C	0.50 0.12
AS46 / pKK223-3 ($phrA^-$) at 25°C	0.50 0.04
AS46 / pKK223-3 ($phrA^-$) at 10°C	0.26 0.19

Table 5.2. Increase in mean survival after 120 minutes of photoreactivation at different temperatures using a fluence-rate of 8.5Wm^{-2}.

Using the increase in mean survival after 60 minutes instead of after 120 minutes, gives an indication of the increase in the rate of the photorecovery at 37°C compared to 25°C - see Table 5.3.

STRAIN AND PHENOTYPE	INCREASE IN SURVIVAL
AS46 / pND03 ($phrA^+$) at 37°C	0.91 0.03
AS46 / pND03 ($phrA^+$) at 25°C	0.50 0.08
AS46 / pKK223-3 ($phrA^-$) at 37°C	0.33 0.19
AS46 / pKK223-3 ($phrA^-$) at 25°C	0.31 0.13

Table 5.3. Increase in mean survival after 60 minutes of photoreactivation at different temperatures using a fluence-rate of 8.5Wm^{-2}.

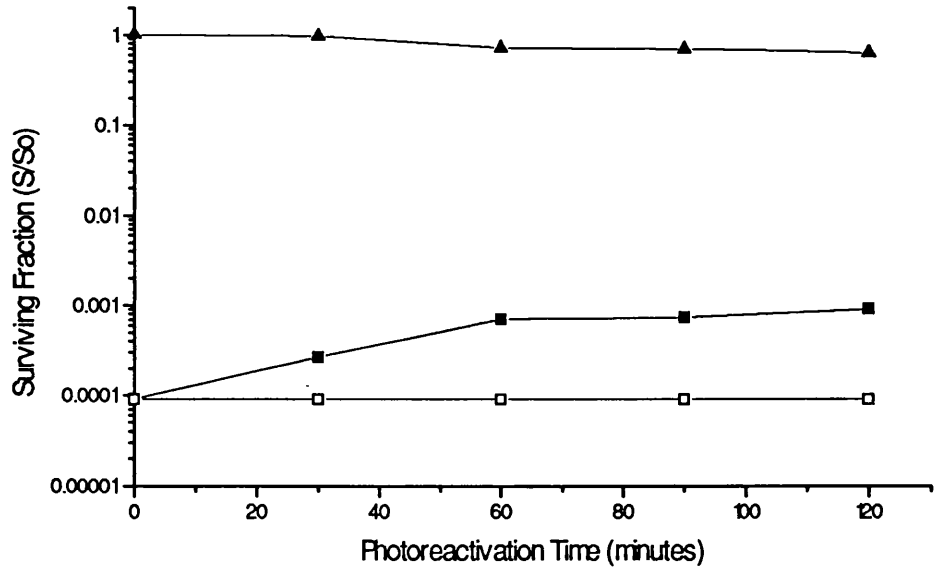

Figure 5.10. Photoreactivation of UV-irradiated AS46/pND03 (■) at 37°C. The controls are UV-irradiated AS46/pND03 (❑) in the dark and unirradiated AS46/pND03 (▲) in the photoreactivating light.

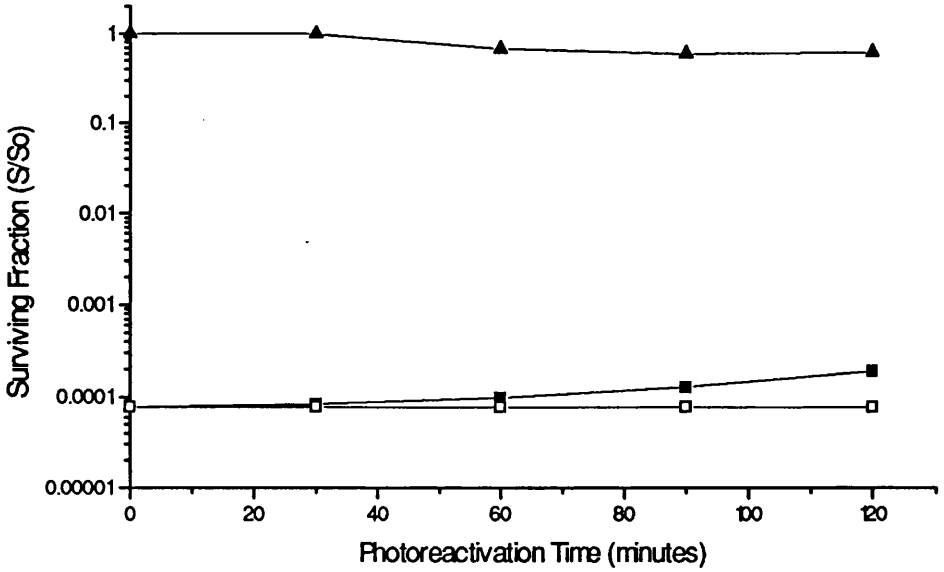

Figure 5.11. Photoreactivation of UV-irradiated AS46/pND03 (■) at 10°C. The controls are UV-irradiated AS46/pND03 (❑) in the dark and unirradiated AS46/pND03 (▲) in the photoreactivating light.

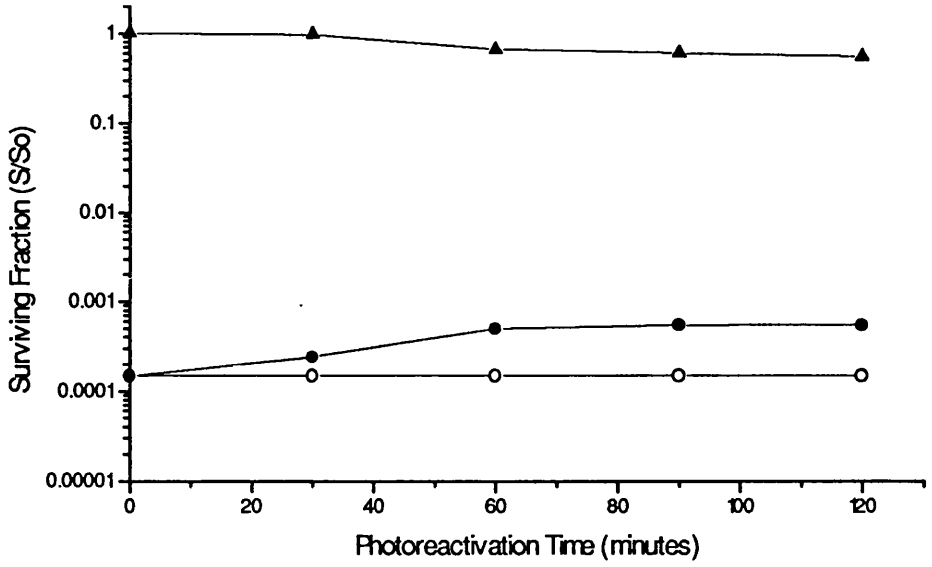

Figure 5.12. Photoreactivation of UV-irradiated AS46/pKK223-3 (●) at 37°C. The controls are UV-irradiated AS46/pKK223-3 (○) in the dark and unirradiated AS46/pKK223-3 (▲) in the photoreactivating light.

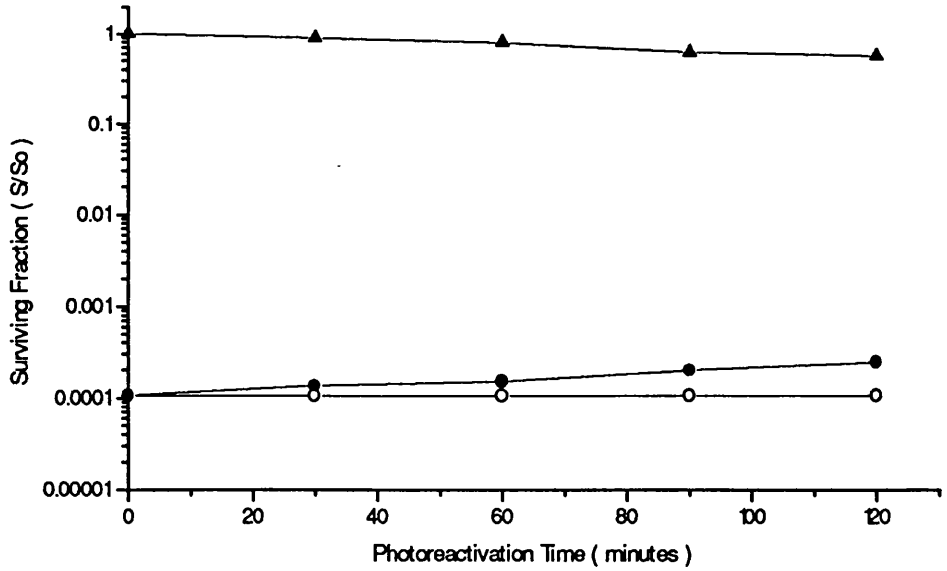

Figure 5.13. Photoreactivation of UV-irradiated AS46/pKK223-3 (●) at 10°C. The controls are UV-irradiated AS46/pKK223-3 (○) in the dark and unirradiated AS46/pKK223-3 (▲) in the photoreactivating light.

5.3.4 DOSE-RATE DEPENDENCE STUDIES

Another feature of Type III photoreactivation is the absence of dose-rate effects. Thus the photoreactivation of AS46 / pND03 at 37°C and 25°C was performed using different fluences of photoreactivating light, using AS46 / pKK223-3 as a control.

PHOTOREACTIVATION USING DIFFERENT FLUENCE RATES OF PHOTOREACTIVATING LIGHT

24 hour secondary cultures of both organisms were produced, harvested and irradiated as described above to reduce the surviving fraction to approximately 1 x 10^3 colony forming units per ml. The irradiated cells were incubated at 25°C for 20 minutes to allow any enzyme-substrate complexation to occur, then the cells were transferred to an illumination vessel which was placed in the temperature control unit and allowed to equilibrate to the experimental temperature for a further 5 minutes. The irradiated cells were then exposed to photoreactivating light for a period of 120 minutes, sampling at 30 minutes intervals.

The comparative estimates of the fluence-rates were made using the calibrated thermopile as described in Section 2.5.4.

The fluence-rate of the photoreactivating light used in the Initial Photoreactivation Studies (see Section 5.3.2) was calculated as approximately 8.5Wm^{-2}.

To decrease the fluence-rate of the photoreactivating light, the temperature control unit was moved further away from the light source, to give the approximate fluence-rates of 5Wm^{-2} and 1Wm^{-2}.

To increase the fluence-rate of the photoreactivating light, the temperature control unit was moved closer to the light source, to give the approximate fluence-rate of 12Wm^{-2}.

Unirradiated cells were also exposed to the photoreactivating light at the same time and samples taken at 30 minute intervals as well. A sample of irradiated cells were held in the

dark at the experimental temperature and samples taken at 30 minute intervals as well. The results are shown in Figures 5.14 to 5.21.

The results showed that at 37°C, reduction of the fluence-rate from approximately 8.5Wm^{-2} to 1Wm^{-2} had very little effect on the rate or extent of repair of strain AS46 / pND03 or strain AS46 /pKK223-3 after 120 minutes of photoreactivation - see Figures 5.14 and 5.15 and Table 5.4.

STRAIN AND PHENOTYPE	INCREASE IN SURVIVAL
AS46 / pND03 ($phrA^+$) at 8.5Wm^{-2}	1.01 0.01
AS46 / pND03 ($phrA^+$) at 1Wm^{-2}	0.96 0.02
AS46 / pKK223-3 ($phrA^-$) at 8.5Wm^{-2}	0.50 0.12
AS46 / pKK223-3 ($phrA^-$) at 1Wm^{-2}	0.45 0.09

Table 5.4. Increase in mean survival after 120 minutes of photoreactivation at different fluence-rates at a temperature of 37°C.

However, using the increase in mean survival after 60 minutes instead of after 120 minutes, shows there is a difference in the rate of the photorecovery at 1Wm^{-2} compared to 8.5Wm^{-2} - see Table 5.5.

STRAIN AND PHENOTYPE	INCREASE IN SURVIVAL
AS46 / pND03 ($phrA^+$) at 8.5Wm^{-2}	0.91 0.03
AS46 / pND03 ($phrA^+$) at 1Wm^{-2}	0.72 0.07

Table 5.5. Increase in mean survival after 60 minutes of photoreactivation at different fluence-rates at a temperature of 37°C.

At 25°C, reduction of the fluence-rate from approximately 8.5Wm^{-2} to either 1Wm^{-2} or 5Wm^{-2} had a dramatic effect on the rate and extent of repair of strain AS46 / pND03 and very little effect on the rate and extent of repair of strain AS46 / pKK223-3 - see Figures 5.16 to 5.19. An increase of the fluence-rate from approximately 8.5Wm^{-2} to 12Wm^{-2} increased the rate and extent of repair of strain AS46 / pND03, and had very little effect on the rate and extent of repair of strain AS46 / pKK223-3 - see Figures 5.20 and 5.21. The changes in mean increase in survival are presented in Table 5.6.

STRAIN AND PHENOTYPE	INCREASE IN SURVIVAL
AS46 / pND03 ($phrA^+$) at 1Wm^{-2}	0.34 0.08
AS46 / pND03 ($phrA^+$) at 5Wm^{-2}	0.51 0.17
AS46 / pND03 ($phrA^+$) at 8.5Wm^{-2}	0.84 0.07
AS46 / pND03 ($phrA^+$) 12Wm^{-2}	1.10 0.16
AS46 / pKK223-3 ($phrA^-$) at 1Wm^{-2}	0.45 0.18
AS46 / pKK223-3 ($phrA^-$) at 5Wm^{-2}	0.53 0.06
AS46 / pKK223-3 ($phrA^-$) at 8.5Wm^{-2}	0.50 0.04
AS46 / pKK223-3 ($phrA^-$) at 12Wm^{-2}	0.45 0.11

Table 5.6. Increase in mean survival after 120 minutes of photoreactivation at different fluence-rates at a temperature of 25°C.

These results are discussed in Section 5.4.

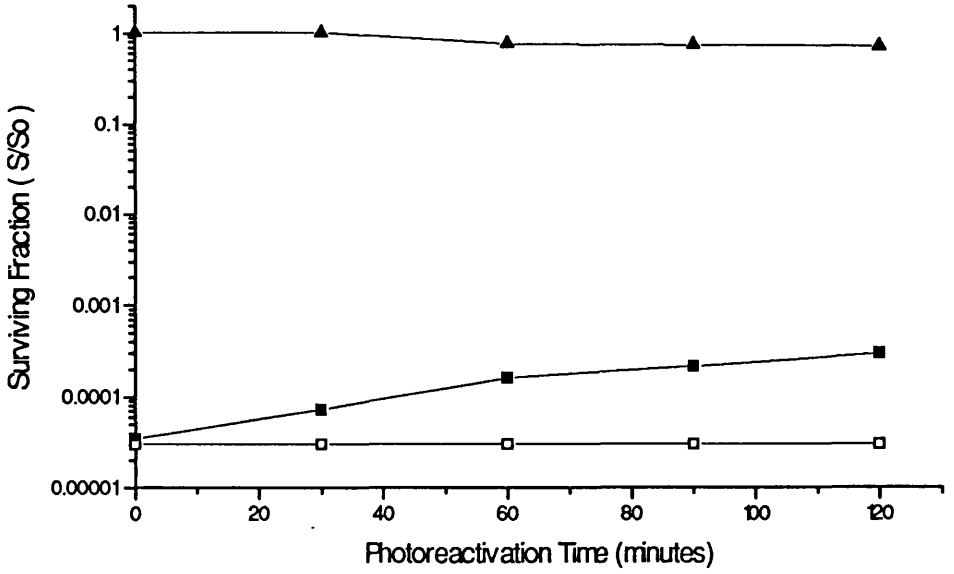

Figure 5.14. Photoreactivation with a low fluence-rate (≅ 1Wm^{-2}) of UV-irradiated AS46/pND03 (■) at 37°C. The controls are UV-irradiated AS46/pND03 (❑) in the dark and unirradiated AS46/pND03 (▲) in the photoreactivating light.

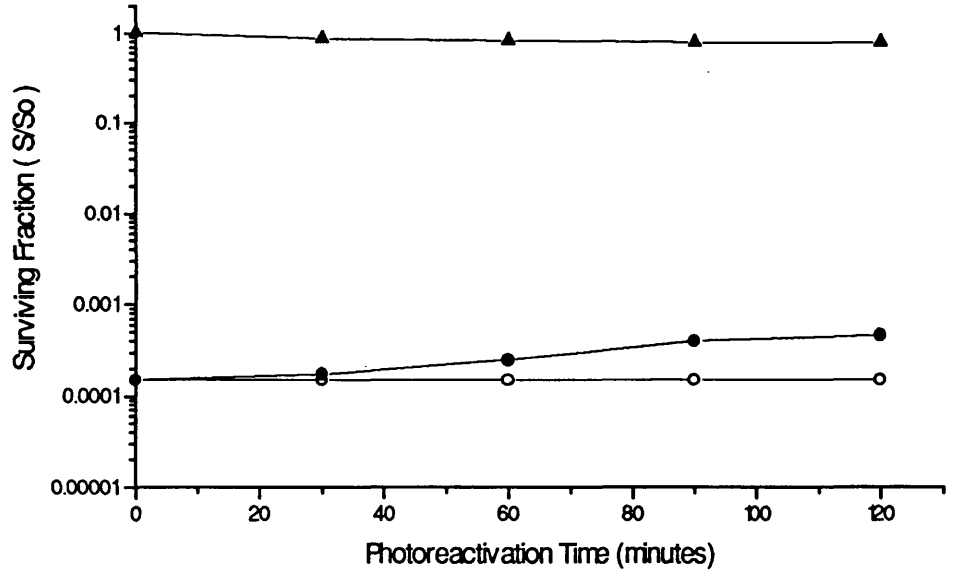

Figure 5.15. Photoreactivation with a low fluence-rate (≅ 1Wm^{-2}) of UV-irradiated AS46/pKK223-3 (●) at 37°C. The controls are UV-irradiated AS46/pKK223-3 (○) in the dark and unirradiated AS46/pKK223-3 (▲) in the photoreactivating light.

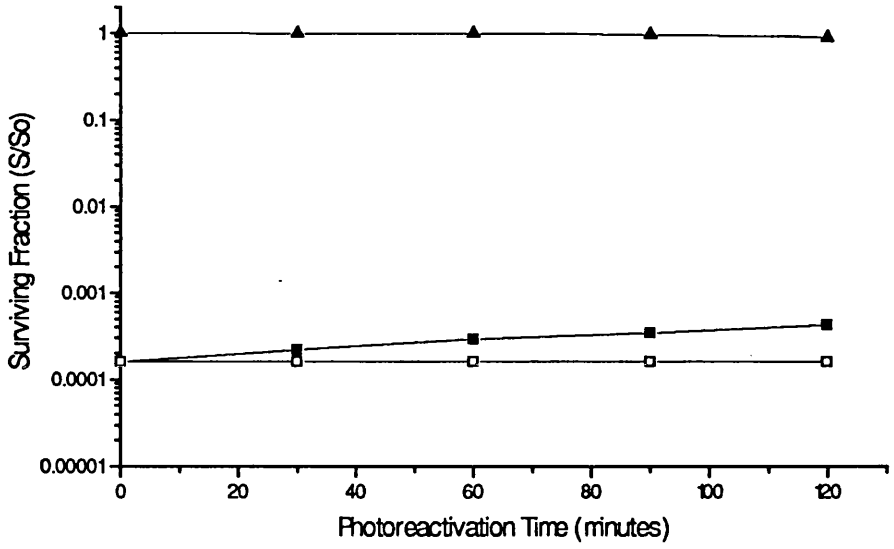

Figure 5.16. Photoreactivation with a low fluence-rate (≅ 1Wm^{-2}) of UV-irradiated AS46/pND03 (■) at 25°C. The controls are UV-irradiated AS46/pND03 (❑) in the dark and unirradiated AS46/pND03 (▲) in the photoreactivating light.

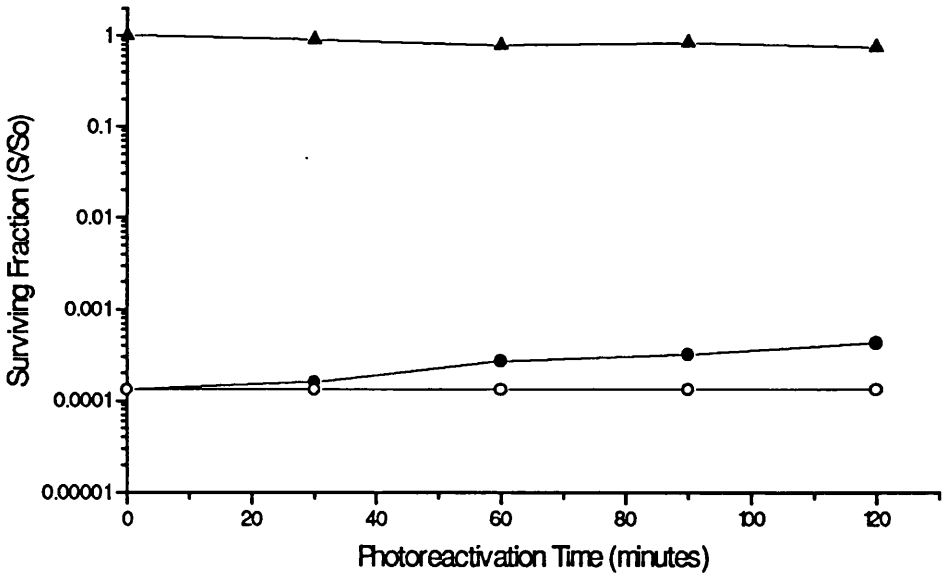

Figure 5.17. Photoreactivation with a low fluence-rate (≅ 1Wm^{-2}) of UV-irradiated AS46/pKK223-3 (●) at 25°C. The controls are UV-irradiated AS46/pKK223-3 (○) in the dark and unirradiated AS46/pKK223-3 (▲) in the photoreactivating light.

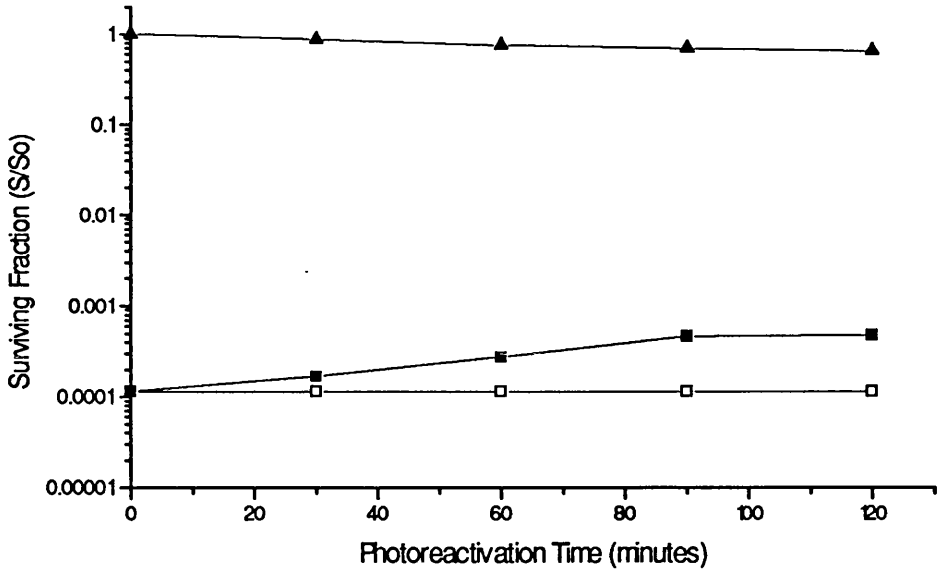

Figure 5.18. Photoreactivation with a low fluence-rate (≅ 5Wm^{-2}) of UV-irradiated AS46/pND03 (■) at 25°C. The controls are UV-irradiated AS46/pND03 (❑) in the dark and unirradiated AS46/pND03 (▲) in the photoreactivating light.

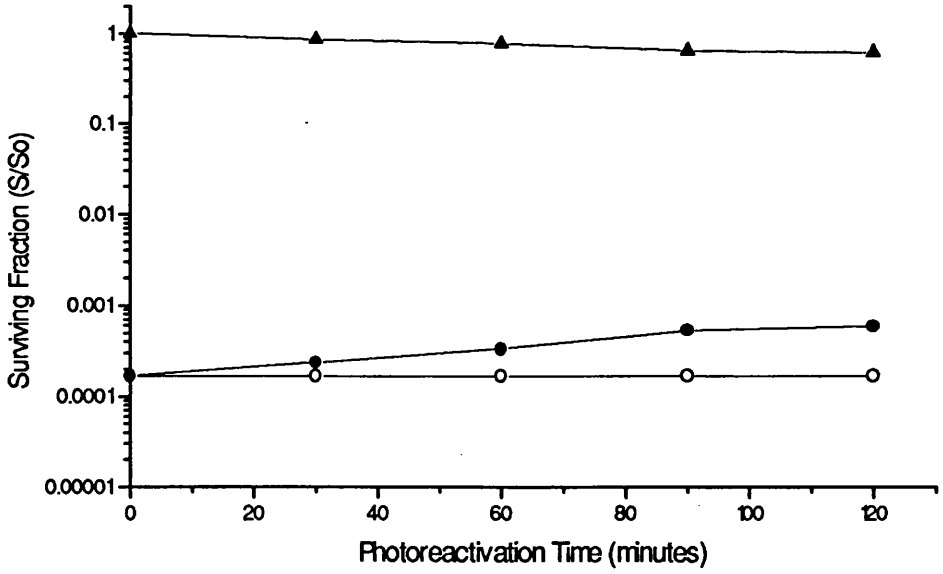

Figure 5.19. Photoreactivation with a low fluence-rate (≅ 5Wm^{-2}) of UV-irradiated AS46/pKK223-3 (●) at 25°C. The controls are UV-irradiated AS46/pKK223-3 (○) in the dark and unirradiated AS46/pKK223-3 (▲) in the photoreactivating light.

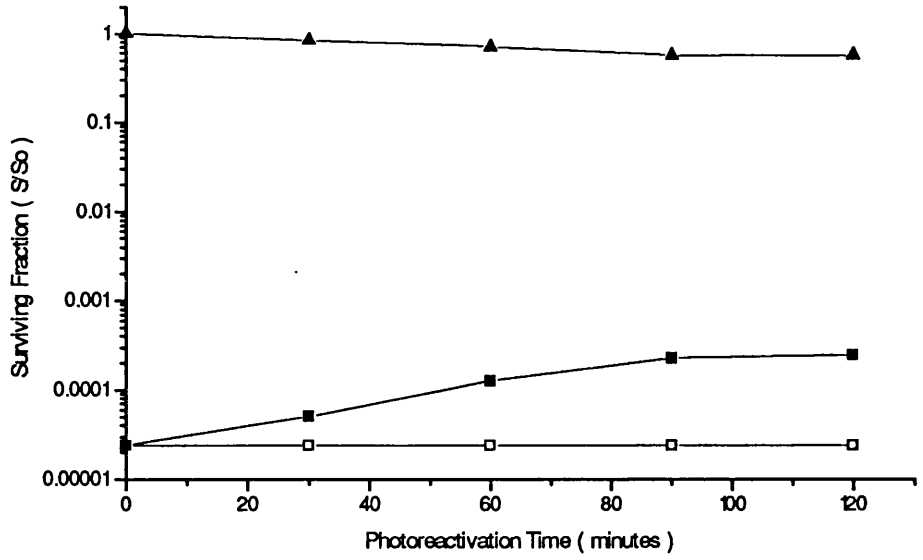

Figure 5.20. Photoreactivation with a high fluence-rate (≅ 12Wm^{-2}) of UV-irradiated AS46/pND03 (■) at 25°C. The controls are UV-irradiated AS46/pND03 (❑) in the dark and unirradiated AS46/pND03 (▲) in the photoreactivating light.

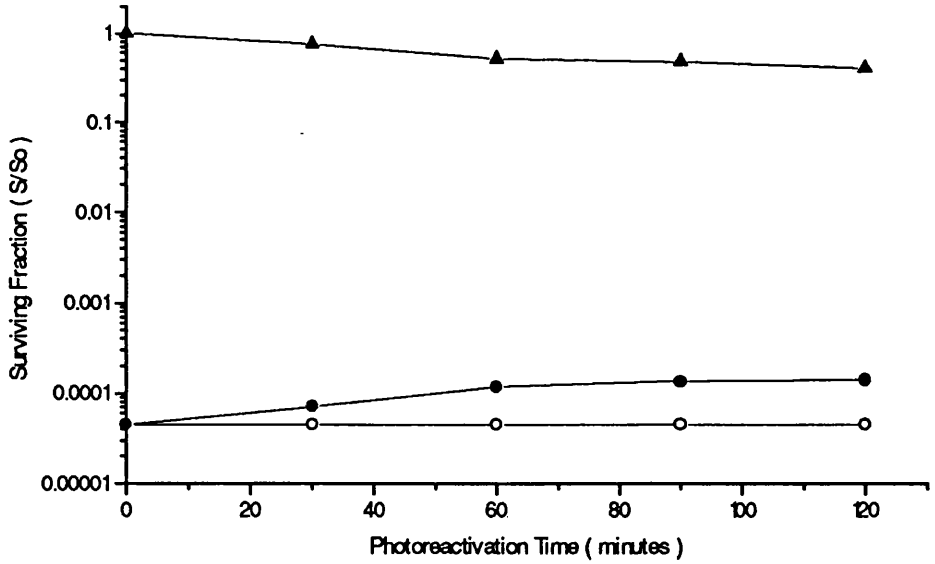

Figure 5.21. Photoreactivation with a high fluence-rate (≅ 12Wm^{-2}) of UV-irradiated AS46/pKK223-3 (●) at 25°C. The controls are UV-irradiated AS46/pKK223-3 (○) in the dark and unirradiated AS46/pKK223-3 (▲) in the photoreactivating light.

5.3.5 NEAR-UV SENSITIVITY STUDIES

Husain and Sancar (1987a) reported their observation that deletion of the *gal-attλ* region in *phr*B mutants made the strains more sensitive to near-UV killing. Their explanation for this was that the increase in killing by near-UV light was due to sensitisation of the cells due to accumulation of coproporphyrin, which was in turn due to the deletion of the *hem*F gene, located within the *gal-attλ* region (Bachmann, 1989) - see Section 1.5.3. The gene sequenced in this study is not the *hem*F gene, and it was decided to investigate whether the presence of this gene decreased the sensitivity to near-UV light (photoreactivating light). This was accomplished by comparing the killing of AS46 / pND01 compared to AS46 / pUC19, and AS46 / pND03 compared to AS46 / pKK223-3, upon exposure of unirradiated cells to the photoreactivating light at 25 °C.

NEAR-UV SENSITIVITY OF *phr*A$^+$ AND *phr*A$^-$ STRAINS IN A DARK REPAIR-DEFICIENT AND *phr*B$^-$ BACKGROUND

24 hour secondary cultures of each organism were produced and harvested to give approximately 1 x 10^7 colony forming units per ml as described above. After the 5 minutes incubation at 25°C, the cells were incubated at room temperature in the dark for 5 minutes, to mimic the time and conditions allowed for while other cells would normally be irradiated. The cells were incubated at 25°C for 20 minutes to mimic the time allowed for any enzyme-substrate complexation to occur, then the cells were transferred to two separate illumination vessels which were placed in the temperature control unit. The cells were then exposed to photoreactivating light of approximate fluence-rate of 8.5Wm^{-2} for a period of 120 minutes, sampling at 30 minutes intervals. The results are shown in Figures 5.22 and 5.23.

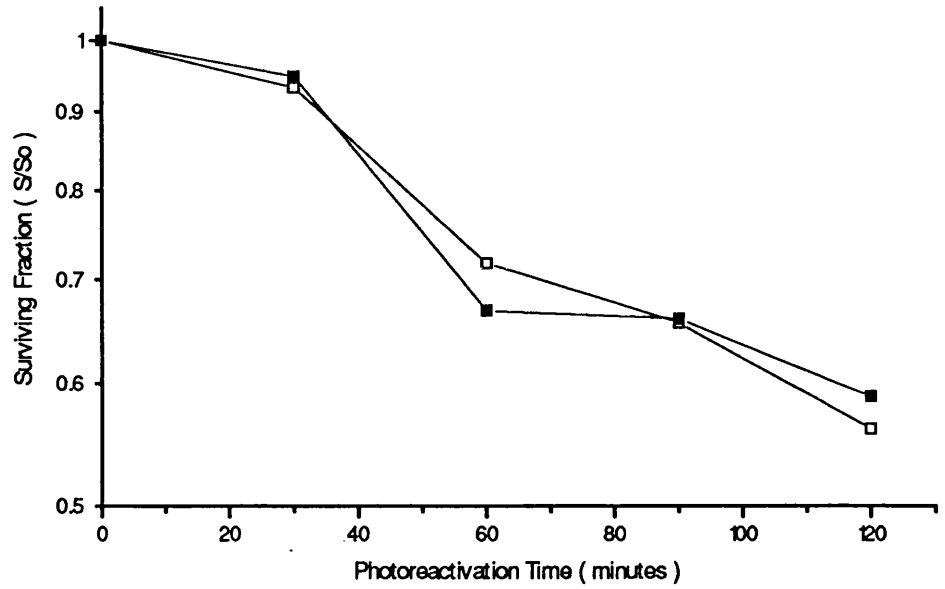

Figure 5.22. Near-UV sensitivity of AS46/pND01 (■) and AS46/pUC19 (❑) when unirradiated cells were exposed to photoreactivating light of a fluence-rate of 8.5Wm^{-2}.

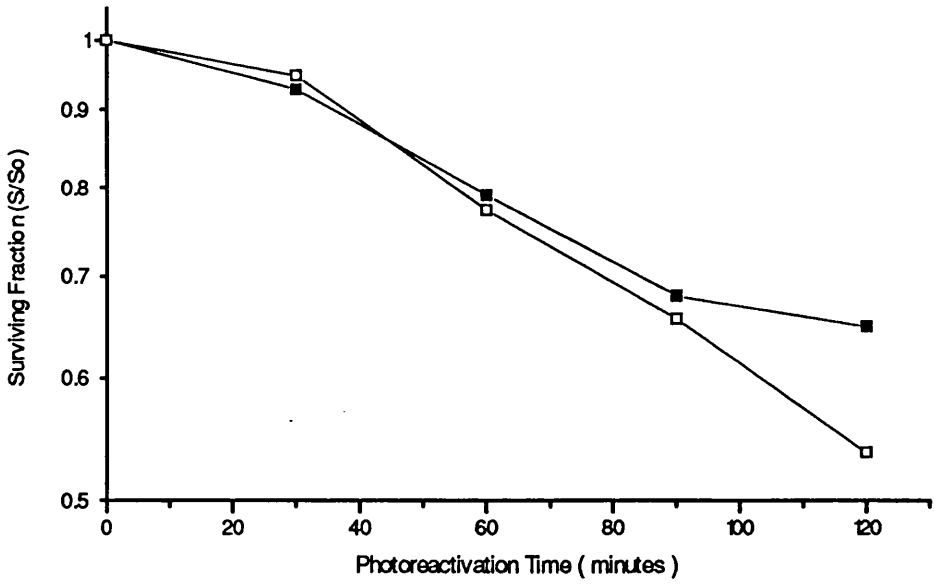

Figure 5.23. Near-UV sensitivity of AS46/pND03 (■) and AS46/pKK223-3 (❑) when unirradiated cells were exposed to photoreactivating light of a fluence-rate of 8.5Wm^{-2}.

The differences in the near-UV sensitivity between AS46 / pND01 and AS46 / pUC19 were not very pronounced - see Figure 5.22., while the differences between AS46 / pND03 and AS46 / pKK223-3 were more noticeable, but not very dramatic. Therefore, using photoreactivating light of a fluence-rate of 8.5Wm^{-2} didn't really emphasise the observation made by Husain and Sancar (1987a). Therefore, the experiments were repeated with strains AS46 / pND03 and AS46 / pKK223-3 using photoreactivating light of a fluence-rate 12Wm^{-2}. The results are shown in Figure 5.24.

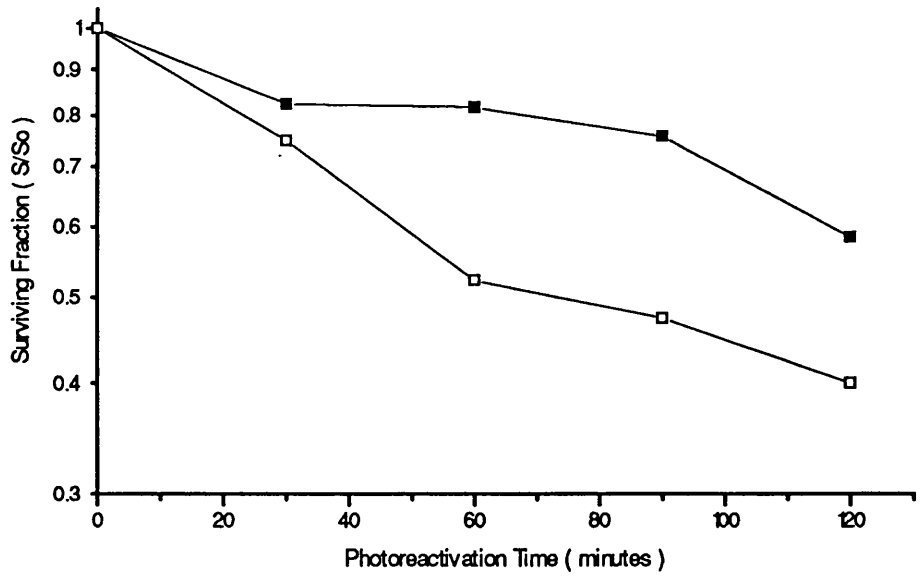

Figure 5.24. Near-UV sensitivity of AS46/pND03 (■) and AS46/pKK223-3 (❑) when unirradiated cells were exposed to photoreactivating light of a fluence-rate of 12Wm^{-2}.

The differences in near-UV sensitivity between AS46 / pND03 and AS46 / pKK223-3 upon exposure to the higher fluence-rate of photoreactivating light were more pronounced.

These results are discussed in Section 5.4.

5.3.6 FURTHER PHOTOREACTIVATION STUDIES

As stated at the beginning of Section 5.3, plasmid pND05 was not produced until much later on in this study. When pND05 was produced (see Section 4.3.5) it was transformed into strain AS46 as described in Section 5.3.1. It was hoped that though no over-expression of the putative *phr*A gene product was observed in Section 4.3.6, the *in vivo* activity would still be seen, as had been the case with pND03.

PHOTOREACTIVATION OF AS46 / pND05

A 24 hour secondary culture of AS46 / pND05 was produced, harvested and irradiated as described above to reduce the surviving fraction to approximately 1 x 10^3 colony forming units per ml. The irradiated cells were incubated at 25°C for 20 minutes to allow any enzyme-substrate complexation to occur, then the cells were transferred to an illumination vessel which was placed in the temperature control unit. The irradiated cells were then exposed to photoreactivating light of a fluence-rate of 8.5Wm^{-2} as described in Section 2.5.4 for a period of 120 minutes at a constant temperature of 25°C, sampling at 30 minutes intervals. Unirradiated cells were also exposed to the photoreactivating light at the same time and samples taken at 30 minute intervals as well. A sample of irradiated cells were held in the dark at 25°C and samples taken at 30 minute intervals as well. The results are shown in Figure 5.25.

The results showed that there was very little difference in the rate and extent of photorepair between AS46 / pND05 and AS46 / pKK223-3 - see Table 5.7. The near-UV sensitivity of AS46 / pND05 was closer to that seen in AS46 / pKK223-3 than AS46 / pND03. This is discussed in Section 5.4.

STRAIN AND PHENOTYPE	INCREASE IN SURVIVAL
AS46 / pND05 ($phrA^+$)	0.36 0.10
AS46 / pKK223-3 ($phrA^-$)	0.50 0.04

Table 5.7. Increase in mean survival after 120 minutes of photoreactivation at 25°C using a fluence-rate of 8.5Wm^{-2}.

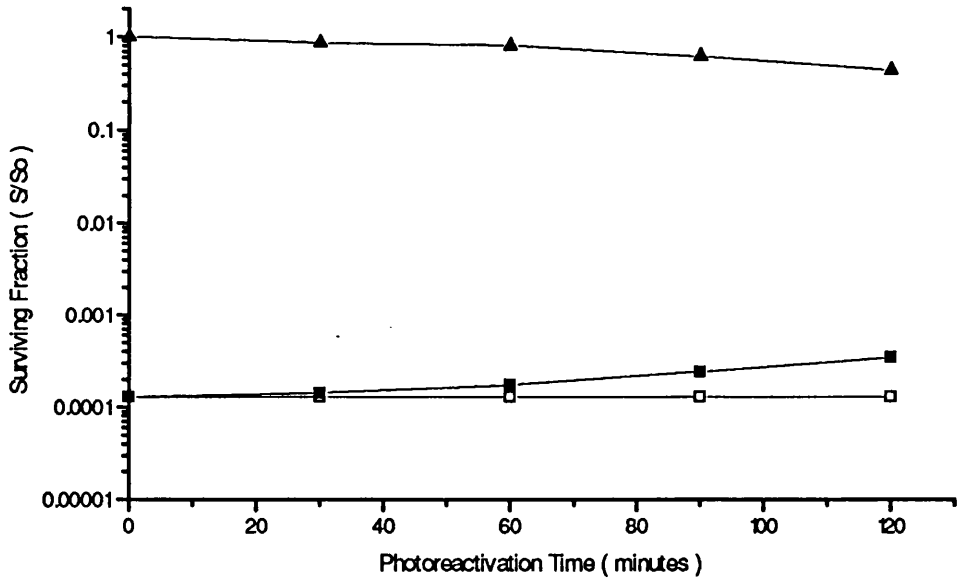

Figure 5.25. Photoreactivation of UV-irradiated AS46/pND05 (■) at 25°C. The controls are UV-irradiated AS46/pND05 (❑) in the dark and unirradiated AS46/pND05 (▲) in the photoreactivating light.

5.4 DISCUSSION

The *in vivo* activity of the putative *phr*A gene in the three vectors pND01, pND03 and pND05 was investigated in this section of the study. Smith (1987) and Smith and Moss (1988) have shown approximately 1 log cycle photorecovery after UV-irradiation reduction of 4 log cycles with strain AS46 / pAS01, which carries the putative *phr*A gene on plasmid pAS01.

The initial photoreactivation studies (see Sections 5.3.1 and 5.3.6) produced some interesting results. Both AS46 / pND01 and AS46 / pND03 showed photorecovery above that of the controls, while AS46 / pND05 did not. The photorecovery seen in AS46 / pND03 proceeded at a faster rate and to a greater extent than that seen in AS46 / pND01. An attractive explanation for this observation from the point of view of this study, is that this is due to the presence of more molecules per cell of the putative *phr*A gene product. The fact that AS46 / pND05 did not photoreactivate above the rate or extent of the control, AS46 / pKK223-3, would suggest that the putative *phr*A gene is not functioning in this plasmid. This is supported by the near-UV sensitivity of AS46 / pND05, which is closer to that observed in the *phr*A$^-$ *phr*B$^-$ background than in the *phr*A$^+$ *phr*B$^-$ background.

Another interesting result was the level of photorecovery seen in the controls, AS46, AS46 / pUC19 and AS46 / pKK223-3. All these strains showed approximately half a log cycle photorecovery over a 120 minute period of exposure to photoreactivating light. This is in contrast to the findings of Smith (1987), Smith *et al.* (1987) and Smith and Moss (1988), who found AS46 to be photoreactivation-deficient. A possible explanation for this is that the results presented in this study are corrected for near-UV induced killing, while those presented by Smith (1987), for example, are not. Smith *et al.* (1987) found that control experiments indicated that the surviving fraction of non-irradiated cells exposed to

photoreactivating light did not fall below a surviving fraction of 0.9 over the time periods studied (180 minutes for AS46), which is why no correction was made for near-UV induced killing. Husain and Sancar (1987a) found that unirradiated cells exposed to photoreactivating light of a fluence-rate of $5Wm^{-2}$ were inactivated by near-UV killing to a much greater extent than that reported by Smith *et al.* (1987), and that strains with deletions of the region Δ(*gal-uvr*B) were more sensitive to near-UV killing. Because of this, the results in the work by Husain and Sancar (1987a) are corrected for near-UV killing. It has been suggested that the differences in photorecovery seen in *phr*A$^+$ *phr*B$^-$ and *phr*A$^-$ *phr*B$^-$ mutants can be explained entirely by the differences in near-UV killing. However, the results presented in Section 5.3, which have been corrected for near-UV killing, would contradict that statement.

The temperature studies (see Section 5.3.3) showed that the photorecovery seen in AS46 / pND03 is dependent on the temperature the irradiated cells are held at during exposure to the photoreactivating light. When this temperature is increased from 25°C to 37°C, the rate and extent of photorecovery observed is increased. When this temperature is decreased from 25°C to 10°C, the rate and extent of photorecovery observed is reduced to a level similar to that seen in the control, AS46 / pKK223-3. At 37°C and 25°C there is very little difference in the rate and extent of photorecovery in AS46 / pKK223-3.
These results would suggest that some part of the photorecovery seen in AS46 / pND03 was not due to Type III photoreactivation, and is possibly due to an unknown enzymatic action due to the putative *phr*A gene product.

The dose-rate studies (see Section 5.4.4) showed that the photorecovery seen in AS46 / pND03 is dependent on the fluence-rate of the photoreactivating light. At 37°C, even a low fluence-rate of $1Wm^{-2}$ didn't effect the rate or extent of photorecovery to any great extent. However, at 25°C, fluence-rates of $1Wm^{-2}$ and $5Wm^{-2}$ reduced the rate or extent

of photorecovery seen in AS46 / pND03 to a level approaching that of AS46 / pKK223-3 at those fluence-rates. At a higher fluence-rate of $12Wm^{-2}$, the rate and extent of photorecovery seen in AS46 / pND03 was slightly increased, but remained unchanged in AS46 / pKK223-3. Why is this fluence-rate dependence observed at 25°C, but not at the higher temperature of 37°C? One possibility is that at 37°C, the putative *phr*A gene product is operating close to the optimum temperature for the enzyme-mediated reaction. Because of this, the enzyme kinetics of binding and catalysis will proceed at a faster rate, and the effects of a lower fluence-rate will be masked. Reference to Table 5.5 shows that at 60 minutes there is a decrease in the increase of mean survival of AS46 / pND03 at $1Wm^{-2}$ compared to at $8.5Wm^{-2}$. Thus, if each enzyme-substrate complex requires a minimum fluence of photoreactivating light to initiate the catalysis reaction, at a lower fluence-rate at a lower temperature, where the kinetics of binding will be affected, the fluence-rate dependence will be more pronounced.

These results would also suggest that some part of the photorecovery seen in AS46 / pND03 was not due to Type III photoreactivation, and would support the hypothesis that it was due to an unknown photoactive protein, the putative *phr*A gene product.
Another interesting aspect of this part of the photoreactivation studies, is that at a fluence-rate of $5Wm^{-2}$ the level of photorecovery seen in AS46 / pND03 and AS46 / pKK223-3 is virtually indistinguishable. This is the fluence-rate used by Husain and Sancar (1987a) when they found that deletion of the putative *phr*A gene had no effect on the rate or extent of photoreactivation seen in either a *phr*B^+ or *phr*B^- mutant background. The results reported here would offer an explanation for the failure of Husain and Sancar (1987a) to detect any photoactivity due to the putative *phr*A gene product.

The near-UV sensitivity results (see Section 5.3.5) agree with the observations made by Husain and Sancar (1987a) that cells with deletion of the *gal-uvr*B interval are more

sensitive to near-UV light. The results reported here would suggest that it is possibly due to deletion of the putative *phr*A gene that causes this increase in sensitivity to near-UV light, and not due to deletion of the *hem*F gene, as proposed by Husain and Sancar (1987a). However, that statement can not be concluded from this work, as the effect of the *hem*F gene is not accounted for, as it is deleted in all the strains used.

An interesting finding of the photoreactivation studies concerns the reproducibility of the results obtained in this study, and previously by other workers studying the effect of the putative *phr*A gene. During the early experimental work when experiments were performed on a single exploratory basis, the fluence-rate of the 254nm UV light source was higher than later on in the study. This produced irradiated cell surviving fractions of less than 1×10^{-4} colony forming units per ml. Later on, when the fluence-rate of the 254nm UV light source had decreased slightly, irradiated cell surviving fractions of greater than 1×10^{-4} colony forming units per ml were produced. In the latter case the effect of the putative *phr*A gene was often indistinguishable from the controls. Upon reducing the surviving fraction below 1×10^{-4} colony forming units per ml, the effect of the putative *phr*A gene was once again observed, while the rate and extent of photorecovery in the controls was unchanged irrespective of the initial irradiated cell surviving fraction.
This casts an interesting light over work performed by other workers in this field, and also over the possible mechanism by which the putative *phr*A gene product functions. This will be expanded upon in the final discussion of the work in this study in Chapter 6.

In conclusion, the results reported in this part of the study support previous work in our laboratory which suggested a role for the putative *phr*A gene in photorepair in *Escherichia coli* K-12.

CHAPTER SIX

DISCUSSION

The work reported in this study is centred on the role of the putative *phr*A gene in photoreactivation in *Escherichia coli* K-12. Sutherland and Hausrath (1979) originally proposed that there were two genes involved in photoenzymatic repair in *E. coli*, terming them *phr*A and *phr*B respectively. Since then, the *phr*B gene and gene product have been cloned, sequenced and extensively characterised. It is now accepted that the *phr*B gene is the major photolyase gene in *E. coli*.

Husain and Sancar (1987a) studied the genetic control of photoreactivation in *E. coli*, and were unable to reproduce previous work which had supported a role for the *phr*A gene in the genetic control of photoreactivation. They concluded that the *phr*A gene played no significant physiological role in photoreactivation and should not be called *phr*A; similarly the *phr*A gene product should not be called a photolyase.

However, Smith *et al.* (1987) also studied the genetic control of photoreactivation in *E. coli*, and found, in contrast to the findings of Husain and Sancar (1987a), that a *phr*A$^+$ *phr*B$^-$ strain did photoreactivate, while a *phr*A$^-$ *phr*B$^-$ strain was photoreactivation-deficient. Smith and Moss (1988) reported the cloning of a SphI restriction fragment from a λ*dgal* transducing 'phage and demonstrated the appearance of a photoreactivable response in the photoreactivation-deficient *phr*A$^-$ *phr*B$^-$ strain.

The work in Chapter 3 involved the sequencing of this SphI restriction fragment from the plasmid pAS01, to investigate whether there was a gene present on this restriction fragment. At this point, it is worthwhile to correct a minor error in the work reported by Smith (1987) and Smith and Moss (1988). It is stated that the plasmid pAS01 carries an

approximately 8kbp insert from a partial SphI digest of the λ*dgal* transducing 'phage. Reference to Agarose Gel 3.1 shows that a complete SphI digest of pAS01 produces two fragments, one the same size to the vector pBR322 into which the restriction fragment was cloned; and one of approximately 1.2kbp. Therefore, the insert sequenced in this study should not correspond to a 8kbp insert as reported previously, but to a 1.2kbp insert. This was confirmed by the sequencing results. Also, the restriction fragment cloned into pBR322 to produce pAS01 is a completely digested SphI fragment, not a partial digest.

The insert sequenced was 1188bp in length, and upon analysis was discovered to contain an open reading frame of 340 amino acids commencing from an ATG start codon. The ORF coded for a protein of 37,894Da. Areas of similarity to consensus sequences for the transcriptional and translational signals in *E. coli* were identified - see Section 3.4. Upon searching for matches for the nucleotide and amino acid sequences on the EMBL and GenBank databases, no significant matches were found. The ORF was thus termed the putative *phr*A gene, and the protein coded for by the putative *phr*A gene termed the putative *phr*A gene product.

Interestingly, the predicted amino acid composition of the putative *phr*A gene product bears little resemblance to the amino acid composition presented by Snapka and Sutherland (1980) for the *phr*A PRE isolated in their laboratory - see Section 3.4.

The work in Chapter 4 involved attempts to show over-expression of the putative *phr*A gene product. Three vectors containing the putative *phr*A gene were studied. pND01 utilised the transcriptional and translational signals already present 5' to the ATG start codon identified in Section 3.4 to initiate expression of the putative *phr*A gene product. pND03 utilised the strong *tac* promoter on the expression vector pKK223-3 (Brosius and Holy, 1984) and the ribosome-binding site present 5' to the ATG start codon of the putative *phr*A gene. pND05 utilised the strong *tac* promoter and the ribosome-binding site

on the expression vector pKK223-3, with the ATG start codon of the putative *phr*A gene immediately 3' to the ribosome-binding site.

However, as predicted in Section 3.4, the over-expression of the putative *phr*A gene product proved to be rather difficult. No discernible over-expression was observed on SDS-PA gels above that of the background protein bands of the controls - see Section 4.3. The results obtained in Chapter 5 cast an interesting light over those results obtained in Chapter 4.

The work in Chapter 5 involved studies of the *in vivo* photoreactivation produced by the putative *phr*A gene. The results indicate that the putative *phr*A gene confers two biological effects to a *phr*A *phr*B mutant. The first is a level of photorecovery above that observed in the *phr*A *phr*B mutant, and the second is an increase in resistance to near-UV induced killing. With this is mind, the results obtained for pND01, pND03 and pND05 cast new light on the results obtained and the strategies used during the sub-cloning work performed in Section 4.3.

AS46 / pND01 showed a level of photorecovery above that of AS46 / pUC19, and a slight increase in resistance to near-UV killing. However, the effect of the putative *phr*A gene in AS46 / pND03 was more pronounced. The rate and extent of photorecovery was above that observed in AS46 / pKK223-3 and above that observed in AS46 / pND01. The increase in resistance to near-UV killing was more pronounced as well. However, AS46 / pND05 did not exhibit a level of photorecovery above that of AS46 / pKK223-3, and the sensitivity of AS46 / pND05 to near-UV light was closer to that of AS46 / pKK223-3 than AS46 / pND03.

These results suggest that the putative *phr*A gene is functioning in pND01, is over-expressed in relation to pND01 in pND03, but not functioning in pND05. This suggests that the strategy to clone the putative *phr*A gene downstream of a strong promoter was successful in increasing the expression of the putative *phr*A gene product. However, when

this strategy was expanded upon to include a strong ribosome-binding site, this resulted in the putative *phr*A gene apparently not functioning.

One possible explanation for this is that the PCR generation of the putative *phr*A gene used in Section 4.3.5 introduced an incorrect nucleotide, thus changing the reading frame and affecting the amino acid composition of the putative *phr*A gene product, and thus its biological activity. This would explain the apparent lack of *phr*A activity in AS46 / pND05. The sequence of an individual DNA molecule cloned from an amplified pool of PCR generated fragments is unreliable (Sambrook *et al.*, 1989). A way to check this would be to sequence a number of independent recombinant clones to confirm the sequence of the putative *phr*A gene. A quicker way would be to isolate a number of the plasmids from independent clones and after transforming the plasmid DNA into AS46, check the biological activity of the putative *phr*A gene by photoreactivation experiments.

However, the above does not explain why if a protein is been produced by the over-expression strategy used in the construction of pND05, this protein, though not biologically active, does not show up after induction by analysis by SDS-PAGE techniques. A possible reason for this has been proposed in Section 4.4, namely the staining system used is not sensitive enough to pick up the low levels of protein produced. Another possible reason is that the putative *phr*A gene product has a low affinity for commonly used protein stains. Snapka and Sutherland (1980) reported similar problems with the enzyme they studied, making its localisation on gels difficult.

This, if it is the cause of the apparent lack of over-expression of the putative *phr*A gene product, rather than the low numbers of molecules per cell, could be investigated by using radio-labelled amino acids, such as ^{35}S Met, in the growth medium used in the induction cultures, and detecting the radio-labelled proteins after SDS-PAGE by autoradiography.

Another possible cause of the lack of over-expression in pND05 is that the expression vectors ribosome-binding site is too far away from the ATG start codon of the putative *phr*A gene. When the expression vector pKK223-3 was purchased from PHARMACIA, the

data sheet stated that to utilise the ribosome-binding site present on pKK223-3, the ATG start codon must be cloned within 10-15 bases 3' to the ribosome-binding site. However, the data sheet has now been revised, stating that the ATG start codon must be now within 5-9 bases 3' to the ribosome-binding site. This is due to problems such as have been experienced with pND05 (S. Pearson, Pharmacia - Personal Communication).

The work performed in Chapter 4 has opened the way for many future experiments on the over-expression of the putative *phr*A gene product. These include :-

a) Running induced samples on a larger gel apparatus and staining with silver salts to detect smaller amounts of protein.

b) Radio-labelling the proteins produced during induction and detecting these proteins by autoradiography after separation by SDS-PAGE.

c) Analysis of the biological activity of the gene present on the PCR generated fragments to check that the integrity of the putative *phr*A gene has been maintained.

It is hoped that this area of the work, in particular, will be continued.

The work in Chapter 5, after showing a photoreactivable response associated with the putative *phr*A gene above the photorecovery of the controls, centred on the statements made by Husain and Sancar (1987a) and Husain *et al.* (1988). They proposed that the photorecovery seen in *phr*B mutants was due to Type III photoreactivation, and also observed that deletion of the *gal-uvr*B region increased the sensitivity of cells to near-UV induced killing.

The results presented in Chapter 5 with the *phr*A *phr*B mutant AS46, carrying the plasmid pND03 which includes the putative *phr*A gene, suggest that part of the photorecovery observed in AS46 / pND03 is not due to Type III photoreactivation, due to its dependence on :-

i) The temperature at which the irradiated cells are held during exposure to the photoreactivating light.

ii) The fluence-rate of the photoreactivating light.

Additionally, the results with the *phr*A *phr*B mutant AS46, carrying the control plasmid pKK223-3, support the hypothesis that the photorecovery seen in *phr*A *phr*B mutants is due to Type III photoreactivation, due to this photorecovery being virtually independent of temperature and dose-rate effects - see Section 5.4. The near-UV sensitivity studies suggest that the putative *phr*A gene does increase the resistance of cells to near-UV killing, which leads to the hypothesis that it is deletion of the putative *phr*A gene which caused the effects reported by Husain and Sancar (1987a) and not deletion of the *hem*F gene as speculated by these workers. However, this can not be concluded from this work - see Section 5.4.

As well as the main conclusions drawn from the results obtained from Chapter 5, two explanations were reached to explain the failure of other workers to reproduce the activity of the putative *phr*A gene product.

At fluence-rates of photoreactivating light below $8.5 Wm^{-2}$, the photorecovery associated with the putative *phr*A gene is virtually indistinguishable from that associated with Type III photoreactivation seen in the control. This covers the fluence-rate ($5 Wm^{-2}$) used by Husain and Sancar (1987a) and would explain why they were unable to show any

biological activity associated with the putative *phr*A gene, in contrast to the findings of workers in our laboratory, who used a fluence-rate of $17Wm^{-2}$ (for example, Smith *et al.*, 1987).

When the irradiated cells initial surviving fraction was reduced below 1×10^{-4}, the effect of the putative *phr*A gene was clearly seen. However, when the irradiated cells initial surviving fraction was above 1×10^{-4}, it was difficult to distinguish between the photorecovery associated with the putative *phr*A gene and the photorecovery associated with Type III photoreactivation observed in the control. This again would explain why the effect of the putative *phr*A gene has been overlooked in the past. No difference in the rate or extent of photorecovery seen in the control was observed when the irradiated cells initial surviving fraction was above or below 1×10^{-4}. To observe a relatively small effect, the surviving fraction needs to be reduced to a level where it can be detected.

It is known that Type III photoreactivation is involved with the photoconversion of (6-4) photoproducts to their Dewar isomers - see Section 1.3.5. The Dewar isomer is thought to be less cytotoxic than the (6-4) photoproduct, but its effect on mutagenesis is as yet unclear. However, Husain and Sancar (1987a) reported a level of photorecovery in *phr*B mutants of 30% of the UV damage, despite their predictions that the (6-4) photoproducts would not constitute more than 15% of the total photoproducts induced by the UV fluences used in their experiments. This would imply that some of the pyrimidine dimers were repaired by exposure to the photoreactivating light.

The second of the two practical observations reported above would suggest that the putative *phr*A gene product acts on a substrate other than pyrimidine dimers. Even with the fluence of 254nm UV-irradiation required to reduce the surviving fraction to 5×10^{-4}, there would be more than enough pyrimidine dimers for the effect of the putative *phr*A gene product to be seen above that of the control.

An explanation would be that the higher fluence of 254nm UV-irradiation induces a higher number of the less important UV-induced photoproducts, to a level where they begin to become biologically significant. Pyrimidine dimers other than the predominant T< >T dimers, such as C< >T dimers, could be formed in significant amounts. While considering the effect of repair of 254nm UV-induced damage, it is also worthwhile considering the effect the putative *phr*A gene has on near-UV sensitivity. Ellison and Childs (1981) showed that at low fluences of 300nm and 313nm light, C< >T dimers were formed more frequently than T< >T dimers, whereas the reverse was true at either longer or shorter wavelengths. This would suggest that any pyrimidine dimers produced in DNA by the photoreactivating light used in this study would be more likely to be T< >T dimers than C< >T dimers - see Figure 2.4 for the transmission properties of the photoreactivating light used in this study, which shows no transmission below 340nm. This reduces the likelihood of C< >T dimers been the substrate for the putative *phr*A gene product.

After pyrimidine dimers, the next most important UV-induced photoproduct is the (6-4) photoproduct. This is the lesion converted to its Dewar isomer by Type III photoreactivation, and if it were the substrate for the putative *phr*A gene product, it would help to explain why at low levels of UV-induced DNA damage it is difficult to distinguish between putative *phr*A gene-mediated photorecovery and Type III photoreactivation, as both processes would be competing for the same lesion.

Husain and Sancar (1987a) showed that deletion of the *gal-attλ* region increased the sensitivity of strains to near-UV killing, in both *phr*B$^+$ and *phr*B$^-$ strains. Tyrrell *et al.* (1973) demonstrated the destruction of *E. coli* PRE by 365nm radiation. This would suggest that over long exposures to photoreactivating light the importance of the *phr*B gene product diminishes due to its inactivation, while the importance of the putative *phr*A gene product would increase. What remains unclear is whether the damage induced by the

photoreactivating light is to DNA, DNA repair systems or membranes; and how and where the putative *phr*A gene product acts.

With this in mind, another possibility is that the photorecovery is due to photoreactivating light-induced growth delay, allowing the putative *phr*A gene product to act in a different manner than that of a photolyase.

Returning to the observation of Husain and Sancar (1987a) that the photorecovery in *phr*B mutants upon long exposures to photoreactivating light results in repair of 30% of the total UV damage, they proposed three possibilities to explain these findings :-

i) The existence of a second photolyase in *E. coli.*

ii) Dimer reversal is photosensitised by chromophoric metabolites.

iii) Pyrimidine dimers are directly reversed by photoreactivating light.

The third explanation was dismissed as it is unlikely that an inefficient photoreversal process would increase cell survival by use of light that introduces more dimers into DNA. In conclusion, they had no satisfactory explanation for the residual photoreactivation observed in *phr*B mutants. The work by Husain *et al.* (1988) showed that in a *phr*A *phr*B mutant, pyrimidine dimer content remained unchanged after exposure to photoreactivating light. This removes the second and third explanations for the residual photoreactivation in *phr*B mutants put forward by Husain and Sancar (1987a), which both involved the removal of pyrimidine dimers. A conclusion not drawn by Husain *et al.* (1988), even though they explained this residual photoreactivation observed in *phr*B mutants as been due to Type III photoreactivation, is that the level of (6-4) photoproducts induced by the 254nm UV-irradiation used in their studies is probably higher than the 15% they quoted,

and closer to 30% of total UV-induced damage, which was the level of photorepair observed.

If this is the case, and the level of (6-4) photoproducts produced by the fluence of 254nm UV-irradiation is in the range of 20-30% in the experiments performed by Husain and Sancar (1987a) and in our laboratory in Bath, then the prospect that the putative *phr*A gene product repairs (6-4) photoproducts is very attractive.

In Section 1.5.4, three major possibilities for the role of *phr*A in *Escherichia coli* K-12 were proposed :-

i) No significant role in photoreactivation.

ii) Photoreactivation by repair of pyrimidine dimers at higher fluence-rates of photoreactivating light.

iii) Photoreactivation by repair of (6-4) photoproducts.

The results obtained in Chapter 5 would suggest that the putative *phr*A gene studied in this work acts by photoreactivation of (6-4) photoproducts rather than pyrimidine dimers. Todo *et al.* (1993) showed that an extract from *E. coli* strain AB1157 bound UV-irradiated DNA depleted of pyrimidine dimers by prior treatment of with *E. coli* DNA photolyase. It would be interesting to repeat this experiment with extracts from AS46 and AS46 / pND03 to see if a (6-4) photoproduct binding factor exists in AS46 / pND03, but not in AS46. If this was the case, repeating the assay for photoreactivation-mediating activity would be the next step. If the results from this were positive, this would confirm the hypothesis that part of the photoreactivation seen in AS46 / pND03 is due to repair of (6-4) photoproducts by the putative *phr*A gene product.

In conclusion, the work presented in this study supports the hypothesis that the putative *phr*A gene studied in our laboratory in Bath does code for a photoactive protein and explanations are put forward for the contradicting results reported in the literature. A hypothesis is proposed that the putative *phr*A gene product acts by repairing (6-4) photoproducts rather than pyrimidine dimers.

REFERENCES

ANDERSON, E.H. (1946) Growth requirements of virus-resistant mutants of *Escherichia coli* B. ***Proc.Natl.Acad.Sci.USA.*** **32,** 120-128.

AOYAMA, T., TAKANAMI, M., OHTSUKA, E., TANIYAMA, Y., MARUMOTO, R., SATO, H. and IKEHARA, M. (1983) Essential structure of *Escherichia coli* promoter : Effects of spacer length between two consensus sequences on promoter function. ***Nucleic Acids Res.*** **11,** 5855-5864.

BACHMANN, B.J. (1983) Linkage map of *Escherichia coli* K-12, Edition 7. ***Microbiol.Rev.*** **47,** 180-230.

BACHMANN, B.J. (1989) Linkage map of *Escherichia coli* K-12, Edition 8. ***Microbiol.Rev.*** **54,** 130-197.

BAER, M. and SANCAR, G.B. (1989) Photolyases from *Saccharomyces cerevisiae* and *Escherichia coli* recognise common binding determinants in DNA containing pyrimidine dimers. ***Mol.Cell Biol.*** **9,** 4777-4788.

BEUKERS, R. and BERENDS, W. (1960) Isolation and identification of the irradiated product of thymine. ***Biochim.Biophys.Acta.*** **41,** 550-551.

BOSE, S.N. and DAVIES, R.J.H. (1984) The photoreactivity of TA sequences in oligodeoxyribonucleotides and DNA. ***Nucleic Acids Res.*** **12,** 7903-7914.

BRASH, D.E., FRANKLIN, W.A, SANCAR, G.B., SANCAR, A. and HASELTINE, W.A. (1985) *Escherichia coli* DNA photolyase reverses cyclobutane pyrimidine dimers but not pyrimidine-pyrimidone (6-4) photoproducts. ***J.Biol.Chem.*** **260,** 11438-11441.

BRASH, D.E. and HASELTINE, W.A. (1985) Photoreactivation of *Escherichia coli* reverses *umu*C induction by UV light. ***J.Bacteriol.*** **163,** 460-463.

BRASH, D.E. (1988) UV Mutagenic photoproducts in *Escherichia coli* and human cells: A molecular genetics perspective on human skin cancer. ***Photochem.Photobiol.*** **48,** 59-66.

BROSIUS, J. and HOLY, A. (1984) Regulation of ribosomal-RNA promoters with a synthetic *lac* operator. ***Proc.Natl.Acad.Sci.USA.*** **74,** 5463-5467.

CHAN, G.L., PEAK, M.J., PEAK, J.G. and HASELTINE, W.A. (1986) Action spectrum for the formation of endonuclease - sensitive sites and (6-4) photoproducts induced in a DNA fragment by ultraviolet radiation. ***Int.J.Radiat.Biol.*** **50,** 641-648.

DAGERT, M. and EHRLICH, S.D. (1979) Prolonged incubation in calcium chloride improves the competence of *Escherichia coli* cells. ***Gene.*** **6,** 23-28.

DAVIES, D.J.G., TYLER, S.A. and WEBB, R.B. (1970) A sequential repair model of photoreactivation in bacteria. ***Photochem.Photobiol.*** **11,** 371-386.

DODSON, M.L. and LLOYD, R.S. (1989) Structure-function studies of the T4 endonuclease V repair enzyme. ***Mutation Res.*** **218,** 49-65.

DULBECCO, R. (1949) Reactivation of ultraviolet inactivated bacteriophage by visible light. *Nature.* **163,** 949-950.

EKER, A.P.M., KOOIMAN, P., HESSELS, J.K.C. and YASUI, A. (1990) DNA photoreactivating enzyme form the cyanobacterium *Anacystis nidulans*. ***J.Biol.Chem.*** **265,** 8009-8015.

ELLISON, M.J. and CHILDS, J.D. (1981) Pyrimidine dimers induced in *Escherichia coli* DNA by ultraviolet radiation present in sunlight. ***Photochem.Photobiol.*** **34,** 465-469.

FERNANDEZ DE HENESTROSA, A.R., CALERO, S. and BARBÉ, J. (1991) Expression of the *rec*A gene of *Escherichia coli* in several species of gram-negative bacteria. ***Mol.Gen.Genet.*** **226,** 503-506.

FRANKLIN, W.A., LO, K. and HASELTINE, W.A. (1982) Alkaline lability of fluorescent photoproducts in ultraviolet light-irradiated DNA. ***J.Biol.Chem.*** **257,** 13535-13543.

FRANKLIN, W.A. and HASELTINE, W.A. (1984) Removal of UV light-induced pyrimidine-pyrimidone (6-4) photoproducts from *Escherichia coli* requires the *uvr*A, *uvr*B and *uvr*C gene products. ***Proc.Natl.Acad.Sci.USA.*** **81,** 3821-3824.

FRIEDBERG, E.C. (1985) "DNA Repair" **W.H.Freeman, New York.**

GALLAGHER, P.E. and DUKER, N.J. (1986) Detection of UV purine photoproducts in a defined sequence of DNA. ***Molec.Cell Biol.*** **6,** 707-709.

GASPARRO, F.P. and FRESCO, J.R. (1986) Ultraviolet-induced 8,8-adenine dehydrodimers in oligo- and polynucleotides. ***Nucleic Acids Res.*** **14,** 4239-4251.

GATES, F.L. (1930) A study of the bactericidal action of UV light. III. The absorption of ultraviolet light by bacteria. ***J.Gen.Physiol.*** **14,** 31-42.

GORDON, L.K. and HASELTINE, W.A. (1982) Quantitation of cyclobutane pyrimidine dimer formation in double- and single-stranded DNA fragments of defined sequence. ***Radiat.Res.*** **89,** 99-112.

GROSSMAN, L. and YEUNG, A.T. (1990) The UvrABC endonuclease of *Escherichia coli*. ***Photochem.Photobiol.*** **51,** 749-755.

HAMILTON, K.K., KIM, P.M.H. and DOETSCH, P.W. (1992) Glycosylase / lyase recognising ultraviolet light-induced pyrimidine dimers. ***Nature.*** **356,** 725-728.

HAMM-ALVAREZ, S., SANCAR, A. and RAJAGOPALAN, K.V. (1990) The folate cofactor of *Escherichia coli* DNA photolyase acts catalytically. ***J.Biol.Chem.*** **265,** 18656-18662.

HARM, H. and RUPERT, C.S. (1968) Analysis of photoenzymatic repair of UV lesions in DNA by single light flashes. I. *In vitro* studies with *Haemophilus influenzae* transforming DNA and yeast photoreactivating enzyme. ***Mutation Res.*** **6,** 355-370.

HARM, W., HARM, H. and RUPERT, C.S. (1968) Analysis of photoenzymatic repair of UV lesions in DNA by single light flashes. II. *in vivo* studies with *Escherichia coli* cells and bacteriophage. ***Mutation Res.*** **6,** 371-385.

HARM, W., RUPERT, C.S. and HARM, H. (1971) The study of photoenzymatic repair in DNA by Flash Photolysis. In *"Photophysiology"* Vol *VI.* A.C. Giese, Ed. **Academic Press, New York.**

HATCHARD, C.G. and PARKER, C.A. (1956) A new sensitive chemical actinometer. II. Potassium ferroxalate as a standard chemical actinometer. ***Proc.Roy.Soc. (London)*** **A235,** 518-536.

HAYS, J.B., MARTIN, S.J. and BHATIA, K. (1985) Repair of non-replicating DNA; co-operative dark repair by *Escherichia coli uvr* and *phr* functions. ***J.Bacteriol.*** **161,** 602-608.

HEELIS, P.F., SANCAR, A. and OKAMURA, T. (1992) Excited quartet states in DNA photolyase. ***J.Photochem.Photobiol. B: Biol.*** **16,** 387-390.

HEELIS, P.F., KIM, S-T, OKAMURA, T. and SANCAR, A. (1993) The photo repair of pyrimidine dimers by DNA photolyase and model systems. ***J.Photochem.Photobiol. B: Biol.*** **17,** 219-228.

HEJMADI, V.S. and VERMA, N.C. (1987) Interaction of the aproprotein of 40kDa photoreactivating enzyme from *Escherichia coli* with deoxyribonucleic acid. ***Indian J.Biochem.Biophys.*** **24,** 189-193.

HÉLÈNE, C., and CHARLIER, M. (1977) Photosensitised splitting of pyrimidine dimers by indole derivatives and by tryptophan-containing oligopeptides and proteins. ***Photochem.Photobiol.*** **25,** 429-434.

HODGES, N.D.M. (1979) Ph.D. Thesis, University of Bath.

HOEIJAMKERS, J.H.J. (1993) Nucleotide excision repair I : From *E. coli* to yeast. ***Trends in Genetics.*** **9,** 173-177.

HOWARD-FLANDERS, P. and THERIOT, L. (1966) Mutants of *Esherichia coli* K-12 defective in DNA repair and genetic recombination. ***Genetics.*** **53,** 1137-1150.

HOWARD-FLANDERS, P. (1981) Inducible repair of DNA. ***Scientific American.*** **245(5),** 56-64.

HUSAIN, I. and SANCAR, A. (1987a) Photoreactivation in *phr* mutants of *Escherichia coli* K-12. ***J.Bacteriol.*** **169,** 2367-2372.

HUSAIN, I. and SANCAR, A. (1987b) Binding of *E. coli* photolyase to a defined substrate containing a single T< > T dimer. ***Nucleic Acids Res.*** **15,** 1109-1120.

HUSAIN, I., SANCAR, G.B., HOLBROOK, S.R. and SANCAR, A. (1987) Mechanism of damage recognition by *Escherichia coli* DNA photolyase. ***J.Biol.Chem.*** **262,** 13188-13197.

HUSAIN, I., CARRIER, W.J., REGAN, J.D. and SANCAR, A. (1988) Photoreactivation of killing in *Escherichia coli* K-12 *phr*$^-$ cells is not caused by pyrimidine dimer reversal. ***Photochem.Photobiol.*** **48,** 233-234.

IKEMURA, T. (1981) Correlation between the abundance of *Escherichia coli* transfer RNAs and the occurrence of the respective codons in its protein genes : A proposal for a synonymous codon choice that is optimal for the *Escherichia coli* translational system. ***J.Mol.Biol.*** **151,** 389-409.

IKENAGA, M., PATRICK, M.H. and JAGGER, J. (1970) Action of photoreactivating light on pyrimidine heteroadduct in bacteria. ***Photochem.Photobiol.*** **11,** 487-494.

IKENAGA, M., PATRICK, M.H. and JAGGER, J. (1971) Photoreactivation of killing in *Streptomyces*. III. Action spectra for photolysis of pyrimidine dimers and adducts in *S. griseus* and *S. griseus* PHR-1. ***Photochem.Photobiol.*** **14,** 175-187.

JAGGER, J. (1960) "Radiation Protection and Recovery" **Pergamon, Oxford.**

JAGGER, J. (1967) "Introduction to Research in Ultraviolet Photobiology" **Prentice Hall, New Jersey.**

JAGGER, J., STAFFORD, R.S. and SNOW, J.M. (1969) Thymine-dimer and action spectra evidence for indirect photoreactivation in *Escherichia coli*. ***Photochem.Photobiol.*** **10,** 383-395.

JAGGER, J., TAKEBE, H. and SNOW, J.M. (1970) Photoreactivation of killing in *Streptomyces* : Action spectra and kinetic studies. ***Photochem.Photobiol.*** **12,** 185-196.

JAGGER, J. (1985) "Solar-UV Actions on Living Cells" **Praeger, New York.**

JOHNS, H.E., PEARSON, M.L., LEBLANC, J.C. and HELLEINER, C.W.J. (1964) The ultraviolet photochemistry of thymidylyl - (3'→5') - thymidine. ***J.Mol.Biol.*** **9,** 503-524.

JOHNSON, J.L., HAMM-ALVAREZ, S., PAYNE, G., SANCAR, G.B., RAJAGOPALAN, K.V. and SANCAR, A. (1988) Identification of the second chromophore of *Escherichia coli* and yeast DNA photolyase as 5,10-metheyltetrahydrofolate. ***Proc.Natl.Acad.Sci.USA.*** **85,** 2046-2050.

JORNS, M.S., SANCAR, G.B. and SANCAR, A. (1984) Identification of a neutral flavin radical and characterisation of a second chromophore in *E. coli* DNA photolyase. ***Biochemistry.*** **23,** 1856-1861.

KELLAND. L.R., MOSS, S.H. and DAVIES, D.J.G. (1983) An action spectrum for ultraviolet radiation-induced membrane damage in *Escherichia coli* K-12. ***Photochem.Photobiol.*** **37,** 301-306.

KELNER, A. (1949) Effect of visible light on the recovery of *Streptomyces griseus conidea* from ultraviolet irradiation injury. ***Proc.Natl.Acad.Sci.USA.*** **35,** 73-79.

KEYSE, S.M., MOSS, S.H. and DAVIES, D.J.G. (1983) Action spectra for inactivation of normal and xeroderma pigmentosum human skin fibroblasts by ultraviolet radiations. ***Photochem.Photobiol.*** **37,** 307-312.

KHATTACK, M.N. and WANG, S.Y. (1972) The photochemical mechanism of pyrimidine cyclobutyl dimerisation. ***Tetrahedron.*** **28,** 945-957.

KIENER, A., HUSAIN, I., SANCAR, A. and WALSH, C. (1989) Purification and properties of *Methanbacterium thermoautotrophicum* DNA photolyase. ***J.Biol.Chem.*** **264,** 13880-13887.

KIM, S-T, LI, Y.F and SANCAR, A. (1992) The third chromophore of DNA photolyase: Trp-277 of *Escherichia coli* DNA photolyase repairs thymine dimers by direct electron transfer. ***Proc.Natl.Acad.Sci.USA.*** **89,** 900-904.

KIM, S-T. and SANCAR, A. (1993) Photochemistry, photophysics and mechanism of pyrimidine dimer repair by DNA photolyase. ***Photochem.Photobiol.*** **57,** 895-904.

KONIGSBERG, W. and GODSON, G.N. (1983) Evidence for use of rare codons in the *dna*G gene and other regulatory proteins of *Escherichia coli.* ***Proc.Natl.Acad.Sci.USA.*** **80,** 687-691.

LI, Y.F. and SANCAR, A. (1990) Active site of *Escherichia coli* DNA photolyase: Mutations at Trp-277 alter the selectively of the enzyme without affecting the quantum yield of photorepair. ***Biochemistry.*** **29,** 5698-5706.

LI, Y.F., HEELIS, P.F. and SANCAR, A. (1991) Active site of DNA photolyase: Trp-306 is the intrinsic H-atom donor essential for flavin radical photoreduction and DNA repair *in vitro*. ***Biochemistry.*** **30,** 6322-6329.

LI, Y.F., KIM, S-T. and SANCAR, A. (1993) Evidence for lack of DNA photoreactivating enzyme in humans. ***Proc.Natl.Acad.Sci.USA.*** **90,** 4389-4393.

LIN, J-J. and SANCAR, A. (1992) Exinuclease - The *Escherichia coli* nucleotide excision repair enzyme. ***Mol.Microbiol.*** **6,** 2219-2224.

LIPPKE, J.A., GORDON, L.K., BRASH, D.E. and HASELTINE, W.A. (1981) Distribution of UV-light induced damage in a defined sequence of human DNA : Detection of alkaline sensitive lesions at pyrimidine nucleoside - cytidine sequences. ***Proc.Natl.Acad.Sci.USA.*** **78,** 3388-3392.

LITTLE, J.W., EDMISTON, S.H., PACELLI, P.Z. and MOUNT, D.W. (1980) Cleavage of the *Escherichia coli* LexA protein by the RecA protease. ***Proc.Natl.Acad.Sci.USA.*** **77,** 3225-3229.

LITTLE, J.W. and MOUNT, D.W. (1982) The SOS regulatory system of *Esherichia coli*. ***Cell.*** **29,** 11-22.

LITTLE, J.W. (1984) Autodigestion of LexA and phage repressors. ***Proc.Natl.Acad.Sci.USA.*** **81,** 1375-1379.

MACMILLAN, S., EDENBERG, H.J., RADANY, E.H., FRIEDBERG, R.C. and FRIEDBERG, E.C. (1981) *denV* gene of bacteriophage T4 codes for both pyrimidine dimer-DNA glycosylase and apyrimidinic endonuclease activities. ***J.Virol.*** **40,** 211-223.

MESSING, J., CREA, R. and SEEBURG, P.H. (1981) A system for shotgun DNA sequencing. ***Nucleic Acids Res.*** **9,** 309-321.

MESSING, J. (1983) New M13 vectors for cloning. ***Methods in Enzymology.*** **101,** 20-78.

MITCHELL, D.L. and NAIRN, R.S. (1989) The biology of the (6-4) photoproduct. ***Photochem.Photobiol.*** **49,** 805-819.

PARK, H-W, SANCAR, A. and DEISENHOFER, J. (1993) Crystallization and preliminary crystallographic analysis of *Escherichia coli* DNA photolyase. ***J.Mol.Biol.*** **231,** 1122-1125.

PAYNE, G., HEELIS, P.F., ROHRS, B.R. and SANCAR, A. (1987) The active form of *Escherichia coli* DNA photolyase contains a fully reduced flavin and not a flavin radical, both *in vivo* and *in vitro*. ***Biochemistry.*** **26,** 7121-7127.

PAYNE, G. and SANCAR, A. (1990) Absolute action spectrum of E-$FADH_2$ and E-$FADH_2$-MTHF forms of *Escherichia coli* DNA photolyase. ***Biochemistry.*** **29,** 6810-6816.

PLATT, T. and YANOTSKY, C. (1975) An intercistronic region and ribosome-binding site in bacterial messenger RNA. ***Proc.Natl.Acad.Sci.USA.*** **72,** 2399-2403.

RADANY, E.H., LOVE, J.D. and FRIEDBERG, E.C. (1981) The use of direct photoreversal of UV-irradiated DNA for the demonstration of pyrimidine dimer-DNA glycosylase activity. In *"Chromosome Damage and Repair"* E. Seeberg and K. Kleppe, Eds. **Plenum, New York.**

RAMABHADRAN, T.V. and JAGGER, J. (1976) Mechanism of growth delay induced in *Escherichia coli* by near ultraviolet radiation. ***Proc.Natl.Acad.Sci.USA.*** **73, 59-63.**

ROSENBURG, M., and COURT, D. (1979) Regulatory sequences involved in the promotion and termination of RNA transcription. ***Annu.Rev.Genet.*** **13,** 319-353.

ROTHMAN, R.H., KATO, T. and CLARK, A.J. (1975) The beginning of an investigation of the role of *rec*F in the pathways of metabolism of ultraviolet-induced DNA in *Escherichia coli.* In *"Molecular mechanisms for the repair of DNA"* P.C. Hanawalt and R.B. Setlow, Eds. **Plenum Publishing Corp.**

RUPERT, C.S., GOODGAL, S.H. and HERRIOTT, R.M. (1958) Photoreactivation *in vitro* of ultraviolet inactivated *Haemophilus influenzae* transforming factor. ***J.Gen.Physiol.*** **41,** 451-471.

SAMBROOK, J., FRITSCH, E.F. and MANIATIS, T. (1989) "Molecular Cloning - A Laboratory Manual" *2nd Edition.* **Cold Spring Harbour Laboratory Press.**

SANCAR, A. and RUPERT, C.S. (1978) Correction of the map location for the *phr* gene in *Escherichia coli* K-12. ***Mutation Res.*** **51,** 139-143.

SANCAR, A. and RUPP, W.D. (1983) A novel repair enzyme - UvrABC excision nuclease of *Escherichia coli* cuts a DNA strand on both sides of the damaged region. ***Cell.*** **33,** 249-260.

SANCAR, A. and SANCAR, G.B. (1984) *Escherichia coli* DNA photolyase is a flavoprotein. ***J.Mol.Biol.*** **172,** 223-227.

SANCAR, A., SMITH, F.W. and SANCAR, G.B. (1984a) Purification of the *Escherichia coli* DNA photolyase. ***J.Biol.Chem.*** **259,** 6028-6032.

SANCAR, A. and SANCAR, G.B. (1988) DNA repair enzymes. ***Annu.Rev.Biochem.*** **57,** 29-67.

SANCAR, A. and TANG, M-S. (1993) Nucleotide excision repair. ***Photochem.Photobiol.*** *57,* 905-921.

SANCAR, G.B., SMITH, F.W. and SANCAR, A. (1983) Identification and amplification of the *E.coli phr* gene product. ***Nucleic Acids Res.*** **11,** 6667-6678.

SANCAR, G.B., SMITH, F.W., LORENCE, M.C., RUPERT, C.S. and SANCAR, A. (1984b) Sequences of the *Escherichia coli* photolyase gene and protein. ***J.Biol.Chem.*** **256,** 6033-6038.

SANCAR, G.B., JORNS, M.S., PAYNE, G., FLUKE, D.J., RUPERT, C.S. and SANCAR, A. (1987) Action mechanisms of *Escherichia coli* DNA photolyase. III. Photolysis of the enzyme-substrate complex and the absolute action spectrum. ***J.Biol.Chem.*** **262,** 494-498.

SANCAR, G.B. and SMITH, F.W. (1989) Interactions between yeast photolyase and nucleotide excision repair proteins in *Saccharomyces cerevisiae* and *Escherichia coli.* ***Mol.Cell.Biol.*** **9,** 4767-4776.

SANCAR, G.B. (1990) DNA photolyases: Physical properties, action mechanism, and roles in dark repair. ***Mutation Res.*** **236,** 147-160.

SANGER, F., MIKLEN, S. and COULSON, A.R. (1977) DNA Sequencing with chain terminating inhibitors. ***Proc.Natl.Acad.Sci.USA.*** **74,** 5463-5467.

SARASTE, M., SIBBALD, P.R. and WITTINGHOFER, A. (1990) The P-loop - a common motif in ATP- and GTP-binding proteins. ***Trends in Biochem. Sci.*** **15,** 430-434.

SEDGWICK, S.G. and GOODWIN, P.A. (1985) Interspecies regulation of the SOS response by the *E. coli lex*A$^+$ gene. ***Mutation Res.*** **145,** 103-106.

SELBY, C.P. and SANCAR, A. (1993) Molecular mechanism of Transcription-Repair coupling. ***Science.*** **260,** 53-58.

SETLOW, R.B. and SETLOW, J.K. (1962) Evidence that ultraviolet-induced thymine dimers in DNA can cause biological damage. ***Proc.Natl.Acad.Sci.USA.*** **48,** 1250-1257.

SETLOW, R.B. and CARRIER, W.L. (1966) Pyrimidine dimers in ultraviolet irradiated DNAs. ***J.Mol.Biol.*** **17,** 237-254.

SETLOW, R.B. (1968) The photochemistry, photobiology and repair of polynucleotides. ***Prog.Nuc.Acid.Res.Mol.Biol.*** **8,** 257-295.

SHARP, P.A., SUGDEN, B. and SAMBROOK, J. (1973) Detection of two restriction endonuclease activities in *Haemophilus parainfluenzae* using analytical agarose - ethidium bromide electrophoresis. ***Biochemistry.*** **12,** 3055-3063.

SHINE, J. and DALGARNO, L. (1974) The 3'-terminal sequence of *Escherichia coli* 16S ribosomal RNA: complementarity to nonsense triplets and ribosome-binding sites. ***Proc.Natl.Acad.Sci.USA.*** **71,** 1342-1346.

SIEBENLIST, U., SIMPSON, R.B., and GILBERT, W. (1980) *E.coli* RNA polymerase interacts homologously with two different promoters. ***Cell.*** **20,** 269-281.

SMITH, A.W. (1987) Ph.D. Thesis, University of Bath.

SMITH, A.W., DAVIES, D.J.G. and MOSS, S.H. (1987) Photoreactivation of ultraviolet radiation damage in dark repair deficient *phr* mutants of *Escherichia coli* K-12. ***Photochem.Photobiol.*** **45,** 247-252.

SMITH, A.W. and MOSS, S.H. (1987) Wavelength-dependence of the photoreactivable response of dark-repair-deficient *phr* mutants of *Escherichia coli* K-12. ***Photochem.Photobiol.*** **45,** 855-857.

SMITH, A.W. and MOSS, S.H. (1988) Photoreactivation in *phr* mutants of *Escherichia coli* K-12: Cloning from the *gal-att*λ interval increases the photoreactivable response in *phr*A strains. ***J.Photochem.Photobiol. B: Biol.*** **2,** 21-32.

SMITH, K.C. and SHARMA, R.C. (1987) A model for the *rec*A-dependent repair of excision gaps in UV-irradiated *Escherichia coli.* ***Mutation Res.*** **183,** 1-9.

SNAPKA, R.M. and SUTHERLAND, B.M. (1980) *Escherichia coli* photoreactivating enzyme : Purification and Properties. ***Biochemistry.*** **19,** 4201-4208.

SUTHERLAND, B.M., COURT, D. and CHAMBERLAIN, M.J. (1972) Studies on the DNA photoreactivating enzyme from *Escherichia coli.* 1. Transduction of the *phr* gene by bacteriophage lambda. ***Virology.*** **48,** 87-93.

SUTHERLAND, B.M., CHAMBERLAIN, M.J. and SUTHERLAND, J.C. (1973) Deoxyribonucleic acid photoreactivating enzyme from *Escherichia coli* : Purification and Properties. ***J.Biol.Chem.*** **248,** 4200-4205.

SUTHERLAND, B.M. and HAUSGRATH, S.C. (1979) Multiple loci affecting photoreactivation in *Escherichia coli*. ***J.Bacteriol.*** **138,** 333-338.

SUTHERLAND, B.M, OLIVEIRA, O.M., CIARROCCHI, G., BRASH, D.E., HASELTINE, W.A., LEWIS, R.J. and HANAWALT, P.C. (1986) Substrate range of the 40,000 dalton DNA-photoreactivating enzyme from *Escherichia coli*. ***Biochemistry.*** **25,** 681-687.

SUTHERLAND, J.C. and GRIFFIN, K.P. (1980) Monomerisation of pyrimidine dimers in DNA by tryptophan-containing peptides : Wavelength dependence. ***Radiat.Res.*** **83,** 529-536.

SVOBODA, D.L., SMITH, C.A., TAYLOR, J-S.A. and SANCAR, A. (1993) Effect of sequence, adduct type and opposing lesions on the binding and repair of ultraviolet photodamage by DNA photolyase and (A)BC exinuclease. ***J.Biol.Chem.*** **268,** 10694-10700.

TABOR, S. and RICHARDSON, C.C. (1989) Effect on manganese ions on the incorporation of dideoxynucleotides by bacteriophage T_7 DNA polymerase and *E.coli* DNA polymerase I. ***Proc.Natl.Acad.Sci.USA.*** **86,** 4076-4080.

TAYLOR, J-S. and COHRS, M.P. (1987) DNA, light and Dewar pyrimidinones : The structure and biological significance of TpT3. ***J.Am.Chem.Soc.*** **109,** 2834-2835.

TAYLOR, J-S., GARRETT, D.S., BROCKIE, I.R., SVOBODA, D.L. and TELSER, J. (1990) ^{1}H NMR assignment and melting temperature study of cis-syn thymine dimer containing duplexes. ***Biochemistry.*** **29,** 8858-8866.

TODO, T., TAKEMORI, H., RYO, H., IHARA, M., MATSUNAGA, T., NIKAIDO, O., SATO, K. and NOMURA, T. (1993) A new photoreactivating enzyme that specifically repairs ultraviolet light-induced (6-4) photoproducts. ***Nature.*** **361,** 371-374.

TYRRELL, R.M. (1971) Ph.D. Thesis, University of Bath.

TYRRELL, R.M., MOSS, S.H. and DAVIES, D.J.G. (1972) The variation in photoreactivating enzyme activity as a function of the stage of growth of three K-12 strains in *Escherichia coli.* ***Mutation Res.*** **19,** 361-364.

TYRRELL, R.M., WEBB, R.B. and BROWN, M.S. (1973) Destruction of photoreactivating enzyme by 365nm radiation. ***Photochem.Photobiol.*** **18,** 249-254.

VERMA, N.C., HEJMADI, V.S. and HOSUR, M.V. (1990) Role of the RNA cofactor of *phr*A photolyase from *E. coli* in its binding with UV-irradiated DNA. ***Current Science.*** **59,** 261-264.

WALKER, G.C. (1984) Mutagenesis and inducible responses to deoxyribonucleic acid damage in *Escherichia coli.* ***Microbiol.Rev.*** **48,** 60-93.

WANG, S.Y. (1960) Reversible behaviour of the ultraviolet irradiated deoxyribonucleic acid and its apurinic acid. ***Nature.*** **188,** 844-846.

WANG, S.Y. (1976) Pyrimidine bimolecular photoproducts. In *"Photochemistry and Photobiology of Nucleic Acids"* Vol *VI*. S.Y. Wang, Ed. **Academic Press, New York.**

WANG, T.V. and SMITH, K.C. (1981) Effect of *rec*B21, *uvr*D3, *lex*A101 and *rec*F143 mutations on ultraviolet radiation sensitivity and genetic recombination in Δ*uvr*B strains of *Escherichia coli*. ***Mol.Gen.Genet.*** **183,** 37-44.

WANG, T.V. and SMITH, K.C. (1983) Mechanisms for *rec*F-dependent and *rec*B-dependent pathways of postreplication repair in UV-irradiated *Escherichia coli uvr*B. ***J.Bacteriol.*** **156,** 1093-1098.

WANG, T.V. and SMITH, K.C. (1986) Post-replication formation and repair of double-stranded breaks in UV-irradiated *Escherichia coli uvr*B cells. ***Mutation Res.*** **165,** 39-44.

WITKIN, E.M. (1976) Ultraviolet mutagenesis and inducible DNA repair in *Escherichia coli*. ***Bacteriol.Rev.*** **40,** 869-907.

WULFF, D.L. and RUPERT, C.S. (1962) Disappearance of thymine photodimers in ultraviolet-irradiated DNA upon treatment with a photoreactivating enzyme from baker's yeast. ***Biochem.Biophys.Res.Commun.*** **7,** 237-240.

YAMADA, H. and HIEDA, K. (1992) Wavelength dependence (150-290nm) of the formation of the cyclobutane dimer and the (6-4) photoproduct of thymine. ***Photochem.Photobiol.*** **55,** 541-548.

YAMAMOTO, K., SATAKE, M., SHINAGAWA, H. and FUJIWARA, Y. (1983a) Amelioration of the ultraviolet sensitivity of an *Escherichia coli rec*A mutant in the dark by photoreactivating enzyme. ***Mol.Gen.Genet.*** **190,** 511-515.

YAMAMOTO, K., SATAKE, M. and SHINAGAWA, H. (1983b) Evidence that the *phr*$^+$ gene enhances the ultraviolet resistance of *Escherichia coli rec*A strains in the dark. ***Mol.Gen.Genet.*** **192,** 282-284.

YANISCH-PERRON, C., VIEIRA, J. and MESSING, J. (1985) Improved M13 phage cloning vectors and host strains : nucleotide sequences of the M13mp 18 and pUC19 vectors. ***Gene*** **33,** 103-119.

YOUNGS, D.A. and SMITH, K.C. (1978) Genetic location of the *phr* gene in *Escherichia coli* K-12. ***Mutation Res.*** **51,** 131-137.

APPENDIX A

Table A1. Bacterial Strains : Derivation and Sources.

STRAIN	GENOTYPE AND DERIVATION	REFERENCE
AS46	Δ(gal-chlA) phr srlA300 : : Tn10 recA56	Smith (1987)
JM83	ara Δ(lac-proAB) rpsL(= strA) thi Φ80dlacZΔM15	Messing (1979)
JM105	supE endA sbcB15 hspR4 rpsL thi Δ(lac-proAB)	Yanisch-Perron
	F' traD36 proAB lacI^q lacZΔM15	(1985)

Table A2. Plasmids used in this study : Derivation and Sources.

PLASMID	FEATURES	SOURCE OR REFERENCE
pBR322	General vector - amp^R + tet^R	Smith (1987)
pAS01	pBR322 + *phr*A gene - amp^R	Smith (1987)
pUC19	General vector - amp^R	PHARMACIA
pAH13	pUC19 + *mdh* gene - amp^R	A.H. Ahmed
pKK223-3	Expression vector - amp^R	PHARMACIA

APPENDIX B1

SOLUTIONS

M9 CONCENTRATES

M9A (50x CONCENTRATE)

NH_4Cl	50g
$MgSO_4.7H_2O$	10g
DDDW	to 1 litre

Made in batches of 500ml and sterilised at 121°C for 30 minutes. Stored at room temperature in the dark.

M9B (12.5x CONCENTRATE)

KH_2PO_4	37.5g
$Na_2HPO_4.2H_2O$	75g
NaCl	6.25g
DDDW	to 1 litre

Made in batches of 500ml and sterilised at 121°C for 30 minutes. Stored at room temperature in the dark.

TRIS SOLUTIONS

The required amount of Tris base (mw 121.1) was dissolved in 400ml of DDDW and the pH adjusted to the desired value by adding concentrated hydrochloric acid (allowing the solution to cool to room temperature before making the final adjustments to pH). The volume was made up to 500ml with DDDW, the solution dispensed into 100ml volumes and sterilised at 121°C for 15 minutes. Stored at 4°C.

0.5M EDTA (pH 8.0)

186.1g of EDTA . $2H_2O$ was added to 800ml of DDDW and stirred vigorously with a magnetic stirrer. The pH was adjusted to 8.0 with 10M NaOH. The solution was made up to 1000ml with DDDW and dispensed into 100ml volumes and sterilised at 121°C for 15 minutes. Stored at 4°C.

10% / 20% w/v SDS

10g or 20g of SDS was dissolved in DDDW and heated to 68°C to aid dissolution. The pH was adjusted to 7.2 by adding a few drops of concentrated hydrochloric acid. The volume was made up to 100ml and the solution dispensed into 20ml aliquots.

SOLUTION I

50mM Glucose

25mM Tris (pH 8.0)

10mM EDTA (pH 8.0)

Made in batches of 100ml and sterilised at 121°C for 15 minutes. Stored at 4°C for 1 month.

SOLUTION II

0.2M NaOH

1% w/v SDS

Freshly prepared from 10M NaOH and 20% w/v SDS stock solutions.

SOLUTION III

5M Potassium Acetate	60ml
Glacial acetic acid	11.5ml
DDDW	28.5ml

The resulting solution is 3M with respect to potassium and 5M with respect to acetate. Stored at 4°C for 1 month.

EQUILIBRATED PHENOL

Phenol was obtained from RATHBURN CHEMICALS LTD, SCOTLAND and stored at -20°C. The volume for equilibration was allowed to warm to room temperature, then hydroxyquinolone added to a final concentration of 0.1% w/v. An equal volume of 0.5M Tris (pH 8.0) was added and mixed with a magnetic stirrer for 15 minutes. The aqueous and organic phases were allowed to partition, then the upper aqueous phase removed. An equal volume of 0.1M Tris (pH 8.0) was then added, mixed for 15 minutes as above, then the upper aqueous phase removed as above. This was repeated until the pH of the aqueous phase was ≅ 8.0 as measured with pH paper. A 0.1 volume of 0.1M Tris (pH 8.0) containing 0.2% v/v β-mercaptoethanol was added, and the equilibrated phenol stored in a light-tight bottle at 4°C for 1 month.

CHLOROFORM : ISOAMYL ALCOHOL (24:1)

4ml of isoamyl alcohol was mixed with 70ml of chloroform and made up to 100ml with chloroform. Stored in a light-tight bottle at 4°C for 1 month.

PHENOL : CHLOROFORM : ISOAMYL ALCOHOL (25:24:1)

A mixture containing equal parts of equilibrated phenol and chloroform : isoamyl alcohol (24:1) was freshly prepared, and used immediately.

RN-ase (DN-ase FREE) 1mg/ml

20mg of pancreatic RN-ase A (SIGMA) was dissolved in 20ml of 10mM Tris (pH 7.5) 15mM NaCl. The solution was heated at 100°C for 15 minutes, then allowed to cool

slowly to room temperature. The solution was sterilised by passage through a 25mm diameter 0.2μm membrane filter, and dispensed into 1ml aliquots and stored at -20°C.

TE (pH 8.0) CONTAINING 20μg/ml RN-ase

10mM Tris (pH 8.0)

1mM EDTA

20μg/ml RN-ase

The solution was sterilised by passage through a 25mm diameter 0.2μm membrane filter, and dispensed into 1ml aliquots and stored at -20°C.

1M $CaCl_2$

54g of $CaCl_2 . 6H_2O$ was dissolved in DDDW and made up to 100ml. This solution was sterilised by passage through a 25mm diameter 0.2μm membrane filter. The sterile solution was dispensed into 1ml aliquots and stored at -20°C.

100mM IPTG

2.383g of IPTG was dissolved in DDDW and made up to 100ml. This solution was sterilised by passage through a 25mm diameter 0.2μm membrane filter. The sterile solution was dispensed into 1ml aliquots and stored at -20°C.

GEL LOADING BUFFER / STOP MIX

0.5% w/v SDS

0.025% w/v Bromophenol Blue

50% v/v Glycerol

Stored at room temperature in glass containers.

λDNA / HindIII MARKER

λDNA pre-digested with HindIII was purchased from SIGMA as a 167μg/ml solution. 20μl of this solution was mixed with 200μl of sterile DDDW and 33μl of gel-loading buffer, and stored at -20°C. 5μl of this solution was used as a marker for the size of DNA fragments on agarose gels. The λDNA / HindIII digest contains eight fragments :- 23,130bps, 9,416bps, 6,557bps, 4,316bps, 2,322bps, 2,027bps, 564bps, and 125bps.

β-MERCAPTOETHANOL

This was purchased as a 14.4M stock solution from SIGMA and stored in the dark at 4°C.

SDS- GEL LOADING BUFFER (2x CONCENTRATE)

100mM Tris (pH 6.8)

4% w/v SDS

0.2% w/v Bromophenol Blue

20% Glycerol

Stored at room temperature in glass containers. Before use, β-mercaptoethanol (14.4M) was added to a ratio of 1:19 and used immediately.

ETHIDIUM BROMIDE 10mg/ml

1g of ethidium bromide (SIGMA) was dissolved in DDDW and made up to 100ml, and the solution stirred using a magnetic stirrer for several hours to ensure all the dye dissolved. The solution was transferred to a light-tight bottle, and stored at room temperature.

COOMASSIE BRILLIANT BLUE STAIN

1.25g of Coomassie Brilliant Blue R250 (BIO-RAD) was dissolved in 450ml of methanol:DDDW (1:1) and 50ml of glacial acetic acid. The solution was filtered through a

Whatman No. 1 filter to remove any particulate matter, and stored in a brown glass ribbed-bottle at room temperature.

APPENDIX B2

MEDIA

NUTRIENT BROTH

OXOID CM1	13g
DDDW	to 1000ml

This was stirred until all the solutes had dissolved, dispensed into 100ml volumes and sterilised at 121°C for 15 minutes. Stored in the dark at room temperature.

LB BROTH

Bacto-Tryptone	10g
Bacto-Yeast Extract	5g
NaCl	10g
DDDW	950ml

This was stirred until all the solutes had dissolved, the pH adjusted to 7.0 with 5M NaOH, the media made up to 1000ml, dispensed into 100ml volumes and sterilised at 121°C for 15 minutes. Stored in the dark at room temperature.

NUTRIENT AGAR

OXOID CM3	28g
DDDW	to 1000ml

This was stirred until all the solutes had dissolved, dispensed into 100ml volumes and sterilised at 121°C for 15 minutes. Stored in the dark at room temperature.

LB AGAR

Bacto-Tryptone	10g
Bacto-Yeast Extract	5g
NaCl	10g
Agar Technical No 3	12g
DDDW	950ml

This was stirred until all the solutes had dissolved, the pH adjusted to 7.0 with 5M NaOH, the media made up to 1000ml, dispensed into 100ml volumes and sterilised at 121°C for 15 minutes. Stored in the dark at room temperature.

APPENDIX B3

BUFFERS

TE BUFFERS

10mM Tris

1mM EDTA

The required pH of TE was prepared by diluting 100mM Tris solution of the same pH. The solutions were sterilised at 121°C for 15 minutes. Stored at 4°C.

TAE BUFFER

A 10x concentrated stock solution was prepared :-

Tris Base	48.4g
Glacial acetic acid	11.4ml
0.5M EDTA (pH 8.0)	20ml
DDDW	to 1000ml

A working concentration of buffer was prepared by diluting the stock solution 1:10 with DDDW.

TBE BUFFER

A 5x concentrated stock solution was prepared :-

Tris Base	54g
Boric Acid	27.5g
0.5M EDTA (pH 8.0)	20ml
DDDW	to 1000ml

A working concentration of buffer was prepared by diluting the stock solution 1:5 with DDDW.

APPENDIX C

SEQUENCING AUTORADIOGRAPHS

IMPORTANT LANES

No. 1 (XI) First Forward (2.5hrs) First Forward (1hr)

No. 2 (XII) First Forward (8hrs) First Forward (4hrs)

No. 3 (XIII) Second Forward (4hrs) Second Forward (2hrs)

No. 4 (XIV) Second Forward (6hrs) Second Forward (9hrs)

No. 5 (XV) Third Forward (2hrs) Third Forward (6hrs)

No. 6 (XVI) Fourth Forward (6hrs) Fourth Forward (2hrs)

No. 7 (XVII) Third Reverse (5hrs) Third Reverse (2hrs)

No. 8 (XIII) Second Reverse (5hrs) Fourth Reverse (5hrs) Fourth Reverse (2hrs)

No. 9 (XIX) Second Reverse (2hrs) First Reverse (5.5hrs)
Third Reverse (5.5hrs) Third Forward (5hrs)

No. 10 (XX) First Reverse (2hrs) Third Reverse (5hrs) First Reverse (4.5hrs)

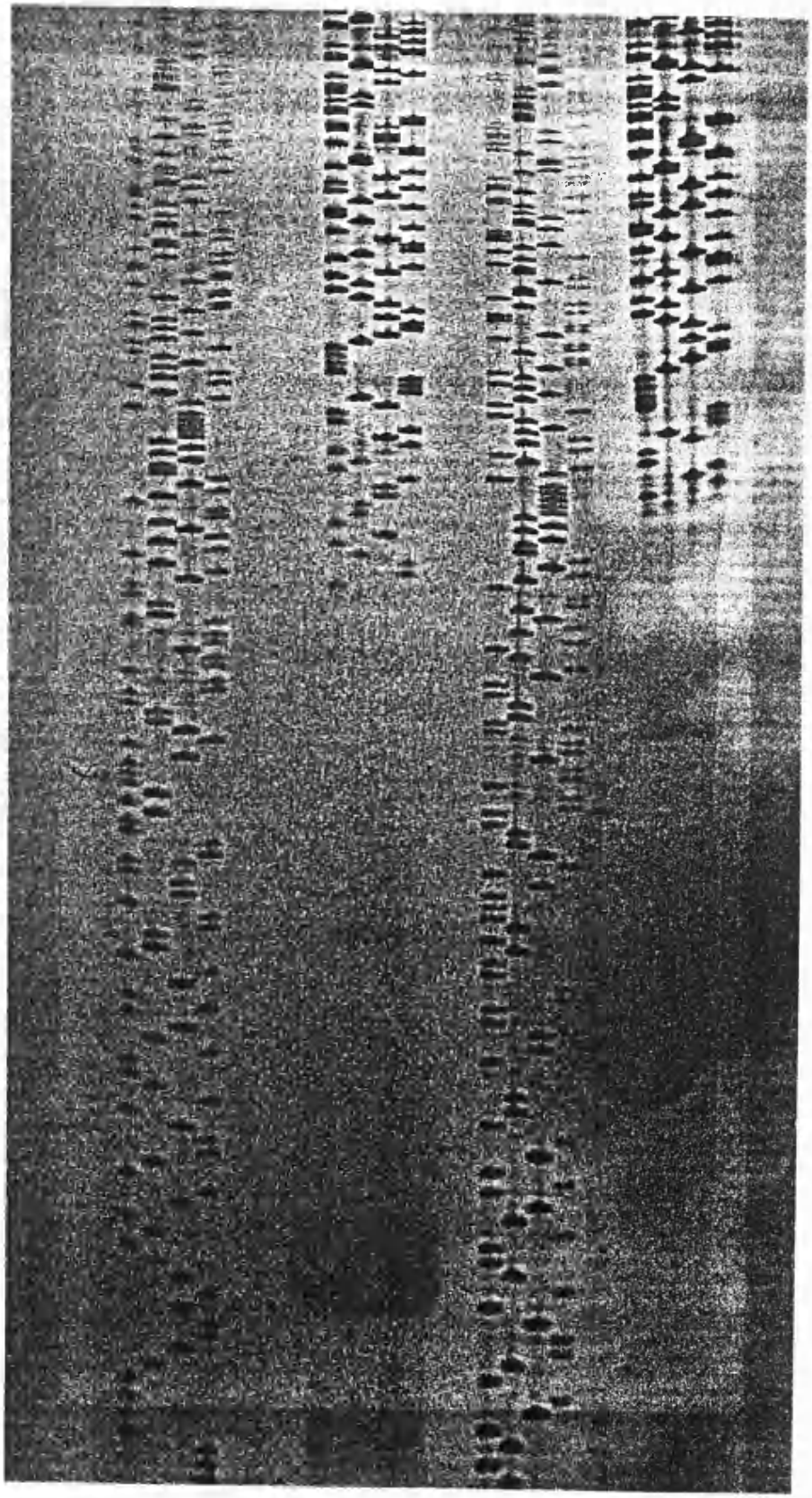

Lane 1) 1st For (2.5hrs), Lane 2) 1st For (1hr).

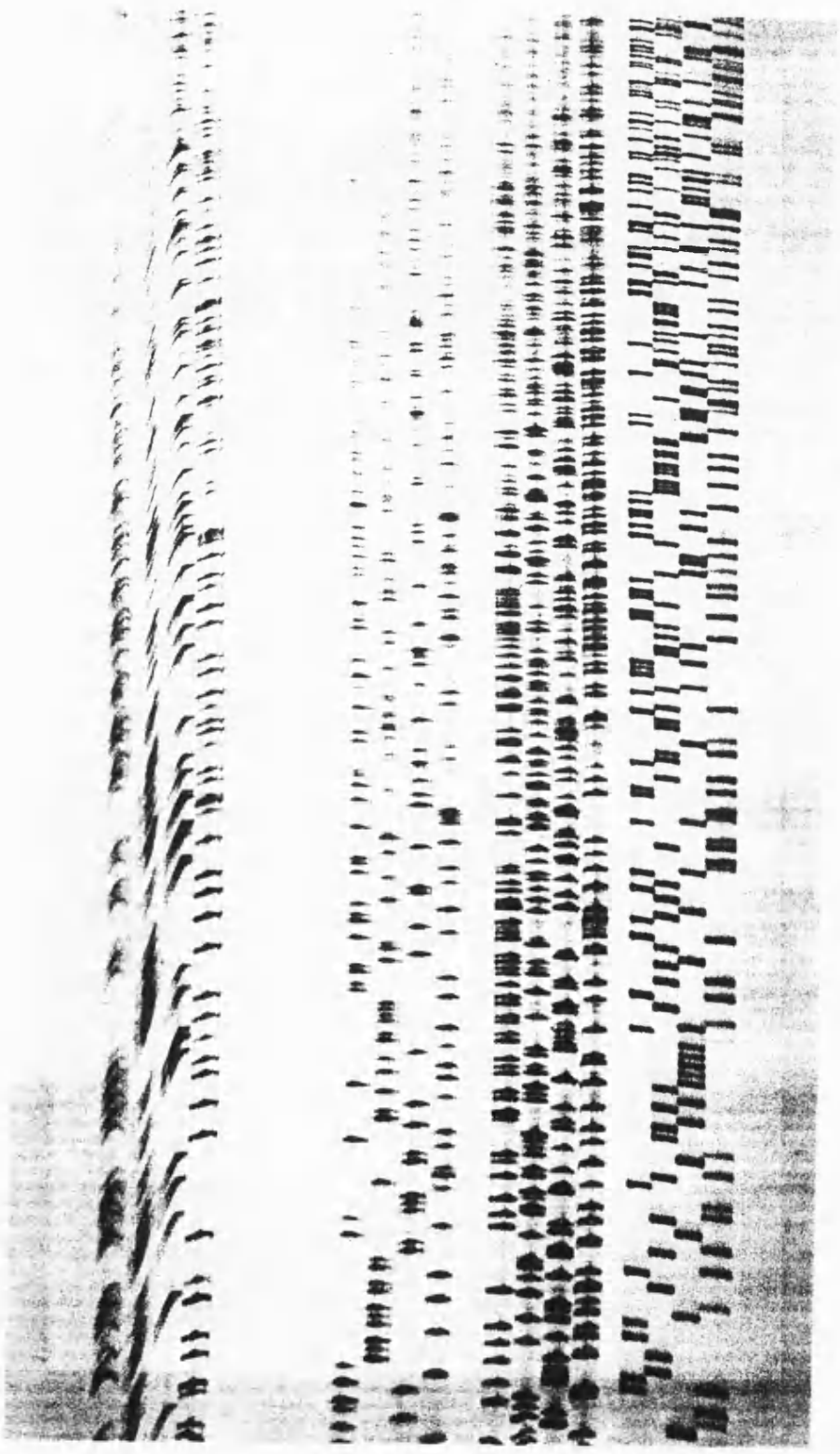

Lane 2) 1st For (8hrs), Lane 4) 1st For (4hrs).

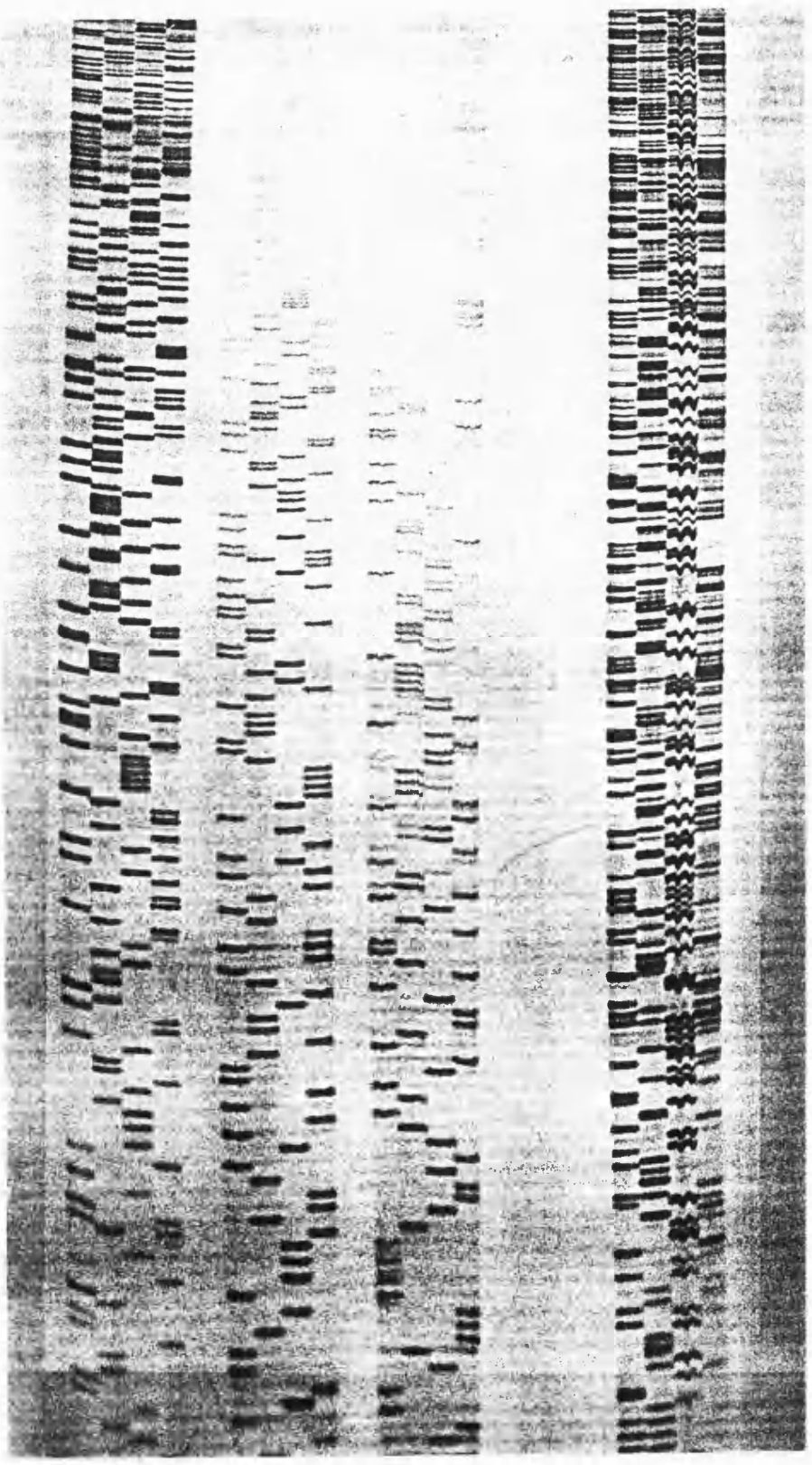

Lane 1) 2nd For (4hrs), Lane 2) 2nd For (2hrs).

Lane 1) 2nd For (6hrs), Lane 2) 2nd For (9hrs).

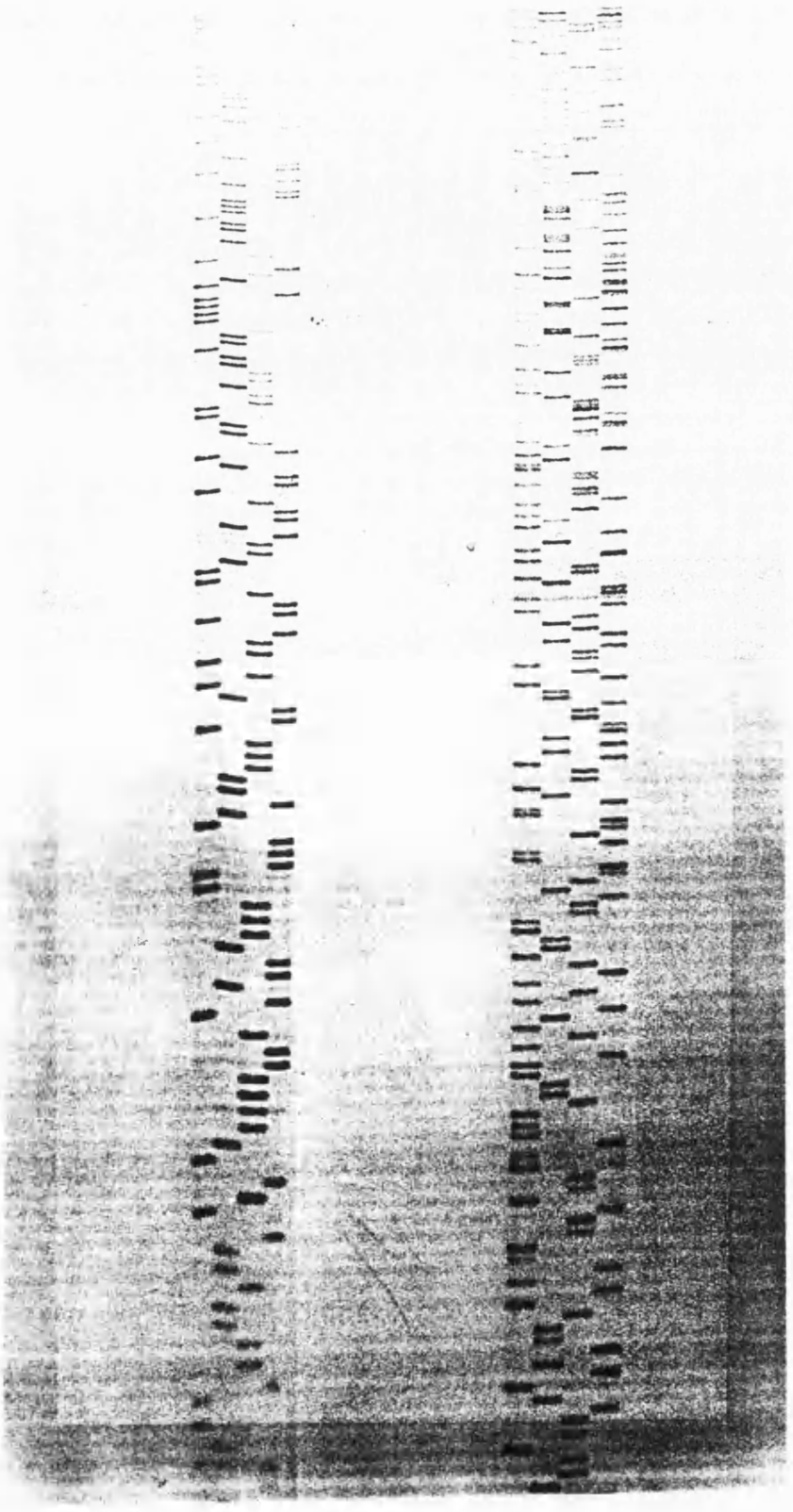

Lane 1) 3rd For (2hrs), Lane 2) 3rd For (6hrs).

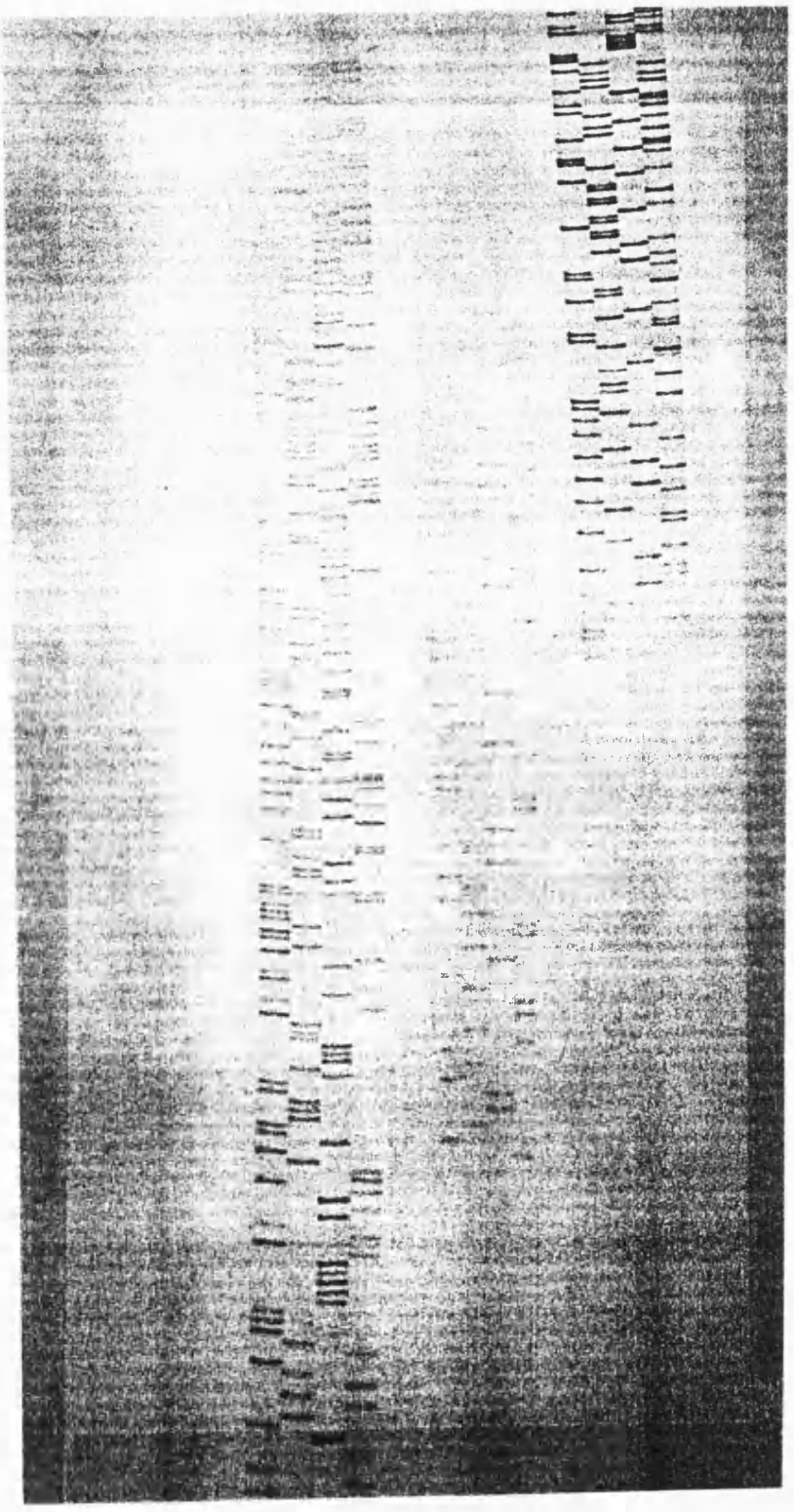

Lane 1) 4th For (6hrs), Lane 3) 4th For (2hrs).

Lane 1) 3rd Rev (5hrs), Lane 2) 3rd Rev (2hrs).

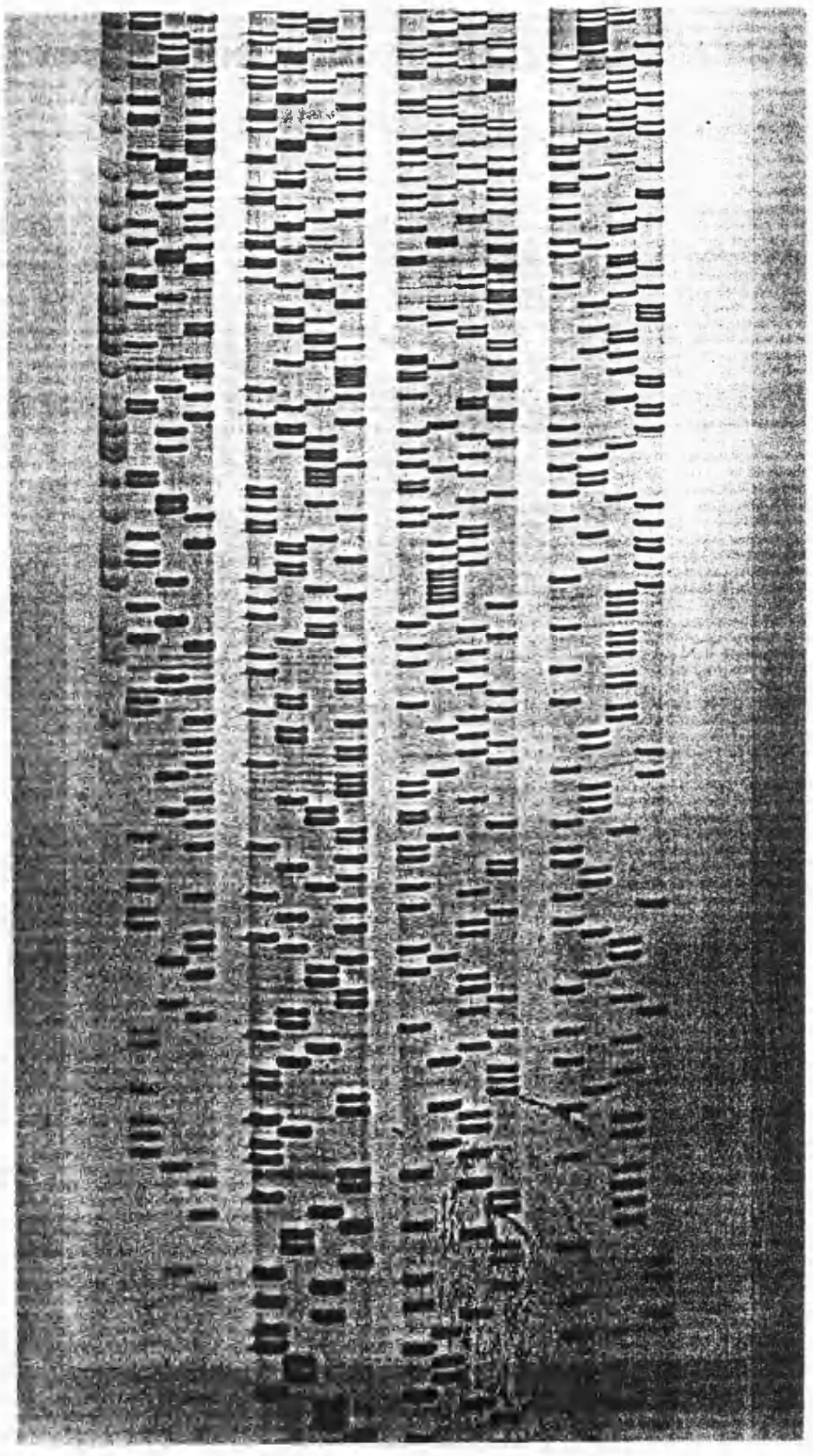

Lane 2) 2nd Rev (5hrs), Lane 3) 4th Rev (5hrs), Lane 4) 4th Rev (2hrs).

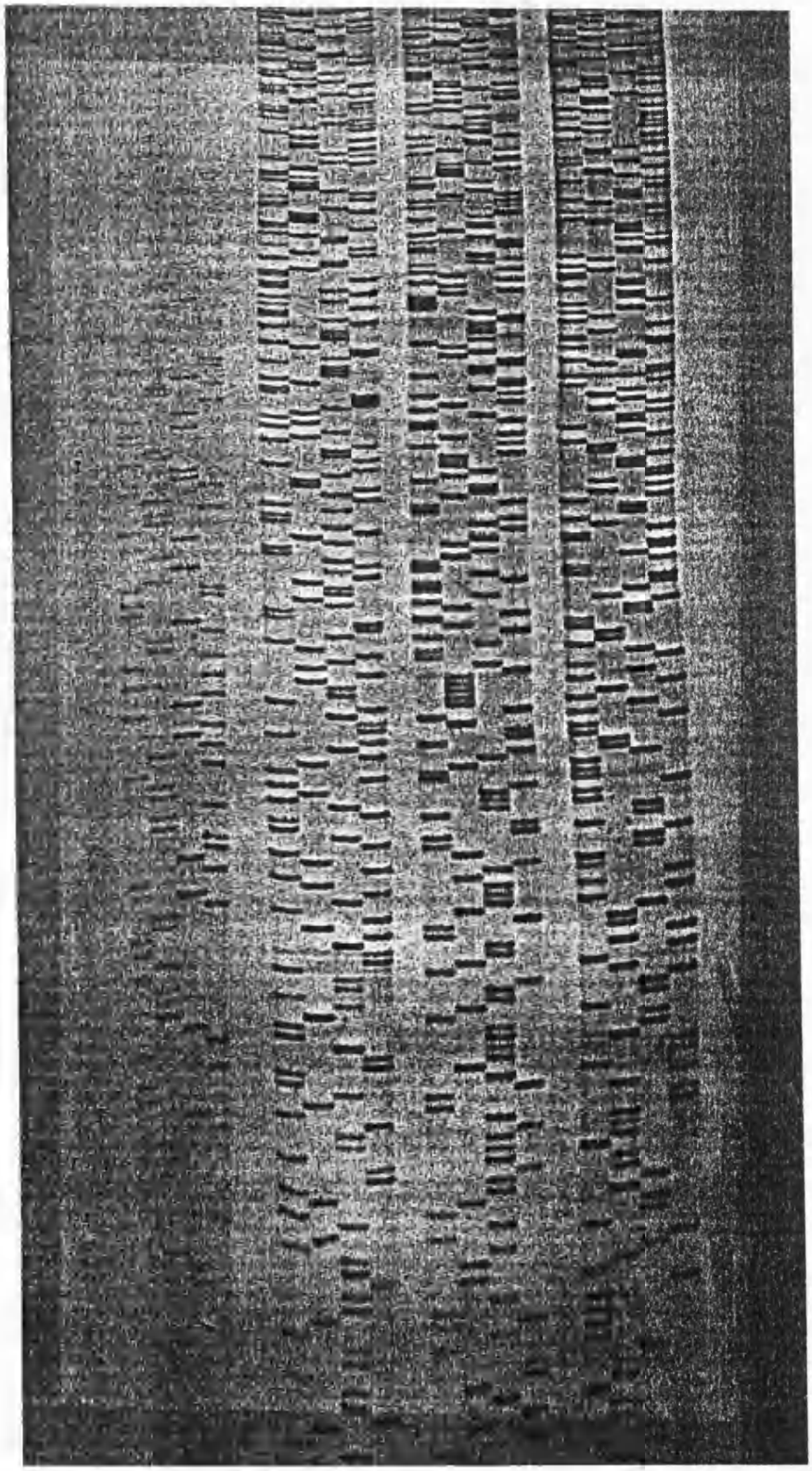

Lane 1) 2nd Rev (2hrs), Lane 2) 1st Rev (5.5hrs), Lane 3) 3rd Rev (5.5hrs),

Lane 4) 1st Rev (4.5hrs).

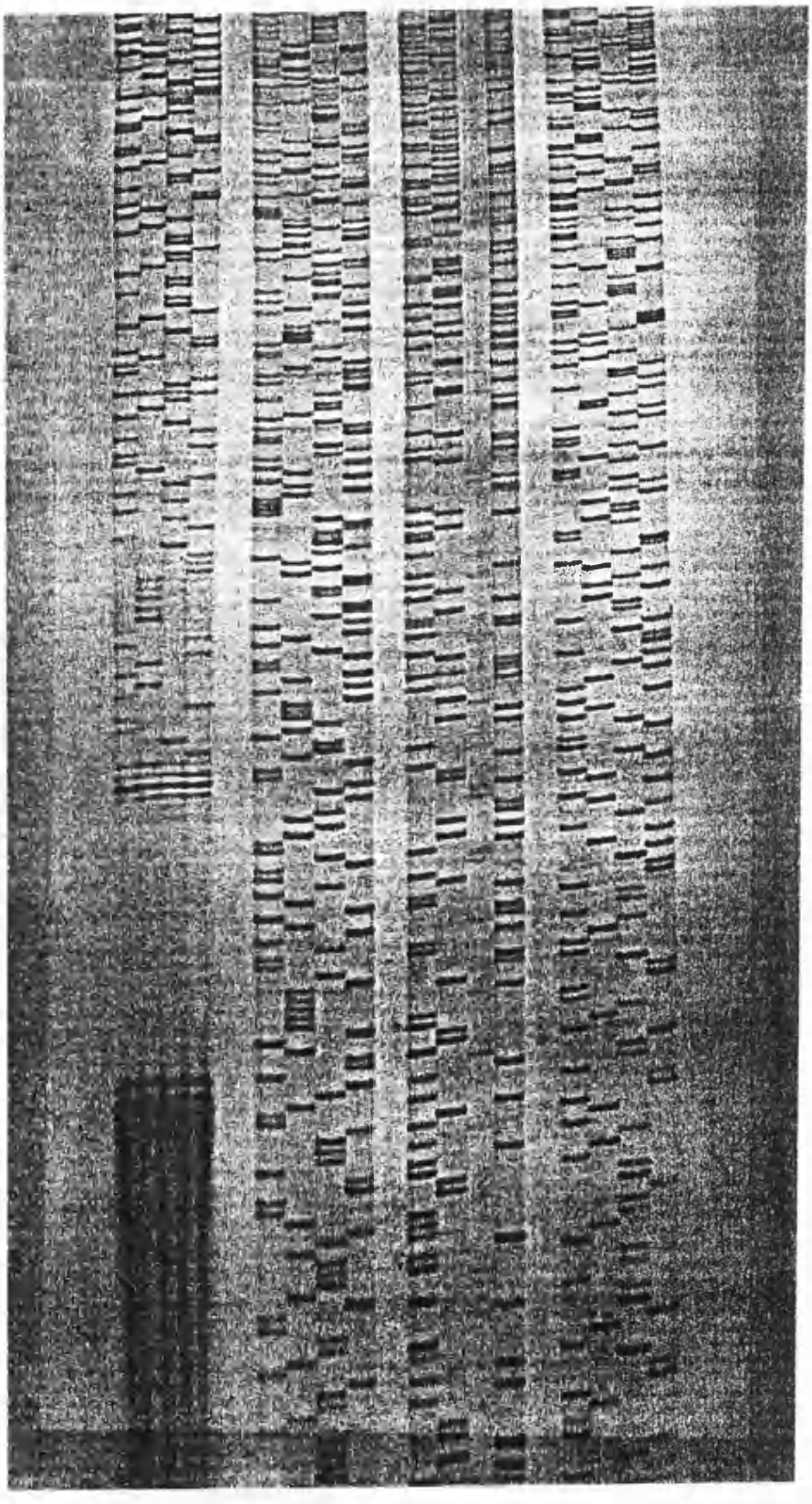

Lane 1) 1st Rev (2hrs), Lane 2) 3rd Rev (5hrs), Lane 4) 1st Rev (4.5hrs).

APPENDIX D

UV-IRRADIATION AND PHOTOREACTIVATION DATA

Table D.1. Survival Curve data for AS46/pND01 irradiated at 254nm (Figure 5.1)

EXPT NO	INITIAL VIABLE COUNT (ml^{-1})	FLUENCE RATE (Wm^{-2})	FLUENCE (Jm^{-2})	SURVIVING FRACTION (S/So)
1a (3.16)	5.63×10^{6}	0.147	0.132	9.65×10^{-2}
			0.260	6.87×10^{-3}
			0.391	6.80×10^{-4}
			0.508	5.68×10^{-5}
1b (3.32)	3.33×10^{6}	0.142	0.131	8.76×10^{-2}
			0.264	6.98×10^{-3}
			0.397	6.91×10^{-4}
			0.524	6.82×10^{-5}
1c (3.04)	2.60×10^{7}	0.150	0.132	1.17×10^{-1}
			0.264	1.24×10^{-2}
			0.401	8.77×10^{-4}
			0.521	7.58×10^{-5}

Table D.2. Survival Curve data for AS46/pUC19 irradiated at 254nm (Figure 5.2)

EXPT NO	INITIAL VIABLE COUNT (ml^{-1})	FLUENCE RATE (Wm^{-2})	FLUENCE (Jm^{-2})	SURVIVING FRACTION (S/So)
2a (3.22)	5.23×10^{6}	0.145	0.131	8.80×10^{-2}
			0.263	8.47×10^{-3}
			0.393	4.26×10^{-4}
			0.524	4.65×10^{-5}
2b (3.34)	6.57×10^{6}	0.145	0.135	8.71×10^{-2}
			0.268	6.92×10^{-3}
			0.403	6.81×10^{-4}
			0.538	6.29×10^{-5}
2c (4.18)	1.08×10^{7}	0.150	0.133	1.19×10^{-1}
			0.262	1.01×10^{-2}
			0.407	9.68×10^{-4}
			0.524	8.98×10^{-5}

Table D.3. Survival Curve data for AS46/pND03 irradiated at 254nm (Figure 5.3)

EXPT NO	INITIAL VIABLE COUNT (ml^{-1})	FLUENCE RATE (Wm^{-2})	FLUENCE (Jm^{-2})	SURVIVING FRACTION (S/So)
3a (3.10)	4.60×10^{6}	0.150	0.136	1.06×10^{-1}
			0.271	5.65×10^{-3}
			0.404	5.07×10^{-4}
			0.521	5.59×10^{-5}
3b (3.24)	2.20×10^{6}	0.145	0.128	1.33×10^{-1}
			0.255	1.18×10^{-2}
			0.382	1.35×10^{-3}
			0.498	1.05×10^{-4}
3c (3.40)	3.43×10^{6}	0.145	0.134	1.65×10^{-1}
			0.270	1.42×10^{-2}
			0.405	1.37×10^{-3}
			0.537	1.31×10^{-4}

Table D.4. Survival Curve data for AS46/pKK223-3 irradiated at 254nm (Figure 5.4)

EXPT NO	INITIAL VIABLE COUNT (ml^{-1})	FLUENCE RATE (Wm^{-2})	FLUENCE (Jm^{-2})	SURVIVING FRACTION (S/So)
4a (3.38)	5.23×10^{6}	0.145	0.125	1.71×10^{-1}
			0.252	1.56×10^{-2}
			0.378	1.51×10^{-3}
			0.499	1.49×10^{-4}
4b (3.42)	2.97×10^{6}	0.145	0.137	1.02×10^{-1}
			0.278	9.31×10^{-3}
			0.415	9.27×10^{-4}
			0.546	9.09×10^{-5}
4c (3.46)	3.60×10^{7}	0.142	0.132	5.32×10^{-2}
			0.271	4.78×10^{-3}
			0.404	4.72×10^{-4}
			0.528	4.67×10^{-5}

Table D.5. Photoreactivation data for AS46/pND01 at 25°C (Figure 5.5)

	PHOTOREACTIVATION TIME (minutes)				
EXPT 5a (3.16)	0	30	60	90	120
UNIRRADIATED S/So	1.000	0.871	0.853	0.737	0.737
IRRADIATED S/So	5.28×10^{-5}	5.56×10^{-5}	1.00×10^{-4}	1.29×10^{-4}	1.67×10^{-4}
CORRECTED S/So	5.28×10^{-5}	6.38×10^{-5}	1.17×10^{-4}	1.75×10^{-4}	2.27×10^{-4}
DARK IRRADIATED S/So	5.28×10^{-5}	5.28×10^{-5}	5.30×10^{-5}	5.33×10^{-5}	5.30×10^{-5}
EXPT 5b (3.07)	0	30	60	90	120
UNIRRADIATED S/So	1.000	0.867	0.847	0.746	0.691
IRRADIATED S/So	9.40×10^{-5}	1.06×10^{-4}	1.43×10^{-4}	1.76×10^{-4}	2.56×10^{-4}
CORRECTED S/So	9.40×10^{-5}	1.22×10^{-4}	1.69×10^{-4}	2.36×10^{-4}	3.71×10^{-4}
DARK IRRADIATED S/So	9.40×10^{-5}	9.40×10^{-5}	9.40×10^{-5}	9.40×10^{-5}	9.40×10^{-5}
EXPT 5c (4.20)	0	30	60	90	120
UNIRRADIATED S/So	1.000	0.897	0.843	0.751	0.682
IRRADIATED S/So	6.48×10^{-5}	6.72×10^{-5}	1.06×10^{-4}	1.38×10^{-4}	1.89×10^{-4}
CORRECTED S/So	6.48×10^{-5}	7.49×10^{-5}	1.26×10^{-4}	1.84×10^{-4}	2.77×10^{-4}
DARK IRRADIATED S/So	6.48×10^{-5}	6.48×10^{-5}	6.48×10^{-5}	6.48×10^{-5}	6.48×10^{-5}

Table D.6. Photoreactivation data for AS46/pUC19 at 25°C (Figure 5.6)

	PHOTOREACTIVATION TIME (minutes)				
EXPT 6a (3.22)	0	30	60	90	120
UNIRRADIATED S/So	1.000	0.893	0.702	0.727	0.713
IRRADIATED S/So	4.65×10^{-5}	4.46×10^{-5}	6.83×10^{-5}	1.05×10^{-4}	1.05×10^{-4}
CORRECTED S/So	4.65×10^{-5}	4.99×10^{-5}	9.73×10^{-5}	1.44×10^{-4}	1.47×10^{-4}
DARK IRRADIATED S/So	4.65×10^{-5}	4.68×10^{-5}	4.67×10^{-5}	4.68×10^{-5}	4.66×10^{-5}
EXPT 6b (3.34)	0	30	60	90	120
UNIRRADIATED S/So	1.000	0.890	0.724	0.701	0.678
IRRADIATED S/So	1.33×10^{-4}	1.38×10^{-4}	1.87×10^{-4}	2.02×10^{-4}	1.72×10^{-4}
CORRECTED S/So	1.33×10^{-4}	1.55×10^{-4}	2.58×10^{-4}	2.88×10^{-4}	2.54×10^{-4}
DARK IRRADIATED S/So	1.33×10^{-4}	1.33×10^{-4}	1.33×10^{-4}	1.33×10^{-4}	1.33×10^{-4}
EXPT 6c (4.18)	0	30	60	90	120
UNIRRADIATED S/So	1.000	0.930	0.749	0.679	0.532
IRRADIATED S/So	8.98×10^{-5}	1.10×10^{-4}	1.19×10^{-4}	1.36×10^{-4}	1.29×10^{-4}
CORRECTED S/So	8.98×10^{-5}	1.19×10^{-4}	1.60×10^{-4}	2.00×10^{-4}	2.42×10^{-4}
DARK IRRADIATED S/So	8.98×10^{-5}	8.98×10^{-5}	8.98×10^{-5}	8.98×10^{-5}	8.98×10^{-5}

Table D.7. Photoreactivation data for AS46/pND03 at 25°C (Figure 5.7)

	PHOTOREACTIVATION TIME (minutes)				
EXPT 7a (3.10)	0	30	60	90	120
UNIRRADIATED S/So	1.000	0.928	0.790	0.679	0.648
IRRADIATED S/So	4.72×10^{-5}	5.80×10^{-5}	1.42×10^{-4}	2.00×10^{-4}	2.46×10^{-4}
CORRECTED S/So	4.72×10^{-5}	6.25×10^{-5}	1.80×10^{-4}	2.95×10^{-4}	3.80×10^{-4}
DARK IRRADIATED S/So	4.72×10^{-5}	4.74×10^{-5}	4.73×10^{-5}	4.75×10^{-5}	4.76×10^{-5}
EXPT 7b (4.16)	0	30	60	90	120
UNIRRADIATED S/So	1.000	0.918	0.838	0.654	0.636
IRRADIATED S/So	4.43×10^{-5}	6.68×10^{-5}	1.15×10^{-4}	1.55×10^{-4}	1.62×10^{-4}
CORRECTED S/So	4.43×10^{-5}	7.28×10^{-5}	1.37×10^{-4}	2.36×10^{-4}	2.55×10^{-4}
DARK IRRADIATED S/So	4.43×10^{-5}	4.43×10^{-5}	4.43×10^{-5}	4.43×10^{-5}	4.43×10^{-5}
EXPT 7c (4.22)	0	30	60	90	120
UNIRRADIATED S/So	1.000	0.915	0.817	0.666	0.639
IRRADIATED S/So	5.78×10^{-5}	7.57×10^{-5}	1.26×10^{-4}	2.04×10^{-4}	2.63×10^{-4}
CORRECTED S/So	5.78×10^{-5}	8.27×10^{-5}	1.54×10^{-4}	3.06×10^{-4}	4.12×10^{-4}
DARK IRRADIATED S/So	5.78×10^{-5}	5.78×10^{-5}	5.78×10^{-5}	5.78×10^{-5}	5.78×10^{-5}

Table D.8. Photoreactivation data for AS46/pKK223-3 at 25°C (Figure 5.8)

	PHOTOREACTIVATION TIME (minutes)				
EXPT 8a (3.66)	0	30	60	90	120
UNIRRADIATED S/So	1.000	0.983	0.901	0.728	0.572
IRRADIATED S/So	2.28×10^{-4}	2.49×10^{-4}	3.21×10^{-4}	3.90×10^{-4}	3.77×10^{-4}
CORRECTED S/So	2.28×10^{-4}	2.53×10^{-4}	3.57×10^{-4}	5.36×10^{-4}	6.59×10^{-4}
DARK IRRADIATED S/So	2.28×10^{-4}	2.28×10^{-4}	2.28×10^{-4}	2.28×10^{-4}	2.28×10^{-4}
EXPT 8b (4.14)	0	30	60	90	120
UNIRRADIATED S/So	1.000	0.924	0.660	0.592	0.548
IRRADIATED S/So	3.66×10^{-5}	4.21×10^{-5}	6.78×10^{-4}	6.61×10^{-4}	7.10×10^{-4}
CORRECTED S/So	3.66×10^{-5}	4.55×10^{-5}	1.03×10^{-4}	1.12×10^{-4}	1.29×10^{-4}
DARK IRRADIATED S/So	3.66×10^{-5}	3.66×10^{-5}	3.66×10^{-5}	3.66×10^{-5}	3.66×10^{-5}
EXPT 8c (4.24)	0	30	60	90	120
UNIRRADIATED S/So	1.000	0.967	0.753	0.651	0.584
IRRADIATED S/So	6.71×10^{-5}	7.89×10^{-5}	9.56×10^{-5}	1.00×10^{-4}	1.21×10^{-4}
CORRECTED S/So	6.71×10^{-5}	8.16×10^{-5}	1.27×10^{-4}	1.54×10^{-4}	2.07×10^{-4}
DARK IRRADIATED S/So	6.71×10^{-5}	6.71×10^{-5}	6.71×10^{-5}	6.71×10^{-5}	6.71×10^{-5}

Table D.9. Photoreactivation data for AS46 at 25°C (Figure 5.9)

	PHOTOREACTIVATION TIME (minutes)				
EXPT 9a (3.18)	0	30	60	90	120
UNIRRADIATED S/So	1.000	0.890	0.890	0.812	0.807
IRRADIATED S/So	8.35×10^{-5}	9.34×10^{-5}	1.48×10^{-4}	1.93×10^{-4}	1.99×10^{-4}
CORRECTED S/So	8.35×10^{-5}	1.05×10^{-4}	1.66×10^{-4}	2.37×10^{-4}	2.47×10^{-4}
DARK IRRADIATED S/So	8.35×10^{-5}	8.35×10^{-5}	8.35×10^{-5}	8.35×10^{-5}	8.35×10^{-5}
EXPT 9b (3.30)	0	30	60	90	120
UNIRRADIATED S/So	1.000	0.792	0.777	0.652	0.744
IRRADIATED S/So	2.91×10^{-4}	3.43×10^{-4}	3.50×10^{-4}	3.55×10^{-4}	3.36×10^{-4}
CORRECTED S/So	2.91×10^{-4}	4.33×10^{-4}	4.51×10^{-4}	5.44×10^{-4}	4.52×10^{-4}
DARK IRRADIATED S/So	2.91×10^{-4}	2.91×10^{-4}	2.91×10^{-4}	2.91×10^{-4}	2.91×10^{-4}
EXPT 9c (3.02)	0	30	60	90	120
UNIRRADIATED S/So	1.000	0.888	0.874	0.744	0.730
IRRADIATED S/So	4.71×10^{-4}	5.06×10^{-4}	6.30×10^{-4}	7.46×10^{-4}	7.46×10^{-4}
CORRECTED S/So	4.71×10^{-4}	5.70×10^{-4}	7.20×10^{-4}	1.00×10^{-3}	1.02×10^{-3}
DARK IRRADIATED S/So	4.71×10^{-4}	4.71×10^{-4}	4.71×10^{-4}	4.71×10^{-4}	4.71×10^{-4}

Table D.10. Photoreactivation data for AS46/pND03 at 37°C (Figure 5.10)

	PHOTOREACTIVATION TIME (minutes)				
EXPT 10a (3.24)	0	30	60	90	120
UNIRRADIATED S/So	1.000	0.952	0.709	0.692	0.639
IRRADIATED S/So	9.09×10^{-5}	2.51×10^{-4}	4.96×10^{-4}	5.05×10^{-4}	5.77×10^{-4}
CORRECTED S/So	9.09×10^{-5}	2.64×10^{-4}	6.99×10^{-4}	7.29×10^{-4}	9.03×10^{-4}
DARK IRRADIATED S/So	9.09×10^{-5}	9.09×10^{-5}	9.09×10^{-5}	9.09×10^{-5}	9.09×10^{-5}
EXPT 10b (3.36) *	0	30	60	90	120
UNIRRADIATED S/So	1.000	0.949	0.756	0.701	0.642
IRRADIATED S/So	2.53×10^{-4}	3.58×10^{-4}	5.58×10^{-4}	5.11×10^{-4}	5.47×10^{-4}
CORRECTED S/So	2.53×10^{-4}	3.77×10^{-4}	7.38×10^{-4}	7.29×10^{-4}	8.52×10^{-4}
DARK IRRADIATED S/So	2.53×10^{-4}	2.53×10^{-4}	2.53×10^{-4}	2.53×10^{-4}	2.53×10^{-4}
EXPT 10c (4.26)	0	30	60	90	120
UNIRRADIATED S/So	1.000	0.962	0.748	0.689	0.641
IRRADIATED S/So	7.12×10^{-5}	1.21×10^{-4}	3.66×10^{-4}	4.14×10^{-4}	4.72×10^{-4}
CORRECTED S/So	7.12×10^{-5}	1.26×10^{-4}	4.89×10^{-4}	6.01×10^{-4}	7.36×10^{-4}
DARK IRRADIATED S/So	7.12×10^{-5}	7.12×10^{-5}	7.12×10^{-5}	7.12×10^{-5}	7.12×10^{-5}

* Data from Expt 10b was not included in the quantitative analysis of the data for reasons explained in Section 5.4.

Table D.11. Photoreactivation data for AS46/pND03 at 10°C (Figure 5.11)

	PHOTOREACTIVATION TIME (minutes)				
EXPT 11a (4.02)	0	30	60	90	120
UNIRRADIATED S/So	1.000	0.904	0.824	0.666	0.624
IRRADIATED S/So	8.70×10^{-5}	9.54×10^{-5}	9.54×10^{-5}	9.54×10^{-5}	1.21×10^{-4}
CORRECTED S/So	8.70×10^{-5}	1.06×10^{-4}	1.16×10^{-4}	1.37×10^{-4}	1.93×10^{-4}
DARK IRRADIATED S/So	8.70×10^{-5}	8.70×10^{-5}	8.70×10^{-5}	8.70×10^{-5}	8.70×10^{-5}
EXPT 11b (3.48)	0	30	60	90	120
UNIRRADIATED S/So	1.000	0.988	0.673	0.590	0.612
IRRADIATED S/So	8.56×10^{-5}	8.36×10^{-5}	6.54×10^{-5}	7.49×10^{-5}	1.16×10^{-4}
CORRECTED S/So	8.56×10^{-5}	8.46×10^{-5}	9.72×10^{-5}	1.27×10^{-4}	1.90×10^{-4}
DARK IRRADIATED S/So	8.56×10^{-5}	8.56×10^{-5}	8.56×10^{-5}	8.56×10^{-5}	8.56×10^{-5}
EXPT 11c (4.28)	0	30	60	90	120
UNIRRADIATED S/So	1.000	0.965	0.754	0.632	0.601
IRRADIATED S/So	7.57×10^{-5}	8.02×10^{-5}	6.74×10^{-5}	5.89×10^{-5}	6.13×10^{-5}
CORRECTED S/So	7.57×10^{-5}	8.31×10^{-5}	8.94×10^{-5}	9.32×10^{-5}	1.02×10^{-4}
DARK IRRADIATED S/So	7.57×10^{-5}	7.57×10^{-5}	7.57×10^{-5}	7.57×10^{-5}	7.57×10^{-5}

Table D.12. Photoreactivation data for AS46/pKK223-3 at 37°C (Figure 5.12)

	PHOTOREACTIVATION TIME (minutes)				
EXPT 12a (3.50)	0	30	60	90	120
UNIRRADIATED S/So	1.000	0.964	0.658	0.603	0.564
IRRADIATED S/So	1.48×10^{-4}	2.30×10^{-4}	3.28×10^{-4}	3.26×10^{-4}	3.10×10^{-4}
CORRECTED S/So	1.48×10^{-4}	2.38×10^{-4}	4.98×10^{-4}	5.41×10^{-4}	5.48×10^{-4}
DARK IRRADIATED S/So	1.48×10^{-4}	1.48×10^{-4}	1.48×10^{-4}	1.48×10^{-4}	1.48×10^{-4}
EXPT 12b (4.30)	0	30	60	90	120
UNIRRADIATED S/So	1.000	0.932	0.701	0.612	0.554
IRRADIATED S/So	6.14×10^{-5}	6.77×10^{-5}	6.11×10^{-5}	6.05×10^{-5}	7.92×10^{-5}
CORRECTED S/So	6.14×10^{-5}	7.26×10^{-5}	8.72×10^{-5}	9.89×10^{-5}	1.43×10^{-4}
DARK IRRADIATED S/So	6.14×10^{-5}	6.14×10^{-5}	6.14×10^{-5}	6.14×10^{-5}	6.14×10^{-5}
EXPT 12c (4.32)	0	30	60	90	120
UNIRRADIATED S/So	1.000	0.941	0.687	0.621	0.571
IRRADIATED S/So	8.97×10^{-5}	9.79×10^{-5}	1.25×10^{-4}	1.47×10^{-4}	1.88×10^{-4}
CORRECTED S/So	8.97×10^{-5}	1.04×10^{-4}	1.82×10^{-4}	2.37×10^{-4}	3.29×10^{-4}
DARK IRRADIATED S/So	8.97×10^{-5}	8.97×10^{-5}	8.97×10^{-5}	8.97×10^{-5}	8.97×10^{-5}

Table D.13. Photoreactivation data for AS46/pKK223-3 at 10°C (Figure 5.13)

	PHOTOREACTIVATION TIME (minutes)				
EXPT 13a (3.88)	0	30	60	90	120
UNIRRADIATED S/So	1.000	0.890	0.789	0.616	0.555
IRRADIATED S/So	1.05×10^{-4}	1.20×10^{-4}	1.19×10^{-4}	1.21×10^{-4}	1.36×10^{-4}
CORRECTED S/So	1.05×10^{-4}	1.35×10^{-4}	1.50×10^{-4}	1.96×10^{-4}	2.45×10^{-4}
DARK IRRADIATED S/So	1.05×10^{-4}	1.05×10^{-4}	1.05×10^{-4}	1.05×10^{-4}	1.05×10^{-4}
EXPT 13b (3.46)	0	30	60	90	120
UNIRRADIATED S/So	1.000	0.982	0.802	0.721	0.730
IRRADIATED S/So	4.67×10^{-4}	4.17×10^{-4}	3.58×10^{-4}	3.86×10^{-4}	3.69×10^{-4}
CORRECTED S/So	4.67×10^{-4}	4.24×10^{-4}	4.47×10^{-4}	5.35×10^{-4}	5.06×10^{-4}
DARK IRRADIATED S/So	4.67×10^{-4}	4.67×10^{-4}	4.67×10^{-4}	4.67×10^{-4}	4.67×10^{-4}
EXPT 13c (4.34)	0	30	60	90	120
UNIRRADIATED S/So	1.000	0.936	0.792	0.654	0.592
IRRADIATED S/So	5.47×10^{-5}	6.37×10^{-5}	6.27×10^{-5}	6.42×10^{-5}	7.76×10^{-5}
CORRECTED S/So	5.47×10^{-5}	6.81×10^{-5}	7.92×10^{-5}	9.82×10^{-5}	1.31×10^{-4}
DARK IRRADIATED S/So	5.47×10^{-5}	5.47×10^{-5}	5.47×10^{-5}	5.47×10^{-5}	5.47×10^{-5}

Table D.14. Photoreactivation data for AS46/pND03 at fluence rate of ≅ 1Wm^{-2} at 37°C (Figure 5.14)

	PHOTOREACTIVATION TIME (minutes)				
EXPT 14a (3.52)	0	30	60	90	120
UNIRRADIATED S/So	1.000	0.993	0.750	0.727	0.721
IRRADIATED S/So	3.44×10^{-5}	7.13×10^{-5}	1.19×10^{-4}	1.56×10^{-4}	2.12×10^{-4}
CORRECTED S/So	3.44×10^{-5}	7.18×10^{-5}	1.58×10^{-4}	2.14×10^{-4}	2.94×10^{-4}
DARK IRRADIATED S/So	3.44×10^{-5}	3.44×10^{-5}	3.44×10^{-5}	3.44×10^{-5}	3.44×10^{-5}
EXPT 14b (4.36)	0	30	60	90	120
UNIRRADIATED S/So	1.000	0.987	0.797	0.751	0.719
IRRADIATED S/So	6.26×10^{-5}	8.94×10^{-5}	2.46×10^{-4}	3.13×10^{-4}	4.27×10^{-4}
CORRECTED S/So	6.26×10^{-5}	9.06×10^{-5}	3.09×10^{-4}	4.17×10^{-4}	5.94×10^{-4}
DARK IRRADIATED S/So	6.26×10^{-5}	6.26×10^{-5}	6.26×10^{-5}	6.26×10^{-5}	6.26×10^{-5}
EXPT 14c (4.38)	0	30	60	90	120
UNIRRADIATED S/So	1.000	0.971	0.782	0.734	0.727
IRRADIATED S/So	7.91×10^{-5}	1.09×10^{-4}	3.89×10^{-4}	4.43×10^{-4}	5.23×10^{-4}
CORRECTED S/So	7.91×10^{-5}	1.12×10^{-4}	4.97×10^{-4}	6.04×10^{-4}	7.19×10^{-4}
DARK IRRADIATED S/So	7.91×10^{-5}	7.91×10^{-5}	7.91×10^{-5}	7.91×10^{-5}	7.91×10^{-5}

Table D.15. Photoreactivation data for AS46/pKK223-3 at fluence rate of ≅ 1Wm^{-2} at 37°C (Figure 5.15)

	PHOTOREACTIVATION TIME (minutes)				
EXPT 15a (3.54)	0	30	60	90	120
UNIRRADIATED S/So	1.000	0.865	0.818	0.774	0.764
IRRADIATED S/So	1.49×10^{-4}	1.49×10^{-4}	2.02×10^{-4}	3.05×10^{-4}	3.49×10^{-4}
CORRECTED S/So	1.49×10^{-4}	1.72×10^{-4}	2.47×10^{-4}	3.94×10^{-4}	4.57×10^{-4}
DARK IRRADIATED S/So	1.49×10^{-4}	1.49×10^{-4}	1.49×10^{-4}	1.49×10^{-4}	1.49×10^{-4}
EXPT 15b (4.40)	0	30	60	90	120
UNIRRADIATED S/So	1.000	0.896	0.808	0.764	0.734
IRRADIATED S/So	6.54×10^{-5}	7.09×10^{-5}	7.79×10^{-5}	8.71×10^{-5}	1.07×10^{-4}
CORRECTED S/So	6.54×10^{-5}	7.91×10^{-5}	9.64×10^{-5}	1.14×10^{-4}	1.46×10^{-4}
DARK IRRADIATED S/So	6.54×10^{-5}	6.54×10^{-5}	6.54×10^{-5}	6.54×10^{-5}	6.54×10^{-5}
EXPT 15c (4.42)	0	30	60	90	120
UNIRRADIATED S/So	1.000	0.901	0.821	0.784	0.746
IRRADIATED S/So	8.76×10^{-5}	9.55×10^{-5}	1.17×10^{-4}	1.69×10^{-4}	2.17×10^{-4}
CORRECTED S/So	8.76×10^{-5}	1.06×10^{-4}	1.43×10^{-4}	2.16×10^{-4}	2.91×10^{-4}
DARK IRRADIATED S/So	8.76×10^{-5}	8.76×10^{-5}	8.76×10^{-5}	8.76×10^{-5}	8.76×10^{-5}

Table D.16. Photoreactivation data for AS46/pND03 at fluence rate of ≅ $1Wm^{-2}$ at 25°C (Figure 5.16)

	PHOTOREACTIVATION TIME (minutes)				
EXPT 16a (3.56)	0	30	60	90	120
UNIRRADIATED S/So	1.000	0.977	0.977	0.967	0.920
IRRADIATED S/So	1.58×10^{-4}	2.13×10^{-4}	2.81×10^{-4}	3.32×10^{-4}	3.98×10^{-4}
CORRECTED S/So	1.58×10^{-4}	2.18×10^{-4}	2.88×10^{-4}	3.43×10^{-4}	4.33×10^{-4}
DARK IRRADIATED S/So	1.58×10^{-4}	1.58×10^{-4}	1.58×10^{-4}	1.58×10^{-4}	1.58×10^{-4}
EXPT 16b (4.44)	0	30	60	90	120
UNIRRADIATED S/So	1.000	0.934	0.797	0.751	0.724
IRRADIATED S/So	5.49×10^{-5}	6.45×10^{-5}	6.72×10^{-5}	7.66×10^{-5}	7.67×10^{-5}
CORRECTED S/So	5.49×10^{-5}	6.91×10^{-5}	8.43×10^{-5}	1.02×10^{-4}	1.06×10^{-4}
DARK IRRADIATED S/So	5.49×10^{-5}	5.49×10^{-5}	5.49×10^{-5}	5.49×10^{-5}	5.49×10^{-5}
EXPT 16c (4.46)	0	30	60	90	120
UNIRRADIATED S/So	1.000	0.946	0.824	0.794	0.746
IRRADIATED S/So	5.12×10^{-5}	6.36×10^{-5}	6.77×10^{-5}	7.81×10^{-5}	7.76×10^{-5}
CORRECTED S/So	5.12×10^{-5}	6.72×10^{-5}	8.22×10^{-5}	9.84×10^{-5}	1.04×10^{-4}
DARK IRRADIATED S/So	5.12×10^{-5}	5.12×10^{-5}	5.12×10^{-5}	5.12×10^{-5}	5.12×10^{-5}

Table D.17. Photoreactivation data for AS46/pKK223-3 at fluence rate of ≡ $1Wm^{-2}$ at 25°C (Figure 5.17)

	PHOTOREACTIVATION TIME (minutes)				
EXPT 17a (3.58)	0	30	60	90	120
UNIRRADIATED S/So	1.000	0.897	0.780	0.827	0.733
IRRADIATED S/So	1.31×10^{-4}	1.41×10^{-4}	2.09×10^{-4}	2.61×10^{-4}	3.12×10^{-4}
CORRECTED S/So	1.31×10^{-4}	1.57×10^{-4}	2.68×10^{-4}	3.15×10^{-4}	4.25×10^{-4}
DARK IRRADIATED S/So	1.31×10^{-4}	1.31×10^{-4}	1.31×10^{-4}	1.31×10^{-4}	$1.31x\ 10^{-4}$
EXPT 17b (4.48)	0	30	60	90	120
UNIRRADIATED S/So	1.000	0.904	0.796	0.764	0.754
IRRADIATED S/So	8.46×10^{-5}	9.01×10^{-5}	1.05×10^{-4}	1.53×10^{-4}	2.46×10^{-4}
CORRECTED S/So	8.46×10^{-5}	9.97×10^{-5}	1.32×10^{-4}	2.41×10^{-4}	3.26×10^{-4}
DARK IRRADIATED S/So	8.46×10^{-5}	8.46×10^{-5}	8.46×10^{-5}	8.46×10^{-5}	8.46×10^{-5}
EXPT 17c (4.50)	0	30	60	90	120
UNIRRADIATED S/So	1.000	0.869	0.776	0.724	0.704
IRRADIATED S/So	5.69×10^{-5}	5.59×10^{-5}	5.93×10^{-5}	6.52×10^{-5}	6.95×10^{-5}
CORRECTED S/So	5.69×10^{-5}	6.43×10^{-5}	7.64×10^{-5}	9.01×10^{-5}	9.87×10^{-5}
DARK IRRADIATED S/So	5.69×10^{-5}	5.69×10^{-5}	5.69×10^{-5}	5.69×10^{-5}	5.69×10^{-5}

Table D.18. Photoreactivation data for AS46/pND03 at fluence rate of ≡ $5Wm^{-2}$ at 25°C (Figure 5.18)

	PHOTOREACTIVATION TIME (minutes)				
EXPT 18a (3.90)	0	30	60	90	120
UNIRRADIATED S/So	1.000	0.901	0.772	0.705	0.671
IRRADIATED S/So	6.00×10^{-5}	7.98×10^{-5}	1.11×10^{-4}	1.50×10^{-4}	1.57×10^{-4}
CORRECTED S/So	6.00×10^{-5}	8.86×10^{-5}	1.44×10^{-4}	2.13×10^{-4}	2.34×10^{-4}
DARK IRRADIATED S/So	6.00×10^{-5}	6.00×10^{-5}	6.00×10^{-5}	6.00×10^{-5}	6.00×10^{-5}
EXPT 18b (3.72)	0	30	60	90	120
UNIRRADIATED S/So	1.000	0.869	0.759	0.700	0.678
IRRADIATED S/So	$1.14x\ 10^{-4}$	1.45×10^{-4}	2.08×10^{-4}	3.25×10^{-4}	3.25×10^{-4}
CORRECTED S/So	1.14×10^{-4}	1.67×10^{-4}	2.73×10^{-4}	4.64×10^{-4}	4.79×10^{-4}
DARK IRRADIATED S/So	1.14×10^{-4}	1.14×10^{-4}	1.14×10^{-4}	1.14×10^{-4}	1.14×10^{-4}
EXPT 18c (4.52)	0	30	60	90	120
UNIRRADIATED S/So	1.000	0.894	0.763	0.712	0.674
IRRADIATED S/So	5.12×10^{-5}	5.55×10^{-5}	5.93×10^{-5}	6.71×10^{-5}	7.15×10^{-5}
CORRECTED S/So	5.12×10^{-5}	6.21×10^{-5}	7.77×10^{-5}	9.42×10^{-5}	1.06×10^{-4}
DARK IRRADIATED S/So	5.12×10^{-5}	5.12×10^{-5}	5.12×10^{-5}	5.12×10^{-5}	5.12×10^{-5}

Table D.19. Photoreactivation data for AS46/pKK223-3 at fluence rate of ≅ 5Wm^{-2} at 25°C (Figure 5.19)

	PHOTOREACTIVATION TIME (minutes)				
EXPT 19a (3.92)	0	30	60	90	120
UNIRRADIATED S/So	1.000	0.912	0.746	0.638	0.606
IRRADIATED S/So	6.35×10^{-5}	8.08×10^{-5}	1.23×10^{-4}	1.24×10^{-4}	1.46×10^{-4}
CORRECTED S/So	6.35×10^{-5}	8.86×10^{-5}	1.65×10^{-4}	1.95×10^{-4}	2.40×10^{-4}
DARK IRRADIATED S/So	6.35×10^{-5}	6.35×10^{-5}	6.35×10^{-5}	6.35×10^{-5}	6.35×10^{-5}
EXPT 19b (3.74)	0	30	60	90	120
UNIRRADIATED S/So	1.000	0.847	0.757	0.633	0.602
IRRADIATED S/So	1.66×10^{-4}	1.99×10^{-4}	2.52×10^{-4}	3.30×10^{-4}	3.52×10^{-4}
CORRECTED S/So	1.66×10^{-4}	2.35×10^{-4}	3.32×10^{-4}	5.22×10^{-4}	5.84×10^{-4}
DARK IRRADIATED S/So	1.66×10^{-4}	1.66×10^{-4}	1.66×10^{-4}	1.66×10^{-4}	1.66×10^{-4}
EXPT 19c (4.54)	0	30	60	90	120
UNIRRADIATED S/So	1.000	0.864	0.767	0.649	0.617
IRRADIATED S/So	5.01×10^{-5}	5.80×10^{-5}	6.32×10^{-5}	7.72×10^{-5}	8.82×10^{-5}
CORRECTED S/So	5.01×10^{-5}	6.71×10^{-5}	8.24×10^{-5}	1.19×10^{-4}	1.43×10^{-4}
DARK IRRADIATED S/So	5.01×10^{-5}	5.01×10^{-5}	5.01×10^{-5}	5.01×10^{-5}	5.01×10^{-5}

Table D.20. Photoreactivation data for AS46/pND03 at fluence rate of ≅ 12Wm^{-2} at 25°C (Figure 5.20)

	PHOTOREACTIVATION TIME (minutes)				
EXPT 20a (4.58)	0	30	60	90	120
UNIRRADIATED S/So	1.000	0.815	0.712	0.593	0.543
IRRADIATED S/So	4.43 x 10^{-5}	5.47 x 10^{-5}	1.00 x 10^{-4}	1.46 x 10^{-4}	2.50 x 10^{-4}
CORRECTED S/So	4.43 x 10^{-5}	6.71 x 10^{-5}	1.40 x 10^{-4}	2.46 x 10^{-4}	4.60 x 10^{-4}
DARK IRRADIATED S/So	4.43 x 10^{-5}	4.43 x 10^{-5}	4.43 x 10^{-5}	4.43 x 10^{-5}	4.43 x 10^{-5}
EXPT 20b (4.10)	0	30	60	90	120
UNIRRADIATED S/So	1.000	0.833	0.699	0.562	0.579
IRRADIATED S/So	2.38 x 10^{-5}	4.19 x 10^{-5}	8.81 x 10^{-5}	1.27 x 10^{-4}	1.43 x 10^{-4}
CORRECTED S/So	2.38 x 10^{-5}	5.03 x 10^{-5}	1.26 x 10^{-4}	2.26 x 10^{-4}	2.46 x 10^{-4}
DARK IRRADIATED S/So	2.38 x 10^{-5}	2.38 x 10^{-5}	2.38 x 10^{-5}	2.38 x 10^{-5}	2.38 x 10^{-5}
EXPT 20c (4.56)	0	30	60	90	120
UNIRRADIATED S/So	1.000	0.824	0.754	0.564	0.521
IRRADIATED S/So	6.71 x 10^{-5}	8.15 x 10^{-5}	1.86 x 10^{-4}	2.83 x 10^{-4}	3.39 x 10^{-4}
CORRECTED S/So	6.71 x 10^{-5}	9.89 x 10^{-5}	2.47 x 10^{-4}	5.02 x 10^{-4}	6.51 x 10^{-4}
DARK IRRADIATED S/So	6.71 x 10^{-5}	6.71 x 10^{-5}	6.71 x 10^{-5}	6.71 x 10^{-5}	6.71 x 10^{-5}

Table D.21. Photoreactivation data for AS46/pKK223-3 at fluence rate of ≅ 12Wm^{-2} at 25°C (Figure 5.21)

	PHOTOREACTIVATION TIME (minutes)				
EXPT 21a (4.12)	0	30	60	90	120
UNIRRADIATED S/So	1.000	0.754	0.513	0.474	0.396
IRRADIATED S/So	4.50×10^{-5}	5.31×10^{-5}	5.98×10^{-5}	6.35×10^{-5}	5.50×10^{-5}
CORRECTED S/So	4.50×10^{-5}	7.04×10^{-5}	1.17×10^{-4}	1.34×10^{-4}	1.39×10^{-4}
DARK IRRADIATED S/So	4.50×10^{-5}	4.50×10^{-5}	4.50×10^{-5}	4.50×10^{-5}	4.50×10^{-5}
EXPT 21b (3.84)	0	30	60	90	120
UNIRRADIATED S/So	1.000	0.722	0.509	0.460	0.400
IRRADIATED S/So	2.08×10^{-4}	2.36×10^{-4}	2.84×10^{-4}	2.88×10^{-4}	3.12×10^{-4}
CORRECTED S/So	2.08×10^{-4}	3.27×10^{-4}	5.58×10^{-4}	6.26×10^{-4}	7.08×10^{-4}
DARK IRRADIATED S/So	2.08×10^{-4}	2.08×10^{-4}	2.08×10^{-4}	2.08×10^{-4}	2.08×10^{-4}
EXPT 21c (4.60)	0	30	60	90	120
UNIRRADIATED S/So	1.000	0.764	0.521	0.469	0.410
IRRADIATED S/So	6.79×10^{-5}	6.20×10^{-5}	5.15×10^{-4}	5.35×10^{-4}	5.99×10^{-4}
CORRECTED S/So	6.79×10^{-5}	8.12×10^{-5}	9.88×10^{-5}	1.14×10^{-4}	1.46×10^{-4}
DARK IRRADIATED S/So	6.79×10^{-5}	6.79×10^{-5}	6.79×10^{-5}	6.79×10^{-5}	6.79×10^{-5}

Table D.22i. Sensitivity of unirradiated AS46/pND01 to the photoreactivating light at fluence rate of ≅ 8Wm^{-2} at 25°C (Figure 5.22)

	PHOTOREACTIVATION TIME (minutes)				
(4.4)					
EXPT 22ia	0	30	60	90	120
S/So	1.000	1.174	0.870	0.709	0.565
EXPT 22ib	0	30	60	90	120
S/So	1.000	0.863	0.493	0.619	0.604
AVERAGE S/So	1.000	0.948	0.668	0.660	0.588

Table D.22ii. Sensitivity of unirradiated AS46/pUC19 to the photoreactivating light at fluence rate of ≅ 8Wm^{-2} at 25°C (Figure 5.22)

	PHOTOREACTIVATION TIME (minutes)				
(3.80)					
EXPT 22iia	0	30	60	90	120
S/So	1.000	0.930	0.749	0.679	0.532
EXPT 22iib	0	30	60	90	120
S/So	1.000	0.935	0.691	0.634	0.586
AVERAGE S/So	1.000	0.932	0.717	0.656	0.561

Table D.23i. Sensitivity of unirradiated AS46/pND03 to the photoreactivating light at fluence rate of ≅ 8Wm^{-2} at 25°C (Figure 5.23)

	PHOTOREACTIVATION TIME (minutes)				
(3.60)					
EXPT 23ia	0	30	60	90	120
S/So	1.000	1.061	0.820	0.689	0.731
EXPT 23ib	0	30	60	90	120
S/So	1.000	0.812	0.763	0.670	0.575
AVERAGE S/So	1.000	0.928	0.790	0.679	0.648

Table D.23ii. Sensitivity of unirradiated AS46/pKK223-3 to the photoreactivating light at fluence rate of ≅ 8Wm^{-2} at 25°C (Figure 5.23)

	PHOTOREACTIVATION TIME (minutes)				
(3.78)					
EXPT 23iia	0	30	60	90	120
S/So	1.000	0.944	0.725	0.595	0.470
EXPT 23iib	0	30	60	90	120
S/So	1.000	0.939	0.825	0.721	0.607
AVERAGE S/So	1.000	0.942	0.773	0.656	0.537

Table D.24i. Sensitivity of unirradiated AS46/pND03 to the photoreactivating light at fluence rate of ≡ 12Wm^{-2} at 25°C (Figure 5.24)

	PHOTOREACTIVATION TIME (minutes)				
(4.6)					
EXPT 24ia	0	30	60	90	120
S/So	1.000	0.840	0.834	0.764	0.604
EXPT 24ib	0	30	60	90	120
S/So	1.000	0.808	0.801	0.741	0.566
AVERAGE S/So	1.000	0.824	0.817	0.757	0.584

Table D.24ii. Sensitivity of unirradiated AS46/pKK223-3 to the photoreactivating light at fluence rate of ≡ 12Wm^{-2} at 25°C (Figure 5.24)

	PHOTOREACTIVATION TIME (minutes)				
(4.8)					
EXPT 24iia	0	30	60	90	120
S/So	1.000	0.745	0.529	0.471	0.418
EXPT 24iib	0	30	60	90	120
S/So	1.000	0.755	0.516	0.475	0.402
AVERAGE S/So	1.000	0.749	0.522	0.473	0.408

Table D.25. Photoreactivation data for AS46/pND05 at 25°C (Figure 5.25)

	PHOTOREACTIVATION TIME (minutes)				
EXPT 25a (3.86)	0	30	60	90	120
UNIRRADIATED S/So	1.000	0.857	0.801	0.614	0.438
IRRADIATED S/So	1.29×10^{-4}	1.21×10^{-4}	1.39×10^{-4}	1.48×10^{-4}	1.51×10^{-4}
CORRECTED S/So	1.29×10^{-4}	1.42×10^{-4}	1.74×10^{-4}	2.40×10^{-4}	3.45×10^{-4}
DARK IRRADIATED S/So	1.29×10^{-4}	1.29×10^{-4}	1.29×10^{-4}	1.29×10^{-4}	1.29×10^{-4}
EXPT 25b (4.62)	0	30	60	90	120
UNIRRADIATED S/So	1.000	0.864	0.790	0.631	0.459
IRRADIATED S/So	7.26×10^{-5}	7.31×10^{-5}	7.75×10^{-5}	7.19×10^{-5}	6.38×10^{-5}
CORRECTED S/So	7.26×10^{-5}	8.46×10^{-5}	9.81×10^{-5}	1.14×10^{-4}	1.39×10^{-4}
DARK IRRADIATED S/So	7.26×10^{-5}	7.26×10^{-5}	7.26×10^{-5}	7.26×10^{-5}	7.26×10^{-5}

APPENDIX E

MISCELLANEOUS DATA

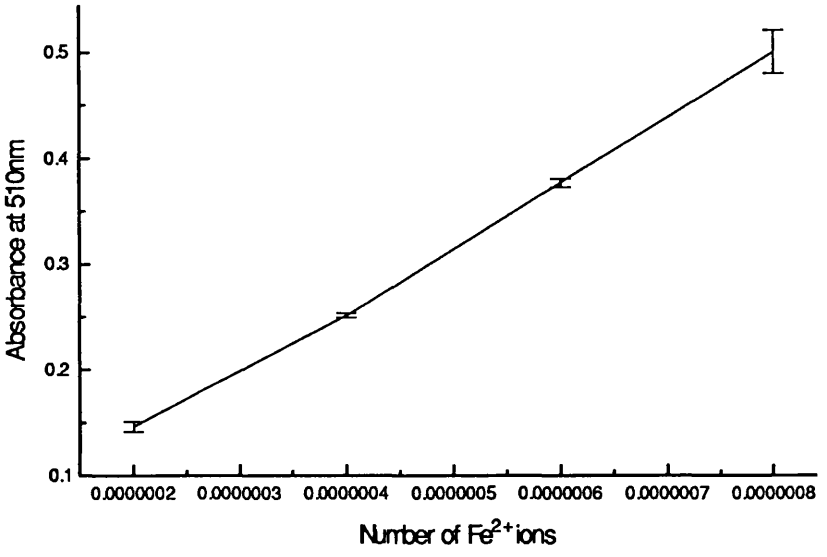

Figure E.1. Calibration curve of the optical density at 510nm against the amount of ferrous ions present in the solution.

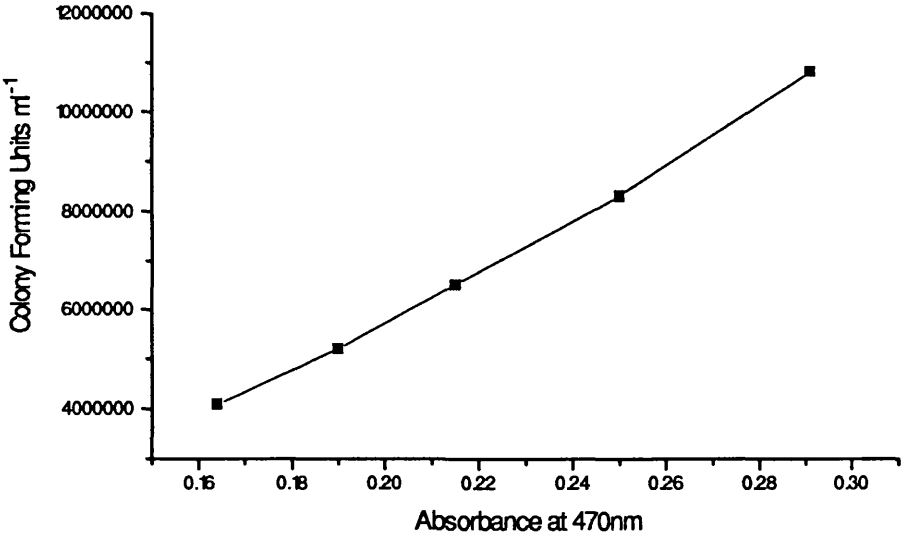

Figure E.2. Calibration curve of the viable count of a cell suspension of AS46 / pND03 against the optical density of the cell suspension mesured at 470nm.